STIMULUS-RESPONSIVE INJECTABLE POLYSACCHARIDE SCAFFOLDS FOR SOFT TISSUE ENGINEERING PREPARED BY O/W HIGH INTERNAL PHASE EMULSION

Shengzhong Zhou

A dissertation submitted to Imperial College London

in fulfilment of the requirements for the degree of

Doctor of Philosophy

and the Diploma of Membership of Imperial College London

Department of Chemistry

Imperial College London

December 2010

DECLARATION

I hereby certify that the work presented in this thesis is the result of my own investigations carried out at Imperial College London during the period from February 2007 to February 2010, except where otherwise stated.

Shengzhong Zhou

December 2010

ACKNOWLEDGEMENTS

I am grateful to the following for their support, help and contribution throughout the course of this work:

- My supervisors Dr Joachim H.G. Steinke and Professor Alexander Bismarck for their great patience, guidance, inspiration and support in the past four years.

- All my friends and colleagues in the JHGS group and PaCE group at Imperial College, for their help and support during my stay in UK. Special thanks go to Sally Ewen, James M. Serginson, Ranting Wu, Wei Yuan, Michael Bajomo, Jonathan Martinelli, Edyta Sidorowicz and Bryn Monnery.

- Dr Fanshun Meng, Dr Natasha Shirshova, Dr Angelika Menner and Dr Jonny J. Blaker, for their advices and help.

- Andrew Chong and Dr Anne E. Bishop, for their help in scaffold cytoxicity assessments.

This thesis is dedicated to my parents and my wife.

ABSTRACT

This thesis describes work on the development of several novel stimuli-responsive porous hydrogels prepared from oil-in-water (o/w) high internal phase emulsion (HIPE) as injectable scaffolds for soft tissue engineering. Firstly, by copolymerising glycidyl methacrylate (GMA) derivatised dextran and *N*-isopropylacrylamide (NIPAAm) in the aqueous phase of a toluene-in-water HIPE, thermo-responsive polyHIPE hydrogels were obtained. The temperature depended modulus of these porous hydrogels, as revealed by oscillatory mechanical measurements, indicated improvements of the mechanical properties of these hydrogels when heated from room temperature to human body temperature, as the polyNIPAAm copolymer segments starts to phase separate from the aqueous phase and causes the hydrogel to form a more compact structure within the aqueous phase of the polyHIPE. Secondly ion responsive methacrylate modified alginate polyHIPE hydrogels were prepared. The physical dimensions, pore and pore throat sizes as well as water uptakes of these ion responsive hydrogels can be controllably decreased in the presence of Ca^{2+} ions and are fully recovered after disruption of the ionic crosslinking using a chelating agent (sodium citrate). These ion-responsive polyHIPE hydrogels also possess good mechanical properties (modulus up to 20 kPa). Both of these polyHIPE hydrogels could be easily extruded through a hypodermic needle while breaking into small fragments (about 0.5 to 3.0 mm in diameter), but the interconnected porous

morphology was maintained after injection as revealed by SEM characterisation. Furthermore, the hydrogel fragments produced during injection can be crosslinked into a coherent scaffold under very mild condition using Ca^{2+} salts and alginate aqueous solution as the ionically crosslinkable adhesive.

In order to increase the pore size of these covalently crosslinked polyHIPE hydrogels and also find a biocompatible nontoxic emulsifier as substitution to traditional surfactants, methyl myristate-in-water and soybean oil-in-water HIPEs solely stabilised by hydroxyapatite (HAp) nanoparticle were prepared. These Pickering-HIPEs were used as template to prepare polyHIPE hydrogels. Dextran-GMA, a water soluble monomer, was polymerised in the continuous phase of the HAp Pickering HIPEs leading to porous hydrogels with a tunable pore size varying from 1.5 μm to 41.0 μm. HAp is a nontoxic biocompatible emulsifier, which potentially provides extra functions, such as promoting hard tissue cell proliferation.

HIPE-templated materials whose porous structure is maintained solely by the reversible physical aggregation between thermo-responsive dextran-*b*-polyNIPAAm block polymer chains in an aqueous environment (for this type of HIPE templated material we coined the name thermo-HIPEs) were prepared. No chemical reaction is required for the solidification of this porous material. This particular feature should provide a safer route to injectable scaffolds as issues of polymerisation/crosslinking chemistry or residual initiator fragments or monomers potentially being cytotoxic do

not arise in our case, as all components are purified polymers prior to HIPE formation. Thermo-HIPEs with soybean oil or squalene as dispersed oil phase were prepared. Also in this HIPE system it was possible to replace the original surfactant Triton X405 with colloidal HAp nanoparticles or pH/thermo-responsive polyNIPAAm-*co*-AA microgel particles. The pore sizes and the mechanical properties of colloidal particles stabilised thermo-HIPEs showed improvement compared with thermo-HIPEs stabilised by Triton X405.

In summary new injectable polyHIPEs have been prepared which retain their pore morphology during injection and can be solidified by either a thermal or ion (Ca^{2+}) or chelating ion (Ca^{2+}) stimulus. The materials used are intrinsically biocompatible and thus makes these porous injectable scaffolds excellent candidates for soft tissue engineering.

CONTENT

LIST OF FIGURES

LIST OF TABLES

LIST OF ABBREVIATIONS

2D	2-dimensional
3D	3-dimensional
AA	acrylic acid
AIBN	2,2'-azobis(isobutyronitrile)
APS	ammonium persulfate
BIS	*N,N'*-methylenebisacrylamide
c/w	CO_2-in-water
D_2O	deuterium oxide
Dex-P	dextran solid-(high internal phase emulsion) with *p*-xylene as oil phase and microgel particle as stabiliser
Dex-S	dextran solid-(high internal phase emulsion) with *p*-xylene as oil phase and Triton X405 as stabiliser
DG1	poly(dextran-glycidyl methacrylate) based poly(high internal phase emulsion) hydrogel
DGN1& DGN2	poly((dextran-glycidyl methacrylate)-*co*-*N*-isopropylacrylamide) based poly(high internal phase emulsion) hydrogels

DGS	poly(dextran-glycidyl methacrylate) hydrogel prepared from dextran-glycidyl methacrylate self-stabilised emulsion
DMAP	4-dimethylaminopyridine
DMEM	Dulbecco's Modified Eagle Medium
DMSO	dimethylsulphoxide
DN0	dextran based solid-(high internal phase emulsion) with *p*-xylene as oil phase and Triton X405 as stabiliser
DN1~DN3	dextran-*b*-poly(*N*-isopropylacrylamide) thermo-responsive-(high internal phase emulsion)s with *p*-xylene as oil phase and Triton X405 as stabiliser
DN-P-1 & DN-P-2	dextran-*b*-poly(*N*-isopropylacrylamide) thermo-responsive-(high internal phase emulsion)s with *p*-xylene as oil phase and microgel particle as stabiliser
DN-S-1 & DN-S-2	dextran-*b*-poly(*N*-isopropylacrylamide) thermo-responsive-(high internal phase emulsion)s with *p*-xylene as oil phase and Triton X405 as stabiliser

DN-S-*p*-Xylene	dextran-*b*-poly(*N*-isopropylacrylamide) thermo-responsive-(high internal phase emulsion) with *p*-xylene as oil phase and Triton X405 as stabiliser
DN-S-Soybean	dextran-*b*-poly(*N*-isopropylacrylamide) thermo-responsive-(high internal phase emulsion) with soybean oil as oil phase and Triton X405 as stabiliser
DN-S-Squalene	dextran-*b*-poly(*N*-isopropylacrylamide) thermo-responsive-(high internal phase emulsion) with squalene as oil phase and Triton X405 as stabiliser
DN-HAp-*p*-Xylene	dextran-*b*-poly(*N*-isopropylacrylamide) thermo-responsive-(high internal phase emulsion) with *p*-xylene as oil phase and hydroxyappetite nanoparticle as stabiliser
DN-HAp-Soybean	dextran-*b*-poly(*N*-isopropylacrylamide) thermo-responsive-(high internal phase emulsion) with soybean oil as oil phase and hydroxyappetite nanoparticle as stabiliser
DN-HAp-Squalene	dextran-*b*-poly(*N*-isopropylacrylamide) thermo-responsive-(high internal phase emulsion) with squalene as oil phase and hydroxyappetite nanoparticle as stabiliser
DVB	divinylbenzene

.FBS	foetal bovine serum
GMA	glycidyl methacrylate
GPC	gel permeation chromatography
HCl	hydrochloric acid
HMDS	hexamethyl disilazane
HIPE	high internal phase emulsion
HAp	hydroxyapatite
LCST	lower critical solution temperature
M_n	number average molecular weight
M_w	weight average molecular weight
MWCO	molecular weight cut off
NaDBS	sodium dodecylbenzenesulfonate
NaOH	sodium hydroxide
NMR	nuclear magnetic resonance
NIPAAm	*N*-isopropylacrylamide
o/w	oil-in-water

o/o	oil-in-oil
OPF	oligo(polyethylene glycol) fumarate
PAA	poly(acrylic acid)
PBS	phosphate buffered saline
PCL	poly(caprolactone)
PDLLA	poly(D,L, lactic acid)
PDMS	poly(dimethoxy silane)
PEG	poly(ethylene glycol)
PGA	poly(glycolic acid)
PHEA	poly(2-hydroxyethyl acetate)
PHMA	methacrylated-modified alginate poly(high internal phase emulsion) hydrogel
PLA	poly(lactic acid)
PLG	poly(lactide-*co*-glycolide)
PLGA	poly(lactic-*co*-glycolic acid)
PLLA	poly(L lactic acid)

PMMA	poly(methyl methaacrylate)
P(PF-*co*-EG)	poly(propylene fumarate-*co*-ethylene glycol)
PPH1~PPH8	poly(dextran-glycidyl methacrylate) poly-Pickering-(high internal phase emulsion) hydrogels with hydroxyappetite nanoparticle as stabiliser
PPO	poly(propylene oxide)
PVA	poly(vinyl alcohol)
PPF	poly(propylene fumarate)
PVA	poly(vinyl alcohol)
PLG	poly(lactide-*co*-glycolide)
PLLA	poly(L-lactic acid)
PolyHIPE	poly(high internal phase emulsion)
PS	poly(styrene)
SEM	scanning electron microscopy
TEMED	*N*,*N*,*N*',*N*'-tetramethylethylenediamine
w/o	water-in-oil

CHAPTER 1

INTRODUCTION

The focus of the work described in this thesis is the preparation of injectable 3 dimensional (3D) scaffolds for soft tissue engineering by using biocompatible hydrophilic natural polysaccharides as the molecular building blocks of the scaffold. Oil in water (o/w) high internal phase emulsion (HIPE) act as a pore template, stimulus-responsive particles as emulsifier both to create highly porous injectable scaffolds with an environmental stimulus to trigger gelation as solidification method (**Figure 1-1**).

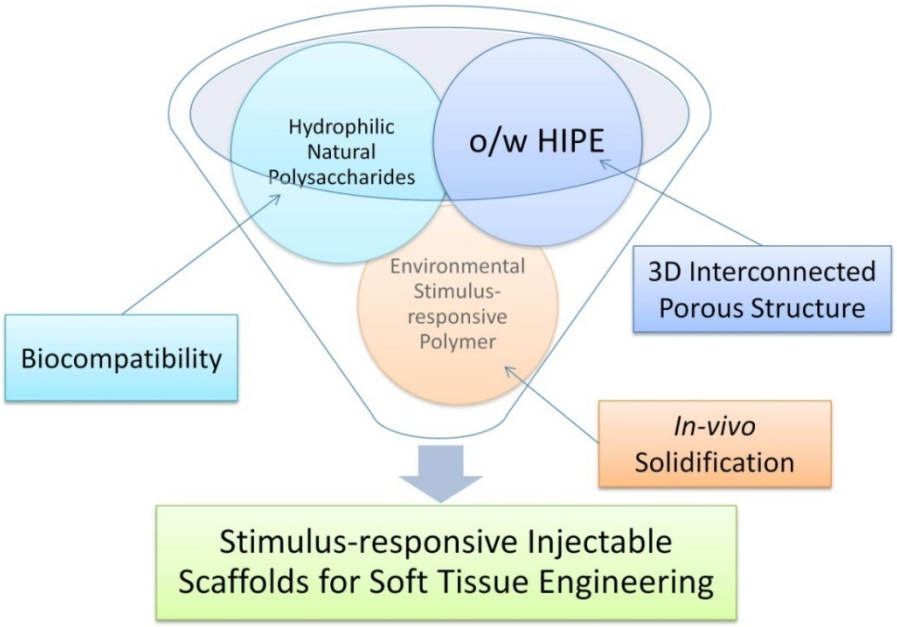

Figure 1-1: General scheme illustrating the key features of stimuli-responsive injectable polysaccharide scaffolds for soft tissue engineering.

A general introduction to the motivation of this project follows in **Section 1.1**. The major objective of the project was the development of novel stimuli-responsive injectable scaffolds and the strategy for achieving this objective is summarised in **Section 1.2**.

1.1 MOTIVATION

Nowadays, a comfortable and long life has become most peoples' desire and expectation. Medical technologies, such as surgical techniques and pharmaceutical developments which extend life and improve the quality of life have shouldered a majority of these demands. But correspondingly, the increase of human life span and quality has created a great demand for organ transplants and tissue replacements. By performing transplant surgeries, organ or tissue loss can be treated by transplanting organs from one individual to another. Although these surgeries have improved and saved countless lives, they remain imperfect solutions. Transplantation is severely limited by a critical donor shortage.[1] It has been reported that 77 people receive transplants in the United States every day in 2009, but nearly 20 die because of organ shortages.[2] Moreover, over 98,000 patients spend more than three years on average waiting for a suitable transplant.[2] The situation is obviously considerably worse in some developing or undeveloped countries.

Currently, transplants or medical prosthetics only offer a partial solution in comparison to the healthy, undamaged physiological state. As an alternative treatment,

tissue engineering, defined as "*understanding the principles of tissue growth, and applying this to produce functional replacement tissue for clinical use*"[3], offers another solution to organ transplantation. By combining the latest technologies in cell proliferation and porous extracellular matrices (scaffold), it is possible to create living tissue either in the laboratory[4] or *in vivo*[5]. It is reported that over 20 different tissues, such as bone, cartilage or skin, have already been engineered.[1,6-7] These engineered tissues could greatly reduce the need for organ transplants and could help to accelerate the development of new drugs.[8]

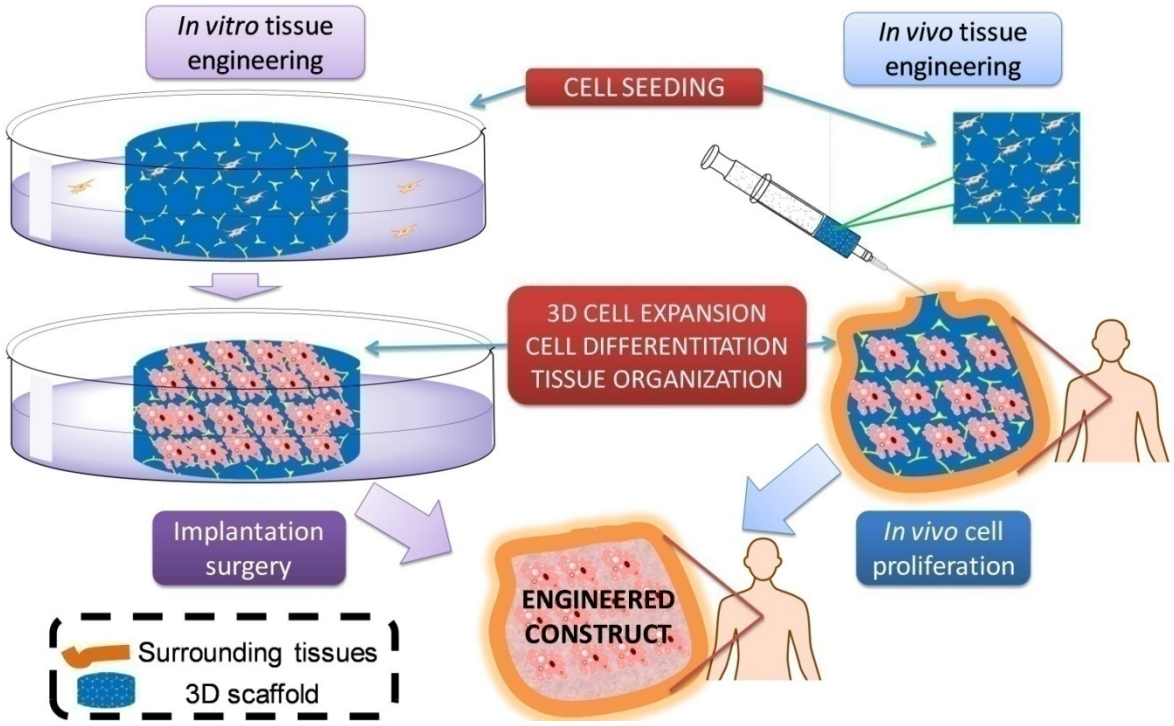

Figure 1-2: Two ways of regenerating tissue using different 3D scaffolds: **Left**: *in vitro* tissue engineering where cells are firstly seeded on a 3D scaffold and then left to proliferate *in vitro*. Thereafter the cell containing scaffold is transferred *in vivo* through invasive implantation surgery. **Right**: *in vivo* tissue engineering where cells are firstly seeded on a 3D scaffold and then injected into the human body together with the scaffold. After the scaffold solidifies, cells start to proliferate and generate tissue *in vivo* which ultimately integrates into the surrounding tissues.

Scaffolds, a critical element in tissue engineering, are usually made from a biocompatible and biodegradable matrix that offers physical support as well as a 3D environment to create living tissue through cell proliferation.[4,6,9] These highly porous matrices are used to foster tissues *in vitro* or *in vivo* to repair or replace diseased organs[10-11]. Constructs of living cells can be formed by seeding cells either within a preformed scaffold or through injection of a solidifiable porous scaffolds together with a cell mixture into the defective tissue[12-13] (**Figure 1-2**). Compared with preformed scaffolds, injectable scaffolds possess many advantageous features from a clinical perspective, such as minimising cost of treatment, patient discomfort, risk of infection and scar formation.[11,14] In addition to cells, also drugs or growth factors could be loaded into the scaffold prior to injection as well providing additional benefits.[11] Moreover, injectable scaffolds can be used to fill irregular defects, which is difficult to achieve with preformed scaffolds.[14]

However the main problem limiting the application of injectable scaffolds for tissue engineering is the difficulty to achieve good injectability and well-defined porous structures for cell proliferation after injection simultaneously. Currently injectable scaffolds that could be easily injected through needles usually possess porous structures with low interconnectivity, or cause irritations to the surrounding tissue during *in vivo* solidification. On the other hand, scaffolds, which have well-defined and controlled porous structure lack either injectability or a mild (non-irritating) *in vivo* solidification mechanism[15-18], and can only be used as preformed scaffolds.

1.2 PROJECT OBJECTIVES

The objectives of this project were to identify and develop novel injectable scaffolds for soft tissue engineering prepared by oil in water (o/w) high internal phase emulsion (HIPE) templating. The overall research objectives were as follows:

- Develop biocompatible scaffolds for soft tissue engineering with a suitable mechanical properties (with modulus between 60 Pa to 3 MPa) and well-defined interconnected porous structure suitable for nutrient/waste diffusion to support cell growth and migration.

- Prepare HIPE templated porous scaffolds fabricated through different types of crosslinking (e.g., covalent crosslinking, thermo-induced physical aggregation or ion crosslinking) compatible with their use as injectable porous scaffold materials.

- Develop and investigate solidification methods that allow o/w HIPE templated injectable scaffolds to be solidified *in vivo* after injection into a 3D porous structure.

- Identify a biocompatible emulsifier (such as nontoxic colloidal particles) to stabilise o/w HIPEs and investigate their application in fabricating porous scaffolds for tissue engineering.

1.3 THESIS STRUCTURE

This thesis presents work on the development of several polysaccharide based injectable scaffolds for soft tissue engineering prepared from o/w HIPE. The injectability, stimuli responsiveness, *in vivo* solidification, cytoxicity and porous structure of these scaffolds were investigated. In **Chapter 2**, the relevant background literature is comprehensively reviewed: scaffolds for tissue engineering (**Section 2.2**) and important elements in the design of injectable scaffolds for soft tissue engineering (**Section 2.3, 2.4 & 2.5**). A brief overview of tissue engineering and regenerative technology (**Section 2.1**) is also provided. In **Chapter 3** and **Chapter 4**, two types of novel stimuli-responsive covalently crosslinked hydrogel scaffolds fabricated from o/w HIPEs are discussed: thermo-responsive poly((dextran-GMA)-*co*-polyNIPAAm) polyHIPE hydrogels (**Chapter 3**) and ion-responsive methacrylate-modified alginate polyHIPE hydrogel (**Chapter 4**). The injectability and *in vivo* solidification methods of these two covalently crosslinked hydrogel scaffolds are discussed in **Chapter 5**. A new type of non-covalently crosslinked injectable HIPEs based on dextran-*b*-polyNIPAAm is described in **Chapter 6**. The use of biocompatible colloidal particles as emulsifiers for o/w HIPEs and the fabrication of porous scaffolds for tissue engineering is described in **Chapter 7**. **Chapter 8** draws overall conclusions from the study and makes suggestions for future work.

CHAPTER 2

BACKGROUND

2.1 INTRODUCTION TO TISSUE ENGINEERING

Tissue engineering is the method of creating 3D living tissues to improve or replace biological functions.[1] It is an interdisciplinary field that aims to create whole tissue, such as cartilage, bone, lung or blood vessel by utilizing combinations of engineering methods and life sciences, to replace damaged or lost organs (**Figure 2-1**).[19] The fabrication of new physiologically fully functioning tissue involves the combined efforts of material scientists, biologists, mathematicians, engineers, geneticists, and clinicians.[20] The first reported example of tissue engineering was recorded in 1933 where mouse tumour cells were encased in a polymer membrane and inserted into a pig abdominal cavity[7,21]. The tumour cells were not destroyed by the immune system. Nowadays, due to the progress in stem cell biology and recognition of the unique biological properties of stem cells, tissue can be engineered either *in vitro* or *in vivo* using stem cells comprising a diverse selections from epithelial surfaces to skeletal tissues.[22] The list of tissue that can potentially be engineered is growing steadily every year.[22]

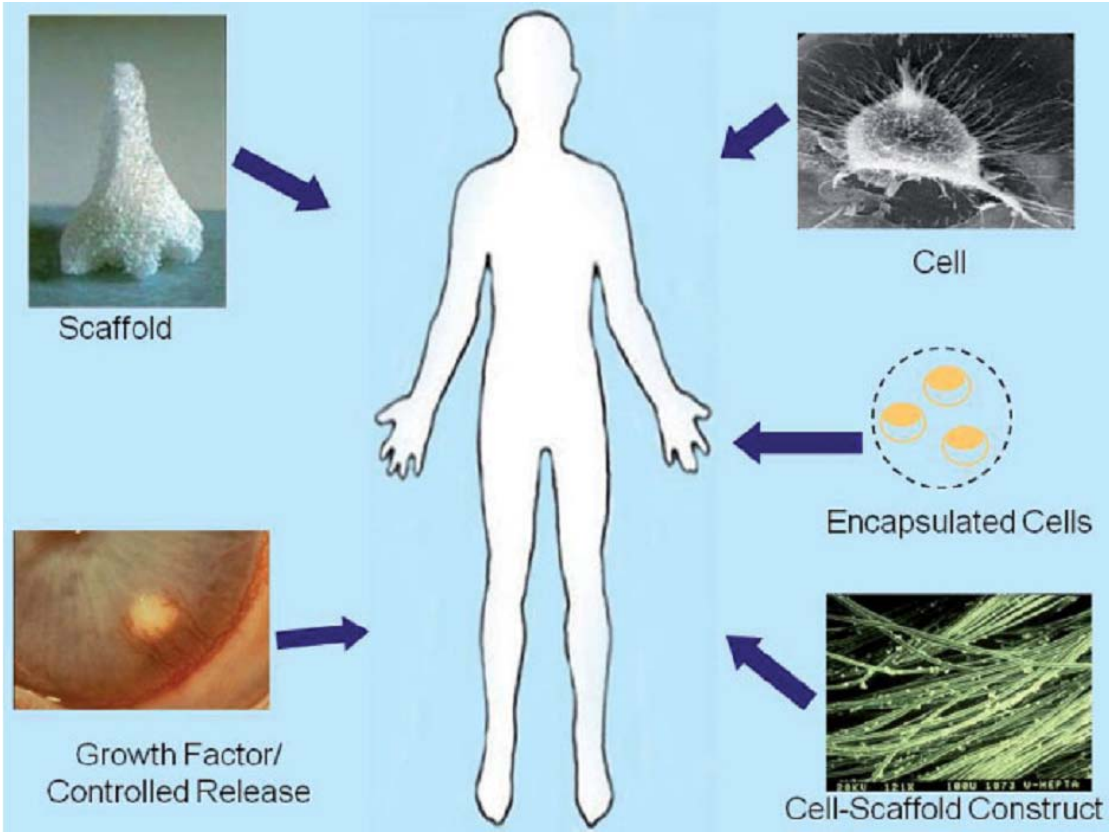

Figure 2-1: Approaches to tissue engineering and regenerative medicine (reproduced from Langer, R. *Adv. Mater.* 21, 3235-3236 (2009))

In tissue engineering and regenerative medicine, three general strategies have been developed to create new tissues:

1. Isolated cells or cell substitutes. This approach allows replacement of only those cells that supply the required function and permits manipulation and expansion of the cells before infusion. This method avoids the complications of surgery, but the potential limitation is the ability of maintaining the function of infused cells in the recipient or immunological rejection of the injected cells.[1]

2. Tissue-inducing substances. This approach is based on the introduction of appropriate signal molecules, such as growth factors, and the methods to deliver these molecules to their targets.[1]

3. Cell seeded scaffolds. Cells are initially seeded onto a porous scaffold *in vitro* or *in vivo*. The scaffold should allow permeation of nutrients and waste but be "invisible physiologically" do that antibodies or immune cells will not be triggered to destroy the transplant. These systems then can be used as extracorporeal devices or implanted directly into the patient and allowed integration with the surrounding tissue.[1]

2.2 SCAFFOLDS FOR TISSUE ENGINEERING

As already mentioned, scaffolds play a very important role in tissue reconstruction. It is known that isolated cells cannot form new tissue by themselves.[23] Numerous strategies currently used to engineer tissue depend on employing a scaffold. Scaffolds serve as templates for cell interaction and the formation of extracellular matrix to provide structural support to the newly formed tissue.

Most of the scaffolds for tissue engineering are biocompatible 3D porous matrices, because in a living organism, cells are surrounded by other cells and the *in situ* environment of such cells is 3D.[24-26] In such an environment, extracellular ligands including collagens and laminin, are involved in providing a matrix which develops between cells and the basal membrane; nutrient diffusion as well as waste exchange can occur easily due to the interconnectivity of the 3D matrices.[11,27] When seeded

onto two dimensional (2D) scaffolds, cells lack the ability to grow in their favoured 3D orientations which defines the anatomical shape of the tissue. Instead, they randomly migrate to form a 2D layer of cells.[28] There are several major drawbacks to 2D scaffolds:

1. Chemical signals or molecular gradients that guide cells differentiation, organ development and other biological processes are absent from a 2D environment[23]

2. The production of the extracellular matrix proteins and the morphological change (e.g., spreading speed) of cells can be significantly changed when the cells are proliferating in a 2D culture. The cells directly exposed to the culture medium have more opportunities to obtain nutrients. On the other hand, the cells attached to the surface may have fewer opportunities for clustering. The asymmetric spreading of cells in 2D culture might lead to the wrong orientation and clustering and also affect communication between cells;

3. In 2D environment, cells isolated directly from higher organisms frequently alter metabolism and gene expression patterns, which results in the adaption of cells to 2D cultures.

The requirements for a scaffold are numerous and often different for different applications; however, there are some general properties a scaffold must fulfil to be considered for tissue engineering applications:

1. The material used as the solid constituent of the scaffold must be biocompatible and biodegradable, possess suitable hydrophilic surface properties for cell adhesion;

2. The scaffold should possess a 3D interconnected pore structure to support cell growth and provide a mass-transport environment for optimal diffusion of nutrients and waste;

3. The modulus of human tissue ranges from 50 Pa[29] for skin or subcutaneous tissue to 100 GPa[30] for trabecular bone (**Table 2-1**). The appropriate mechanical properties of a scaffold are required to temporarily substitute those of the native tissue and support everyday functional demands within a defect until sufficient tissue has formed to take over the function.[4] Scaffolds must be designed not only to avoid failure of providing sufficient mechanical strength to withstand biomechanical loading to and offer reliable yet temporary support for the growing cell culture but should also not be too stiff compared to surrounding and regenerating tissues to cause adverse physiological responses, such as tissue resorption;

4. The scaffold, both preformed or injectable, should initially fill complex 3D defects, subsequently guiding the tissue to shape itself to match the original 3D defect structure.[31]

Table 2-1: Tangent/Young's modulus range of biologic tissues from the stiffest tissue (bone) to the most compliant tissue (skin). (Table adapted from Scott, J. H. Scaffold Design and Manufacturing: From Concept to Clinic. *Adv. Mater.* 21, 3330-3342 (2009))

Tissue (Species)	Tangent/Young's Modulus Range in MPa	References
Trabecular Bone	100-100000	[30]
Meniscus	1.6-3.2	[32]
Articular Cartilage	0.3-2.1	[32]
Medial Collateral Ligament	0.3	[33]
Intervertebral Disc – Fibrocartilage	0.05-0.07	[34]
Fat	0.002	[35]
Heart Valve	0.00153	[36]
Skin/Subcutaneous Tissue	0.000057	[29]

2.2.1 PREFORMED SCAFFOLDS

When the porous scaffold is preformed outside the human body, the living tissue is engineered within this matrix *in vitro* and then implanted into patients through invasive surgery, the scaffold is classified unsurprisingly as a preformed scaffold. Preformed scaffolds are investigated either in therapeutic applications as tissue substitute, in diagnostic applications, for instance for drug testing[13] or even in edible meat production[37]. A flow chart that describes the general approach of repairing

defects and generating native tissues by using preformed scaffolds is shown in **Figure 2-1**.

As mentioned before, compared with injectable scaffolds, preformed scaffolds can be fabricated into complex 3D matrices by many methods without the requirement of injectability. As the solidification of preformed scaffolds is triggered *in vitro*, the processing conditions of preformed scaffolds (e.g. pressure, temperature, solvent and devices) are less limited compared with injectable scaffolds. Harmful chemicals that are used or produced during scaffolds preparation can be easily removed before cell seeding. Surface modifications that improve cell-surface adhesion can also be preformed after the porous scaffold was fabricated, which enlarges the materials selection considerably since some synthetic polymers (e.g. poly(styrene) (PS)[38]) do not posses proper biocompatible surfaces for cell adhesion but could also be modified and used as scaffolds in this way. Porogen leaching[39], emulsion templating[40], gas foaming[41], freeze drying[42], fiber mesh fabrication[43], molding[44], phase separation[45] or even computer-aided prototyping[4,46] have been used to produce preformed scaffolds.[44] Details about the fabrication of preformed scaffolds will be given in **Section 2.5**.

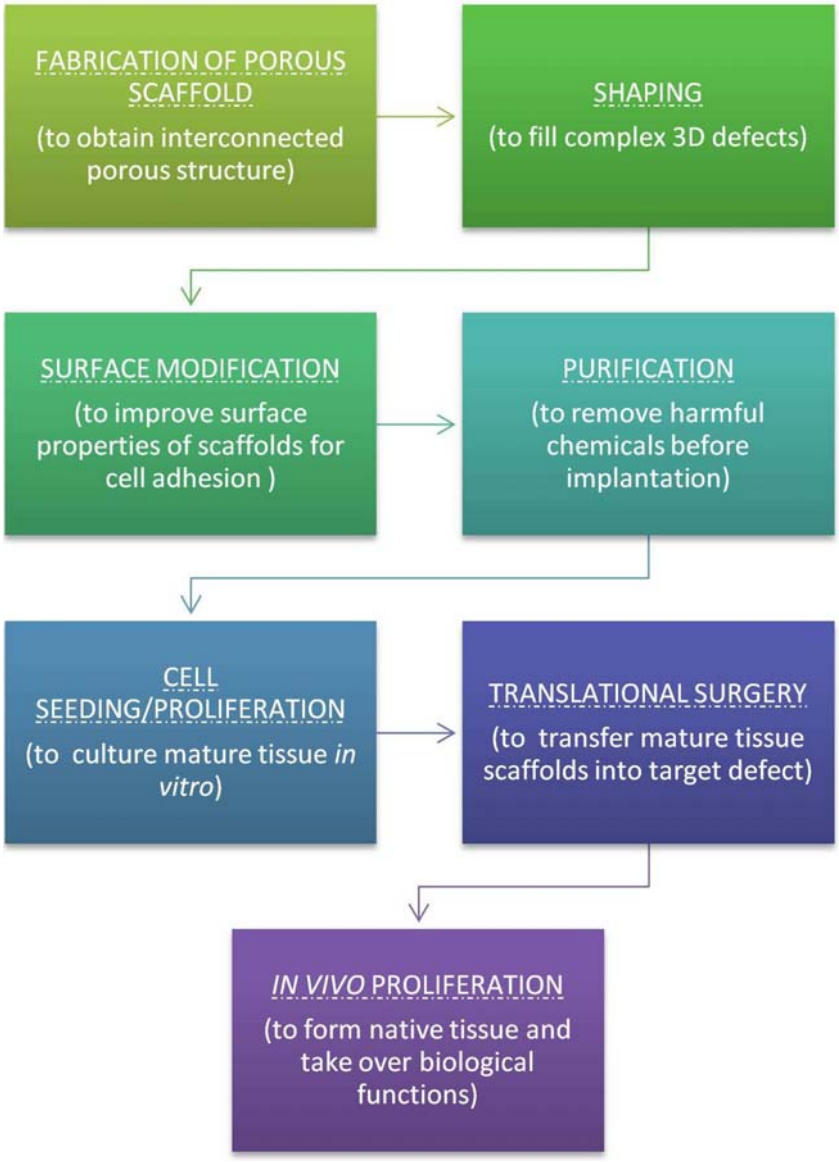

Figure 2-2: Flow chart illustrating the general approach of using preformed scaffolds to generate tissue in vitro, which subsequently are being implanted in a patient to take over biological functions.

2.2.2 INJECTABLE SCAFFOLDS

Clinically, there is a great demand for minimal invasive surgery procedures in order to minimise patient discomfort and risk of infection[11]. Surgical micro-techniques have proven to be effective and are frequently used for many operations.

Biocompatible/biodegradable matrixes with open porous structures and designed as carrier systems for cell transplants, also known as injectable scaffolds, meet this demand for minimal invasive surgery procedures. A flow chart describing one possible approach of repairing defects by using an injectable scaffold is shown in **Figure 2-3**. Compared with preformed scaffolds, injectable scaffolds, owing to their injectability, offer many advantages such as minimising cost of treatment, scar formation, patient discomfort, and risk of infection.[11] Moreover, injectable scaffolds can easily be used to fill irregular defects, which is much more difficult to achieve when using preformed scaffolds. Also cells, drugs and other bioactive molecule can easily be incorporated into the matrix.

The challenges in designing and producing an injectable scaffold are also clear. After injection, it is impossible to use any machines or apparatus to fabricate an interconnected porous structure during the solidification *in vivo* and therefore the pore structure has to be in place before injection or during the injection process. Many methods of fabricating 3D porous scaffolds, such as fibre spinning or moulding, are not amenable for direct injection of porous structures. Also surface modification of such potential scaffolds is impossible *in vivo*. Imposing severe limits on the selection and processing of materials for scaffold fabrication. Materials that are naturally biocompatible and biodegradable, such as alginate or fibrin, became therefore first choice for producing injectable scaffolds.[11] The variability in the mechanical properties between the liquid state before injection and the solid state *in vivo* also

limits the choice of materials. Moreover, minimising cytotoxicity and inflammation to damage the surrounding tissue also limits the choice of solidification mechanism. And finally the methods and the process with which cells can be safely loaded into the scaffolds without exposure to any hazard chemicals also need to be carefully considered.

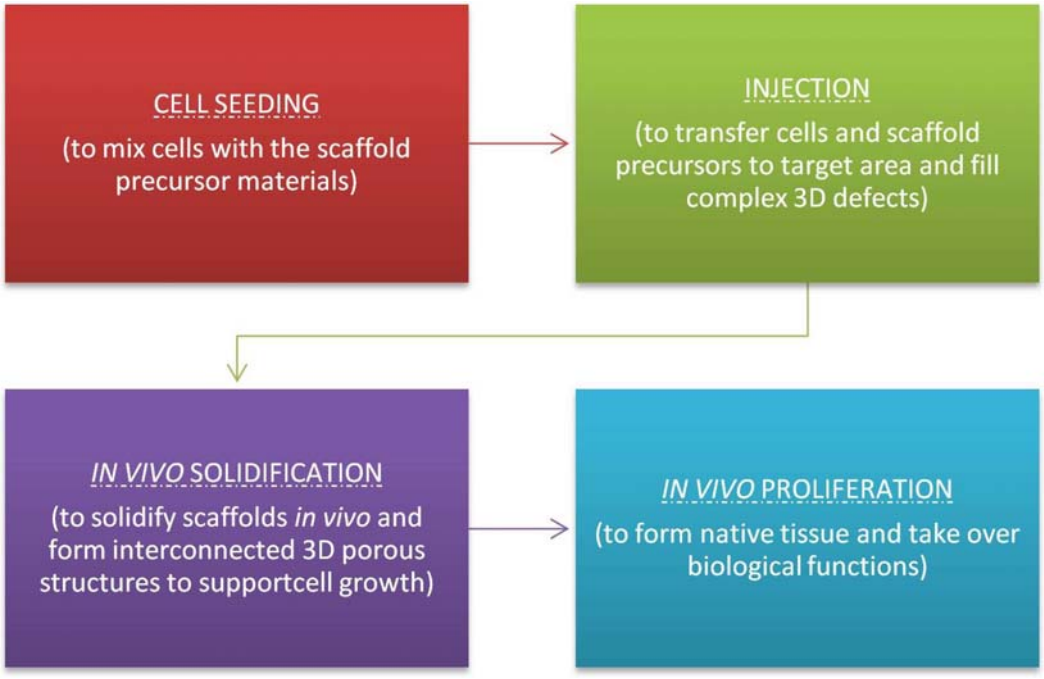

Figure 2-3: A flow chart that illustrates a possible approach of using injectable scaffold to fixed defect.

In contrast to scaffolds for hard tissue engineering (such as bone), scaffolds for soft tissue engineering, such as muscle, cartilage, liver or kidney, often have to fill large volumes but require only moderate mechanical strength. When engineering soft tissues which have specific biomechanical requirements, such as mechanical simulation modulated cell differentiation or increase extracellular matrix synthesis, the mechanical properties of the scaffolds can be crucial to obtain full tissue

function.[47-48] In accordance with the general design principles of scaffolds, the requirements for injectable scaffolds follow the basic design principles as summarised in **Table 2-2**.

Table 2-2: Requirements for injectable scaffolds used in soft tissue engineering[11,14,27]

Requirements	Explanation
Injectability	The porous scaffolds should be injectable through the needle prior to solidification.
Solidification *in vivo*	A mild and safe solidification process is required to avoid damage to the surrounding tissues and while retaining high bioactivity and cell viability.
Pore morphology	*In situ* formed injectable scaffolds should possess a 3D porous structure with a interconnected pore morphology with pore throats between pores in order to support the growth of cells and facilitate the exchange of nutrients and cellular waste. Normally, the diameter of pores should be at least 3 times as big as the cell size.
Biocompatibility	Scaffolds should be nontoxic and have similar hydrophilic surface properties to human living system. The solid constituents of scaffolds should naturally integrate with the host tissue and their degradation products should not demonstrate cytotoxicity or immunogenicity, or elicit an inflammatory response.
Degradation property	During tissue development, the scaffolds should be able to degrade at a rate in accordance with the generation of new tissue. Degradation products should also be biocompatible.
Bioactivity	The scaffold should be bioactive so as to guide and promote proliferation and differentiation of cells. It should retain the bioactivity of growth factors and release them to the target with optimal dosage, timing and in the correct sequence.
Mechanical strength	The scaffolds should possess good dimensional stability in the body after injection and solidification. It should also provide sufficient mechanical strength to withstand biomechanical loading and offer reliable yet temporary support for the growing cell culture. The mechanical parameter of the scaffolds, such as modulus or strength, scaffolds should be similar to native tissues.

2.3 INJECTABLE MATERIALS FOR SOFT TISSUE ENGINEERING

As shown in **Table 2-1**, the modulus of soft tissue (tissue with lower mechanical properties compared to bone or cartilage) range from around 50 Pa to 3.2 MPa. Considering the requirement of mechanical robustness (including elastic behaviour), polymers are better candidates for soft tissues when compared to ceramics or metals. The high stiffness of ceramics or metals may lead to mechanical stimulation[49] or some other problems (such as stress-shielding and subsequent implant loosening[50]) to the surrounding tissue. Polymers used in the preparation of injectable scaffolds for soft tissue can be divided into two categories: synthetic and natural.

2.3.1 SYNTHETIC POLYMERS

The long and successful history of synthetic polymers in regenerative medicine combined with the ability to tailor their properties has attracted much interest for their application as injectable scaffolds for soft tissue engineering. The most widely investigated synthetic biodegradable polymers for soft tissue repair are poly (α-hydroxy esters) such as poly(glycolic acid) (PGA)[51], poly(L-lactic acid) (PLLA)[52], and their copolymers poly(L-lactide-*co*-glycolide) PLGA[53-56]. Also poly(ethylene glycol) (PEG)[57-59], poly(vinyl alcohol) (PVA)[60], poly(propylene fumarate) (PPF)[61-65] and their copolymer such as PLLA-*b*-PEG, PEG-*b*-PPO-*b*-PEG have been used to develop injectable scaffolds through radical polymerisation or crosslinking and

alternatively by self-assembly (**Figure 2-4**). Most of these synthetic polymers are biologically inert, non-immunogenic and able to degrade through hydrolysis into metabolic products.[11] The majority of these materials can be processed in solutions for injection and *in viv*o polymerised or crosslinked at the site of defect. Since surface modification post injection is very difficult, some synthetic polymers selected for the fabrication of preformed scaffolds, such as polystyrene, are seldom used as injectable scaffolds.

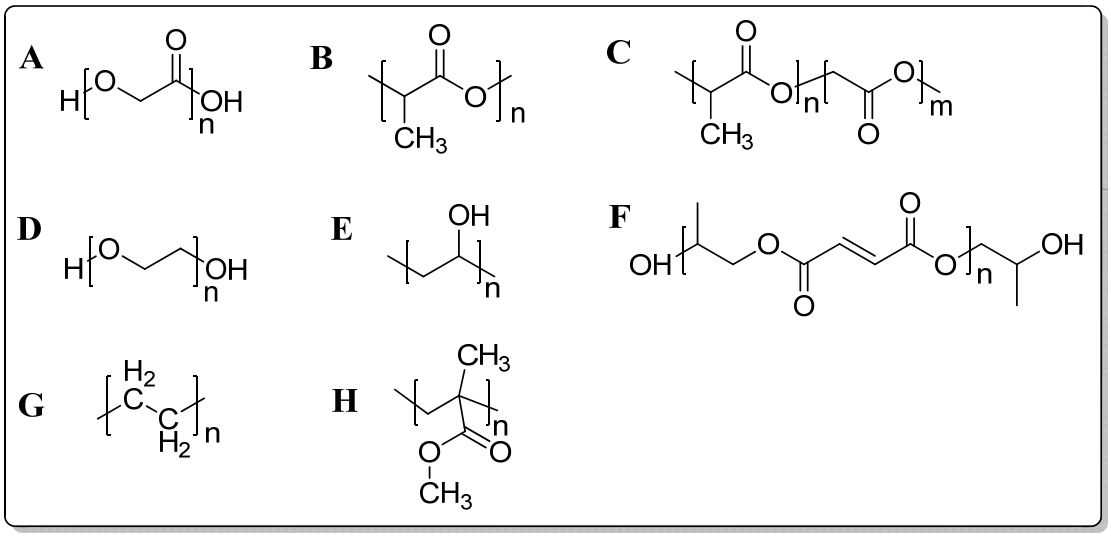

Figure 2-4: Chemical structures of synthetic polymer materials that can be polymerised or crosslinked to create 3D porous scaffolds and used as injectable scaffolds. **A**: PGA; **B**: PLLA; **C**: PLGA; **D**: PEG; **E**: PVA; **F**: PPF; **G**:HDPE; **H**: PMMA.

Perhaps surprisingly, biodegradability is not always required. The biocompatible "non-degradable" synthetic polymers high-density polyethylene (HDPE)[66] and poly(methyl methacrylate) (PMMA)[67] are also used as permanent implants or injectable microspheres/scaffolds for tissue reconstruction. But the limitation is that

these permanent and rigid materials cannot adapt to a growing craniofacial skeleton for instance and should be used with caution in children.[67]

2.3.2 NATURAL POLYMERS

Research focusing on natural polymer as injectable scaffolds most commonly investigates polysaccharides such as chitosan[68-69], dextran[70-74], pullulan[75], agarose[76] alginate[77-78] and cellulose[11]; polysaccharides with additional functionqal groups such as glycosaminoglycans (e.g. hyaluronic acid[79]); and poly(α-amino acid)s (polypeptides) such as fibrin[80-81] and gelatin[82-83]. These natural polymers may present a more natural biological environment to the cells, since they usually contain domains that can provide important receptor sites to guide cells at various stages during their growth. Most of these natural polymers are highly hydrophilic, and therefore better tolerated by the human body than synthetic polymers. By functionalising natural polymers with polymerisable groups they can be radical polymerised/crosslinked and form highly porous hydrogels. Some of these natural materials, such as chitosan[84] or alginate[85], are also stimuli-responsive and such that they can be crosslinked and thereby form hydrogels triggered through environment signals such as temperature and Ca^{2+} concentration.

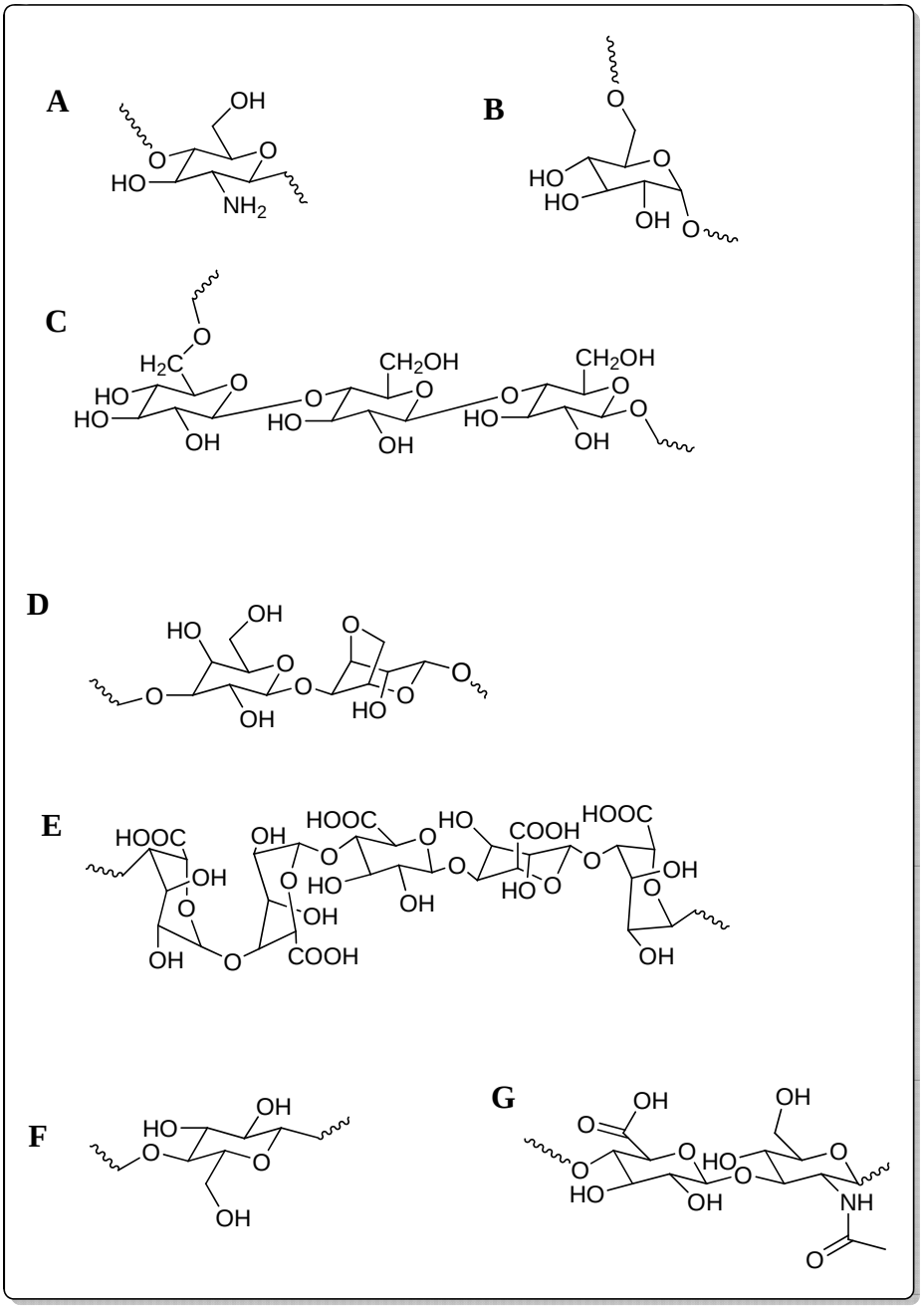

Figure 2-5: Chemical structures of natural polymers that have been used to prepare injectable scaffolds. **A**: chitosan; **B**: dextran; **C**: pullulan; **D**: agarose; **E**: alginate; **F**: cellulose; **G**: hyaluronic acid.

2.4 SOLIDIFICATION METHODS USED TO SYNTHESISE INJECTABLE SCAFFOLDS

The solidification of injectable scaffolds normally means solidifying the constituent precursors or monomers into an interconnected 3D scaffold in the presence of living cells within a limited time period.[11] During the solidification of the precursors of biomaterials should be a very mild process and proceed close to physiological conditions to retain high cell viability as well as to avoid damage to the surrounding native tissues. The temperature and the pH of the scaffold should be close to 37˚C and pH 7.4 during solidification and should not be significantly changed. After solidification, a scaffold with an existing interconnected porous structure should have been formed. Currently the reported solidification methods of injectable scaffolds for soft tissue engineering mainly include thermo-initiated radical polymerisation[14,61-64,86-88], photo-initiated polymerisation[89-93], thermo-gelation[80-81,83-84,94-96] and ionic crosslinking[14,97].

2.4.1 IN VIVO RADICAL CROSSLINKING

A series of synthetic polymers, such as PPF[61-64,86], oligo(polyethylene glycol) fumarate (OPF)[87] or poly(propylene fumarate-*co*-ethylene glycol) (P(PF-*co*-EG))[88] can be solidified by free radical crosslinking by thermally initiated or redox initiation free. This initiation polymerisation/crosslinking system can be triggered simply by a temperature change. The time it takes to solidify must be as short as possible in order

to avoid tissue necrosis around the injected material. Some cytocompatible initiators, such as ammonium persulfate/*N*,*N*,*N*',*N*'-tetramethylethylenediamine (APS/TEMED), produce radicals in aqueous environments at 37˚C[14], which provides the possibility of radical polymerisation of monomers with unsaturated bonds *in vivo*.

Controlled by the presence of light, photo-initiated polymerisations can provide more precise control of the initiation process compared to other initiation methods, such as thermo-initiated free radical or redox initiation.[89] Photo-crosslinkable polymers reported as injectable scaffolds include PPF[93], PEG[90], PVA[91] and their copolymers and phosphoester-derived polymers[92]. The concentration of photo-initiator, the wavelength and intensity of light can be used to control the polymerisation time.[89]

Crosslinking can be used to adjust the mechanical properties of the scaffolds to obtain the desirable stiffness for different soft tissues. Radically crosslinkable materials are often used in the form of hydrogels or microparticles in order to fabricate 3D porous structure and retain their injectability at the same time.

2.4.2NON-COVALENT STIMULUS-RESPONSIVE SOLIDIFICATION OF INJECTABLE SCAFFOLDS

Many polymers, both synthetic and natural, exhibit environmentally responsive behaviour. They undergo drastic conformational changes upon experiencing a trigger, e.g. pH, ion concentration or temperature.[98-99] This conformational change occurs within a narrow range around a certain critical point (e.g. a narrow temperature or pH range, or the presence of ions). Stimuli-responsive polymers are also referred as "smart" materials, in some cases mimicking basic functions of biological systems. They are successfully applied in a broad-range of soft matter applications, specific examples being outside the area of injectable scaffolds[11], drug release systems[100], microfluidic devices[101] and actuators[102]. Stimulus-responsive polymers can be prepared by employing environmentally available stimuli as automatic triggers for scaffold formation by utilizing the human physiology (e.g. body temperature or ions in body fluids) chemical signals *in vivo*. As the chemistry for solidification is non-covalent in nature, it is not only much milder than the use of covalent strategies such as radical polymerisation but also no additional chemicals such as initiators or crosslinkers are required either.

2.4.4.1 Thermo-responsive Solidification of Injectable Scaffolds

Triggered by a change in temperature, some polymer solutions undergo gelation and form hydrogels in an aqueous environment. Both natural (such as chitosan[84],

gelation[83] and fibrin[80-81]) and synthetic (such as PEG, PLGA, polyNIPAAm and its copolymers[94]) thermo-gelling polymer systems have been developed and tested for soft tissue engineering.

Among the thermo-reversible polymers, copolymers of NIPAAm (**Figure 2-6)** are most widely used because as its lower critical solution temperature (LCST) leads to solidification at around 32°C (near body temperature) in aqueous solution.[103-104] The LCST is the temperature at which thermo-reversible polymers undergo a solution-to-gelation transition when heated across this temperature. Below LCST, polyNIPAAm is able to absorb water and exists as isolated, flexible extended coils in aqueous solution; when the temperature is raised above LCST, the polymer reconstructs with abrupt sudden decrease in volume and become hydrophobic (**Figure 2-7**). This temperature dependent solubility change is due to the enthalpic contribution of water hydrogen-bonded to the polymer chain is overtaken by the entropic gain of the system as a whole and consequently, hydrogen bonding between water and polyNIPAAm is disrupted thereby leading to an increase in entropy as the driving force behind such a transition.[98-99] The conformationally amphiphilic polyNIPAAm chains hide their hydrophilic amide groups and expose the hydrophobic isopropyl groups in the compact globule conformation.[105]

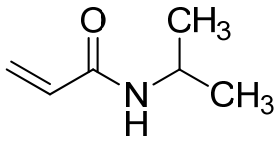

Figure 2-6: *N*-isopropylacrylamide

The LCST of polyNIPAAm (and other polymers showing a LCST) can be tuned to a certain extent (about 20°C to more than 100°C[106]) by making polyNIPAAm copolymers and thereby changing the composition of functional groups. The LCST of polyNIPAAm copolymers can be raised by copolymerizing NIPAAm with hydrophilic monomers (e.g. sulfonic acid-containing polyNIPAAm copolymers have LCST more than 100°C[106]) and can be reduced by introducing hydrophobic (e.g. after copolymerised with *p*-acrylamido-benzoic acid, its LCST could be lowered to 25°C[106]).[98] Once the gels are formed, the gelation is still thermo-reversible.[11] Thermo-reversible hydrogels derived from polyNIPAAm copolymers, such as poly(NIPAAm-*co*-AA)[95], poly(chitosan-*g*-NIPAAm) copolymer[107] and poly(NIPAAm-*co*-poly(ethyleneglycol) dimethacrylate)[96], are frequently reported as injectable scaffolds or drug-carrier matrices.

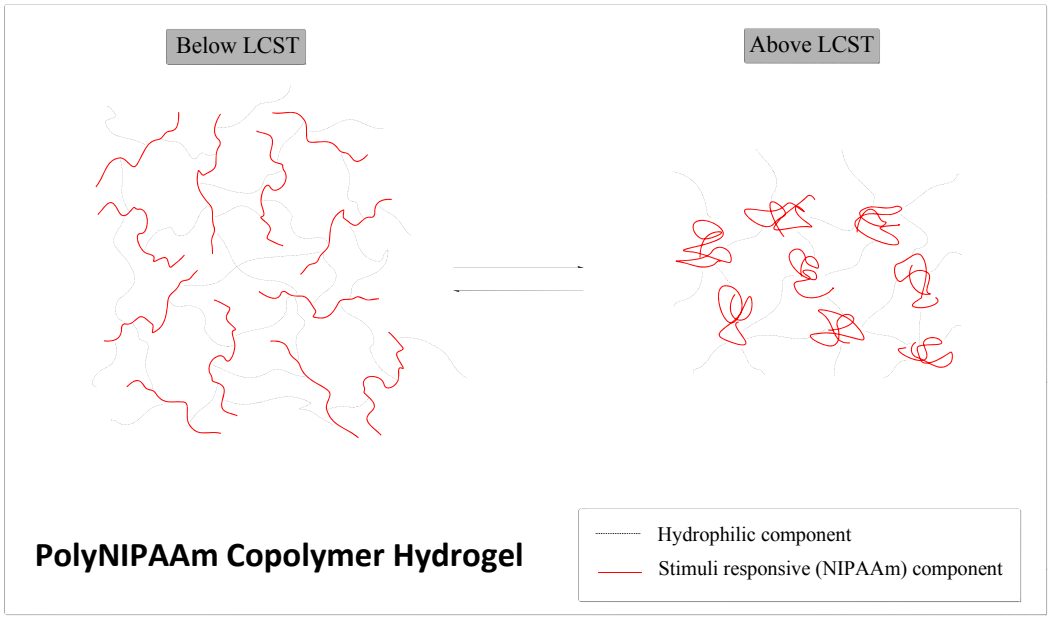

Figure 2-7: Simplified illustration of the structural changes of a polyNIPAAm copolymer hydrogel at temperatures below and above its LCST.

2.4.4.2 Ion-responsive Solidification of Injectable Scaffolds

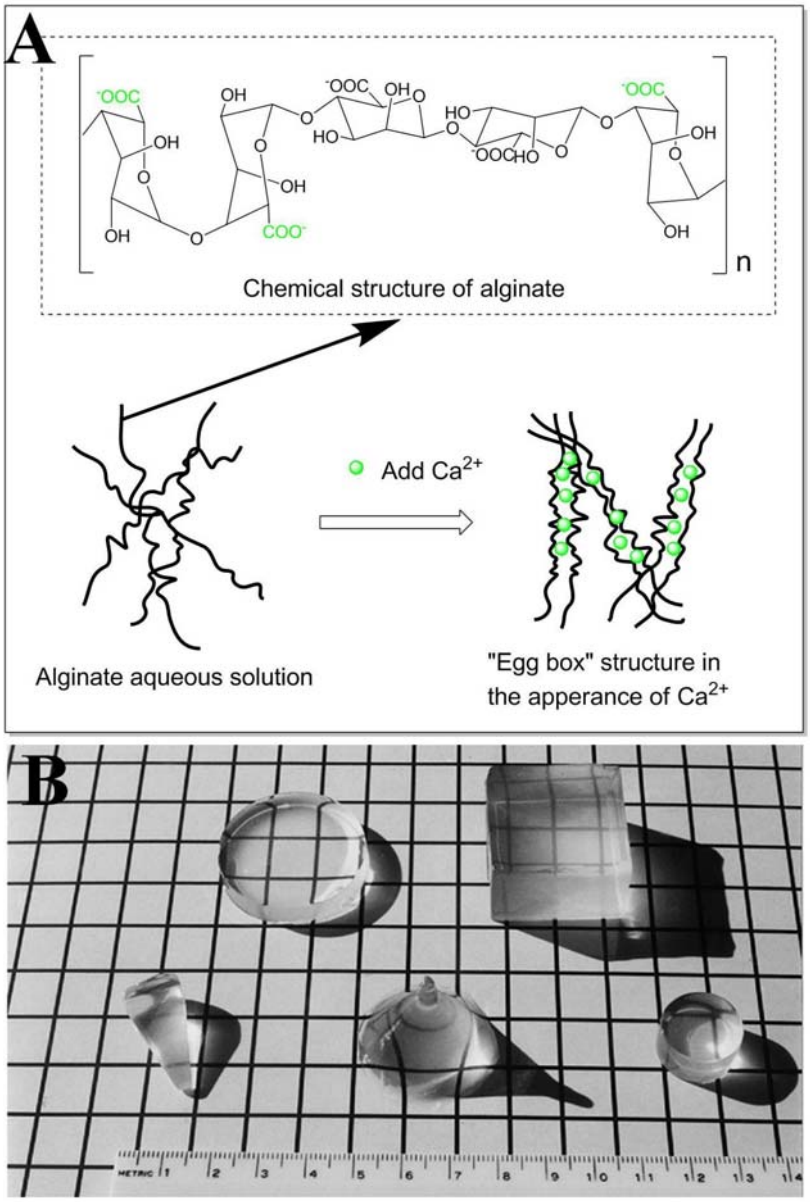

Figure 2-8: Gelation of alginate aqueous solution by addition of calcium ions and formation of "egg box" structure. **A**: a schematic diagram of the gelation progress; **B**: Ca^{2+}-crosslinked alginate gels of various molded shapes (adapted from Kuo, C. & Ma, P. *Biomaterials* **22**, 511-521, (2001).).

Ion-responsive hydrogels can utilise the presence of ions as trigger for gelation. In the presence of divalent or trivalent cations, aqueous solution of polysaccharides, such as

alginate, crosslink and form gels.[97] Ubiquitous divalent ions, such as Ca^{2+}, are typically used as the trigger for gelation.[97] By controlling parameters, such as the concentration and molecular weight of the polysaccharide, type and concentration of cations, it has been shown that hydrogels with desirable mechanical properties and injectability can be formed.[14,97]

Alginate is a particularly attractive naturally derived ion-responsive polysaccharide and has been studied widely for its biocompatibility, biodegradability and reversible aqueous gelation chemistry with di- or trivalent cations (**Figure 2-8**).[85,108-109] Applications include adsorbents for removal of heavy metals from contaminated environments[110-112], scaffolds for tissue engineering[113-115], wound dressings[116-117] and as delivery vehicles for drugs[118-119]. Alginate is a block copolymer composed of (1-4)-linked β-D-mannuronic acid (M units) and α-L-guluronic acid (G units). Divalent cations such as Ca^{2+} ions cooperatively bind between the G-units of adjacent alginate chains, creating ionic interchain links which cause gelling of aqueous alginate solutions.[120-121] The typical level of Ca^{2+} concentration in the human body is 1.8 mM[122-123], the Ca^{2+} concentration in a human knee joint however is equivalent to 4.0 mM $CaCl_2$[124], so that the Ca^{2+} needed for gelation could be supplied directly by the human body. Thus the Ca^{2+}-induced gelling of alginate under very mild aqueous conditions makes alginate a very attractive stimuli-responsive material for use *in vivo*.

2.4.2 PARTICLES METHOD

Different from the two solidification methods described above, when using particles to prepare injectable scaffolds, the crosslinking of the matrix and the fabrication of the porous structure are usually triggered before injection. After cell seeding and *in vitro* cell growth, the particles having particle sizes between 100 μm and 200 μm, usually prepared from PLGA[125-127] , PLA[128-129] or PPF[65], were injected into the body together with the entrapped cells and aggregate at the site of the defect (**Figure 2-9**).[125] In order to improve the *in vivo* mechanical performance and durability of these particles and to keep them highly cohesive at the injection site, a "biocompatible adhesive", such as fibrin[130], polycarbonate (PCL) [131], poly(lactide-*co*-glycolide)(PLG)[65] or PVA[126], were used as bonding agents to glue these particles together and to form a continuous scaffold *in vivo*. Currently the development of injectable microspheres is moving from using solid particles[128,132-133] to open porous particles[129,134-135]. Compared with solid particles, microparticles with an open porous structure are able to carry cells and provide much more suitable physical support for cell proliferation. These open porous spheres are usually prepared by emulsion-solvent evaporation[129], double emulsion templating[135], and grafting–coating method[134].

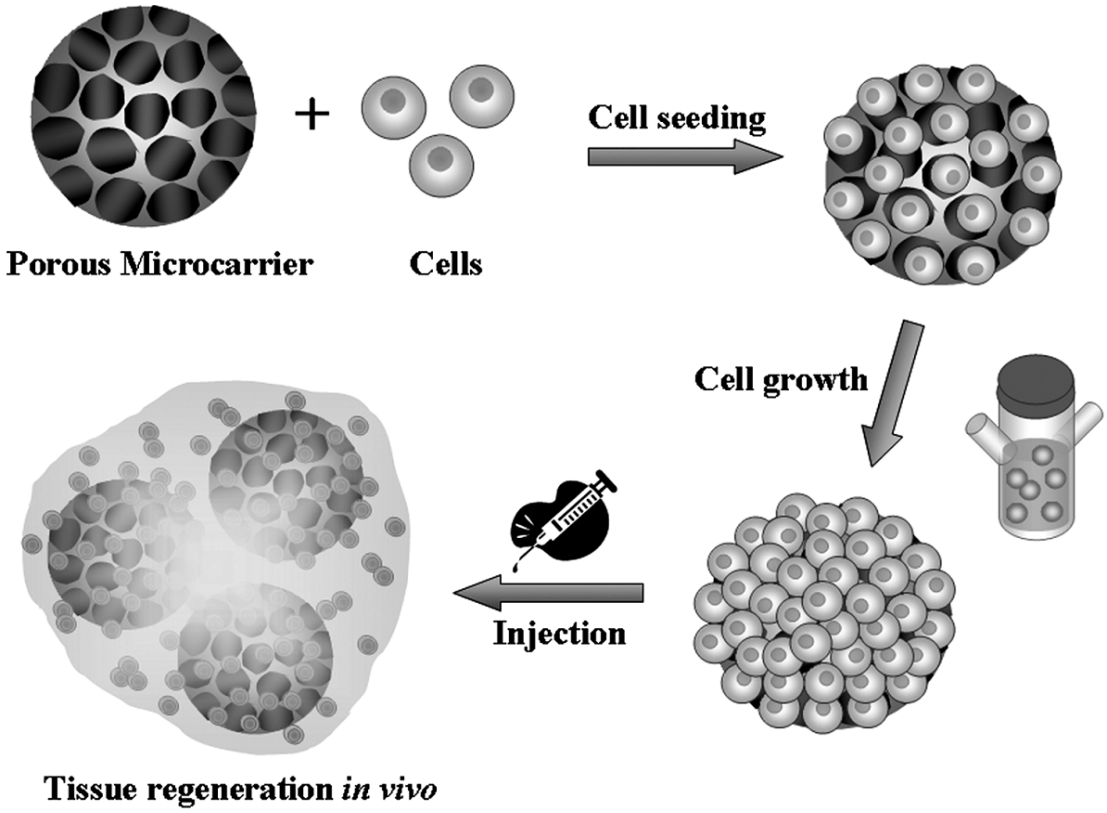

Figure 2-9: A schematic diagram of biodegradable porous microcarriers for injectable cell therapy. Porous microcarriers are seeded with cells, expanded *in vitro* in a bioreactor and injected into the patients' body at the site of the defect. (reproduced from Chung, H. J., Kim, I. K., Kim, T. G. & Park, T. G. *Tissue Eng. Part A* 14, 607-615, (2008).)

2.5 METHODS FOR THE FABRICATION OF POROUS MATERIALS

According to the classification made by IUPAC (International Union of Pure and Applied Chemistry)[136], porous materials can be categorized according to their pore sizes: (a) nanoporous materials (pore sizes < 2 nm); (b) mesoporous material (2 nm < pore sizes < 50 nm); (c) macroporous materials (pore sizes > 50 nm). The diameter of cells ranges from 1 μm (nerve cells) to 100 μm (human eggs) and the minimum

average pore size of scaffolds for tissue engineering should be larger than the cell diameter[137], which means only macroporous materials can be used for tissue engineering scaffolds.

Also the *in vivo* formed macroporous scaffolds should not only possess pores large enough to accommodate cells, but also have interconnections which allow nutrient and waste diffusion making porosity, pore size and the dimensions of the pore interconnects the most important parameters of a porous network.

Considering the fact that a hydrophilic surface provides usually better cell adhesion[4], hydrogels are the most interested scaffolds for soft tissue engineering and a large proportion of research into scaffold fabrication focuses on to the creation and tailoring of 3D interconnected porous structures of hydrogels. Hydrogels are crosslinked polymer networks that swell, but do not dissolve in water. Normally the hydrophilic functional groups in the polymeric backbone give hydrogels the ability to absorb water, with the chemical crosslinks defining the dimensions of the hydrogel and the level to which it can shrink and swell in water. Usually hydrogel precursors are mixed with cells *in vitro* and then the mixture is injected and gelled *in situ* triggered by a physical (such as temperature[84], ion-concentration[138] or UV irradiation[139]) or chemical (such as initiator[140]) trigger to form a 3D scaffold *in vivo*.

A variety of methods exists to prepare injectable macroporous hydrogels for soft tissue engineering. These can be classified into "non-porous structure controlled"

polymerisation/crosslinking, gas forming, leaching, prototyping, fibre architectures and HIPE templating, which will be introduced in the following sections (**Section 2.5.1-2.5.5**).

2.5.1 LEACHING METHODS TO FABRICATE POROUS STRUCTURES

The process of porogen leaching is one of the most common techniques used to fabricate scaffolds, especially preformed scaffolds.[28,31] Briefly, salt, sugar, polymers (such as chitosan) or paraffin[141] are first ground into small particles and these porogens of a desired size are transferred into a mould. A biodegradable polymer dissolved in a volatile solvent is then cast into the porogen-filled mould. After the evaporation of the solvent, the porogens are leached away by solvent to form the pores of the scaffold (**Figure 2-10**). The porosity of scaffold fabricated with this technique can be even higher than 95%[141]. Having to use solvents for the removal of the porogens is the drawbacks of the leaching method and limits its applications as injectable scaffolds fabrication.

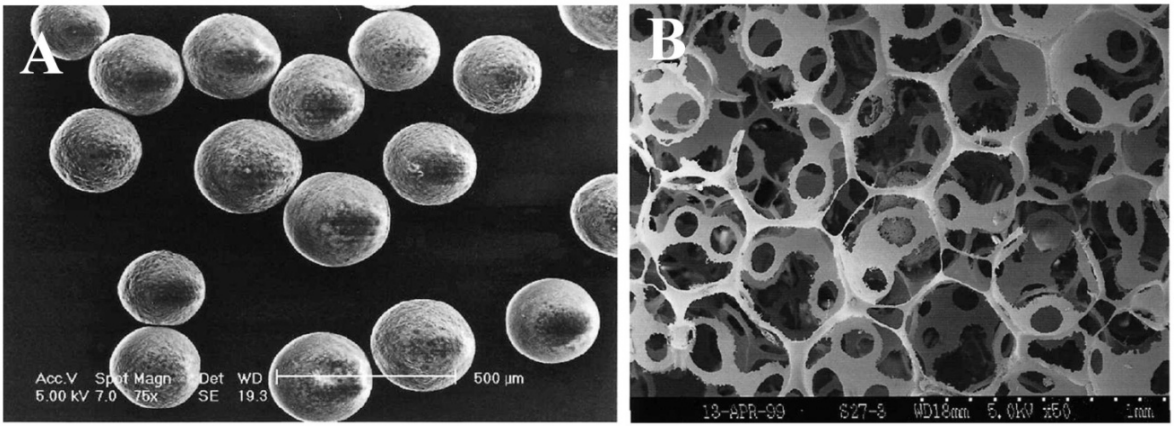

Figure 2-10: SEM micrographs of **A**: paraffin particles used as porogen; **B**: PLGA foams prepared by leaching of paraffin spheres. (reproduced from Ma, P. X. & Choi, J.-W. *Tissue Eng.* 7, 23-33, (2001).)

2.5.2 "NON-POROUS-STRUCTURE CONTROLLED" POLYMERISATION/CROSSLINKING

One of the simplest ways to prepare a hydrophilic scaffold is to polymerise or crosslink water soluble monomers/precursors in an aqueous environment to form a hydrogel. When no special porous fabrication methods (e.g. leaching, freeze drying) are applied during the solidification of the scaffolds, the porous fabrication methods could be classified to "non-porous-structure controlled" polymerisation/crosslinking. As the high degree of swelling ensures hydrogels to possess relatively large pores when swollen hydrogels are the most frequently investigated scaffolds employing this fabrication method. Both natural polymers (such as crosslinked dextran[84], fibrin[138] and collagens[84]) and synthetic copolymers (such as PEG-PLGA copolymer[142] and PPF-PEG copolymer[143]) have produced such hydrogel.[144] Because of the poor ability to create and turn 3D interconnected porous structure, these hydrogels were only for

the study of cytoxicity or biodegradability of the material, but not as scaffold for cell proliferation.

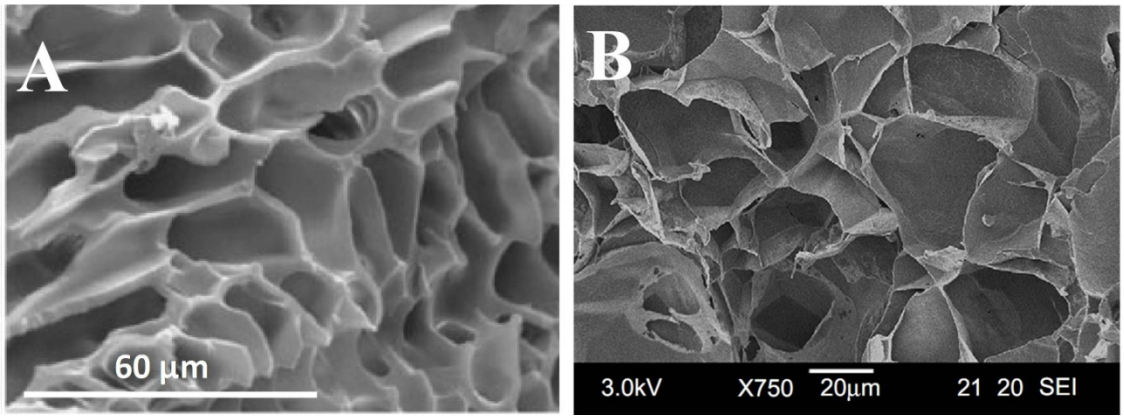

Figure 2-11: Morphologies of different injectable hydrogels fabricated though "non-porous-structure controlled" polymerisation/crosslinking: **A**: *N*-palmitoyl chitosan based pH-responsive hydrogel (reproduced from Chen, J. & Cheng, T. *Macromol. Biosci.* 6, 1026-1039 (2006).) **B**: thermo-responsive polyNIPAAm based hydrogel (reproduced from Chiu, Y.-L. *et al. Biomaterials* 30, 4877-4888 (2009).)

Hydrogels used in regenerative medicine may also be formed by using the junctions or tie points that cause gel formation as stimuli-responsive non-covalent crosslinks (e.g. crosslinks formed though physical entanglements, microcrystallites, ion-bonds, or hydrogen-bonded structures)[145] similar in behaviour to those formed with covalent crosslinks.[2] Compared with covalently crosslinked hydrogels, "non-porous structure controlled" stimulus-responsive crosslinking methods are more practical for the preparation of injectable scaffolds (**Figure 2-11**). Its relatively mild solidification chemistry would allow cell encapsulation in the hydrogel prior to the formation of a porous structure.

2.5.3 GAS FOAMING METHODS TO FABRICATE POROUS STRUCTURES

Gas foaming is a method using a gas as a porogen to prepare porous materials. Gases could be obtained either from physical or chemical blowing agents or produced during the polymerisation/crosslinking of monomers/pre-polymer. A polyurethane based injectable scaffold system is selected as an example and showed in **Figure 2-12**. A highly porous structure, either closed or open cell, can be produced by trapped gas bubbles (usually CO_2 gas[146]). This method avoids the use of organic solvents or high temperatures. It is also possible to control the porosity and pore structure of the resulting foams.[147] On the other hand, some types of gas produced during foaming are potentially harmful to human and should not be injected into human body together with the matrix. The volume change during foaming and *in vivo* solidification (**Figure 2-12 A**) also limits the application of gas foaming in scaffold preparation, especially for the preparation of injectable hydrogels.

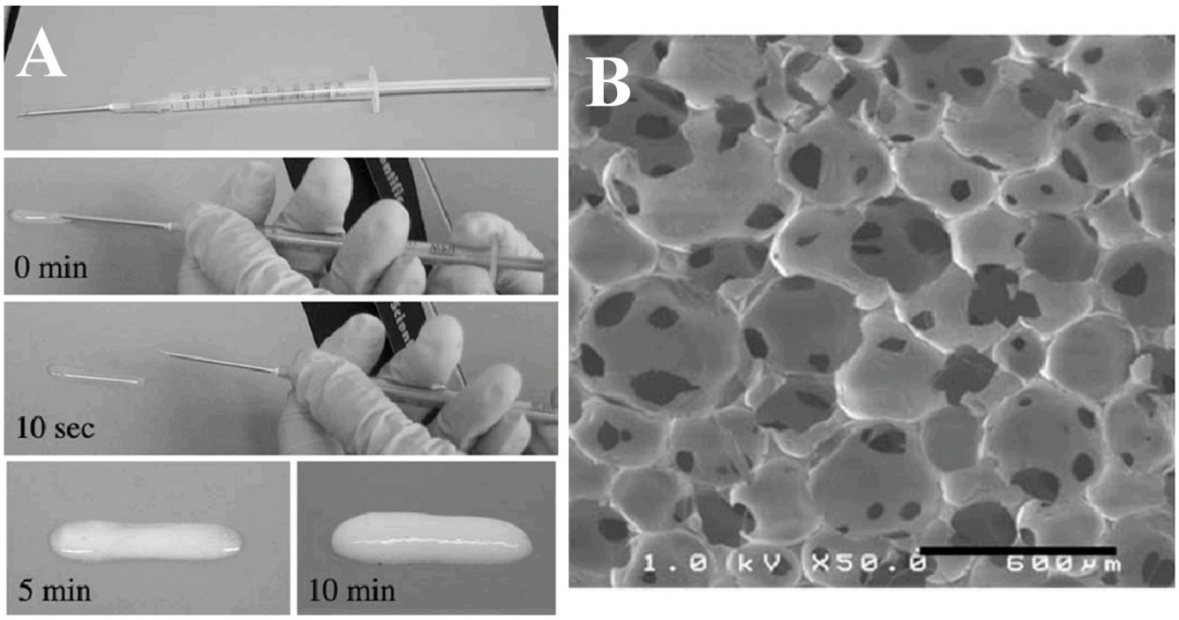

Figure 2-12: Injection of a gas formed polyurethane scaffold: **A**: A series of time-lapse photographs showing the injection of a reactive liquid system; **B**: SEM image of the polyurethane foam. (reproduced from Hafeman, A. *et al. Pharm. Res.* **25**, 2387-2399 (2008).)

2.5.4 Rapid Prototyping Methods to Fabricate Porous Structures

By combing computer aided design and advanced polymer manufacturing, rapid prototyping enables scaffolds to be fabricated with precise control over micro- and macrostructure (**Figure 2-13**). The main advantage of rapid prototyping is the ability to produce complex 3D scaffolds with pore size ranges from 10 μm to 1000 μm[148] from a computer model rapidly by joining liquids, powders and sheet materials. Rapid prototyping offers the potential to precisely control the pore morphology and overall shape of the scaffold to match the anatomical defect site.[4,46] However the required processing conditions of rapid prototyping, such as machines used for selective laser

sintering and 3D printing, makes it unsuitable for the preparation of injectable scaffolds.[148]

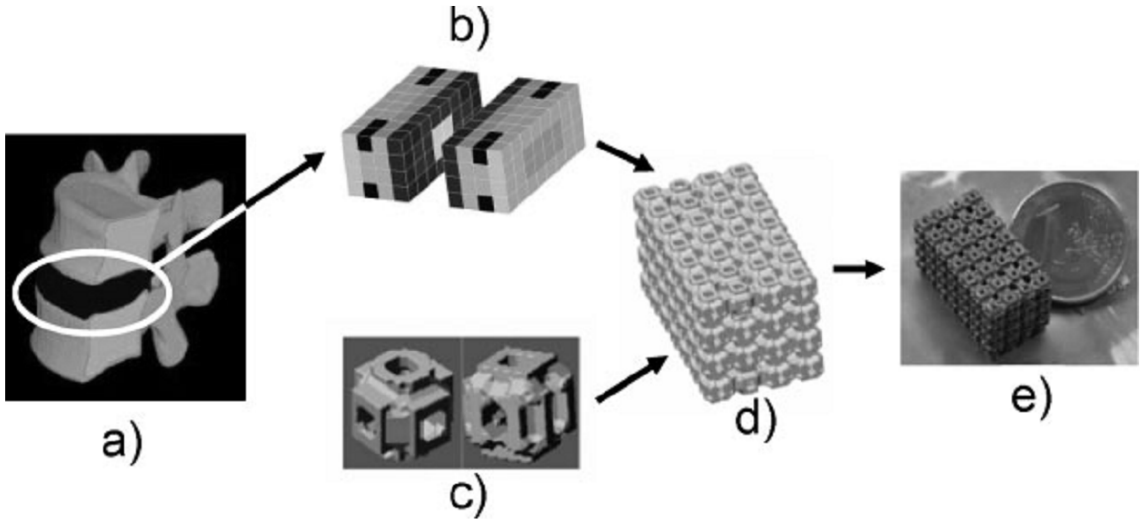

Figure 2-13: Example of using a rapid prototyping technique to fabricate both the exterior shape and dimension of a scaffold shape and an internal 3D porous structure. **a**) A global design domain is created according to the shape of the defect (white circle). **b**) A global view of material distribution within the design domain. **c**) A basic unit used to create porous microstructures. **d**) & **e**) Final scaffold. (Reproduced from Scott, J. H. *Adv. Mater.* 21, 3330-3342 (2009).)

2.5.5 FIBRE ARCHITECTURE METHODS TO FABRICATE POROUS STRUCTURES

Fibres, the basic materials unit of textile and fabrics, are usually produced by spinning technologies (such as electro spinning, melt spinning and solution spinning). Fibres can be used to create porous scaffolds with pore size more than 60 μm from a number of natural and synthetic polymers.[149-153] Fibre-based structures allow for a wide range of morphologies and geometric structures, from textile to fibrous, to be created. These

structures can be tailored for specific tissue engineering applications (**Figure 2-14**). For example, many tissues, such as nerve, muscle, have tubular or fibrous bundle architectures and anisotropic properties.[149] The assembled fibre usually possesses a highly porous interconnected pore structures and good mechanical strength (elastic modulus up to 100 MPa[154]).

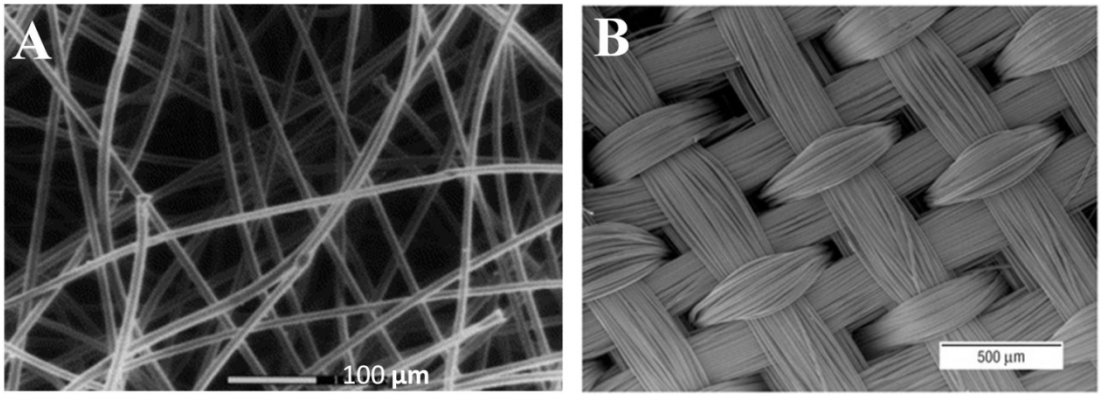

Figure 2-14: Scanning electron micrograph of fibrous scaffolds **A**: Poly(glycolic acid) (PGA) nonwoven scaffold (reproduced from (Ma, P. X. *Materials Today* 7, 30-40 (2004).); **B**: PGA anisotropic woven fibrous scaffold (reproduced from Moutos, F. T., Freed, L. E. & Guilak, F. *Nat Mater* 6, 162-167 (2007).).

2.5.6 HIGH INTERNAL PHASE EMULSION TEMPLATING METHODS TO FABRICATE POROUS STRUCTURES

High internal phase emulsion (HIPE) templating is a method to produce porous materials with interconnected pore structures.[15] The pore size/pore throat size of the HIPE templated materials can be turned by changing the emulsifier concentrations, dispersion speed or ripening time during HIPE preparation.[155-156] In this research, high internal phase emulsion templating is the method that being explored and exploited to

fabricate the porous structure of injectable scaffolds for soft tissue engineering and will be detailed introduced in the following paragraphs.

An emulsion is a mixture of two immiscible liquids. One liquid, the dispersed phase, is dispersed in the other, the continuous phase, in the form of droplets. Usually, at least one of these two phases is water or an aqueous solution. If the organic phase of the emulsion consists of monomers (o/w or water-in-oil (w/o) emulsions), it can be polymerised in three ways to obtain different products: colloidal particles, poly(high internal phase emulsion) (polyHIPE) materials and polymer composites (**Figure 2-15**).

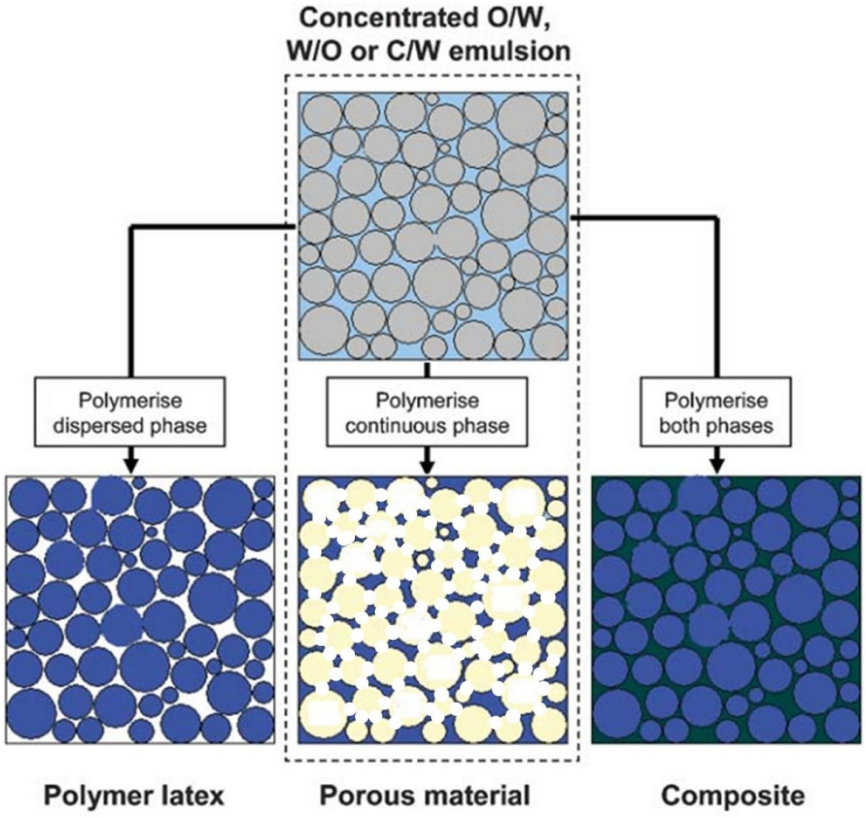

Figure 2-15: Schematic representation of polymerisation of the dispersed phase, continuous phase, or both phases simultaneously in an emulsion for the preparation of colloids, porous materials and composites. (Reproduced from Zhang, H. & Cooper, A. I. *Soft Matter* **1**, 107 (2005).)

When only the monomers in the dispersed phase are polymerised, colloidal particles will be obtained; when the polymerisation is initiated in the dispersed phase and the internal phase is removed afterwards, polyHIPE materials will be obtained and if both phases of emulsion contain the monomers are polymerised, polymer composites will be produced.

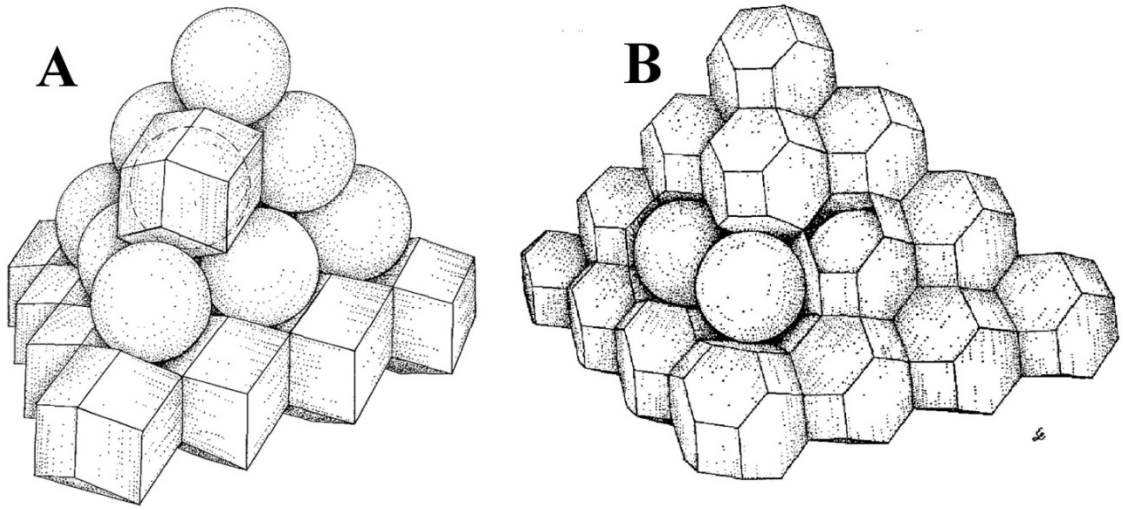

Figure 2-16: Two droplet packing and ordering systems in HIPEs: **A**: Rhomboidal dodecahedral packing (usually occurring in emulsions containing 74% to approximately 94% internal phase ratio); **B**: Tetrakaidecahedral packing (usually occurring in emulsions with an internal phase above 94%) (reproduced from Lissant, K. J. The geometry of high-internal-phase-emulsion ratios. *J. Colloid Interface Sci.* 22, 462-468 (1966).)

The defining feature of a HIPE is its internal phase volume defined as being greater than 74%, which corresponds to the maximum packing fraction (rhomboidal dodecahedral packing and tetrakaidecahedral packing, **Figure 2-16**) of mono-dispersed droplets.[15,157] When the internal phase ratio of the emulsion exceeds 74%, either the droplets have to be flattened or the emulsion must be become polydisperse.[158] If monomers in the continuous phase of a HIPE are polymerised, the

emulsion droplets are embedded in the remaining material and the is porous matrix characterised by a final high porosity in the range 70% to 90% produced after removing the internal phase (usually through solvent drying or extraction).[15] A polyHIPE preparation method is shown in **Figure 2-17**. PolyHIPE materials have a interconnected porous structure. Prior to the polymerisation of HIPEs, the emulsion droplets are separated by a very thin monomer film and normally the thickness of these films is inverse to the surfactant concentration. Then after curing the continuous phase and removing the dispersed phase, a polyHIPE with interconnecting pore throats (windows) may be formed induced due to mechanical action exerted during the post-synthesis processing of the porous polyHIPE monolith. The mechanical action leads to the rupture of the thinnest sections of the polymer film, which are those covering the faces between the closest neighbouring droplets.[159] The pore diameter of a polyHIPE is usually determined by the droplet diameter of HIPEs. Increased emulsion stability usually accompanied by a smaller interfacial tension will lead to smaller droplets, which means that the pore size of a polyHIPE can be enlarged by lowering the emulsion stability, such as changing the concentration or type of surfactant[160], or adding specific solvents into the emulsion to promote Ostwald ripening.[161] The average void diameter in a polyHIPE material can vary from around 1 μm to more than 100 μm.[15]

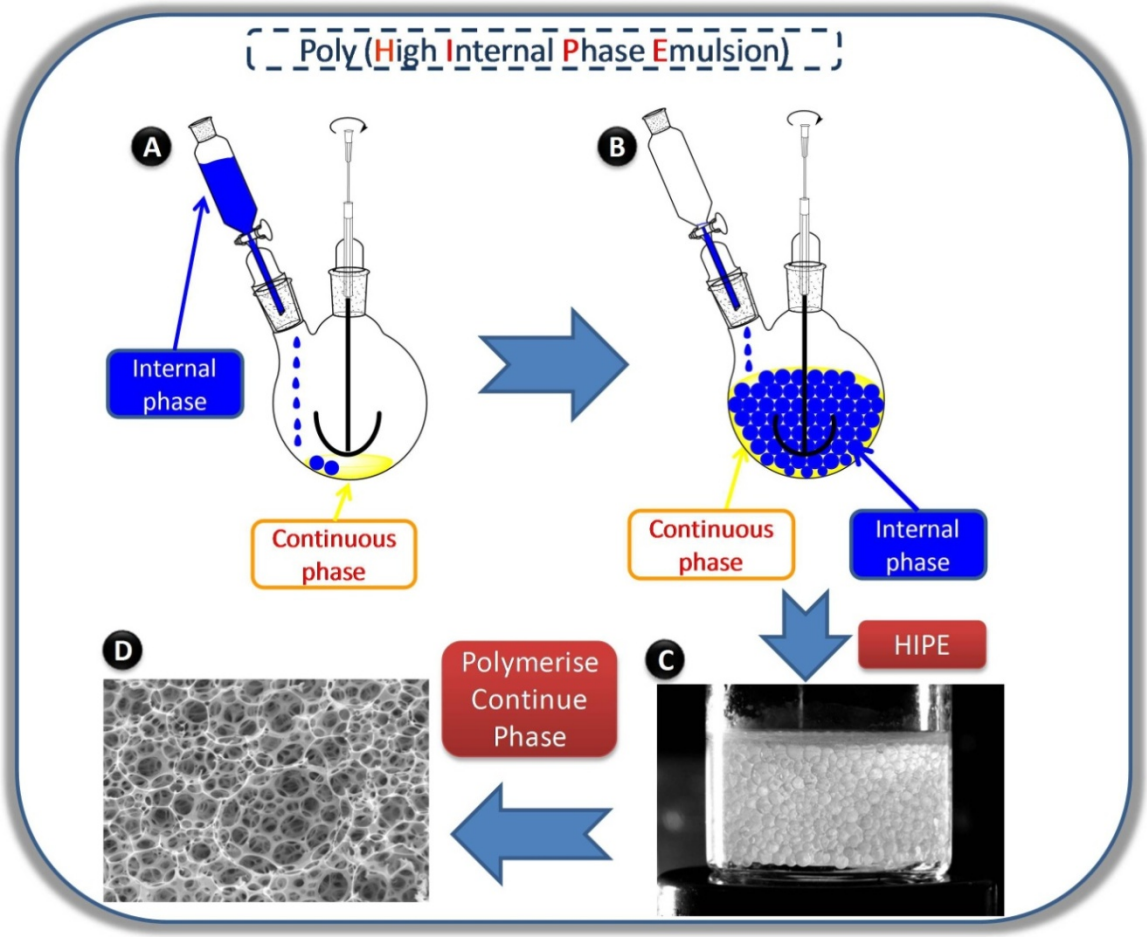

Figure 2-17: Schematic diagram of a polyHIPE preparation method: **A**: dropwise addition of the dispersed phase into the continuous phase (usually containing polymerisable monomers and surfactants) under stirring; **B**: the dispersed phase volume ratio is increased to 0.74 or greater; **C**: a HIPE is obtained after the addition of the disperse phase; **D**: a polyHIPE material is obtained after polymerisation of the monomer in the continuous phase of the HIPE.

HIPEs can be divided into four categories: w/o HIPE, o/w HIPE, oil-in-oil (o/o) and CO_2-in-water (c/w) HIPE. Except for the o/o HIPE (such as petroleum ether in dimethyl sulfoxide HIPE[15]), the other three types were reported as templates for the fabrication of porous scaffolds for tissue engineering (**Table 2-3**).[40,155,162] the preparation of c/w HIPEs usually requires specialised and therefore expensive equipment and very harsh preparation conditions (usually refers to high pressure)[162-

[164]. w/o and o/w HIPEs are those which have been most widely studied. The interconnected porous structure of polyHIPEs meets the pore morphology requirements for scaffolds for tissue engineering. Based on the pore morphology control methods described above, it is possible to prepare polyHIPE materials with pore sizes in the range from 20 μm to 80 μm. The pores of these polyHIPEs are interconnected and suitable for cell seeding.

Table 2-3: Three different types of HIPEs used for porous scaffolds fabrication for tissue engineering

	w/o HIPE	o/w HIPE	c/w HIPE
Continuous Phase	hydrophobic monomers:	hydrophilic monomers:	hydrophilic monomers:
Constituent of the Solid Foam	styrene, divinylbenzene, propylene fumarate	acrylic acid, dextran, pullulan, alginate	acrylamide, dextran,
Dispersed Phase	Water	organic solvent	supercritical CO_2
Phase Order	water-in-oil	oil-in-water	supercritical CO_2-in-water

2.5.5.1 W/O HIPEs for the Fabrication of Interconnected Porous Structure

One of the most widely investigated systems of polyHIPEs prepared from w/o HIPE templates is the styrene system crosslinked using divinylbenzene (DVB) (**Figure 2-18 A**). Styrene is a water-immiscible liquid monomer, which is used as the continuous phase of the HIPE. In the presence of a suitable emulsifier, usually a non-ionic

surfactants such as Span 80[165] or particles such as titania nanoparticles[166], water is slowly added into styrene and emulsified yielding w/o HIPEs. The internal phase (water) is usually removed after the dispersed phase is completely solidified. If these polystyrene based polyHIPEs were coated with aqueous solutions of for example poly-D-lysine and laminin, their biocompatibility has been dramatically improved providing a better surface suitable for the attachment of cells.[167]

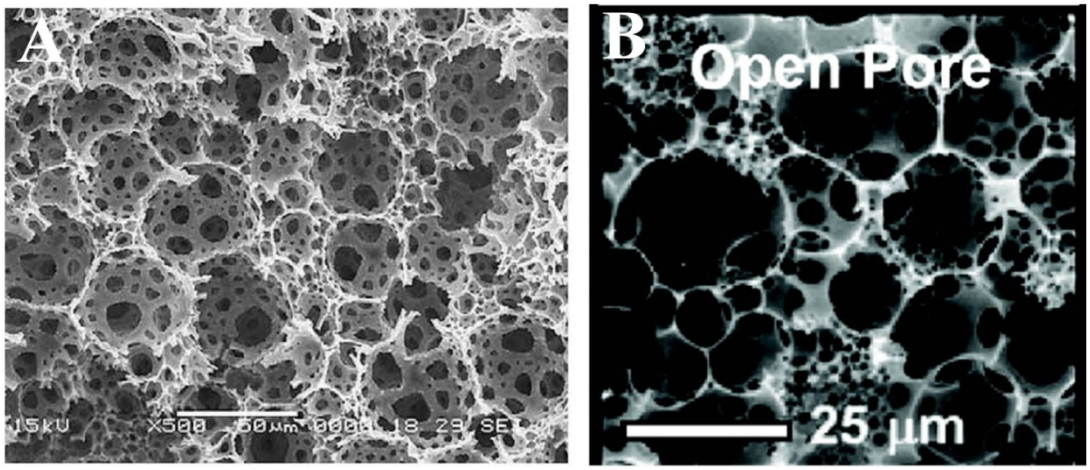

Figure 2-18: Two types of w/o polyHIPEs: **A**: PS-DVB based polyHIPE (reproduced from Zhang, S., Chen, J. & Perchyonok, V. T. *Polymer* 50, 1723-1731 (2009).) **B**: PPF based polyHIPE (reproduced from Christenson, E. M., Soofi, W., Holm, J. L., Cameron, N. R. & Mikos, A. G. *Biomacromolecules* 8, 3806-3814 (2007).)

Besides polystyrene based polyHIPEs, some other polymers, such as PPF[40] (**Figure 2-18 B**) and polyurethane[168], have been studied to prepare w/o polyHIPE scaffolds for tissue engineering. Rat skin explants, individual human skin stem or osteoblast cells were used in the studies of cell seeding on to these scaffolds.[16,169] The results showed that cells seeded onto the polymer attached and proliferated on these scaffolds. [16,169-170]

But all these polymers are hydrophobic, which is considered not be a very suitable environment for cell growth without surface modification. The wettability of a scaffold for tissue engineering is considered very important for cell seeding[171], because cells do not grow into hydrophobic areas and so it is difficult to uniformly distribute cells throughout hydrophobic scaffolds. Because the major constituents of human body are hydrophilic, it is recognised that the materials, with similar hydrophilic surface to the surrounding tissue, are more biocompatible and easier to be accepted by the body. To this end, the hydrophobic polyHIPEs were surface modified with other polymers, such as poly-D-lysine, to enhance biocompatibility.[167] But the remaining unreacted toxic monomers, additives and organic solvents are still not easy to be removed completely, which may bring damage to the surrounding tissue and some growth factors may be inactivated.

2.5.5.2 O/W HIPEs for the Fabrication of Interconnected Porous Structures

In order to avoid the problems outlined above for the w/o polyHIPEs, hydrophilic polyHIPEs were prepared by polymerisation of o/w HIPEs. K. Naotaka[172-173] first reported the production of polyHIPEs produced from entirely hydrophilic monomers. Normally o/w HIPEs contain a hydrophilic/water-soluble monomer and a water-soluble/hydrophilic crosslinker in the aqueous continuous phase, an organic solvent as dispersed phase and an emulsifier with high HLB value (usually 7 to 10) to stabilise

the o/w emulsion. Once a stable o/w HIPE was prepared, the monomers in the aqueous phase were polymerised to form a porous solid. The constituent of these solid foams are derived from hydrophilic polymers, such as poly(acrylic acid)[174] (**Figure 2-19 A**), derivatized polysaccharides[155] (**Figure 2-19 B**), gelatin[137] and poly(hydroxyethyl methacrylate)[175]. The dispersed phase is usually toluene[155] or cyclohexane[175], which are completely removed after solidification.

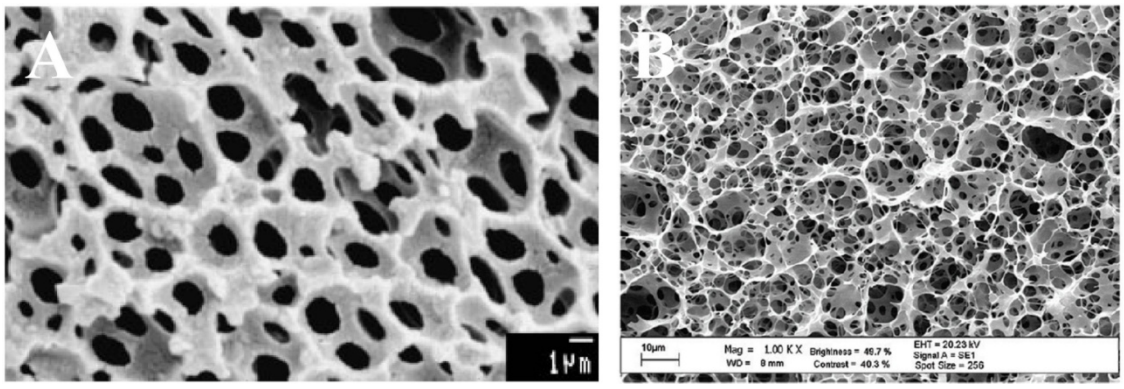

Figure 2-19: Two types of w/o polyHIPEs: **A**: Poly(acrylic acid) based polyHIPE (reproduced from Krajnc, P., Stefanec, D. & Pulko, I. *Macromol. Rapid Commun.* 26, 1289 (2005)); **B**: Alginate based polyHIPE hydrogel (reproduced from Barbetta, A., Barigelli, E. & Dentini, M. *Biomacromolecules* 10, 2328-2337, (2009).)

Barbetta has extended the application of inverse polyHIPE for scaffolds in tissue engineering by using derivatised polysaccharide and gelatin.[18,137,155,162] These natural polymers with hydrophilic surfaces provide a suitable environment to nerve cells, since they are very hydrophilic and are better tolerated by the human body than synthetic polymers. They can provide important signals to guide cells at different stages of growth.[176] However, it is worth to mention that all these inverse polyHIPEs need to be solidified and the dispersed phase has to be removed afterwards. These still

provide some challenges that need to be addressed, such as *in vivo* solidification and mechanical strength, to render o/w polyHIPEs into injectable scaffolds for soft tissue.

2.5.5.3 Pickering HIPEs for the Fabrication of Interconnected Porous Structures

Conventional o/w HIPEs are usually stabilised by large amount of surfactant, such as polyethylene glycol tert-octylphenyl ether (Triton X405)[156,174-175,177-179], sodium dodecyl sulphate[178] or polyethylene glycol dodecyl ether (Brij 35)[180], most of which are not biocompatible or even toxic[181-186]. Besides surfactant, colloidal particles, such as inorganic particles[166,187-189], carbon nanotube (CNT)[190-191] or microgel particles[192], have also been used to stabilize HIPEs (also referred to as Pickering-HIPEs). Compared with conventional surfactant stabilised HIPEs, particle stabilised HIPEs or Pickering HIPEs possess a number of advantages: firstly, the particles are absorbed at the interface between the continuous and dispersed phase and act as a barrier to droplet coalescence, since due to their high energy of attachment they render the resulting emulsion extremely stable.[193-194] Secondly, the use of particles as emulsifiers can also be used to functionalise the pore walls of the macroporous materials produced by polymerisation of the continuous emulsion phase with a layer of particles and in this way introduce additional properties, e.g. improved biocompatibility, electrical conductivity and/or slow drug release properties, etc., which may lead to a variety of applications in the future (such as scaffolds for tissue engineering with

particle functionalised inner surface). Currently several hydrophobic particles, such as surface modified silica particles[187], bacterial celluloses[195] and titania nanoparticles[166] were reported to stabilise w/o Pickering HIPEs, which could be used to produce hydrophobic macroporous materials. Only silica particles[189] and poly(N-isopropylamide)-*co*-(methacrylic acid) microgel particles[192] have been reported as effective emulsifiers for o/w Pickering HIPEs. As mentioned above, o/w Pickering HIPE possesses several advantages compared with surfactant stabilised HIPE, it can be used to prepare hydrogels as scaffolds for tissue engineering. But so far the application of o/w Pickering HIPE templating in tissue engineering is not explored yet and no covalently crosslinked hydrogel prepared from Pickering HIPE was reported, which is most universal porous materials for tissue engineering produced from HIPE templating.[196]

2.6 OVERALL ASSESSMENTS

In summary, currently the main problem in injectable scaffolds for soft tissue engineering, is that scaffolds possess interconnected pore structure (such as scaffolds prepared by HIPE templating or leaching) are usually not injectable or lack of safety solidification methods; injectable scaffolds (such as stimuli responsive hydrogels) do not have proper pore structure (their pores are usually not well interconnected) for tissue engineering. This research aims at solving this problem and preparing injectable scaffolds systems for soft tissue engineering. The scaffolds should be able to be

injected through a hypodermic needle and be able to solidified in a mild environment (e.g. no toxic chemicals will be produced during solidification), should be fabricated by biocompatible materials, and should have turntable interconnected pore structure for the proliferation of different cells.

CHAPTER 3

THERMO-RESPONSIVE POLY((DEXTRAN-GMA)-*CO*-NIPAAM) POLYHIPE HYDROGEL SCAFFOLDS

3.1 INTRODUCTION

In this chapter, a injectable macroporous thermo-responsive polyNIPAAm based polyHIPE hydrogel made from o/w HIPE templates is described. Thermo-responsive polyNIPAAm was used to fabricate this hydrogel. Because polyNIPAAm and its copolymer became hydrophobic after being heated above their LCST[103-104] and lead to lower biocompatibility, in order to improve the biocompatibility of this injectable scaffold system, dextran, a hydrophilic naturally occurring polysaccharide, which is better tolerated by the human body than most synthetic polymers and exhibits good biocompatibility[197], was employed as part of the constituents of the hydrogel matrix together with polyNIPAAm. The pore structure, thermo-responsiveness behaviour and cytoxicity of this thermo-responsive polyHIPE hydrogel are being studied and discussed in this chapter. The injectability and "*in vivo*" solidification of this thermo-

responsive polyHIPE hydrogel will be discussed in **Chapter 5** together with another stimuli-responsive alginate based polyHIPE hydrogel, as similar solidification method could be applied in both of these two hydrogels.

Scaffolds for tissue engineering, either preformed or injectable, have to mimic the *in vivo* environment as accurately as possible and offer physical support as well as a 3D environment to create functional tissue through cell proliferation to regenerate, repair or replace biological functions.[12-13] In spite of the great variety of fabrication methods of scaffolds for tissue engineering, HIPEs, especially oil-in-water (o/w) HIPEs, which can be used to produce highly interconnected hydrophilic macroporous materials, have been recently studied extensively to prepare scaffolds.[16,40,137,164,169-170,198-203] A high degree of interconnectivity, a feature of polyHIPEs, is considered to be a necessary requirement for nutrient/waste diffusion to support cell growth. In the case of o/w HIPEs[156,174-175,177-180,189,192], if water soluble monomers contained in the continuous aqueous phase were polymerised and the dispersed phase was removed afterwards, highly macroporous hydrogels with a well-defined porous structure can be obtained.[156,162-164,174-175,177-180,189,192]

PolyNIPAAm is a typical thermo-sensitive polymer with a lower critical solution temperature (LCST) in aqueous solution of about 32 °C.[103-104] Below LCST, polyNIPAAm chains have a random coil structure in water, but at a temperature above LCST, polyNIPAAm expel water and start to collapse[204]. With its swelling and

de-swelling behaviour being close to body temperature, which could be utilised to control and release drugs or as a *in vivo* solidification methods triggered by heating to human body temperature, polyNIPAAm and its copolymers are widely investigated in tissue engineering and drug delivery.[14] Moreover, the temperature dependent modulation of hydrophilic/hydrophobic surface properties of polyNIPAAm hydrogels was found to be useful for the controlled detachment of cultured cells.[205-206] Confluent cell sheets used for tissue engineering may be detached from the culture substrate without enzymes or chelating agents, which damage cells.[207]

3.2 RESULTS AND DISCUSSIONS

Dextran is commercially available with a molecular weight of 40 kg mol^{-1} and it is reported that the viscosity of a 20 % w/v dextran aqueous solution is easy to be dispersed and suitable for o/w polyHIPE preparation.[155] Glycidyl methacrylate (GMA) was chose to functionalise dextran because using dextran-GMA to prepare polyHIPE hydrogel is reported as a very good method.[155] The synthesis of dextran-GMA was carried out following an established procedure.[208] and the details of the reaction and analysis are described in **9.2**. Dextran-GMA can be copolymerised with NIPAAm in an aqueous environment to obtain a hydrogel. Because dextran-GMA and NIPAAm are water soluble, a toluene-in-water HIPE could be used as template to prepare poly(dextran-GMA) and poly((dextran-GMA)-*co*-NIPAAm) polyHIPE hydrogels. Dextran-GMA itself acts as covalent crosslinker for the hydrogel[209]**.** Triton X405

(hydrophilic-lipophilic balance, HLB ≈ 18[32]) was used as surfactant, because it was proved to be the one of the most effective surfactants to stabilise o/w HIPEs.[155] A covalently crosslinked hydrogel porous network was obtained after radical copolymerisation of dextran-GMA and NIPAAm in the aqueous phase of the HIPE (**Figure 3-1**), a poly(dextran-GMA) polyHIPE hydrogel is also prepared as control (the experimental details are in **9.3**).

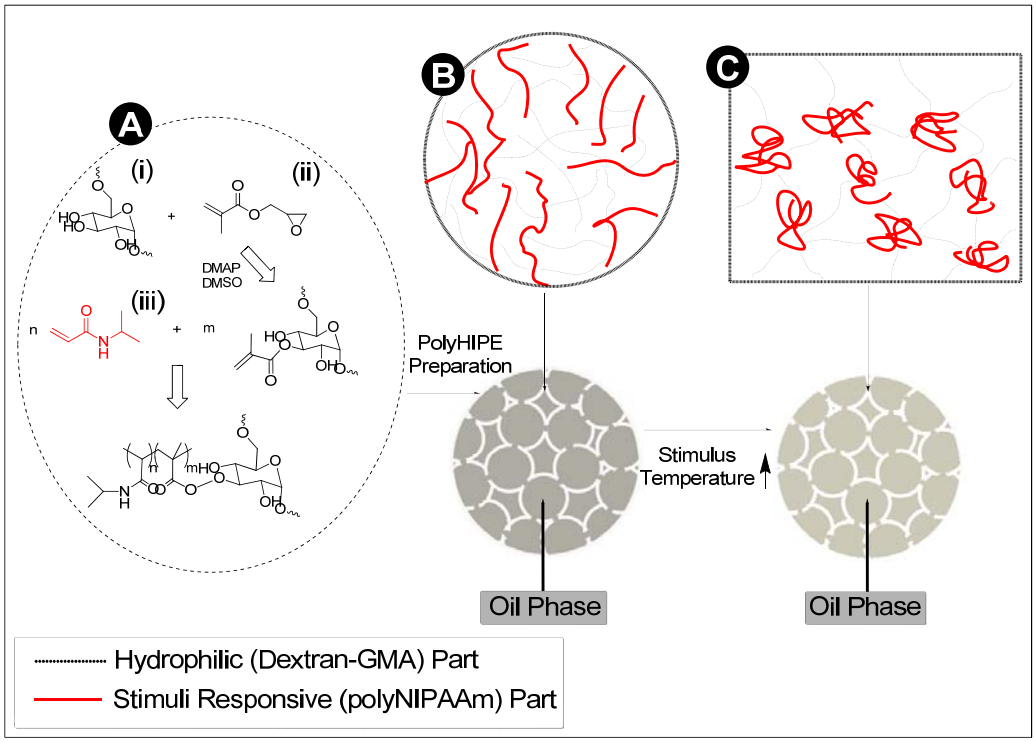

Figure 3-1: A schematic of the preparation of poly((dextran-GMA)-*co*-NIPAAm) polyHIPE hydrogel and its thermo-responsive behaviour in an aqueous environment: **A** & **B**: dextran was functionalised with GMA and then radically copolymerised with NIPAAm in the aqueous phase of an o/w HIPE in an oven at 60 °C for 24 h ((i), dextran, (ii), GMA, (iii) NIPAAm); **C**: poly((dextran-GMA)-*co*-NIPAAm) hydrogel undergoes a phase change to form a more compact structure within the aqueous phase of t he polyHIPE after being heated above the LCST of polyNIPAAm.

A poly(dextran-GMA) polyHIPE (**DG1**) and two poly((dextran-GMA)-*co*-NIPAAm) based polyHIPEs with different NIPAAm/dextran-GMA weight ratios (**DGN1** &

DGN2) were prepared (**Table 3-1**). In order to investigate the effect of introducing NIPAAm on thermo-responsiveness of the polyHIPE, the weight ratio of NIPAAm to dextran-GMA was varied from 0 (**DG1**) to 1 (**DGN1**) until 4(**DGN2**). The ratio was stopped at 4 because dextran-GMA was used as crosslinker of the hydrogel, higher NIPAAm to dextran-GMA ratio may result in lower mechanical performance of the porous scaffold. The composition of poly((dextran-GMA)-*co*-NIPAAm) polyHIPEs was determined by elemental analysis. The ratio of NIPAAm/glucose units is 0.8:1 in **DGN1** and 1.73:1 in **DGN2**.

Table 3-1: Emulsion compositions, pore size and pore throat size (determined from SEM images) of poly(dextran-GMA) and poly((dextran-GMA)-*co*-NIPAAm) polyHIPE hydrogels.

Sample Code	Aqueous phase [a] (volume fraction)	Aqueous phase composition [b]: Dextran-GMA/ NIPAAm/ Triton X405/ AIBN (% w/v : % w/v : % w/v: % w/v)	Pore diameter range[c] (μm)	Pore throat diameter range[c] (μm)
DG1	10	20 : 0 : 8.5 : 9	10-30	1-11
DGN1	10	10 : 10 : 8.5: 9	6-28	1-11
DGN2	10	4 : 16 : 8.5: 9	5-15	1-9

[a] Volume of the organic phase relative to the total volume of the emulsion.

[b] Concentration of dextran-GMA, NIPAAm, Triton X405 and initiator AIBN in distilled water.

[c] Pore and pore throat diameter ranges were determined from the SEM images of freeze dried hydrogels (in their swollen state in water).

SEM images of the polyHIPEs with the same nominal pore volume (the volume fraction of the oil phase) but different dextran-GMA and NIPAAm contents have the characteristic open porous structure of typical polyHIPEs[155] (**Figure 3-2)**. PolyHIPE hydrogel **DG1** and **DGN1** have similar pore size (in the range from 6 μm to 30 μm) and pore throat size (1 μm to 11 μm). When the weight ratio of NIPAAm to dextran-GMA was increased to 4, the pore throat size of **DGN2** slightly decreased to 1 μm to 9 μm, but its pore size fallen to 5 μm to 15 μm. The small pore size/pore throat size of **DGN2** (compared with **DG1** and **DGN2**) might be caused by the relative high ratio of amphiphilic NIPAAm monomer in the continuous phase of **DNG2** before radical polymerisation and resulted in smaller droplets and thus produced smaller pores.

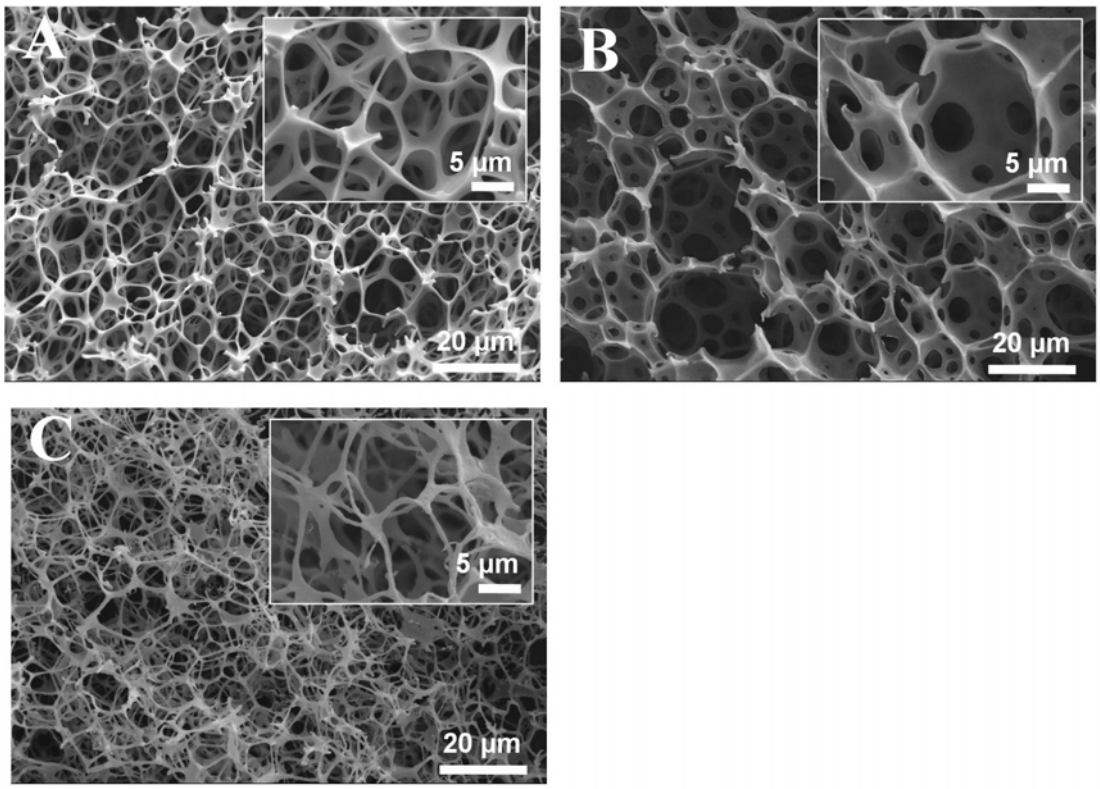

Figure 3-2: SEM images of poly(dextran-GMA) and poly((dextran-GMA)-*co*-NIPAAm) polyHIPE hydrogels: **A**: **DG1**; **B**: **DGN1**; **C**: **DGN2**.

In order to gain insight into the mechanical properties of these polyHIPE hydrogels, oscillatory mechanical measurements were performed to determine the shear modulus of these polyHIPEs a function of temperature (the experimental details are in **9.5**). Changes in the shear storage modulus G' and shear loss modulus G" as a function of temperature are shown in **Figure 3-3**. G' of polyHIPE **DG1** slightly decreases from 28 Pa to 25 Pa with increasing temperature from 25 ^{o}C to 50 ^{o}C while G" remains unaffected. When NIPAAm was introduced into the system, the G' of **DGN1** increased by 34% and the G' of **DGN2** increased by 300% with temperature changed from 25 ^{o}C to 50 ^{o}C. The slope of the G' and G" curves sharply increased around 30 °C to 35 °C, which indicates that the polyNIPAAm segments of the copolymer had started to phase separate from the aqueous phase, which caused the entire hydrogel to form a more compact structure within the aqueous phase of the polyHIPE. The observed transition temperature is around 34 ^{o}C to about 38 ^{o}C is similar to value for the LCST of most polyNIPAAm based hydrogels[210-212]. The higher the polyNIPAAm weight ratio, the more pronounced is the thermo-responsive behaviour. At the same time, the moduli, especially the storage shear modulus G', drops dramatically (up to 78% at 25 ^{o}C) as compared with the shear modulus of poly(dextran-GMA) polyHIPEs. Dextran-GMA also is a crosslinker and the crosslink density decreases with the weight content of dextran-GMA, which explains the decrease in G' with decreasing dextran-GMA content.

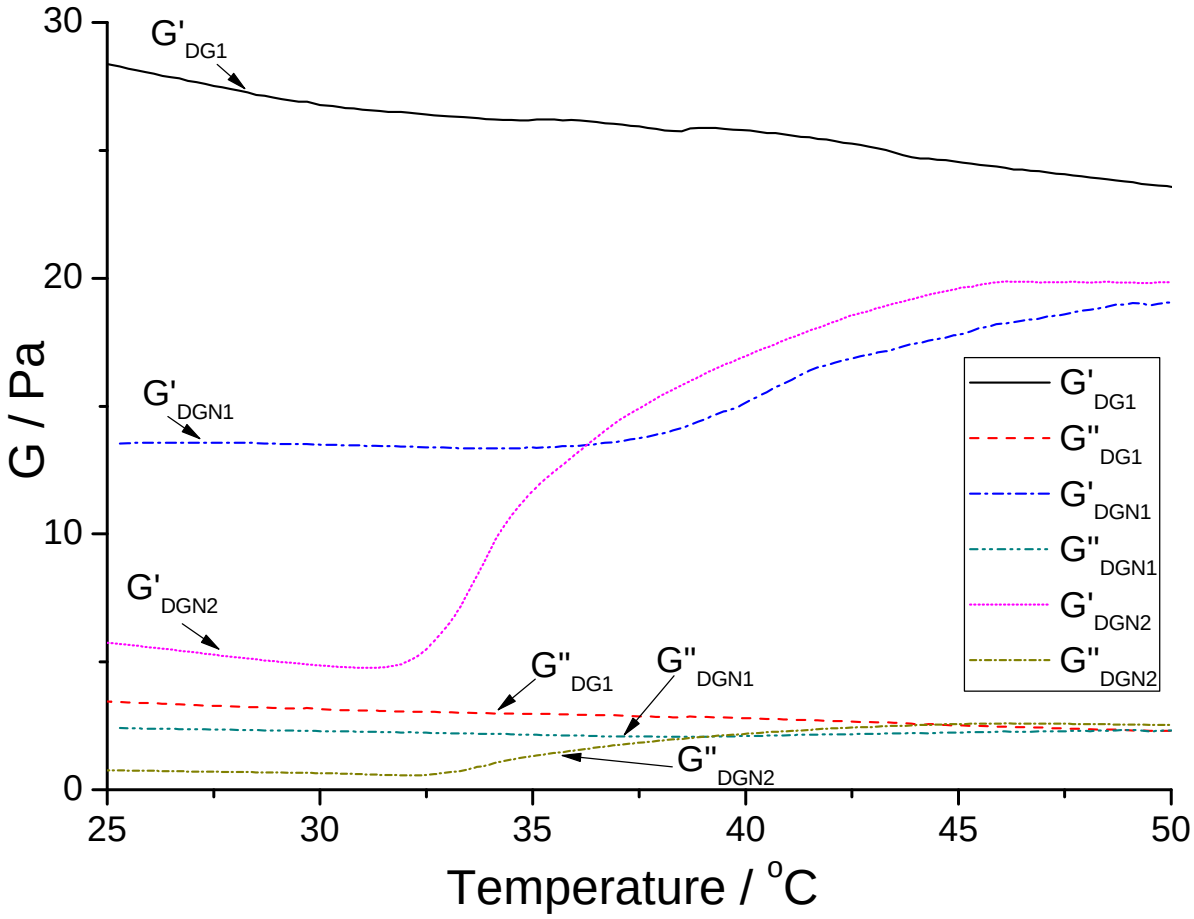

Figure 3-3: Change in storage G' and loss G" modulus as a function of temperature for polyHIPE hydrogel **DG1**, **DGN1** and **DGN2**.

In order to assess the biocompatibility of poly((dextran-GMA)-*co*-NIPAAm) polyHIPE hydrogels, an *in vitro* cytoxity study was performed by cultivating A549 human alveolar adenocarcinoma cells on the surface of a hydrogel monolith (**Figure 3-4**) (the experimental details are in **9.32**). A549 cells are human pneumocyte-like cells derived from an alveolar cell carcinoma, which have previously been used as a model to study cell-material interactions.[213-214] However, it could be observed in **Figure 3-4** that, the relative small pore throat size (less than 11 μm) limited the

penetration/migration of cells into the interior of the scaffold resulting in fewer cells to be found inside the scaffold.

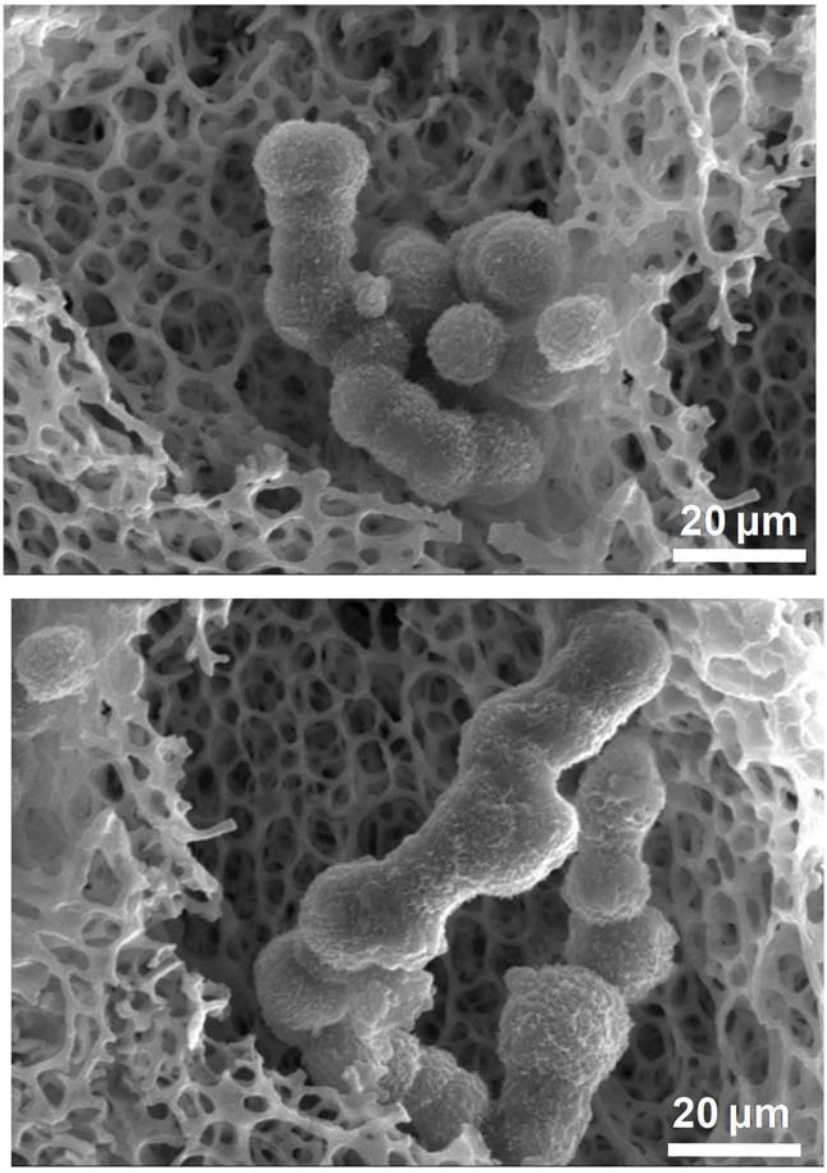

Figure 3-4: SEM images of A549 cells growing on poly((dextran-GMA)-*co*-NIPAAm) **DGN2**

3.3 CONCLUSIONS

Highly macroporous, biocompatible and thermo-responsive poly((dextran-GMA)-*co*-NIPAAm) polyHIPE hydrogels with a well-defined interconnected pore structure were prepared by copolymerising dextran-GMA and NIPAAm in the aqueous phase of a toluene-in-water HIPE. The thermo-responsive behaviour, attributed to the NIPAAm units in the dextran copolymer, was clearly observed in oscillatory mechanical measurements. With increasing temperature, the hydrogels undergo a phase transition in water to form a more compact structure, which lead to a clear increase (up to 300%) of the storage modulus. The thermally induced transition, which occurred between 30 °C to 35 °C, is below but relatively close to body temperature. The research of poly((dextran-GMA)-*co*-NIPAAm) polyHIPE hydrogels is the initial work toward the development of stimuli-responsive polyHIPE hydrogels as injectable scaffolds for soft tissue engineering. The injectability of this polyHIPE hydrogel will be detailed discussed in detail in **Chapter 5**. The methods used to enlarge/improve the pore size/pore throat size of polyHIPE hydrogels are introduced in **Chapter 6**. Moreover, based on this thermo-responsive polyHIPE hydrogel, a improved thermo responsive injectable hydrogel system is introduced in **Chapter 7,** which used reversible physical aggregation between polyNIPAAm chains to replace covalently crosslinking in order to obtain better injectability.

CHAPTER 4

ION-RESPONSIVE METHACRYLATE-MODIFIED ALGINATE POLYHIPE HYDROGEL SCAFFOLDS

4.1 INTRODUCTION

In this chapter, the preparation of a novel ion-responsive biocompatible methacrylate-modified alginate hydrogel produced from o/w HIPE templating is described. The approach reported here is novel as the interconnected pore features of polyHIPEs is combined with the excellent biocompatibility and ionic crosslinking feature of alginate. A covalently crosslinked methacrylate-modified alginate polyHIPE hydrogel (sample code: **PHMA)** was prepared. The covalent crosslinks gives it permanent porosity. Ion-responsiveness is achieved via ionic crosslinking of alginate segments, leading to hydrogels which can be swollen and shrunk controllably while possessing a high degree of permanent porosity and a well-defined interconnected pore structure. Besides scaffolds for tissue engineering, other potential uses for this hydrogel could be controlled drug release[215], microactuators,[216] filtration or separation devices to

remove heavy metal ions[217] and generally biomedical applications requiring a responsive material that can be controllably swollen and shrunk.

Beside thermo-responsive hydrogels, ion-responsive hydrogels, which can utilise Ca^{2+} ions from the surrounding tissue as a very safe trigger for gelation, have also been widely investigated as scaffolds for soft tissue engineering.[85] Alginate is a particularly attractive naturally derived ion-responsive polysaccharide widely investigated for its biocompatibility and reversible gelation chemistry with aqueous di- or trivalent cations.[85,108-109] Rapid Ca^{2+}-induced gelling of alginate under very mild aqueous conditions makes this a very attractive stimuli-responsive material for use *in vivo*.

Ion-responsive hydrogels that have been studied previously include poly(acrylic acid-*co*-2-hydroxyethylmethacrylate)[218], poly(methacrylic acid-*co*-acrylonitrile)[219-220] and poly(acrylamide-*co*-maleic acid)[221]. Ion-responsive hydrogels undergo abrupt changes in volume in response to changes in ionic strength[218,222-223]. The simplest way to prepare ion-responsive covalently crosslinked hydrogels is to polymerise and thus covalently crosslink ion-responsive water soluble monomers and a crosslinker in an aqueous environment[219-220]. Other ion-responsive hydrogels preparation methods include lyotropic surfactant phases[218] and nanofibre crosslinking[221]. Most of these hydrogels possess relatively low porosity (less than 60%) or poorly interconnected pore morphology, which limits the application of these hydrogels as scaffolds for tissue engineering.[218,221]

The preparation of Ca^{2+}-crosslinked alginate based polyHIPEs has been recently reported[198], but the focus was on ionic crosslinking as substitute for the conventional covalent crosslinking used for polyHIPEs.[155,174] Neither ion-response behaviour nor injectability was investigated.

4.2 RESULTS AND DISCUSSION

Similar to the strategy used to prepare poly((dextran-GMA)-*co*-NIPAAm) polyHIPE hydrogel in **Chapter 3**, the first step to prepare alginate based polyHIPE concerns the introduction of vinylic functionalities onto the biopolymeric chains of alginate in order to covalently crosslink alginate in the aqueous phase of an o/w HIPE. This allowed us to obtain a physically stable porous hydrogel monolith after the oil template was removed. Etherification of hydroxyl groups of alginate with methacrylic anhydride to synthesis methacrylated alginate proved to be a relative easy and effective method to vinyl functionalises alginate for covalently corsslinking.[224-225] The synthesis of methacrylate-modified alginate was carried out following an established procedure (the chemistry of the modification was shown in **Figure 4-1** and the experimental details are in **9.6**).[225] With the same reason as described in **Chapter 3**, a toluene-in-water HIPE stabilised by Triton X405 was employed to prepare methacrylated-modified alginate polyHIPE. Because methacrylate-modified alginate with a degree of substitution of 1.00:0.44 (glucose to methacrylate groups, quantified using ^{1}H-NMR and the calculation method is described in **9.6**) is water soluble, a

toluene-in-water HIPE was used as template to prepare methacrylate-modified alginate based macroporous hydrogels. Compared with other water-soluble monomers used to prepare o/w polyHIPEs, such as acrylic acid[174] or dextran[155], the viscosity of our alginate solution is relatively high to be dispersed (the viscosity of 2% alginate from brown algae at 25 °C is about 250 mPa.s). A compromise between the need for a high concentration of methacrylate-modified alginate to obtain a mechanically robust gel on the one hand[209] and a sufficiently low viscosity to be able to prepare a stable and homogeneous HIPE with full incorporation of the oil phase on the other hand had to be identified. After several trials, it was found that the appropriate methacrylate-modified alginate concentration in the aqueous phase of the o/w HIPE was 7.0 % w/v. Above this concentration, the viscosity of the aqueous continuous phase made it extremely difficult to be dispersed using just an overhead stirrer and therefore no homogeneous emulsion was obtained. Also we had to extend the duration of the dropwise addition of the organic phase from 30 min to 4 h (at 500 rpm stirring speed at room temperature) in order to avoid phase inversion during emulsification, higher dropwise addition speed could lead to phase separation. Once the stable o/w HIPE was obtained it was then heated to 60 °C for 24 h for radical polymerisation. Afterwards, the polymerised hydrogel was soxhlet extracted with methanol followed by acetone to remove the dispersed phase and then dried in an oven at 60 °C for another 24 h to remove acetone. The product was finally re-swollen in deionised

water. (**Figure 4-1 A & B**). The experimental details of methacrylate-modified alginate polyHIPE hydrogel preparation are in **9.7**.

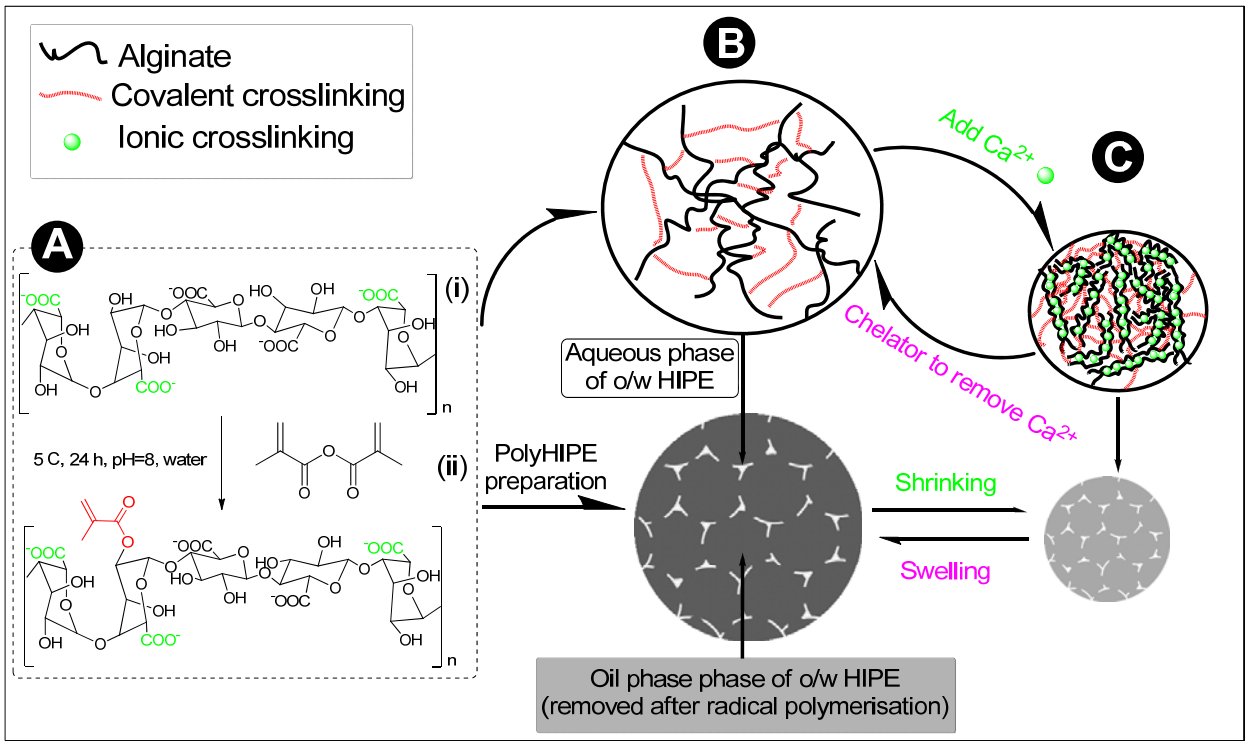

Figure 4-1: A schematic of the preparation of a methacrylate-modified alginate polyHIPE hydrogel **PHMA** and its ion-responsive behaviour in an aqueous environment: **A**: functionalisation of alginate with methacrylate groups ((i), alginate, (ii), methacrylic anhydride); **B**: methacrylate-modified alginate covalently crosslinked in the aqueous phase of an o/w HIPE after radically polymerised at 60 °C for 24 h.; **C**: methacrylate-modified alginate polyHIPE hydrogel **PHMA** in its shrunken state after ionic crosslinking with a $CaCl_2$ solution.

Alginate can be ionically crosslinked in the presence of divalent cations such as Ca^{2+} ions to form stable hydrogels. A purely Ca^{2+}-crosslinked alginate based polyHIPE hydrogel has already been reported.[198] In this study ionic crosslinking serves solely as a non-covalent mode of crosslinking instead of the more conventional covalent approach and no swelling/shrinking of the hydrogel that was caused by the change of the ion concentration was reported .[155,174]

In our work, the main purpose of introducing methacrylate functionalities into alginate is to allow the hydrogel to be crosslinked in two different ways: one is covalently to maintain the porous structure generated during emulsion templating and the other is ionically through formation of ionic crosslinking sites between alginate chains [120-121], which imparts the ability to response to divalent or trivalent cations in a aqueous environment and consequently allow us to control the external dimension and internal pore size/pore throat size of the porous structure as well as the mechanical properties of macroporous hydrogels. Our experiments on ion responsiveness showed that the polyHIPE hydrogel starts to shrink after immersing it into aqueous $CaCl_2$ solution with Ca^{2+} concentration ranging from 1.8 mM to 100 mM (1.8 mM $CaCl_2$ concentration was chosen because it is the typical level of Ca^{2+} concentration in the human[122-123], 100 mM $CaCl_2$ concentration was chosen to facilitate the observation of shrinking phenomenon). Upon exposure to Ca^{2+}, the hydrogel polyHIPE turns from translucent to pale white (**Figure 4-2**). As shown in **Figure 4-2 A**, the diameter of the polyHIPE gradually decreases from 2.1 cm to 1.2 cm in a 100 mM $CaCl_2$ aqueous solution. A series of experiments indicated that, as long as there was a high enough supply of Ca^{2+} (200 ml 1.8 mM $CaCl_2$ is enough to ionically crosslink 0.1 g methacrylate-modified alginate), the final shrunken dimension of methacrylate-modified alginate polyHIPE hydrogel **PHMA** was constant independent from whether it had been immersed in 1.8 mM or 100 mM $CaCl_2$ solution. Before ionic crosslinking, the water uptake of the only covalently crosslinked alginate polyHIPE hydrogel

PHMA was approximately 8000% w/w (determined by gravimetrically comparing the weight of fully swollen hydrogel before and after freeze drying), which is high while the water uptake of other porous alginate based materials ranges from 500% w/w to 3000% w/w[226-228]. Consistent with the volume shrinkage during the ionic crosslinking, water was expelled from the hydrogel and the water content decreased to approximately 3000% w/w (**Table 4-1**). The details of these experiments are in **9.8**, **9.10** and **9.11**.

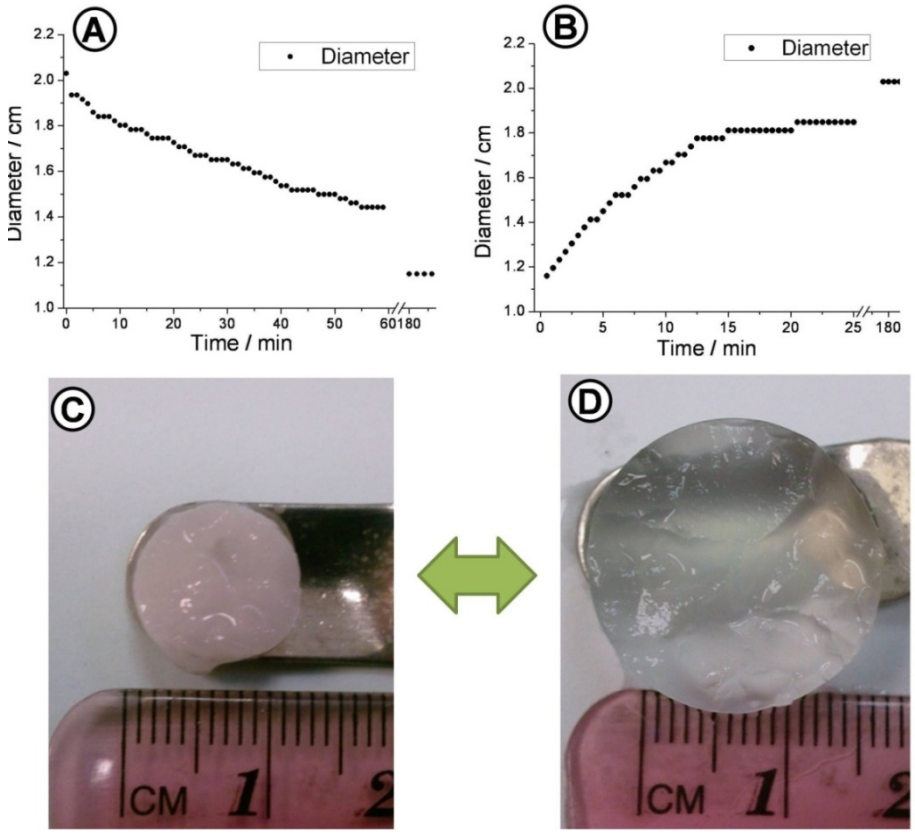

Figure 4-2: Reversible shrinking and swelling of a methacrylate-modified alginate polyHIPE **PHMA** monolith triggered by an alternating exposure to a 100 mM aqueous $CaCl_2$ solution followed by a 100 mM aqueous sodium citrate solution. **A**: change of diameter of the cylindrical polyHIPE monolith with time during shrinking; **B**: change of diameter of the cylindrical polyHIPE monolith with time during swelling; **C**: digital image of a hydrogel after Ca^{2+}-crosslinking; **D**: digital image of a hydrogel after removal of Ca^{2+} ions with excess sodium citrate.

Figure 4-3 allows the comparison of SEM images of methacrylate-modified alginate polyHIPE hydrogel **PHMA** before and after Ca^{2+}-crosslinking. The typical polyHIPE pore structure is clearly observed in all cases. Consistent with the volume shrinkage (50% shrinkage in its diameter), the pore sizes of the polyHIPE hydrogel, which were determined from the SEM images of the freeze dried hydrogels (in their swollen state in water before freeze drying), decreased from 14~31 μm (**Figure 4-3 A**) to 7 ~12 μm (**Figure 4-3 B, C & D)** after Ca^{2+}-crosslinking. Ca^{2+}-crosslinking also led to a slight decrease (about 50%) in the pore throat size (**Table 4-1**). The decrease in pore size and pore throat size of methacrylate-modified alginate polyHIPE are consistent with the external dimension change before and after ionic crosslinking. Moreover, the macroporous alginate hydrogel was a closed cell type after preparation (**Figure 4-3 A**) and gradually produced interconnections between pores evident after already one shrinking cycle.

Table 4-1: Properties of cylindrical methacrylate-modified alginate polyHIPE hydrogel **PHMA** with 80% nominal pore volume in its fully swollen state and fully shrunken state.

Methacrylate-modified alginate polyHIPE hydrogel **PHMA**	Pore size range[a] (μm)	Pore throat size range[a] (μm)	Water uptake[b] (% w/w)	Diameter of hydrogel monolith (cm)
fully swollen	14.4~31.6	2.5~12.3	8000±250	2.1
fully shrunken	6.8~11.8	1.9~5.9	3000±100	1.2

[a] Pore size and pore throat sizes of the polyHIPE hydrogel was determined from the corresponding SEM micrographs. [b] Determined by gravimetrically comparing the weight of fully swollen hydrogel with freeze dried hydrogel.

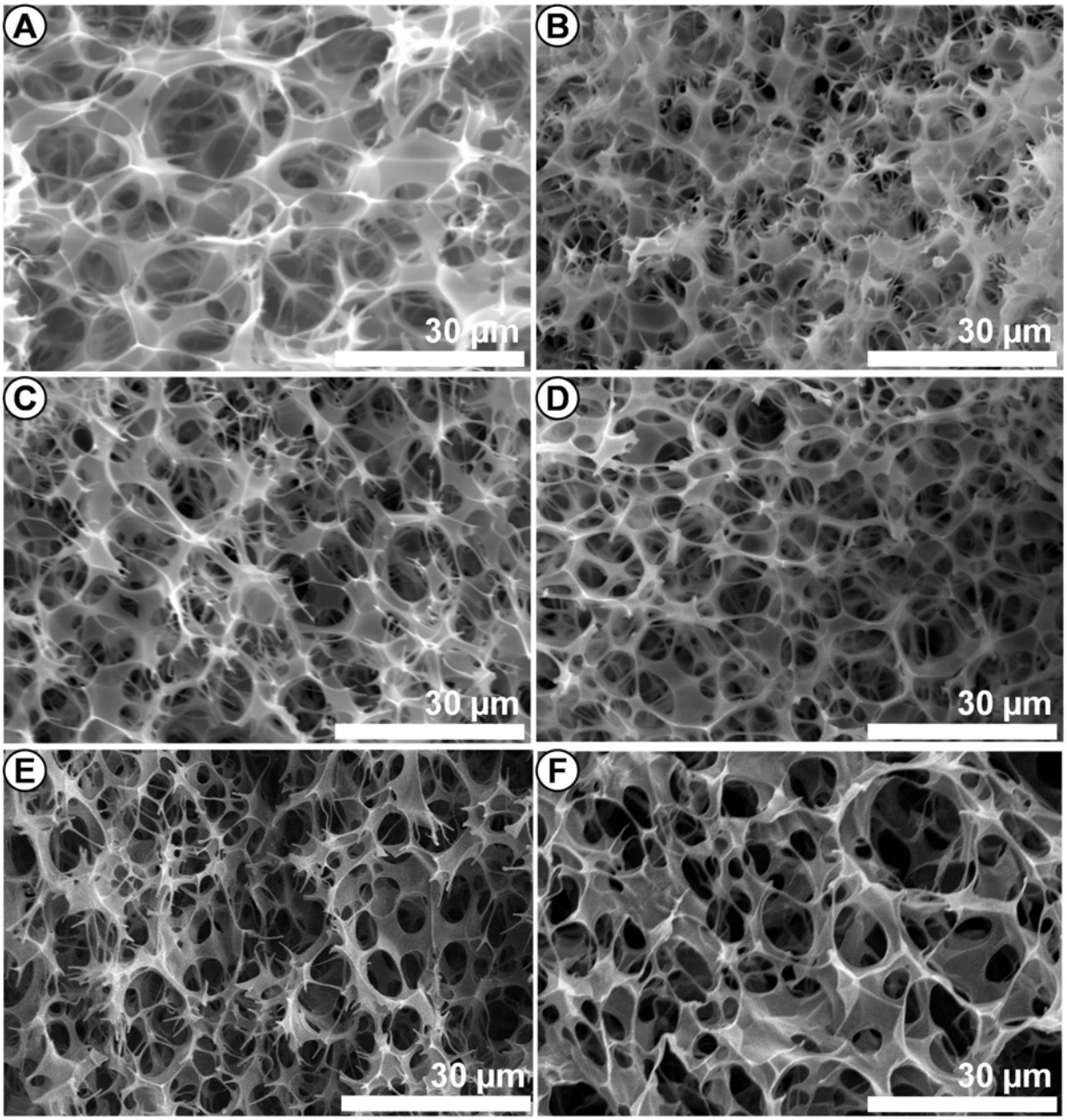

Figure 4-3: SEM images of methacrylate-modified alginate polyHIPE hydrogel **PHMA**: **A**: before shrinking and swelling experiments and after being exposed to **B**: 1.8 mM, **C**: 4.0 mM and **D**: 100 mM $CaCl_2$ solutions; **E**: after 2 cycles of sequential exposure to a 100 mM aqueous $CaCl_2$ solution followed by 100 mM aqueous sodium citrate solution after final immersion in 100 mM aqueous $CaCl_2$ solution (i.e. shrunken state); **F**: after 3 cycles of sequential exposure to a 100 mM aqueous $CaCl_2$ solution followed by 100 mM aqueous sodium citrate solution (i.e. swollen state).

Sodium citrate is a strong tridentate chelator for divalent cations at very mild conditions[229-230] and is commonly used as anticoagulant in blood transfusions[231]. When the covalently and Ca^{2+}-crosslinked methacrylate-modified alginate polyHIPE hydrogel **PHMA** was exposed to an aqueous solution of sodium citrate (100 mM), Ca^{2+} ions were chelated and thus removed from the hydrogel network leading to the removal of the ionic crosslinks expressed physically as swelling of the cylindrical hydrogel monolith. In this swelling experiments, the excess water from the Ca^{2+}-crosslinked monolith was firstly wiped out by tissue paper, and then the monolith was immersed in a beaker contained 200 ml 100 mM aqueous citrate solution. After about 3 h of exposure sodium citrate solution, its diameter finally recovered to 2.1 cm (**Figure 4-2 B**). The SEM image (**Figure 4-3 F**) confirms that also the pore sizes of the methacrylate-modified alginate polyHIPE hydrogel **PHMA** recovered from about 2~6 μm to its original dimension before Ca^{2+}-crosslinking. The swelling-shrinking cycle could be repeated at least three times without visually observing any volume loss or changes in colour or physical dimensions.

The results of the oscillatory mechanical measurements on cylindrical methacrylate-modified alginate polyHIPE hydrogel **PHMA** are shown in **Figure 4-4** and the experimental details are in **9.9**. Before any shrinking-swelling cycle, the storage modulus of the hydrogels was approximately 20 kPa, which is larger than the storage modulus of 1% alginate crosslinked by Ca^{2+} ions [232-233] (approximately 1~ 12 kPa depended in the molecular weight or M to G unit). After the first exposure to Ca^{2+}, a

sharp decrease in the shear storage modulus to 5 kPa was observed and remained at this value after subsequent swelling-shrinking cycles. It is evident from the SEM images that after 3 shrinking-swelling cycles, both in the shrunk (**Figure 4-3 E**) and in the swollen state (**Figure 4-3 F**), the pore walls became thinner compared to the hydrogel polyHIPE prior to shrinking-swelling experiments (**Figure 4-3 A**). The reason for the fourfold drop of the shear storage modulus after the first Ca^{2+}-crosslinking is that the thin films initially separating the pores in the polyHIPE[234] ruptured and so the structure becomes open porous. Another possible reason might be that the methacrylate-modified alginate in the hydrogel polyHIPEs were initially conformationally strained and the first Ca^{2+}-crosslinking/Ca^{2+}-sequestration process allowed for the relaxation of the alginate chains, leading to a lower modulus.

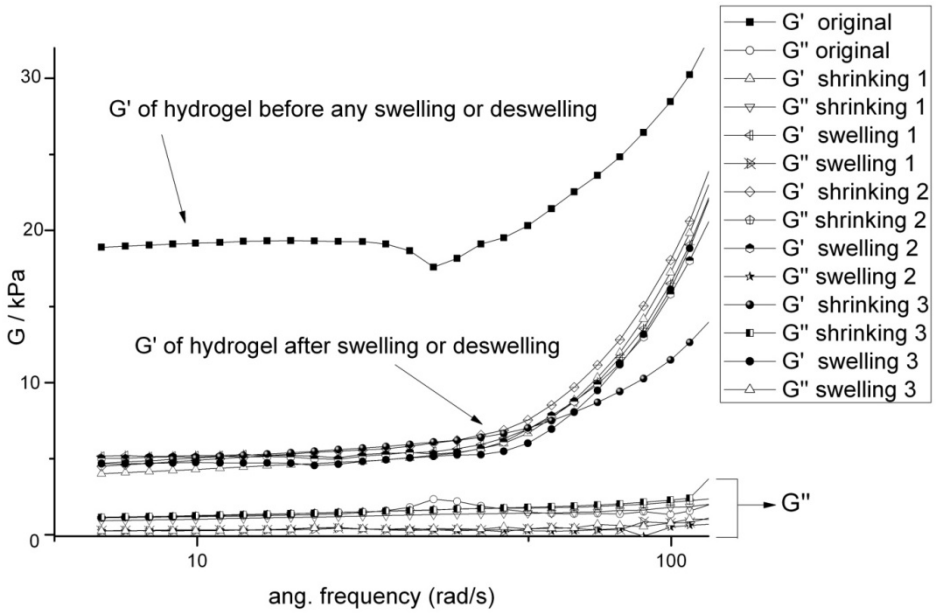

Figure 4-4: Change in shear storage modulus G' and shear loss modulus G" of methacrylate-modified alginate polyHIPE hydrogel **PHMA** triggered by alternating exposure to a 100 mM $CaCl_2$ solution followed by citrate chelation/extraction of Ca^{2+} with a 100 mM sodium citrate solution.

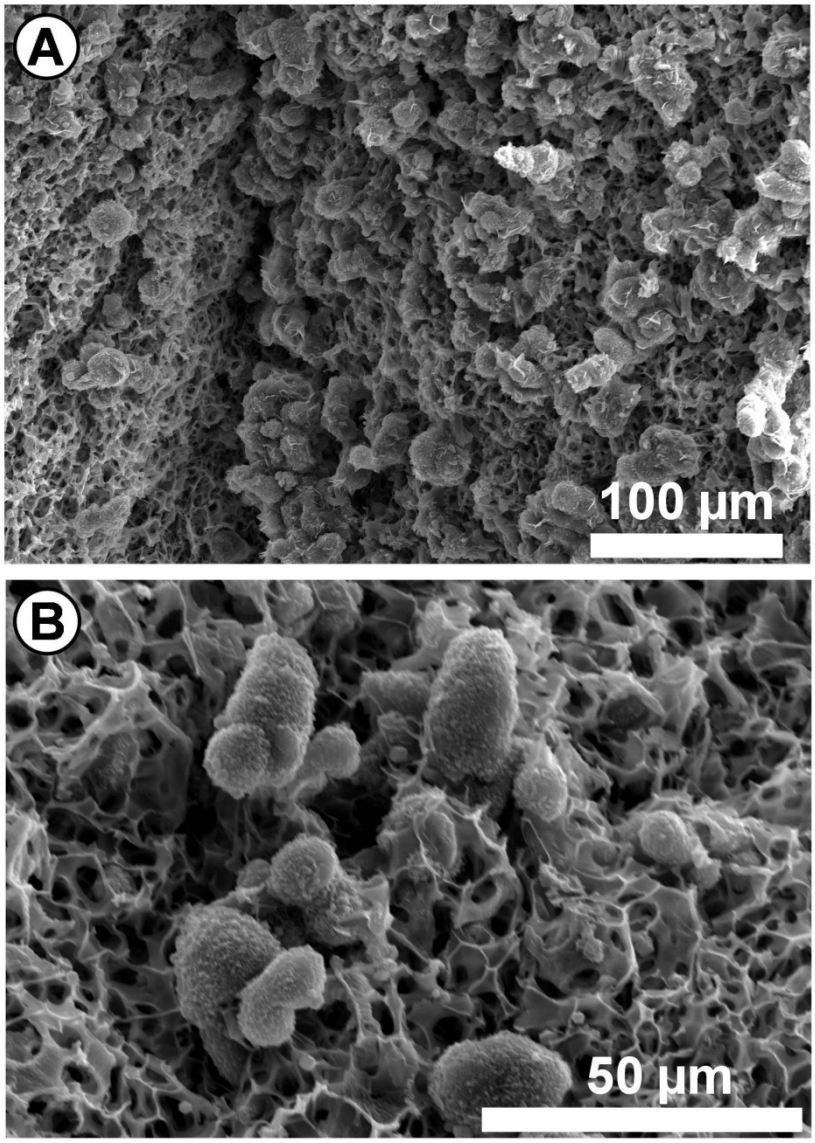

Figure 4-5: SEM images of A549 cells cultured on methacrylate-modified alginate polyHIPE **PHMA**: **A**: cells attached on the surface after culture; **B**: cells that proliferated into the pores of polyHIPE hydrogel after culture.

In order to assess the biocompatibility of the hydrogel, *in vitro* cytoxicity evaluation was performed by culturing A549 human alveolar adenocarcinoma cells on the methacrylate-modified alginate polyHIPE hydrogels (the experimental details are in **9.32**). Extensive colonisation of cells was clearly observed on the surface of the porous hydrogel (**Figure 4-5 A**) and even inside of the hydrogel (**Figure 4-5 B**). Most

cells had assumed squamous epitheloid morphologies. But compared with A549 cell size, the relative small pore throat size limited the penetration/migration of cells into the inside of the scaffold resulting in fewer cells to be found inside the scaffold. However, judging from the rapid colonisation of the scaffolds by A549, and the typical squamous, epithelial morphologies, A549s are able to establish connections with the hydrophilic network of methacrylate-modified alginate polyHIPE **PHMA**.

4.3 CONCLUSIONS

Highly porous and biocompatible methacrylate-modified alginate hydrogel polyHIPE **PHMA** with a well-defined porous structure were prepared. The introduction of methacrylate allowed to covalently crosslink the alginate based hydrogel which also maintains the ability to be ionically crosslinked. The second but ionic crosslinking could be easily reversed using the chelating agent sodium citrate. Both the ionic crosslinking and disruption of ionic crosslinking could be trigged in a mild environment and led to shrinking and swelling phenomenon of polyHIPE hydrogel, which also resulted in the change of the dimension, water uptake and pore size of the hydrogel. After first shrinking, the pore structure of methacrylate-modified alginate polyHIPE was interconnected regardless whether the polyHIPE was in the shrunken or swollen state. The controllable ion-responsive feature and well-controlled pore morphology makes this methacrylate-modified alginate hydrogel polyHIPEs promising scaffolds for soft tissue engineering. The initial data suggests this porous

scaffold is not preventing cell growth but more cytoxicity assessment need to be carried out. Other potential applications in bioseparation, drug delivery, as artificial muscles biosensors, actuators and immobilization of enzymes and cells could also be considered.

CHAPTER 5

INVESTIGATION OF THE INJECTABILITY AND SOLIDIFICATION OF STIMULI-RESPONSIVE POLYHIPE HYDROGELS

5.1 INTRODUCTION

In tissue engineering, constructs of living cells can be formed either by seeding cells onto a preformed scaffold or by injection of a solidifiable porous scaffolds together with a cell mixture to the tissue to be regenerated[12-13]. Compared with preformed scaffolds, injectable scaffolds possess many attractive features from a clinical perspective, such as minimising cost of treatment, patient discomfort, risk of infection and scar formation[11,14]. In addition, cells, drugs or growth factors can be loaded quite simply into the scaffold by mixing prior to injection.[11] Moreover, injectable scaffolds are capable of filling irregular defects, which is difficult to achieve with preformed scaffolds.[14] Because it is usually believed that covalently crosslinked polyHIPEs are

not injectable, most activities concerning the use HIPE-templated monoliths as scaffolds for tissue engineering concentrated on preformed scaffolds[16,164,199-201] in contrast to the work reported here.

An injectable scaffold should be able to solidify *in vivo* after injection without any irritation to the surrounding tissue and possess a interconnected 3D porous structure with proper pore size and sufficient mechanical strength to withstand biomechanical loading.[11] Typical solidification mechanisms during the scaffold formation usually include radical polymerisation/crosslinking[235-237], ceramic setting[238], self-assembly mechanisms[239] and environmental-stimuli triggered solidification, which usually includes thermal gelation[11,240], ionic cross-linking[198,241]. Considerable attention has been given to environmentally-stimuli-responsive materials, or so-called smart hydrogels, as *in vivo* solidification for injectable scaffold for tissue engineering because these toxic monomers can be avoided and relative mild solidification condition can be applied. As mentioned in **Section 2.4.4.2**, among these stimuli-responsive materials, the rapid Ca^{2+}-induced gelation of alginate makes it a very attractive stimuli-responsive material for *in vivo* use. [97]

In **Chapter 2** and **Chapter 3**, two novel stimuli-responsive polyHIPE hydrogels namely: a thermo-responsive poly((dextran-GMA)-*co*-NIPAAm) polyHIPE hydrogel and an ion-responsive methacrylate-modified alginate polyHIPE hydrogel have been

introduced. Both of these hydrogels posses a well-defined interconnected porous structure and good biocompatibility as revealed by a preliminary cytoxicity assessment, which makes them good candidates as preformed scaffolds for soft tissue engineering. In this Chapter, the injectability and solidification of these two types of stimuli-responsive hydrogels are being discussed.

5.2 RESULTS AND DISCUSSION

5.2.1 INJECTABILITY OF METHACRYLATE-MODIFIED ALGINATE POLYHIPE HYDROGEL PHMA

A very simple experiment was conducted in order to investigate the injectability of methacrylate-modified alginate polyHIPE hydrogel **PHMA** (the experimental details are in **9.12**). Several pieces of **PHMA** (diameter > 1 cm) were loaded into a syringe and gently squeezed through a hypodermic needle (inner diameter = 1.1 mm). As expected from a covalently crosslinked hydrogel, the gel particles broke up into smaller fragments during extrusion through the needle. The SEM images (**Figure 5-2 A**) of the extruded gel show that the diameter of the hydrogel fragments produced by extrusion of the polyHIPE gel through the needle ranged from 1 mm to 3 mm. The sizes greater than the needle diameter are a result of the very compliant nature of the porous soft polyHIPE which can be deformed and compressed to a smaller size reversibly upon exerting physical pressure. The pore morphology of these polyHIPEs

was not destroyed by the extrusion process as is evident from the corresponding SEM images (**Figure 5-2 B**). The interconnected pore structure was retained without change of size of pores or pore throats. (The experimental details are in **9.12**.)

Some target areas for injectable scaffolds are confined defects surrounded by soft tissue. Ideally after injection, these 1 mm to 3 mm fragments of polyHIPE hydrogel would fill the confined space fully and act as a continuous (i.e. monolithic) scaffold *in vivo*. At the same time, the surrounding soft tissue would confine and compress the porous hydrogel fragments and force/hold them together (**Figure 5-1**). One simple experiment was carried out for demonstration. The hydrogel was injected into a piece of fresh dead pork muscle (purchased from local supermarket), which was then freeze dried within the muscle after injection. After freeze drying, the interconnected porous structure of the polyHIPE was still clearly observable in the pork muscle (**Figure 5-2 C & E**). The surrounding soft tissue tightly packed the porous hydrogels fragments (**Figure 5-2 C**) and no gap could be observed at the boundary between the pork muscle and the hydrogel (**Figure 5-2 D**).This experiment demonstrated that covalently crosslinked methacrylate-modified alginate polyHIPE **PHMA** is injectable and its porous structure is not changed before and after injection.

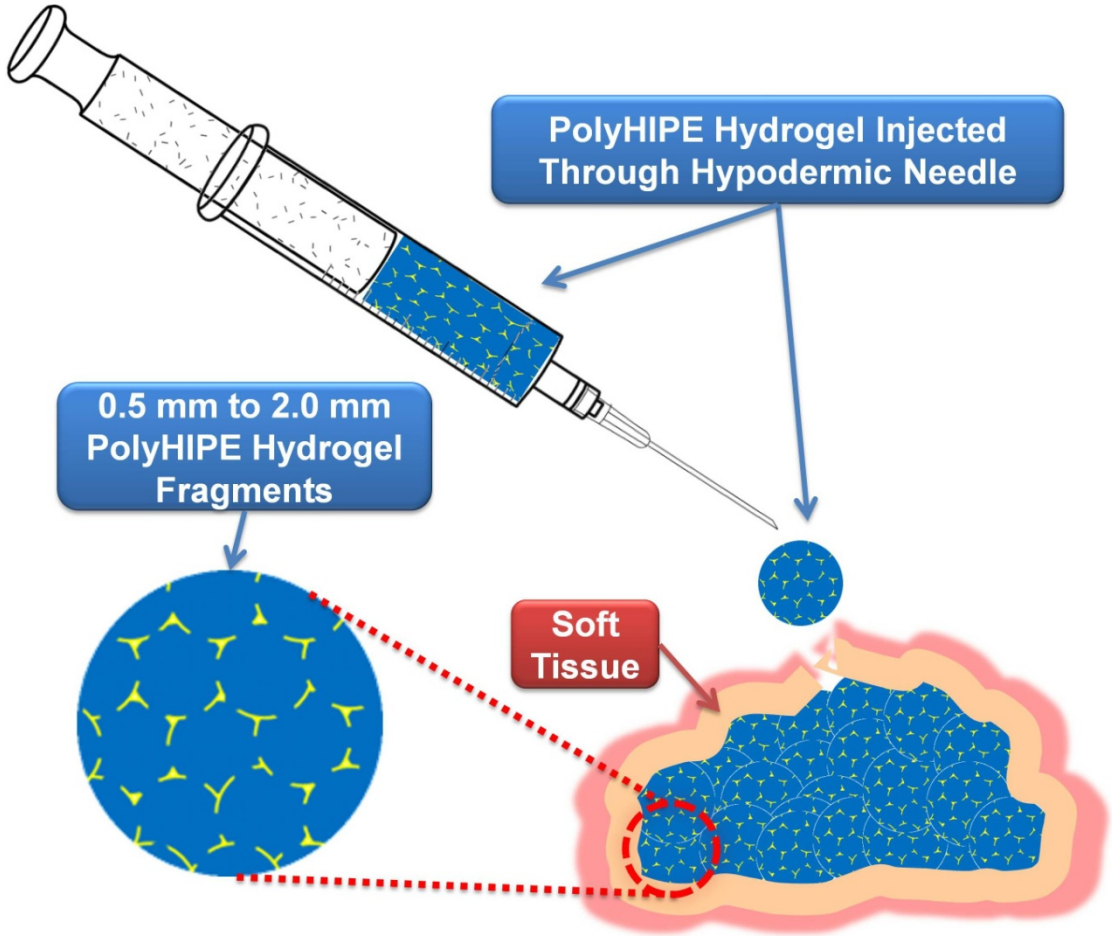

Figure 5-1: A schematic diagram of polyHIPE injection into soft tissues.

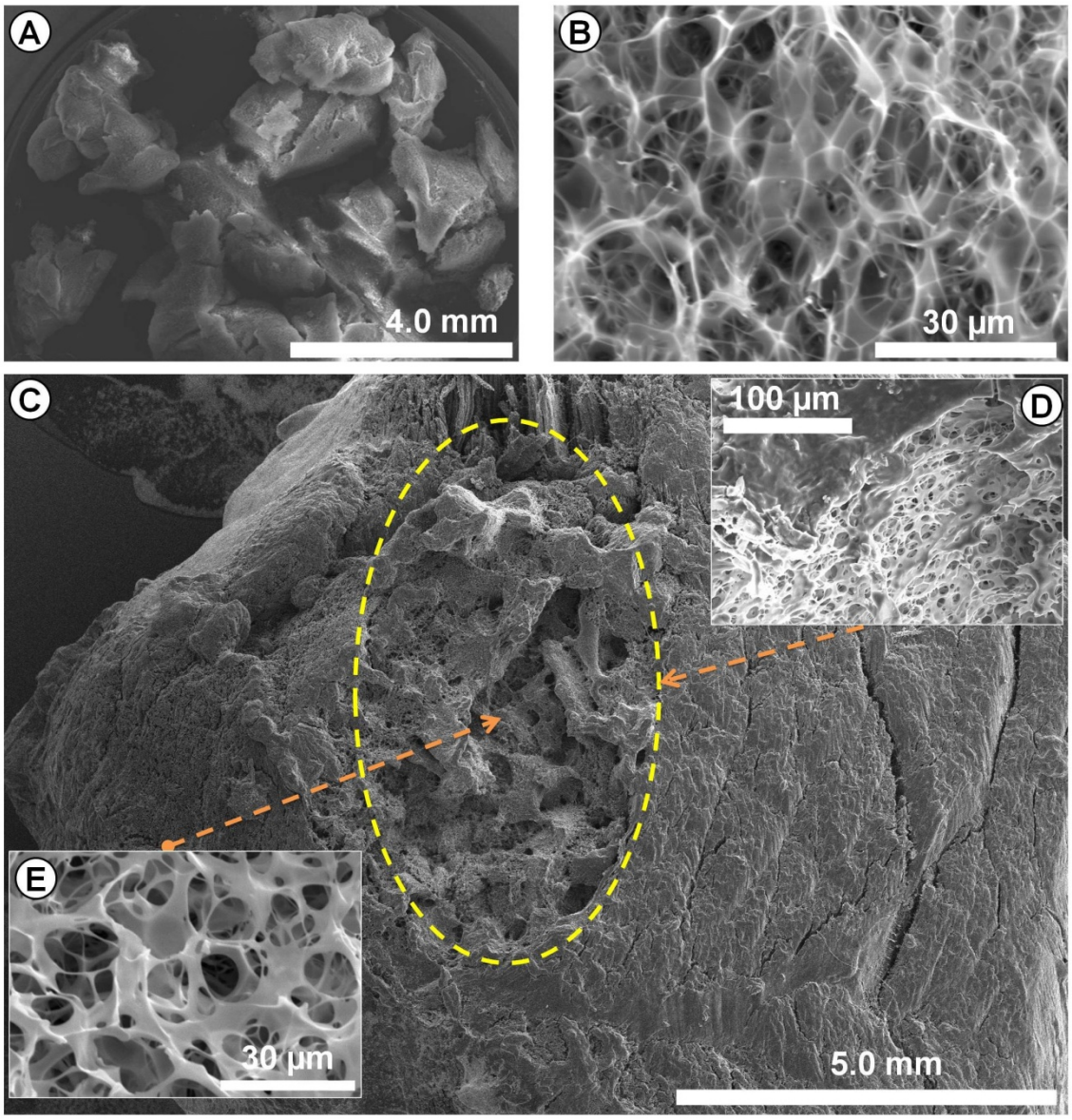

Figure 5-2: SEM images of methacrylate-modified alginate polyHIPE hydrogel **PHMA** after injection through the needle: **A** & **B**: hydrogel passed through a needle with 1.1 mm inner diameter (**A**: low magnification, **B**: high magnification); **C**, **D** & **E**: hydrogel after being injected into a dead pork muscle.

5.2.2 SOLIDIFICATION OF METHACRYLATE-MODIFIED ALGINATE POLYHIPE HYDROGEL PHMA AFTER INJECTION

Considering the possibility that the target area of injectable scaffold maybe not confined space, another potential approach of producing a monolithic structure from fragmented polyHIPE hydrogel particles after injection is explored to utilise the Ca^{2+}-responsive feature of the alginate. If a sufficient number of interparticle Ca^{2+} crosslinks could be introduced through exposure of the fragments to a $CaCl_2$ solution, methacrylate-modified alginate polyHIPE **PHMA** as a coherent monolithic scaffold should form after injection. However only hydrogel fragments were found when the hydrogel **PHMA** was injected into a 50 mM $CaCl_2$ solution (**Figure 5-4 D**). As soon as the particle came in contact with the Ca^{2+} ions, they will crosslink at the surface of the individual particle and make them shrink and with the shrinking one will not get cohesion/adhesion between particles. As the crosslinking is directly associated with shrinking of the particles, it seems likely that the latter process prevented any significant interparticle crosslinks from forming.

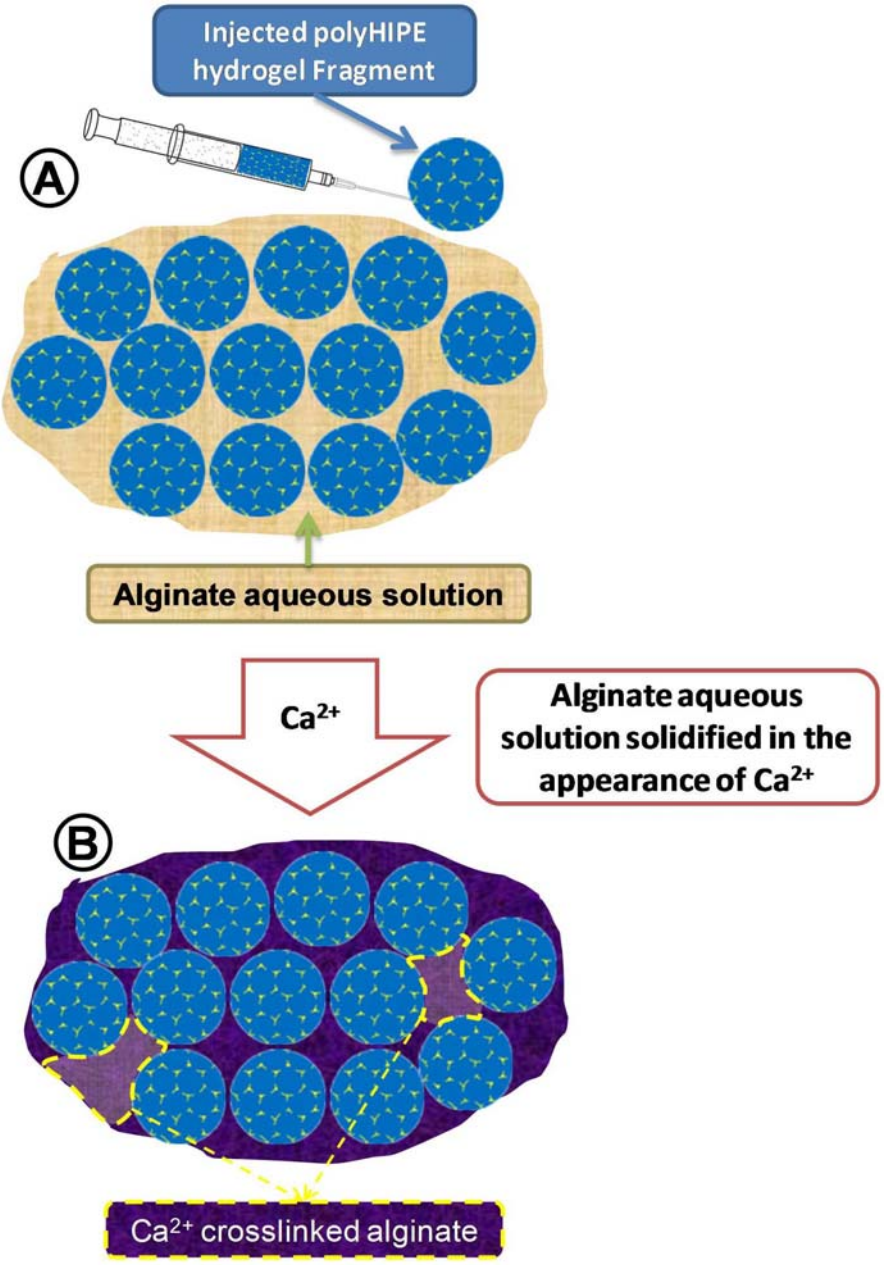

Figure 5-3: A schematic of using Ca^{2+} crosslinkable alginate to bond polyHIPE hydrogel fragments. **A**: aqueous alginate solution diffused into polyHIPE hydrogel fragments; **B**: aqueous alginate solution gelled in the presence of Ca^{2+} and bonded polyHIPE hydrogel fragments together.

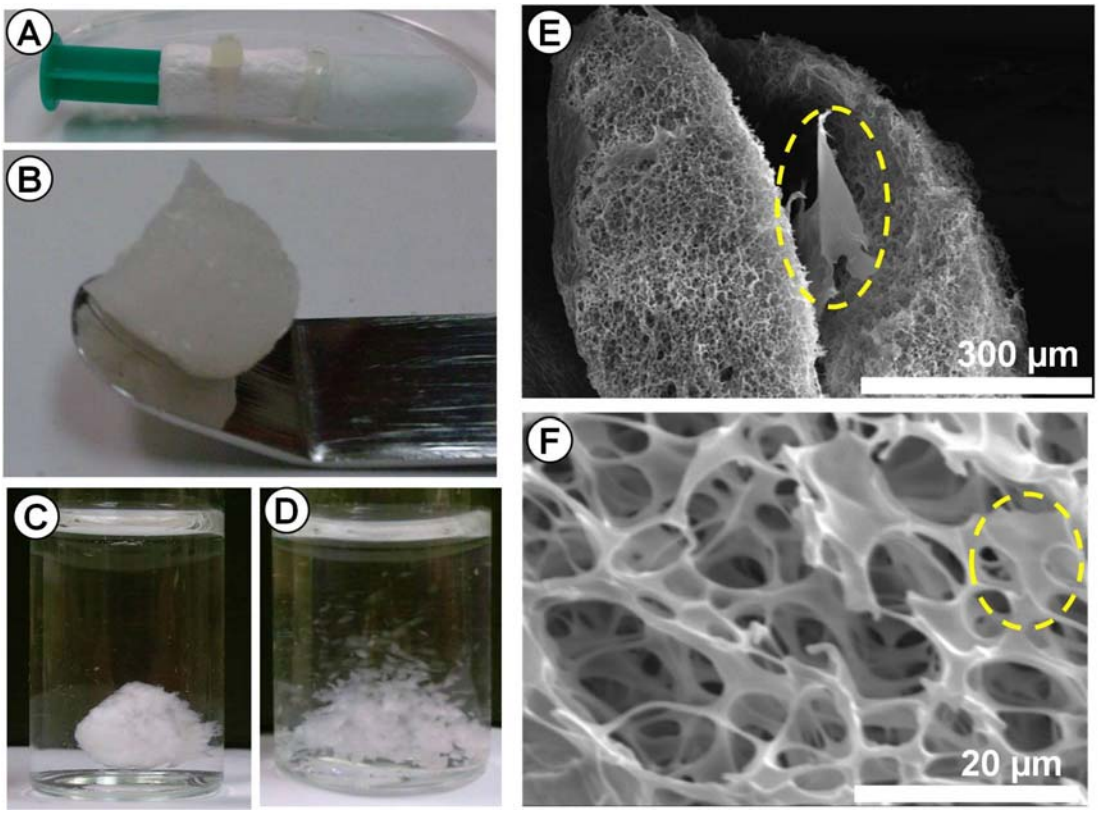

Figure 5-4: Attempts of reforming injected methacrylate-modified alginate polyHIPE hydrogel **PHMA** fragments by bringing the hydrogel particles into contact with either a Ca^{2+} solution alone or a combination of Ca^{2+} solution plus alginate. **A**: reforming set-up composed by a syringe plunger and a cellulose extraction thimble; **B**: one piece of scaffold after the reforming step (the width of the spatula is 1.0 cm); **C**: reformed scaffold immersed in distilled water; **D**: the same methacrylate-modified alginate hydrogel being injected into a $CaCl_2$ solution (50 mM) but without using alginate in the presence of Ca^{2+} as adhesive to bind the hydrogel fragments produced during extrusion together; **E** & **F**: SEM pictures of the inner structure of a reformed scaffold.

In order to reform a hydrogel monolith from the extruded hydrogel fragments under very mild conditions, a solution of unmodified alginate was used as adhesive to bind hydrogel fragments together in the presence of Ca^{2+} ions (**Figure 5-3**). A cellulose soxhlet thimble was chosen as the mould for forming a monolithic scaffold because in addition to offering confinement it is also permeable to Ca^{2+} ions and alginate (**Figure**

5-4 A). After methacrylate-modified alginate polyHIPE hydrogel were immersed in distilled water to reach equilibrium and were then soaked in 50 ml aqueous alginate solution with difference alginate concentrations (0.2 % w/v or 1.0 % w/v) for 24 h. The alginate solution acted as adhesive and an aqueous $CaCl_2$ solution acted as crosslinker to solidify the alginate solution, and so the hydrogel monolith fragments were stuck together and remodelled in to one cylindrical piece of hydrogel (diameter ≈ 1.3 cm, height ≈ 1 cm) (**Figure 5-4 B & C**) (the details of this experiment is in **9.13**). When handling the reformed hydrogel, it seems to have a similar strength and toughness to the touch compared with the same polyHIPE hydrogel before injection. Increasing the concentration of alginate from 0.2 % w/v to 1.0 % w/v led to a slight enhancement of the mechanical performance. The reformed scaffold did maintain its shape in water (**Figure 5-4 C**) without breaking into the original polyHIPE hydrogel fragments after gently shaking the glass tube. In sharp contrast, only hydrogel fragments could be observed when the same hydrogel was injected into thimble and soaked in $CaCl_2$ solution but without using alginate solution as adhesive to bond the hydrogel fragments produced during extrusion together (**Figure 5-4 D**). Ca^{2+}-crosslinked alginate thin films (**Figure 5-4 E** dashed circle), which act as binder for the whole scaffold, could be clearly observed between individual hydrogel fragments (**Figure 5-4 E**). Meanwhile, the interconnected porous structure could be clearly observed throughout the reformed scaffold without obvious pore size change

compared with the scaffold before injection (**Figure 5-4 F**). When the concentration of alginate "adhesive" used was 1.0 % w/v (higher alginate concentration was not selected because of the worries of the blockage of the pores caused by Ca^{2+}-crosslinked alginate), Ca^{2+}-crosslinked alginate films also could be observed in part of the pores inside the methacrylate-modified alginate polyHIPE **PHMA** and the pore walls became slightly thicker (**Figure 5-4 F,** dashed circle). However when the concentration of the alginate "adhesive" was decreased to 0.2 % w/v (lower alginate concentration was not selected because the worries of low mechanical strength of the reformed hydrogel), the change in pore morphology of the methacrylate-modified alginate polyHIPE hydrogel that brought by alginate adhesive was obviously lowered and so that it was difficult to notice the change in the morphology of polyHIPE matrix that brought by similar Ca^{2+}-crosslinked alginate films.

It is important to note that Ca^{2+}-crosslinked alginate is degradable *in vivo* within several days after implantation[242-243], which means these thin films will gradually disappear and will not affect the growth the cells loaded into the porous scaffolds before reforming. It has also been reported that the mechanical strength of the cell-seeded scaffolds increases substantially with the continuous construction of living tissue[244], which means the loss of alginate "adhesive" may be compensated by the growing tissue which may not necessarily lead to a overall loss of mechanical strength of the scaffolds during cell growth.

5.2.3 INJECTABILITY OF POLY((DEXTRAN-GMA)-CO-NIPAAM) POLYHIPE HYDROGELS

As described in **5.1**, the investigate of poly(dextran-GMA) polyHIPE hydrogels were focus on preformed scaffolds but not injectable scaffolds[155,162], because it is usually believed that covalently crosslinked polyHIPEs are not injectable. This section described the investigation of the injectability of poly((dextran-GMA)-*co*-NIPAAm) polyHIPE hydrogels and a safe solidification methods for these hydrogels.

Similar to the injectability experiment of ion-responsive methacrylate-modified alginate polyHIPE hydrogel **PHMA**, the injectability of thermo-responsive poly((dextran-GMA)-*co*-NIPAAm) polyHIPE hydrogel was studied as follows: several pieces of poly((dextran-GMA)-*co*-NIPAAm) hydrogel **DGN1** (diameter > 1 cm) were loaded into a syringe and gently squeezed through a hypodermic needle with inner diameter of 1.1 mm. The result of this type of injectability experiment of poly((dextran-GMA)-*co*-NIPAAm) polyHIPEs was similar to the methacrylated alginate polyHIPEs: the covalently crosslinked poly((dextran-GMA)-*co*-NIPAAm) hydrogel broke into smaller hydrogel fragments after being extruded through the needle. As expected the polyHIPE hydrogel easily deformed and could be compressed through the needle which resulted in 0.5 mm to 2.0 mm hydrogel polyHIPE fragments during extrusion (**Figure 5-5 A**). The sizes greater than the needle diameter are a

result of the highly porous soft foam nature of the polyHIPE which can be deformed and compressed to a smaller size reversibly upon exerting physical pressure. Despite the compression and shear the polyHIPE was exposed to during extrusion, the pore morphology and dimensions of the resulting polyHIPE fragments were not affected by the extrusion process (**Figure 5-5 B**), which attributes to the elasticity of the material. The interconnected pore structure of the polyHIPE hydrogel was retained without change of pore/pore throat size.

Similar to the investigation of injectability of methacrylate-modified alginate polyHIPEs, a follow-up experiment was designed to simulate a target area for injectable scaffolds, therefore we simulated the injection of the polyHIPE hydrogels into a piece of pork meat. A poly((dextran-GMA)-*co*-NIPAAm) polyHIPE hydrogel **DGN1** was injected into a piece of dead pork, which was then freeze dried within the muscle. An SEM image (**Figure 5-5 D**) shows that after freeze drying, the interconnected porous structure of poly((dextran-GMA)-*co*-NIPAAm) hydrogels was still clearly observable in the pork muscle. The surrounding soft tissue tightly surrounded the porous hydrogels (**Figure 5-5 C**) and no gap could be observed at the boundary between the pork muscle and hydrogel (**Figure 5-5 E**). No chemical reaction was required to generate the scaffold or an agglomeration scaffolds in the body, which should provide a safer route to injectable scaffolds as issues with *in situ*

polymerisation/crosslinking or residual initiator fragments or monomer do not arise during this injection and solidification procedure.

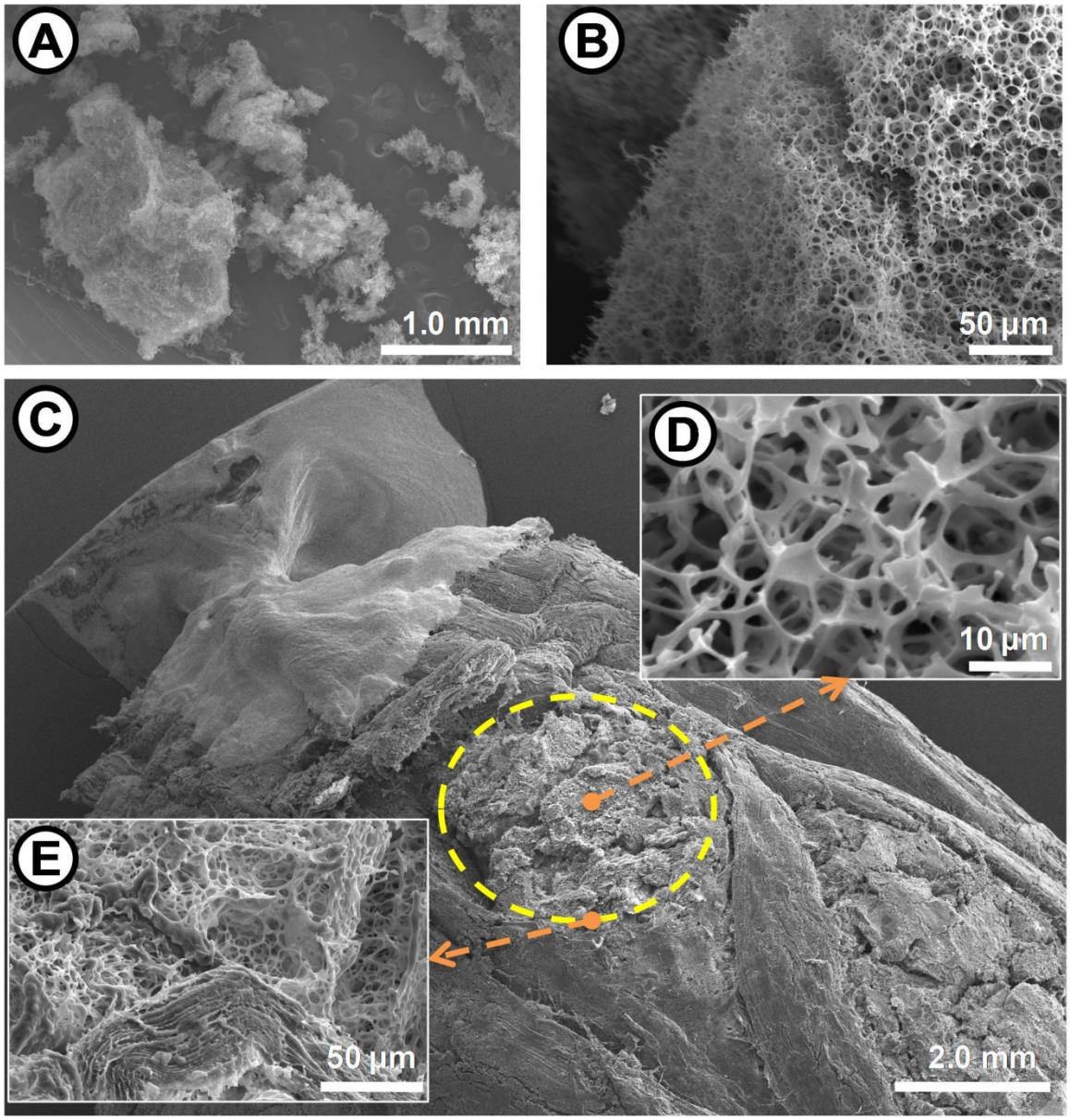

Figure 5-5: SEM images of a poly((dextran-GMA)-*co*-NIPAAm) polyHIPE hydrogel extruded through a needle. **A** & **B**: SEM image of hydrogel **DGN1** (the hydrogel was firstly freeze dried and then was immersed in distilled water to reach equilibrium before injection) passed through a needle with 1.1 mm inner diameter (A: low magnification, B: high magnification); **C**, **D** & **E**: hydrogel **DGN1** after being injected into a dead pork muscle.

5.2.4 SOLIDIFICATION OF POLY((DEXTRAN-GMA)-CO-NIPAAM) POLYHIPE HYDROGELS AFTER INJECTION

Aqueous alginate was used as adhesive to bond the hydrogel fragments produced during injection together into a monolithic scaffold because it can form hydrogel in the presence of Ca^{2+} (**Figure 5-6**). The Ca^{2+} needed for the gelation of the alginate solution could be directly obtained from the human body because the normal level of Ca^{2+} in the human body is 1.8 mM[122-123]. As illustrated in **Figure 5-6 B**, after being triggered by Ca^{2+} after injection, the solidified thermo-responsive poly((dextran-GMA)-*co*-NIPAAm) polyHIPE hydrogel fragments were embedded in a matrix of Ca^{2+}-crosslinked alginate. And the temperature rise caused by body temperature of the injected thermo-responsive polyHIPE might lead to the improvement of the mechanical performance of the scaffold. As mentioned before, Ca^{2+}-crosslinked alginate is degradable within several days in an aqueous environment[242-243]. But simultaneously it is expected that the mechanical strength of the cell-seeded scaffold increases substantially with the continuous construction of tissue[244] which means the loss of alginate adhesive could be compensated by the growing tissue which may not necessarily lead to a loss of the mechanical strength of the scaffold required to support the cells (**Figure 5-6 C**) [244].

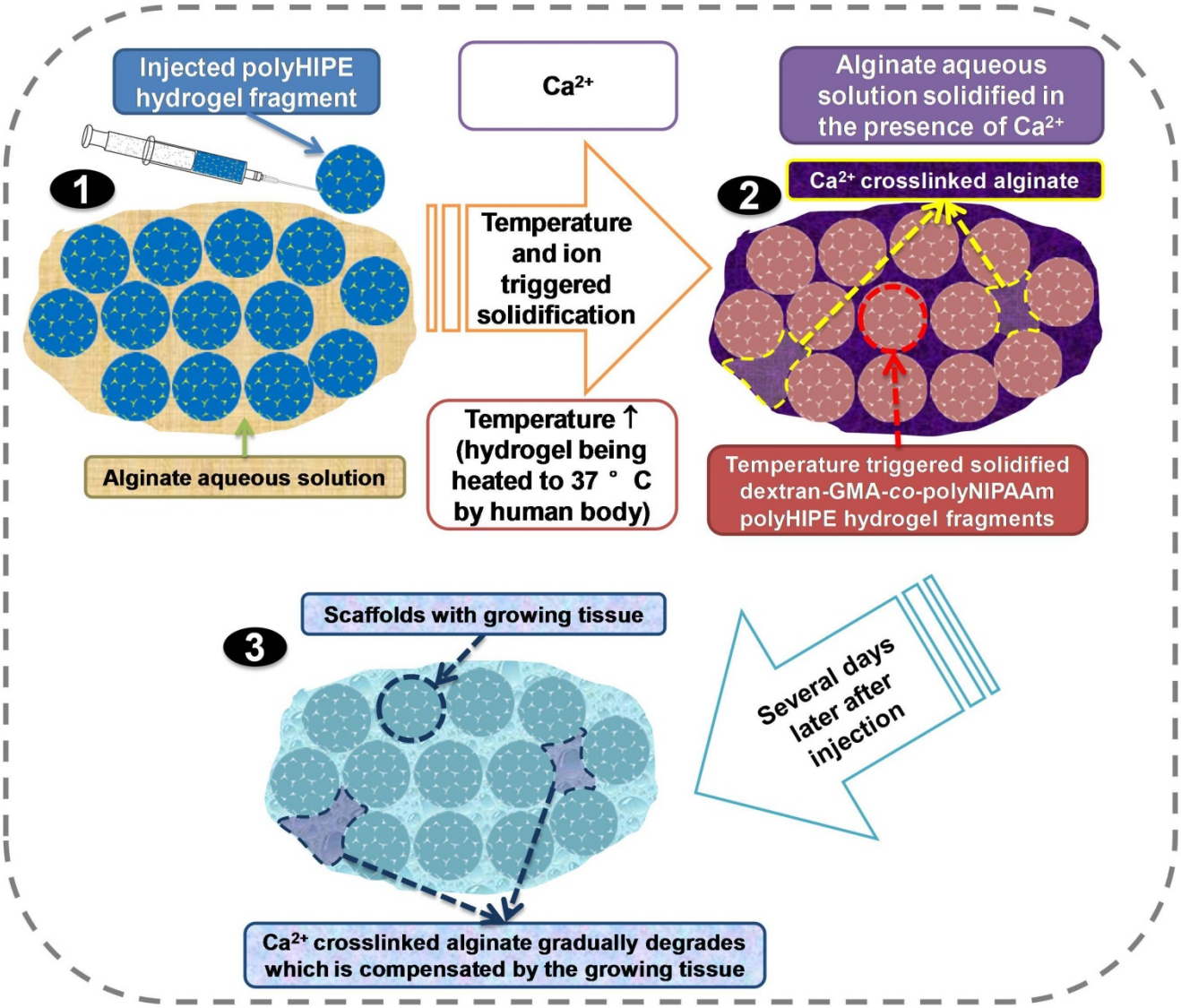

Figure 5-6: Schematic diagram of stimuli-responsive solidification of a thermo-responsive poly((dextran-GMA)-*co*-NIPAAm) polyHIPE hydrogel using a Ca^{2+} crosslinkable aqueous alginate solution as "adhesive" to bond the hydrogel fragments produced during injection/extrusion. (**1**): polyHIPE hydrogel is injected into the target area together with an aqueous alginate solution (hydrogel breaks into fragments during injection); (**2**): aqueous alginate solution gels in the presence of Ca^{2+} which bonds the generated polyHIPE hydrogel fragments together; meanwhile, the modulus of the thermo-responsive hydrogel increases triggered by body temperature; (**3**): Ca^{2+}-crosslinked alginate is degradable *in vivo* within several days after implantation while the mechanical strength of the cell-seeded scaffolds increases substantially with the continuous construction of tissue.

Similar to the experiment of reforming methacrylate-modified alginate polyHIPE hydrogels, a cellulose soxhlet thimble was chosen as the mould to reform poly((dextran-GMA)-*co*-NIPAAm) polyHIPE scaffold. 1.0 % w/v aqueous alginate solution was used as adhesive and 50 mM aqueous $CaCl_2$ solution (this concentration is higher than the average Ca^{2+} concentration in human body in order short gelation time to facilitate observation) as crosslinker to solidify the alginate solution. The polyHIPE hydrogel fragments were bonded together and remodelled into a single cylindrical piece of hydrogel with a diameter of about 0.8 cm and height of about 1 cm (**Figure 5-7 A**). After removing it from the mould and immersing it in a glass container filled with water, the reformed scaffold did maintain its shape without disintegrating into fragments even after shaking the container. When handling the reformed hydrogel, it seems to have a similar strength and toughness to the touch compared with the hydrogel before injection. Some thin films, which could be Ca^{2+}-crosslinked alginate, were clearly observed throughout the reformed scaffold (**Figure 5-7 B**). Although parts of the pore walls of polyHIPE hydrogel became thicker because of the presence of Ca^{2+}-crosslinked alginate, the interconnected porous structure could still be clearly observed without changing the pore size in the reformed scaffold together with some Ca^{2+}-crosslinked alginate films (**Figure 5-7 B**).

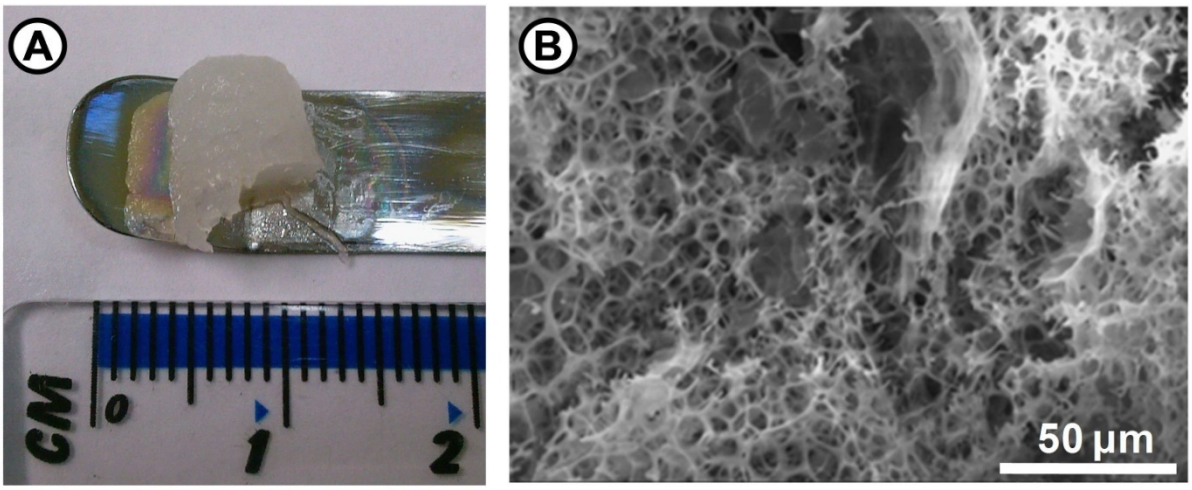

Figure 5-7: Reformed polyHIPE hydrogel **DGN1** scaffold fragments bonded by aqueous alginate solution in presence of Ca^{2+} ions: **A**: one piece of scaffold after re-crosslinking; **B**: SEM image of reformed scaffold.

5.3 CONCLUSIONS

It was shown that the well-defined pore structure of two different types of covalently crosslinked polyHIPEs hydrogel could be maintained after extrusion through a hypodermic needle. The resulting polyHIPE hydrogel particles could be reformed into a monolithic scaffold with a solution-based alginate "adhesive" in biocompatible conditions. This approach is a generic and potentially versatile method to produce porous hydrogels intended as injectable scaffolds for soft tissue engineering.

CHAPTER 6

THERMO-HIPES AS INJECTABLE SCAFFOLDS FOR TISSUE ENGINEERING

6.1 INTRODUCTION

In **Chapter 3** and **Chapter 4**, o/w HIPEs have been used to produce stimuli-responsive highly interconnected porous scaffolds for tissue engineering through covalent crosslinking as a means of introducing and maintaining the desired pore structure and a stimuli-responsive methods. We also have demonstrated that the well-defined pore structure of these two covalently crosslinked polyHIPEs could be maintained even after injection through a needle in **Chapter 5**. In this Chapter, we describe injectable HIPEs produced by using only thermo-responsive dextran-*b*-polyNIPAAm with a lower critical solution temperature (LCST) close to body temperature providing the function of crosslinking and thermo-responsiveness at the same time.

In most cases, crosslinking of HIPEs is carried out by radical polymerisation[15-16], sol-gel reaction[17] or enzymatic crosslinking[18]. If significant crosslinking occurs before

injection, one will have reached the point at which solidification causes the polyHIPE scaffold to break into smaller gel particles after extrusion through a hypodermic needle, as shown in **Chapter 5**; if radical polymerisation or sol-gel reactions of HIPEs occur *in vivo* after injection, irritation may be brought to the surrounding tissue. In the case of enzymatic crosslinking[18], HIPEs may not solidify fast enough *in vivo* to provide sufficient mechanical support. Producing a HIPE through a phase change of a thermo-sensitive polymer may offer a solution to the limitations of currently employed crosslinking chemistries.

We speculated that the physical aggregation between thermo-reversible polymer chains, such as polyNIPAAm, upon phase transition (LCST) may provide enough interpolymer chain interactions to maintain a porous structure such as the one generated in a HIPE. The gel or emulsion system can then be moulded (shaped) below the LCST of the polyNIPAAm components.

In our design we also tried to take account of the fact that the wettability of a scaffold for tissue engineering is very important for cell seeding in three dimensions.[171] Cell adhesion on synthetic polymer surfaces is generally poor due to their low hydrophilicity and lack of cell recognition sites on the scaffold surface.[245-247] In order to improve the biocompatibility of scaffolds, NIPAAm was grafted to dextran, a hydrophilic naturally occurring polysaccharide, which is better tolerated by the human body than most synthetic polymers and exhibits good biocompatibility.[197] Indeed by

using the HIPE templating method to this general approach, we were able to produce thermo-responsive scaffolds with solely interconnected pores.

6.2 RESULTS AND DISCUSSION

Following the strategy outlined in **Section 6.1**, we describe a versatile method to prepare thermo-responsive o/w HIPEs and solid-HIPEs (i.e. porous interconnected solids produced from HIPEs without covalent crosslinking) from thermo-responsive linear polymers, which can potentially be used as injectable scaffolds for tissue engineering (**Figure 6-1**).

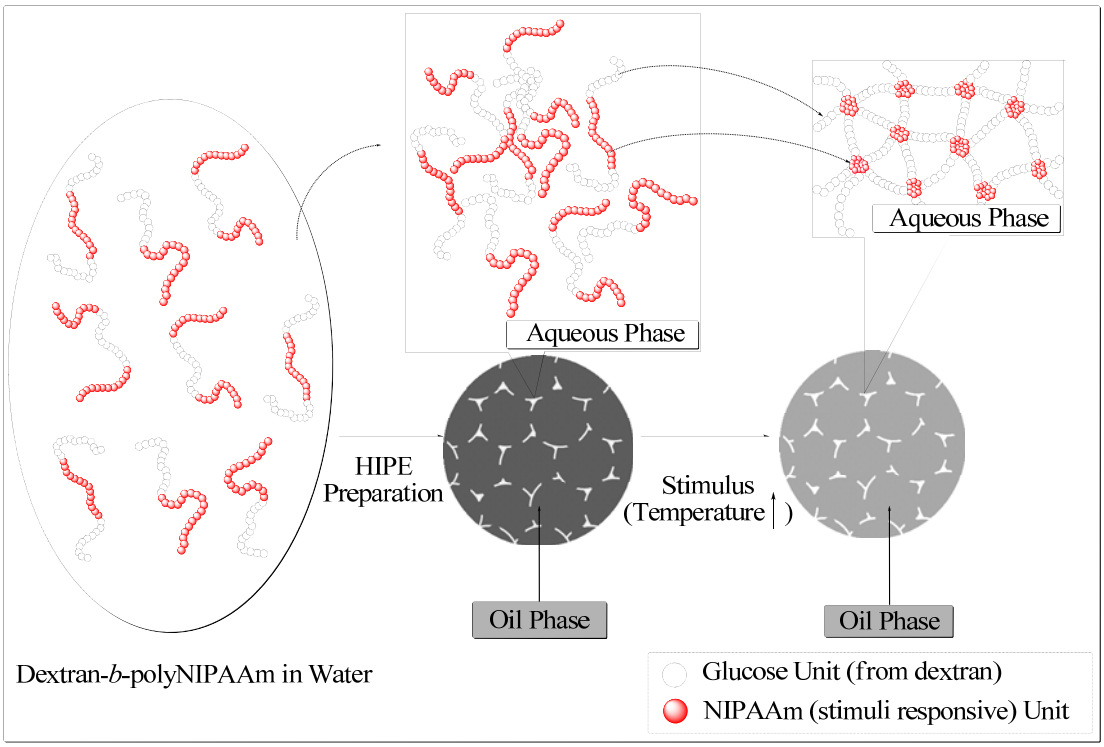

Figure 6-1: Scheme illustrating the proposed formation of crosslinked o/w HIPEs ("Thermo-HIPEs") employing the temperature-triggered phase transition (LCST) of polyNIPAAm segments and their aggregation as non-covalent crosslinking strategy.

We synthesised polyNIPAAm grafted dextran using ammonium cerium (IV) nitrate as a radical redox initiator, as described by Wang et al.[248] (the experimental details with NMR analysis are in **9.14**). According to detailed investigations by Chauvierre et al.[249] and Bertholon et al.[250], the product of the radical polymerisation between dextran and water-soluble vinyl monomers initiated by the redox system dextran and cerium (IV) salts at low pH, leads to linear block copolymers. A block copolymer (dextran-*b*-polyNIPAAm) was synthesised in this way with molecular weight averages of M_w = 28,000 Da and M_n = 13,600 Da as determined by aqueous gel permeation chromatography (GPC). The LCST of this block copolymer was determined to be 34 °C by turbidometry of a 0.2 % w/v aqueous solution heated from 24 °C to 38 °C (this experiment is described in **9.16**). It was observed that the viscosity/mechanical properties of a 20 % w/v dextran-*b*-polyNIPAAm aqueous solution clearly increased after being heated from room temperature to 38 °C (**Figure 6-2**).

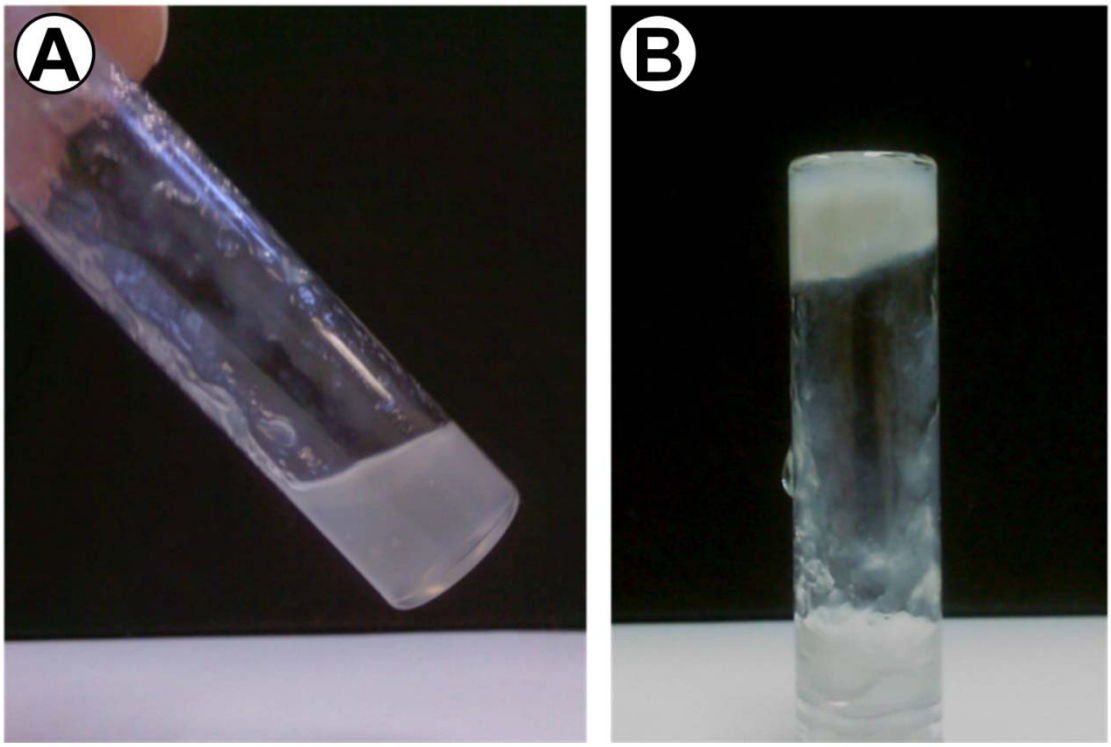

Figure 6-2: 20 % w/v dextran-*b*-polyNIPAAm aqueous solution: **A**: at room temperature; **B**: 10 min after being placed in oven at 38 °C.

Several thermo-responsive solid-HIPEs with different nominal pore volume or polymer concentration in the aqueous phase (i.e. solid-HIPEs prepared with thermo-responsive linear block copolymer) were prepared by o/w high internal phase emulsion templating with dextran-*b*-polyNIPAAm copolymer as the constituent of the continuous aqueous phase. Octylphenol ethoxylate (Triton X405, hydrophilic-lipophilic balance, HLB ≈ 18[251]) was chosen as the surfactant. In order to obtain solid-HIPEs, *p*-xylene was used as oil phase as it can be removed directly by freeze drying, unlike other water-immiscible solvents (e.g. toluene). The emulsification was carried out under stirring at 450 rpm and the formulations studied are listed in **Table 6-1**. Prior to lyophilisation of the HIPE, a syringe was filled with the HIPE and the emulsion was injected into a flask, followed by heating to 38 °C for 30 min to be above the LCST of the polyNIPAAm copolymer. A HIPE (**DN0**) purely made from

dextran (M_w=40,000) was also prepared as a reference. The experimental details are in **9.20**.

Table 6-1: Composition of dextran and dextran-*b*-polyNIPAAm copolymer HIPE formulations

Sample Code	Aqueous phase /oil phase (v:v)	Polymer in aqueous phase	Aqueous phase composition[a]: Polymer/Triton X405 (% w/v : % w/v)	Organic Phase
DN0	1 : 9	dextran	20 : 8.5	*p*-xylene
DN1	1 : 9	dextran-*b*-polyNIPAAm	20 : 8.5	*p*-xylene
DN2	1 : 4	dextran-*b*-polyNIPAAm	20 : 8.5	*p*-xylene
DN3	1 : 9	dextran-*b*-polyNIPAAm	25 : 8.5	*p*-xylene

[a] Concentration of dextran or dextran-*b*-polyNIPAAm copolymers and Triton X405 in distilled water

In the SEM images of dextran solid-HIPEs and dextran-*b*-polyNIPAAm thermo-responsive solid-HIPEs, the open-porous structure typical for polyHIPEs can be seen clearly (**Figure 6-3 A, B, D & E**). It was visually observed that the dimensions of HIPEs were not changed before and after freeze drying and it could believe that freeze drying allowed to maintain the pore dimensions. The pore diameters range from 4~7 μm (**Table 6-2**). Compared to the dextran-*b*-polyNIPAAm thermo-responsive solid-HIPEs (**DN1, DN2 and DN3**), the dextran solid-HIPE possesses no clear pore throats (**Figure 6-3 C**) and its pore size is smaller (approx. 2 μm).

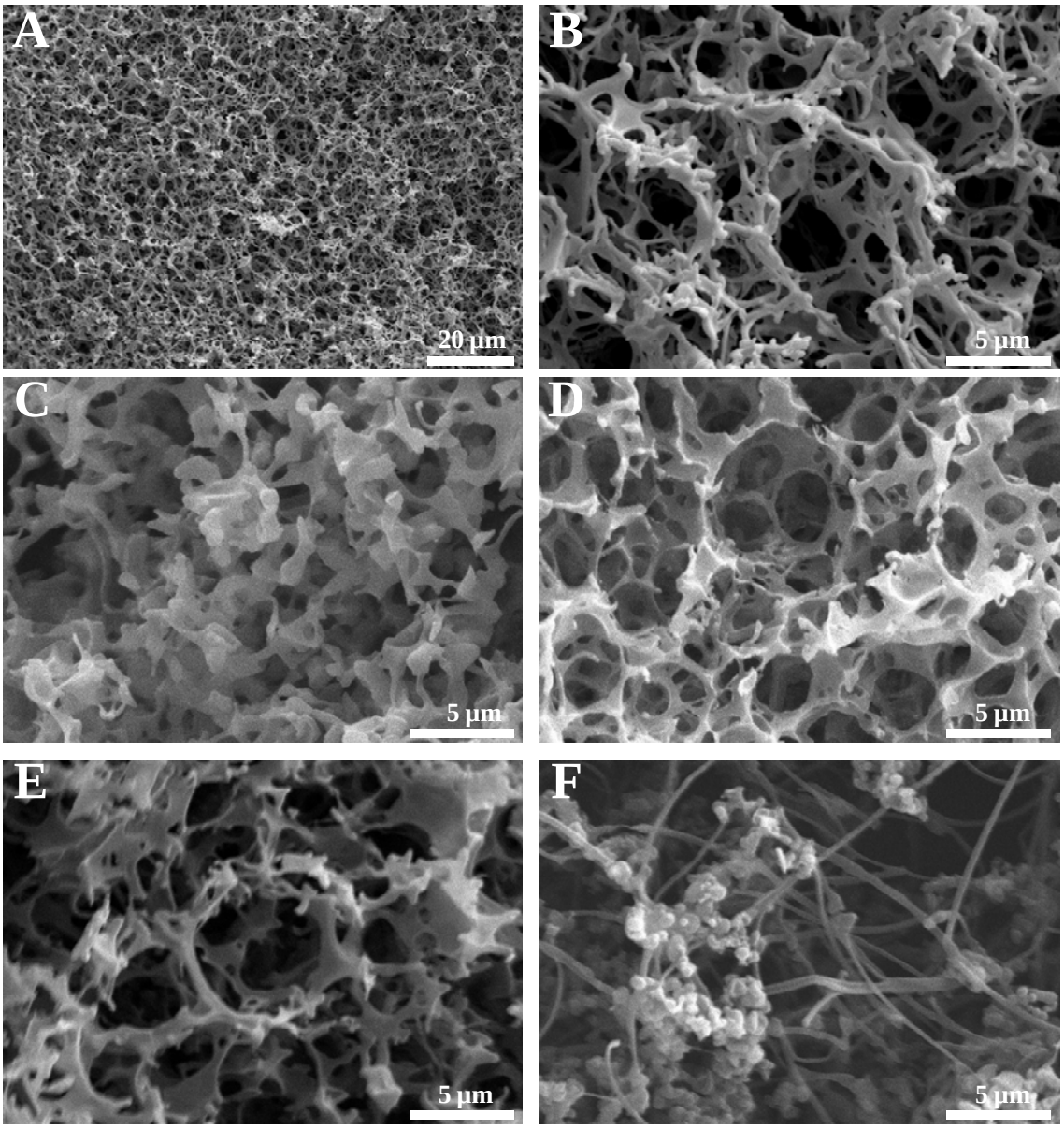

Figure 6-3: SEM images of dextran solid-HIPE and dextran-*b*-polyNIPAAm thermo-responsive solid-HIPEs showing the changes in pore size, pore morphology and connectivity for the three polyHIPEs **DN0**, **DN1** and **DN2**: **A** & **B**. dextran-*b*-polyNIPAAm thermo-responsive solid-HIPE with 90 % v/v nominal pore volume and 20 % w/v polymer concentration (**DN1**); **C**. dextran solid-HIPE with 90 % v/v nominal pore volume and 20 % w/v polymer concentration (**DN0**); **D**. dextran-*b*-polyNIPAAm thermo-responsive solid-HIPE with 80 % v/v nominal pore volume and 20 % w/v polymer concentration (**DN2**); **E**. dextran-*b*-polyNIPAAm thermo-responsive solid-HIPE with 90 % v/v nominal pore volume and 25 % w/v polymer concentration (**DN3**); **F**. thermo-responsive solid-HIPE **DN1** soaked in 38 °C water for 14 d.

Table 6-2: Density, porosity, pore volume, pore/pore throat size and pore wall thickness of solid-HIPE and thermo-responsive solid-HIPEs **DN0-DN3**

Sample Code	Absolute Density (g/cm^3) [a]	Envelope Density (g/cm^3) [b]	Porosity (%)[b]	Pore Volume (cm^3/g) [b]	Pore Size (μm) [c]	Pore Throat Size (μm) [c]	Pore Wall Thickness (μm) [c]
DN0	1.490	0.245	83.6	3.416	1.4~2.4	N/A	0.3~1.4
DN1	1.438	0.131	90.0	6.928	3.6~7.5	0.4~1.3	0.2~1.6
DN2	1.500	0.145	90.4	6.243	4.0~7.0	0.5~1.8	0.5~3.4
DN3	1.466	0.123	91.6	7.448	4.7~7.3	1.0~2.7	0.5~2.5

[a] Determined using GeoPyc 1360. [b] Determined using AccuPyc 1330. [c] Determined from SEM images.

The pore walls became slightly thicker when the concentration of the dextran-*b*-polyNIPAAm in the aqueous phase was increased from 20 % w/v (**Figure 6-3 B**) to 25 % w/v (**Figure 6-3 E**). Reducing the volume percentage of the dispersed phase also resulted in thicker pore walls (**Figure 6-3 D**).

The LCST of polyNIPAAm is reported to be 32 °C[98], whilst we measured the LCST of dextran-*b*-polyNIPAAm copolymer to be 34 °C using turbidity experiments. The raise of the LCST of polyNIPAAm copolymers is caused by copolymerising NIPAAm with hydrophilic dextran. Several experiments were conducted in order to investigate and compare the dissolution behaviour of thermo-responsive solid-HIPEs in water below and above their LCST (**Figure 6-3**) (the experimental details are in **9.22**). A solid-HIPE made of dextran (**DN0**) was placed in distilled water, which

dissolved instantly at 24 °C and 38 °C as was expected for pure dextran. Dextran-*b*-polyNIPAAm thermo-responsive solid-HIPE (**DN1**) was treated in the same way and also dissolved completely at 24 °C (below the LCST), but the process took about 10 min to complete. We compared this with a freeze-dried sample of a polyNIPAAm homopolymer (**N1**) (M_n = 37,600 Da and M_w = 96,200 Da) dehydrated above LCST (the experimental details are in **9.21**) which required a similar period of time (around 12 min) to dissolve at 24 °C, whereas covalently crosslinked polyNIPAAm hydrogels with relatively similar pore size and/or porosity to our solid-HIPEs, are reported to take about 20 s[252] in one example (for 10~50 μm pore sizes) and in another one 1 min[253] (10 μm pore size, 80% porosity) to reach their fully swollen state (below LCST) starting from a fully shrunken state (above LCST). In stark contrast, at 38 ^oC no volume change of the thermo-responsive solid-HIPE was detected even after having been left to float on water for 14 d. This behaviour can be explained because the polyNIPAAm block segments phase inverted above the LCST of the block copolymer while simultaneously producing physical crosslinks through aggregation of neighbouring. The dextran-*b*-polyNIPAAm thermo-responsive solid-HIPEs were freeze dried after this 14 d period of being exposed to water and again characterised by SEM. Interestingly the interaction between polymer and water caused the pore morphology of the thermo-responsive solid-HIPEs to change. Two different morphologies, globular and fibrous (**Figure 6-3 F**) were observed. The globular morphology (diameter ≈ 0.5~0.9 μm) might be caused by the reorganisation/reshaping

of the walls around the pore throats into aggregates of globules in the continuous phase. The fibrous morphology (width ≈ 0.2~0.9 μm) can be rationalised by plasticisation of the polymer through water driven by the minimisation of interfacial energy (**Figure 6-3 F**).

Table 6-3: Observations made during solubility tests of solid-HIPEs and thermo-responsive solid-HIPEs in water above and below the LCST of dextran-*b*-polyNIPAAm

	24 °C Water	38 °C Water
Dextran solid-HIPE (**DN0**)	Dissolves instantly	Dissolves instantly
Dextran-*b*-polyNIPAAm thermo-responsive solid-HIPE (**DN1**)	Disintegrates into small pieces which sink to the bottom of container and dissolve completely within 10 min	Floats in water, no apparent volume loss observed visually during a period of 14 d

In order to assess the biocompatibility of the thermo-HIPE matrix, in vitro cell-seeding experiment was performed by cultivating A549 human alveolar adenocarcinoma cells onto thermo-HIPEs (the experimental details are in **9.32**). Judging from the colonisation of the cells in the scaffolds in SEM images (**Figure 6-4**), and their assumption of typical squamous, epithelial morphologies in these regions, A549s will likely be able to populate the inner regions as well should these appropriate modifications be made. It seems that some of the cells were encapsulated in the thermo-HIPE matrix.

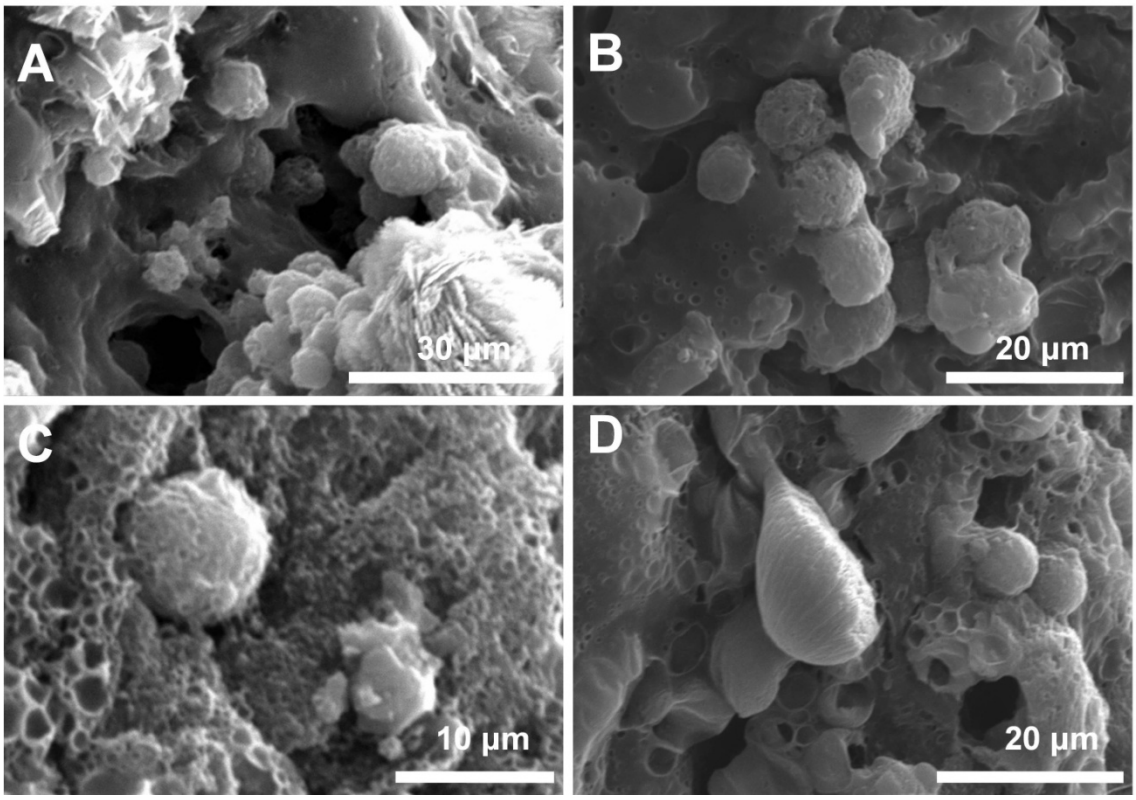

Figure 6-4: SEM images of A549 cells growing on thermo-HIPEs: **A** & **B**: thermo-HIPE **DN2**; **C** & **D**: thermo-HIPE **DN3**.

6.3 CONCLUSIONS

Experiments with dextran-*b*-polyNIPAAm thermo-responsive solid-HIPEs demonstrated that it is possible to prepare very high porosity (> 90%) solid macroporous hydrogels without the need for chemical crosslinks. The interconnected porous structure of the thermo-responsive solid-HIPE forms by aggregation of polyNIPAAm blocks within the copolymer. We have shown that the porous structure is maintained in an aqueous environment above 37 °C. This is a new, versatile method to prepare o/w HIPEs and fabricate interconnected porous hydrogels using a thermal

trigger in the guise of thermo-responsive polymers i.e. using non-covalent interactions. No chemical reaction is required during the preparation of the solid-HIPEs. This particular feature should provide a safer route to injectable scaffolds as issues of polymerisation/crosslinking chemistry or residual initiator fragment or monomer being biocompatible do not arise in our case, as all components can be supplied pure prior to HIPE formation. For the purpose of *in vivo* use, the internal oil phase can be easily displaced by other water-immiscible non-cytotoxic liquids, such as squalene or herring oil.[254-255]

CHAPTER 7

POROUS SCAFFOLDS PREPARED BY O/W PICKERING-HIPE TEMPLATING FOR TISSUE ENGINEERING

7.1 INTRODUCTION

Conventional o/w HIPEs, including the HIPEs introduced in **Chapter 3 & 4**, are usually stabilised by surfactants, most of which are not biocompatible or even toxic[181-186]. Besides surfactant, colloidal particles, such as inorganic nanoparticles[166,187-189] or microgel particles[192] have also been used to stabilise HIPEs (also called Pickering-HIPEs).[193] Compared with conventional surfactant stabilised HIPEs, particle stabilised HIPEs (i.e. Pickering-HIPEs) possess a number of advantages; the resulting emulsions are extremely stable, pore walls of the resulting porous materials are functionalised with a layer of particles and so additional properties can be introduced in this way, such as improved biocompatibility, electrical conductivity and/or drug release properties, etc. are introduced.

HAp (hydroxyapatite, $Ca_{10}(PO_4)_6(OH)_2$) is the main inorganic compound of bones and teeth and it is biocompatible, bioactive, biodegradable, nontoxic and noninflammatory.[256-258] It has been demonstrated that HAp plays an important role in biomineral formation[257,259] and can be used as a dental filling material[260] or implant material for periodontal bone defects[256]. Moreover, as HAp has the advantage of absorbability and high binding affinity with a variety of molecules, it have also been used as carrier for the delivery of a variety of pharmaceuticals[258,261-262], growth factors[263] or genes[264-265]. In Pickering-HIPEs, the emulsifying particles are absorbed at the interface between the continuous and dispersed phase[193-194]. It was reported that after polymerisation of the continuous phase, the particles are present on the surface of pore walls[266]. Taking account of this fact, using HAp nanoparticles as emulsifier for emulsion templating is not only simply looking for a biocompatible biodegradable emulsifier as a substitute to conventional surfactants, but also it is possible to introduce the biomedical merits of HAp (e.g. noninflammatory.[256-258] and promote biomineral formation[257,259]) into the emulsion templated macroporous materials. HAp particles are usually hydrophilic[267] and hydrophilic particles do stabilise o/w Pickering emulsions[268]. Fujii et al.[269] have reported o/w emulsion stabilised by HAp nanoparticles with long-axis length ranges of 40 nm to 2320 nm, but the internal phase volume of Pickering emulsion did not go above 50%. To date no reports of HAp stabilised o/w HIPEs and their resulting polyHIPE hydrogels are available.

Beside HAp nanoparticle as stabiliser for emulsions, stimuli-responsive microgel particle stabilised emulsions are also a new field of research in Pickering emulsions. One advantage of this type emulsifier is that microgels are relatively easy to synthesise compared to hybrid particles like surface-modified latices or other inorganic/polymer hybrid particles.[270] Stimuli-responsive microgel particles, especially polyNIPAAm based microgel particles, exhibit an response to changes in temperature, pH or ionic strength, which lead to changes in hydrophilicity, particle size and water content of the microgels over a small (about 5 °C to 10 °C) temperature range.[271] The variable properties of this kind of emulsifier provide extended emulsion control (e.g. breaking the emulsion on demand). Moreover, these stimuli-responsive microgel emulsifiers absorb at the interface between the continuous and dispersed phase in Pickering-HIPEs[193-194] and therefore, they could potentially be used as drug/growth factor carrier.

In **Chapter 3 to 6,** we introduced several novel stimuli-responsive HIPE templated macroporous scaffolds, including covalently crosslinked polyHIPE hydrogels and non-covalently crosslinked thermo-HIPEs. However the desired features introduced so far to render these materials suitable as potential scaffolds for tissue engineering fall short of what is ultimately required. For example the emulsifier Triton X405 used to prepare o/w thermo-HIPEs is not biocompatible or biodegradable. Also the pore and pore throat sizes of these porous materials are relatively small for some types of cells (e.g. the skin cell size is about 30 μm, which is 10 μm to 20 μm bigger than the

pore sizes of polyHIPEs introduced in **Chapter 3** to **6**).[272] A possible approach to solve both of these problems is to use particles to substitute conventional surfactants in order to stabilise o/w HIPEs. An additional benefit may arise as the use of particles as emulsifiers can be exploited to functionalise the pore walls of the monolith with a layer of such particles and introduce additional properties, such as improved biocompatibility and/or drug release properties.

In this Chapter, we report o/w Pickering-HIPEs solely stabilised by either commercially available hydroxyapatite (HAp) nanoparticles or stimuli-responsive poly(*N*-isopropylamide)-*co*-(acrylic acid) (PolyNIPAAm-*co*-AA) microgel particles, which could be used as template to prepare surfactant-free thermo-HIPEs. These colloidal particles are adsorbed at the o/w interface to hinder extensive droplet coalescence. Limited coalescence is still taking place, which depends on the particle concentration and the interfacial area generated. The pore dimension and pore morphologies of the Pickering-HIPE templated porous materials can be tailored by ripening or simply changing the particle concentration.

7.2 RESULTS AND DISCUSSION

7.2.1 HYDROXYAPATITE BASED POLY-PICKERING-HIPES AND THERMO-HIPES

We prepared o/w Pickering-HIPEs solely stabilised by commercially available HAp nanoparticles with 150 nm to 200 nm average particle size as determined from its SEM image (**Figure 7-1**). The HAp nanoparticles were used without any modification because o/w emulsions were intended to be stabilised and moreover it would be desirable to retain the biological merits of HAp (such as noninflammatory.[256-258] and promote biomineral formation[257,259]). Methyl myristate-in-water Pickering-HIPEs with 80% internal phase volume were prepared simply by homogenising a mixture of 4.0 ml methyl myristate, and 1.0 ml 1.0 % w/v or 0.5 % w/v HAp particles aqueous suspension for 15 s to 25 s (longer dispersion time could lead to destabilisation of emulsions). The homogenising speed was more than 5,000 rpm to provide enough energy to break droplets and form a HIPE at room temperature (the experimental details are in **9.23**). With methyl myristate as the internal phase, the Pickering-HIPEs were stable at room temperature for more than one month and only a thin layer of the oil phase above the sedimented emulsion could be observed after one month. **Figure 7-2** shows the digital photographs of methyl myristate-in-water Pickering-HIPEs with 80% internal phase volume 20 min after homogenisation stopped. Deformed HIPE

droplets[157] ranging from 0.5 mm to 2.7 mm could be clearly observed. These results show that HAp particles are able to stabilise o/w HIPEs.

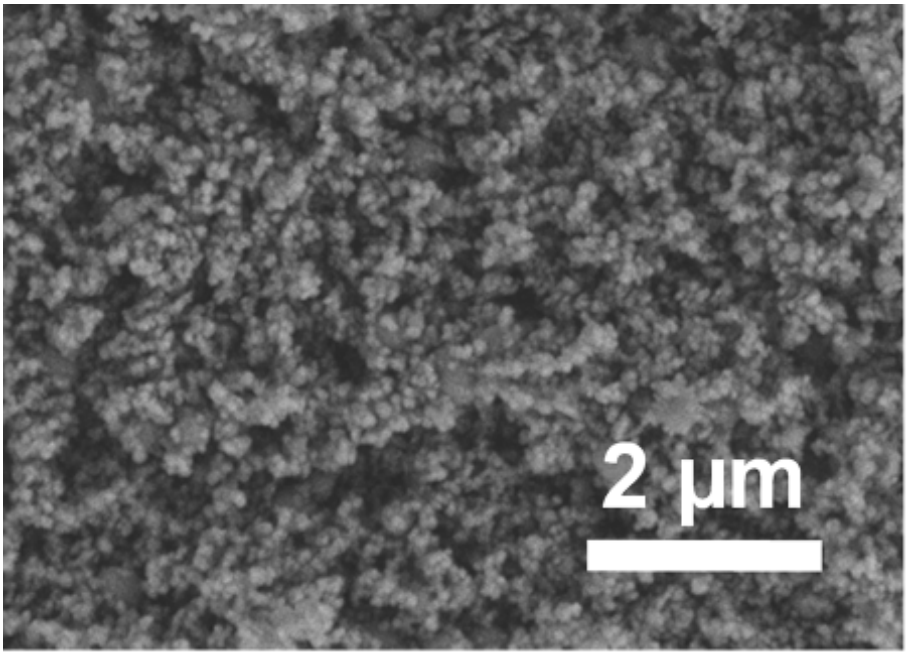

Figure 7-1: SEM image of commercial available HAp nanoparticles used. (HAp was purchased from Sigma-Aldrich Company Ltd. (Poole, UK) with particle size less than 200 nm)

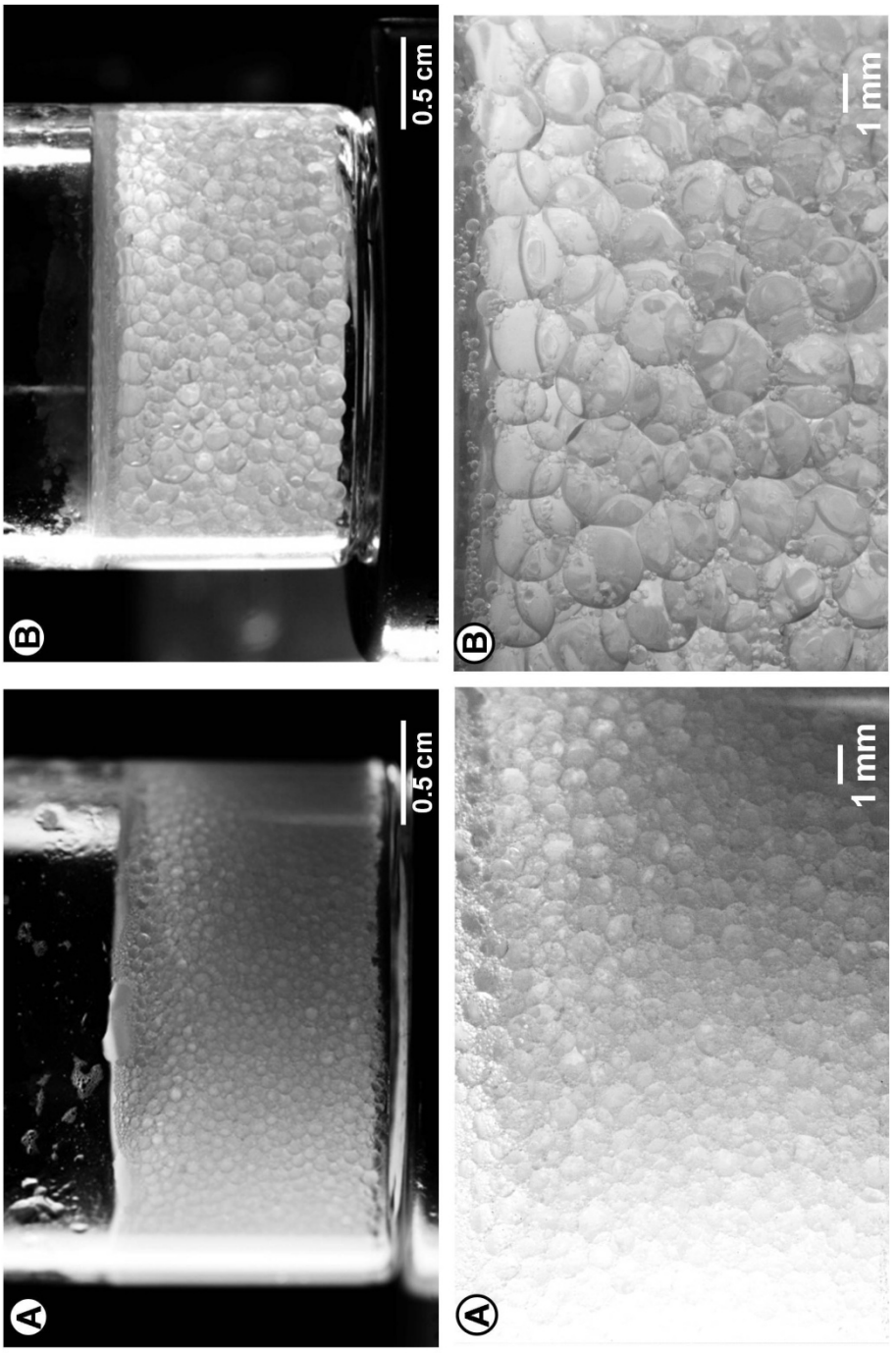

Figure 7-2: Digital photographs taken 20 min after preparation of methyl myristate-in-water Pickering-HIPE solely stabilised by HAp nanoparticles. The emulsions here were prepared by homogenisation at 5,000 rpm for 15 s: **A**: 1.0 % w/v particle concentration in its aqueous phase, **B**: 0.5 % w/v particle concentration in its aqueous phase. (Bottom row at higher magnification)

A smaller droplet size of HAp stabilised Pickering HIPE (decreased from 1.2 ~ 2.7 mm to 0.5 ~ 1.1 mm) was observed when increasing HAp particle concentration in the aqueous phase from 0.5 % w/v (**Figure 7-2 B**) to 1.0 % w/v (**Figure 7-2 A**), while the dispersion condition (homogenised at 5,000 rpm for 15 s) is unchanged. That is because the increased particle concentration allows to stabilise more interface[273] and also results in denser particle layers which limits coalescence[15]. Meanwhile, using the same nanoparticle concentration (1.0 % w/v) but increasing the homogenising speed form 5,000 rpm to 15,000 rpm leads to a sharp decrease of about 30-40 fold of the droplet size from 1.2 ~ 2.7 mm to 30~130 μm. This is because the emulsion is broken up into smaller droplets at a higher input energy. The droplet size of the Pickering-HIPE produced by homogenisation at 15,000 rpm is below the optical resolution of a standard digital camera and thus was detected using optical microscopy (**Figure 7-3**).

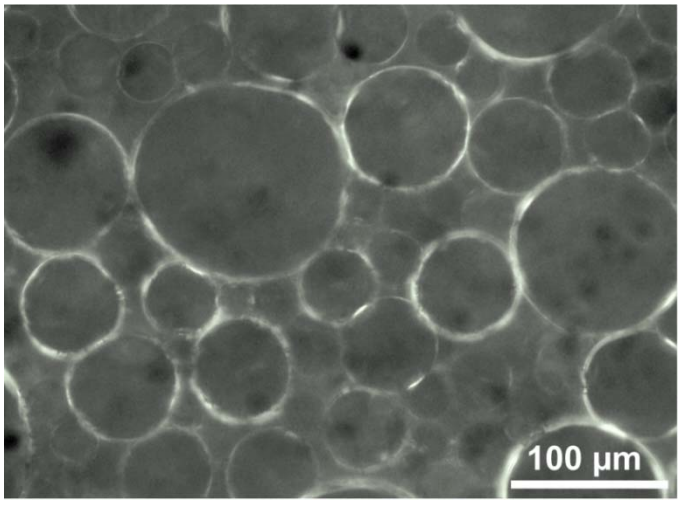

Figure 7-3: Optical microscope image of a methyl myristate-in-water Pickering-HIPE solely stabilised by 1.0 % w/v HAp nanoparticles produced through homogenisation at 15,000 rpm for 25 s.

As we wanted to prepare o/w Pickering-HIPE hydrogels that meet from both a chemical composition and processing point of view, the demands placed on porous materials for applications in the medical field (e.g. scaffolds in tissue engineering or drug carrier in drug delivery), dextran-GMA was polymerised and thus crosslinked in the aqueous phase of Pickering-HIPEs. For this water soluble and highly biocompatible methacrylated polysaccharide[155], a porous hydrogel with tunable pore sizes varying from 1.5 μm to 41.0 μm were obtained (**Table 7-1**). A series dextran-GMA poly-Pickering-HIPE hydrogels were prepared from HIPE templates stabilised by different amounts of HAp nanoparticles (the HAp nanoparticle concentrations in the aqueous phase of Pickering HIPEs ranged from 0.3 % w/v to 1.0 % w/v). Different homogenising and curing conditions were explored in order to investigate their influences on pore size and pore morphology of Pickering polyHIPEs (**Table 7-1**, entries **PPH1** to **PPH7**) (the experimental details are in **9.24**). After the oil phase (methyl myristate or soybean oil) was removed by soxhlet extraction using methanol followed by acetone, the percentage of HAp nanoparticles incorporation into these hydrogels was confirmed by thermogravimetric analysis (TGA) (the experimental details are in **9.25**). The percentage weight of HAp nanoparticles embedded into the hydrogel is in proportion to their initial concentration in the original HIPE (**Table 7-1**).

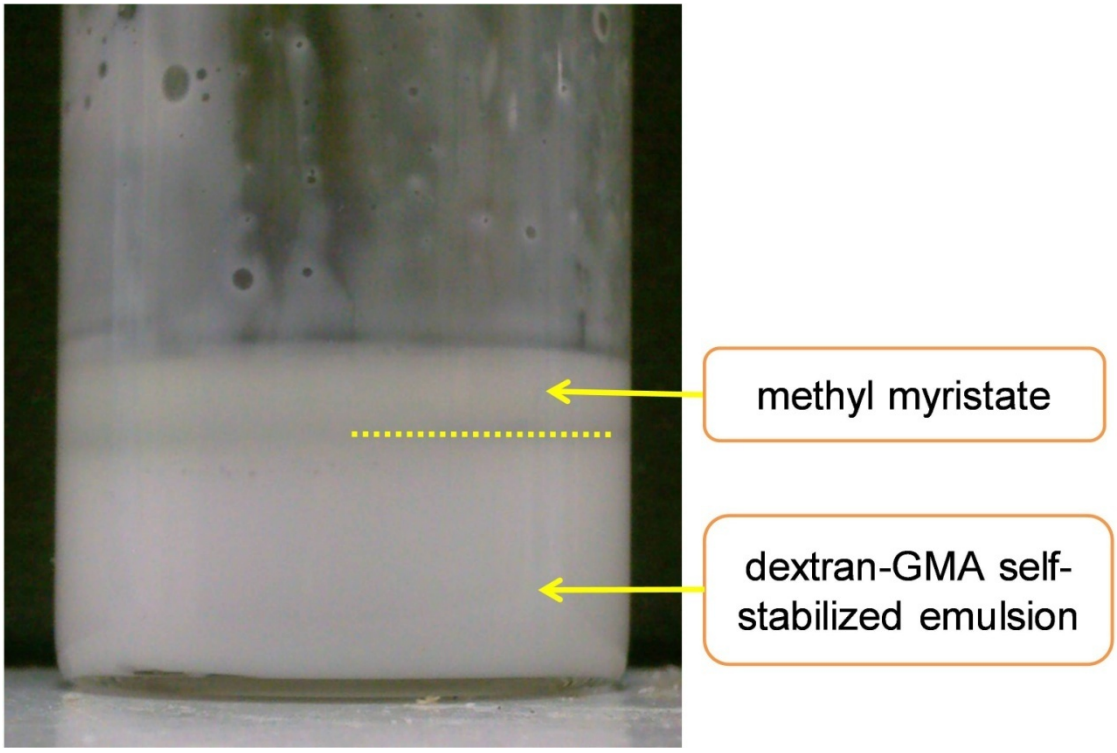

Figure 7-4: Mixture of 20 % w/v aqueous dextran-GMA solution and methyl myristate after homogenising at 20,000 rpm for 60 s (dextran-GMA solution: methyl myristate = 1:4 v/v). The maximum nominal internal phase volume of a dextran-GMA stabilised emulsion was only close to 70% and excess methyl myristate could not be dispersed into the aqueous phase of the emulsion.

As a control, we also homogenised a mixture of a 20 % w/v aqueous dextran-GMA solution and methyl myristate without HAp nanoparticles at 20,000 rpm for 60 s (**Figure 7-4** and **Table 7-1**, **DGS**). Since dextran is hydrophilic and the grafted glycidyl methacrylate moiety is hydrophobic, dextran-GMA itself could act as an emulsifier to stabilise a methyl myristate-in-water emulsion. But without HAp nanoparticles, the maximum nominal internal phase volume of a dextran-GMA stabilised emulsion was only close to 70 % v/v (aiming for 80 % v/v) and thus it is clear that excess methyl myristate could not be dispersed into the aqueous phase of the emulsion (the oil phase volume of the emulsion was calculated from the original

composition and the volume of methyl myristate that did not dispersed into the aqueous phase). A significant amount (about 30 % v/v) of the internal oil phase was expelled after homogenising stopped (**Figure 7-4**).

Different form the closed pore morphology in dextran-GMA self-stabilised sample **DGS** (**Figure 7-5 A**), an open porous structure[15] typically for polyHIPEs was clearly observed in the SEM micrographs of **PPH1** to **PPH7** (**Figure 7-5 B** to **Figure 7-5 I**). The pore size of the dextran-GMA poly-Pickering-HIPEs ranges from 1 μm to 40 μm, about 100 times smaller than the droplets size of Pickering-HIPEs **PPH1** and **PPH2** (**Figure 7-2**). A possible explanation for this change is that the monomer dextran-GMA also acts as nonionic surfactant and co-stabilises the HIPE together with HAp nanoparticles. Introducing dextran-GMA monomer/co-emulsifier into Pickering-HIPE may increase emulsion stability and consequently results in a smaller average droplet size, due to the (presumed) lower interfacial strength.[15]

Table 7-1: Compositions and properties of hydrogel polyHIPEs **PPH1-PPH8** obtained from dextran-GMA HAp nanoparticle stabilised poly-Pickering-HIPEs and a dextran-GMA stabilised emulsion template **DGS**.

Sample	Aqueous phase composition[a]: Dextran-GMA/APS/HAp Particle (% w/v:% w/v:% w/v)	Homogenising speed and duration	Oil phase type	Ripening time before polymerisation	Average pore size (μm[d])	Average pore throat size (μm[d])	Incorporated HAp nanoparticle proportion (% w/v[e])
PPH1[b]	20:5:1	15,000 rpm, 25 s	methyl myristate	0 d	1.51	0.62	3.9
PPH2[b]	20:5:1	5,000 rpm, 15 s	methyl myristate	0 d	17.27	2.55	4.4
PPH3[b]	20:5:1	5,000 rpm, 15 s	methyl myristate	7 d	27.54	2.61	1.8
PPH4[b]	20:5:1	5,000 rpm, 15 s	methyl myristate	14 d	41.00	7.72	2.3
PPH5[b]	20:5:0.5	5,000 rpm, 15 s	methyl myristate	0 d	16.13	3.82	1.6
PPH6[b]	20:5:0.3	5,000 rpm, 15 s	methyl myristate	0 d	17.12	4.78	1.4
PPH7[b]	20:5:1	5,000 rpm, 15 s	soybean oil	0 d	3.50	1.46	3.9
PPH8[b]	20:5:1	5,000 rpm, 15 s	soybean oil	7 d	13.04	2.95	1.9
DGS[c]	20:5:0	20,000 rpm, 60 s	methyl myristate	0 d	1.64	-	0.3

[a] The aqueous phase of all samples is a 20 % w/v dextran-GMA aqueous solution with 50 mg/ml ammonium persulfate (APS) as radical initiator and HAp nanoparticles as emulsifier. [b] Dextran-GMA poly-Pickering-HIPEs with 80% nominal pore volume. [c] Dextran-GMA stabilised emulsion templated hydrogel with about 70% nominal pore volume. [d] Determined from the corresponding SEM micrographs. [e] Determined by thermo gravimetric analysis (TGA) in air for temperature range greater than 600 °C

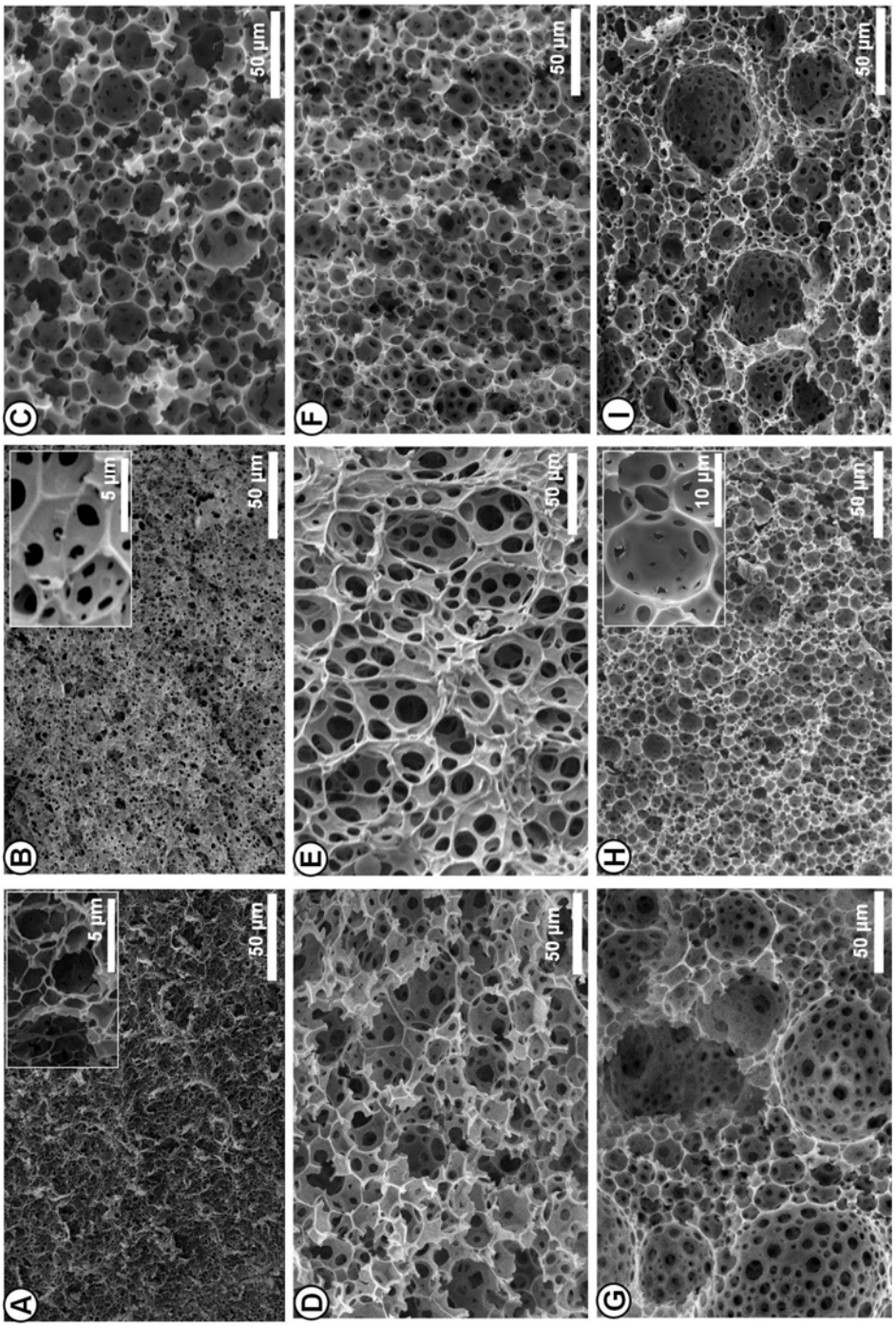

Figure 7-5: SEM micrographs of a poly(medium internal phase emulsion) (polyMIPE) produced from a dextran-GMA stabilised MIPE template and dextran-GMA HAp stabilised poly-Pickering-HIPE hydrogels: **A**: **DGS**; **B**: **PPH1**; **C**: **PPH2**; **D**: **PPH3**; **E**: **PPH4**; **F**: **PPH5**; **G**: **PPH6**; **H**: **PPH7**; **I**: **PPH8**.

Different applications require porous materials with different pore dimensions. For example, the pore sizes of drug delivery systems vary from 5 nm to 50 μm[274-275], but the pores of scaffolds in tissue engineering should be in the range of 15 μm to 300 μm depending on the cell type to be cultured[276]. In order to prepare Pickering-HIPE templated hydrogels with a range of pore sizes, we demonstrated several simple but effective tuning of parameters to control the pore size and pore throat size of dextran-GMA polyHIPE hydrogels, namely we tried to change the dispersion speed, ripening time before polymerisation, HAp nanoparticle concentration and the chemical nature of the oil phase.

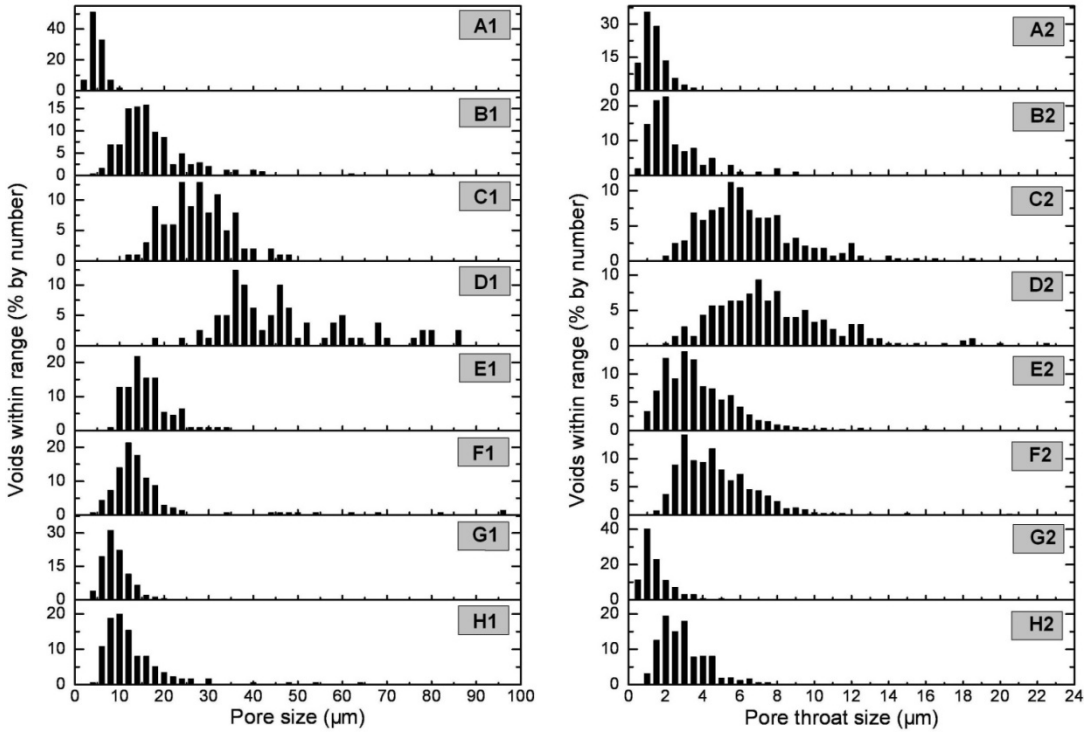

Figure 7-6: Pore size distributions (**left**) and pore throat size distributions (**right**) of dextran-GMA poly-Pickering-HIPE HAp nanoparticle stabilised hydrogels as measure from the corresponding SEM micrographs: **A1** & **A2**. **PPH1**; **B1** & **B2**. **PPH2**; **C1** & **C2**. **PPH3**; **D1** & **D2**. **PPH4**; **E1** & **E2**. **PPH5**; **F1** & **F2**. **PPH6**; **G1** & **G2**. **PPH7**; **H1** & **H2**. **PPH8**. (the experimental details are in **9.26**)

Increasing the homogenisation speed from 5,000 rpm to 15,000 rpm during the HIPE preparation caused larger droplets to break up into smaller ones and so dramatically reduce both the pore and the pore throat dimensions of polyHIPE hydrogels. The average pore size decreased form 17.3 μm to 1.5 μm and the average pore throat size decreased from 2.5 μm to 0.6 μm (**Figure 7-5 B & C**). Also the corresponding pore size and pore throat size distributions was narrower (**Figure 7-6 A1** & **A2**).

The droplet size of emulsions is time dependent[277] and larger droplets result with time caused by 1) limited coalescence[189] and 2) Ostwald ripening[278]. Following this strategy, Pickering-HIPEs were polymerised after 7 d (**PPH3**, **Figure 7-5 E**) and 14 d (**PPH4**, **Figure 7-5 F**) of their preparation (emulsification). Compared with a sample polymerised within 20 min after preparation (**PPH2**, **Figure 7-5 D**), both pore size and pore throat size of the polyHIPEs gradually became larger with ripening time of the emulsion template and finally reach an average pore of 41 μm size and pore throat size of 7.7 μm after ripening for two weeks, which is about 2 times larger than the pore size and pore throat size of **PPH2**. The statistical analysis of the pore size/pore throat size dimensions demonstrated a broader distribution with increasing ripening time (**Figure 7-6**).

Decreasing the HAp nanoparticle concentration from 1.0 % w/v (**PPH2**, **Figure 7-6 C**) to 0.5 % w/v (**PPH5**, **Figure 7-6 F**) did not result in a significant increase of the pore size of the resulting poly-Pickering-HIPEs. Actually these two polyHIPEs have

similar pore size (16 μm to 17 μm) and pore throat size (around 3 μm). This is very different from the observed 50% decrease in droplet size in the o/w Pickering-HIPEs (**Figure 7-2**), which is probably because of the co-stabilization of dextran-GMA. However after further decreasing the HAp nanoparticle concentration to 0.3 % w/v (**PPH6**), the HIPEs become less stable and limited coalescence produced bigger droplets which after polymerisation resulted in large pores with diameters of more than 40 μm (**Figure 7-5 G**). These larger pores are surrounded by many smaller pores with a diameter ranging from 10 to 20 μm. Statistical analysis (**Figure 7-6 F**) showed that the diameter of more than 90% of the pores in PPH6 are between 5 to 25 μm, which explains that the average pore size was still 17 μm while most of the volume of the polyHIPE was occupied by several larger pores with pore size more than 60 μm. Moreover, the pore throat size and pore throat size distributions widened for **PPH6** (**Figure 7-6 B2**, **E2** and **F2**) because of ripening.

Compared with methyl myristate-in-water Pickering-HIPEs, soybean-in-water Pickering-HIPEs are relatively unstable and phase separate within 2 h after homogenisation stopped. But again, after adding dextran-GMA, which appears to act once again as a co-emulsifier, stable Pickering-HIPEs were obtained. The average pore size of the resulting poly-Pickering-HIPE hydrogel (**PPH7**, **Figure 7-5 H**) was 3.5 μm, which was 80% smaller compared to the poly-Pickering-HIPEs made from templates with methyl myristate as internal phase (**PPH2**). After ripening the HIPE

template for 7 d, the pore size of poly-Pickering-HIPE **PP8** reached 13.0 μm (**Figure 7-5 I**) and the distribution became slightly broader because of ripening (**Figure 7-6**).

HAp nanoparticles can also be used as a nontoxic stabiliser to replace Triton X405 to prepare dextran-*b*-polyNIPAAm based thermo-HIPEs. The same preparation conditions of Pickering thermo-HIPEs, including dispersing conditions, dextran-*b*-polyNIPAAm concentration, internal phase ratio, were used as those identified for Triton X405 stabilised thermo-HIPEs (as described in **Chapter 6**). In order to characterise the porous structure of Pickering solid-HIPEs, *p*-xylene was used as oil phase as it can be removed directly by freeze drying. A Pickering-solid-HIPE was obtained after lyophilisation of the oil phase of a Pickering thermo-HIPE **DN-HAp-*p*-Xylene** and the experimental details are in **9.30**. This Pickering solid-HIPE was much firmer to the touch than solid-HIPEs obtained from Triton X405 stabilised emulsions. In the SEM images of HAp-Pickering dextran-*b*-polyNIPAAm thermo-responsive solid-HIPEs the open-porous structure is clearly observed (**Figure 7-7 A & B**). The pore diameter of this solid-HIPE ranges from 20~40 μm, which is about 5 times larger compared to the same Triton X405 stabilised solid-HIPEs (4~7 μm). The diameter of the pore throats of Pickering solid-HIPEs is about 8 μm, which is also 5 times larger compared to the same Triton X405 stabilised solid-HIPEs (0.4 ~ 2.7 μm) and many of small windows could be observed in the pore walls of solid-HIPEs (**Figure 7-7 B**), which may have been produced during lyophilisation of the HIPE (removing both aqueous and oil phase).

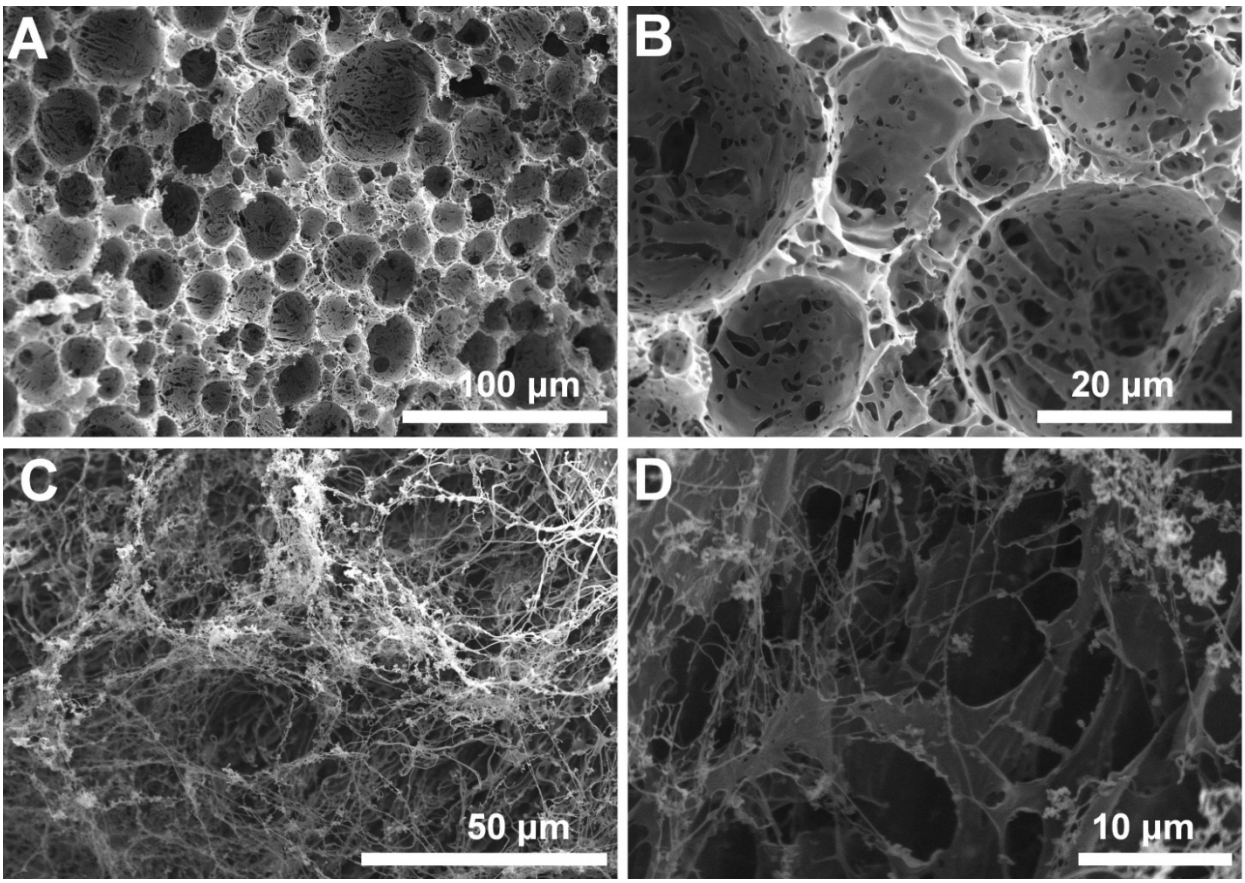

Figure 7-7: SEM images of dextran-*b*-polyNIPAAm thermo-responsive solid-HIPEs **DN-HAp-*p*-Xylene** produced from HAp nanoparticles stabilised thermo-HIPEs with 90 % v/v nominal pore volume and 20 % w/v polymer in the aqueous phase before (**A** & **B**) and after soaking in 38 °C water for 14 d (**C** & **D**). Interconnected porous structure could be clearly observed in these SEM images.

In order to investigate and compare the dissolution behaviour of Pickering thermo-responsive solid-HIPE in water below and above the LCST of the block copolymer, the Pickering solid-HIPE **DN-HAp-*p*-Xylene** made from dextran-*b*-polyNIPAAm was placed in distilled water at 24 °C, in which it dissolved slowly and taking more than 10 min. Similar to the thermo-HIPEs **DN1** to **DN3** described in **Chapter 6** the Pickering thermo-responsive solid-HIPEs floated on water for 14 d at 38 °C without any obvious volume change. This is for the same reasons as discussed in **Chapter 6**,

the polyNIPAAm block segments phase inverts above the LCST of the block copolymer while simultaneously producing physical crosslinks through aggregation of neighbouring segments, As revealed by SEM, some fibrous pore (**Figure 7-7 C**) morphology could be observed after conditioning the solid-HIPE in 38 °C water for 14 d, which is again may be due to plasticisation of the polymer through water driven by minimising the interfacial energy, through reorganisation/reshaping of the pore walls.

Table 7-2: Compositions of dextran-*b*-polyNIPAAm copolymer HIPEs with soybean oil or squalene as oil phase, Triton X405 or HAp nanoparticles as emulsifier.

Sample Code [a]	Oil phase	Emulsifier [b]		Polymer dissolved in aqueous phase [c]	Aqueous phase volume/oil phase volume (v:v)
		Triton X405 (mg/ml)	HAp nanoparticles (mg/ml)		
DN-S-*p*-Xylene	*p*-Xylene	85	0	Dextran-*b*-polyNIPAAm	1:4
DN-S-Soybean	Soybean oil	85	0		
DN-S-Squalene	Squalene	85	0		
DN-HAp-*p*-Xylene	*p*-Xylene	0	10		
DN-HAp-Soybean	Soybean oil	0	10		
DN-HAp-Squalene	Squalene	0	10		

[a] The internal phase volume of all samples 80 % v/v. [b] Concentration of emulsifiers in aqueous phase (distilled water). [c] Dextran-*b*-polyNIPAAm concentration in aqueous phase (distilled water) of all samples is 20 % w/v. The experimental details are in **9.28**.

Thermo-HIPEs are intended to be injected with their oil phase into defect area in human body. However the oil phase of the thermo-responsive HIPEs has so far been limited to *p*-xylene or toluene to facilitate the morphological investigations. As *p*-xylene or toluene is toxic and thus not suitable for *in vivo* applications other hydrophobic molecules to make up the oil phase need to be chosen. For the purpose of drug or gene delivery, many oils[254], such as lard oil, soybean oil or squalene, have been reportedly used as the oil phase in o/w emulsions for *in vivo* use. Therefore we prepared dextran-*b*-polyNIPAAm thermo-HIPEs with either soybean oil or squalene as oil phase (**Table 7-2**). A set of thermo-HIPEs either stabilised by Triton X405 (**DN-S-Soybean & DN-S-Squalene**) or HAp nanoparticles (**DN-HAp-Soybean & DN-HAp-Squalene**) were prepared. The droplet size of **DN-HAp-Soybean** ranges from 15 μm to 40 μm (**Figure 7-8 C**). All of these thermo-HIPEs are stable at room temperature after more than 2 weeks without undergoing phase separation. Interestingly at 38 °C **DN-HAp-Soybean** and **DN-HAp-Squalene** are much more stable than Triton X405 stabilised thermo-HIPEs as no phase separation could be observed for more than 10 d. Of all the formulations tested (**Table 7-2),** only the compositions of **DN-HAp-Soybean** and **DN-HAp-Squalene** did not contain toxic components.

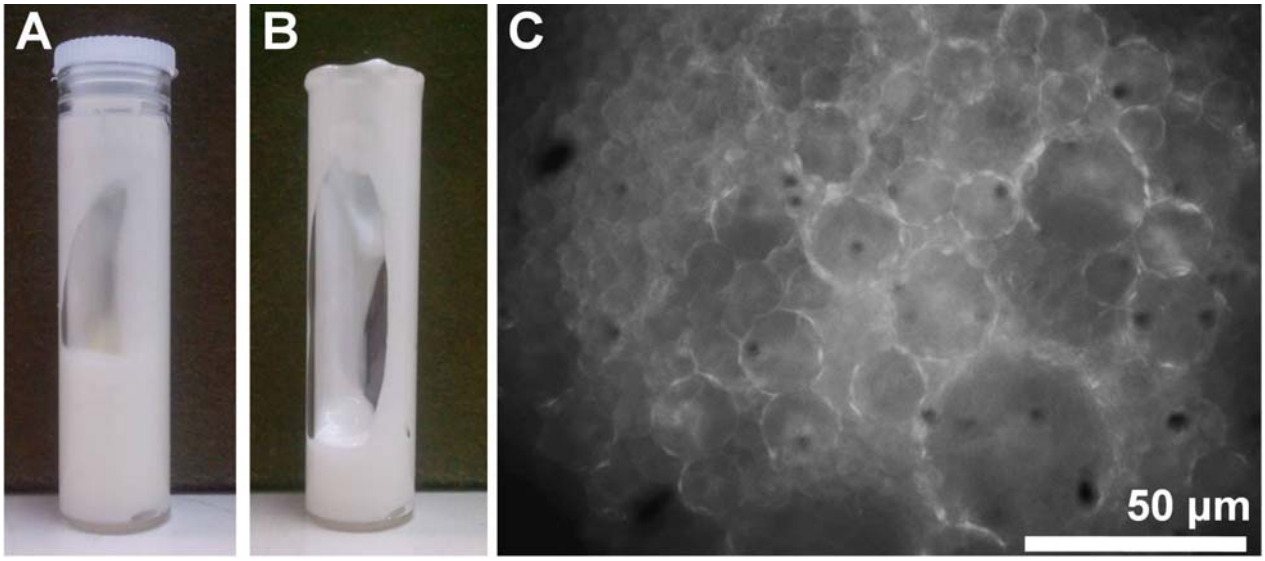

Figure 7-8: Thermo-HIPEs with soybean oil or squalene as oil phase: photographs of **A**: **DN-HAp-Soybean; B**: **DN-HAp-Squalene;** and **C**: optical microscope image of **DN-HAp-Soybean**.

7.2.2 DOUBLE RESPONSIVE PICKERING THERMO-HIPES

Besides HAp nanoparticle stabilised thermo-HIPEs, we also prepared thermo-responsive dextran-*b*-polyNIPAAm based Pickering *p*-xylene in water (o/w) HIPEs by using pH and thermo-responsive polyNIPAAm-*co*-acrylic acid (polyNIPAAm-*co*-AA) microgel particles. One important reason of using stimuli-responsive microgel particles as an emulsifier in the preparation of emulsion templates is that these particles could be potentially useful as "built-in" drug carriers (**Figure 7-9**).

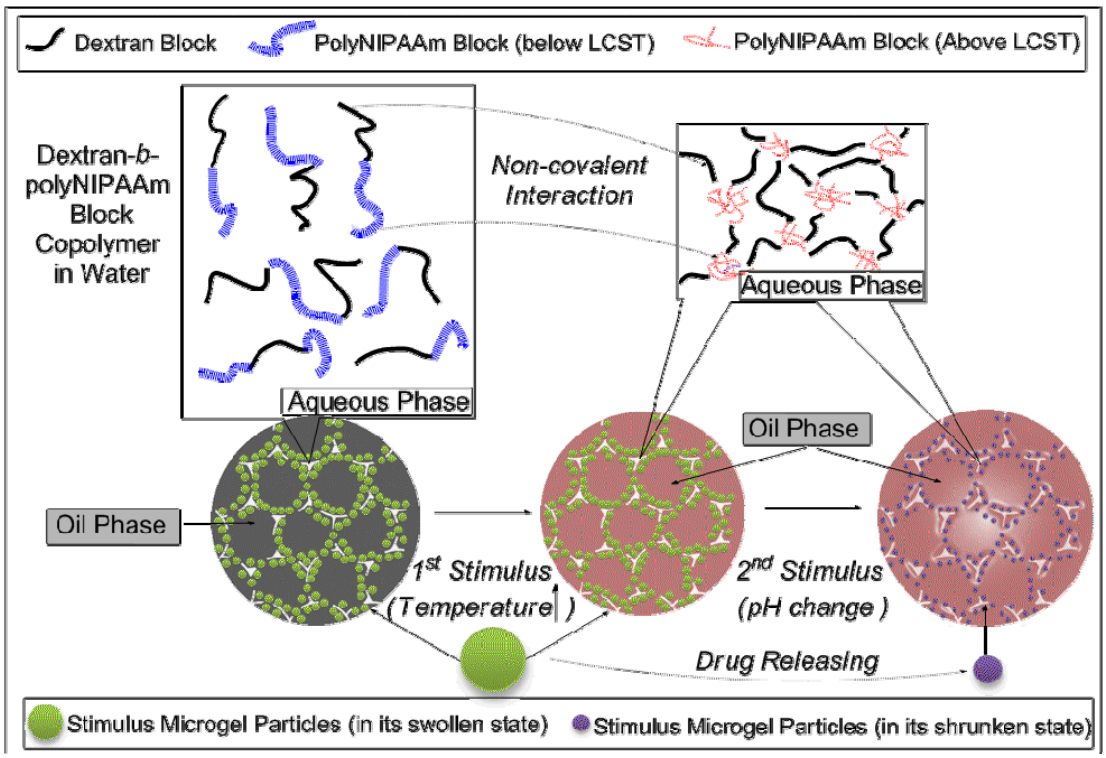

Figure 7-9: Schematic illustrating the formation of o/w "double responsive Pickering-HIPEs" (HIPEs that not only are responsive during in their polymer phase but also the emulsifier is stimuli-responsive) employing the temperature-triggered polyNIPAAm block aggregation as non-covalent crosslinking strategy and pH/temperature responsive microgel particles as both emulsifier and potential drug/growth factor carrier vehicle.

PolyNIPAAm-*co*-AA microgel particles were kindly synthesized by Wei Yuan in the following way: an aqueous redox polymerisation using sodium dodecylbenzene sulfonate (NaDBS) as a surfactant was employed to prepare polyNIPAAm-*co*-AA microgel particles from a monomer solution containing NIPAAm, AAc and BIS, as described by Ito et al[279] and the experimental details are in **9.29**.The size of this microgel particles vary depending on temperature and pH as well as ionic strength.[279-280] Recently, it has been demonstrated that emulsions can be effectively stabilised by such stimuli-responsive microgel particles.[192,271]

Two types of double-responsive solid-HIPEs **DN-P-1** & **DN-P-2** were prepared by o/w high internal phase emulsion templating with dextran-*b*-polyNIPAAm copolymer as the constituent of the continuous aqueous phase and stimuli-responsive microgel particles as sole emulsifier. In order to obtain solid-HIPEs, *p*-xylene was used as oil phase as it can be removed directly by freeze drying to simplify SEM analysis. The emulsification was carried out under stirring at 400 rpm and the formulations studied are listed in **Table 7-1**. Triton X405, (hydrophilic-lipophilic balance, HLB ≈ 18[32]), was used to stabilise solid-HIPEs (**DN-S-1** & **DN-S-2**) and dextran based solid-HIPEs (**Dex-S** & **Dex-P**) were also prepared as control. Prior to lyophilisation of the oil phase, a syringe was filled with the HIPE and the emulsion was injected into a flask. After injection, samples **DN-S-2** and **DN-P-2** were heated to 38 °C for 30 min to trigger the phase inversion of the polyNIPAAm copolymer. The experimental details are in **9.31**.

Table 7-3: Composition of dextran and dextran-*b*-polyNIPAAm copolymer HIPEs stabilised by polyNIPAAm-*co*-AA microgel particles

Sample Code [a]	Polymer in aqueous phase [b]	Aqueous phase[c]			Post treatment after HIPE was prepared	Pore size range (μm)[d]
		Triton X405 (mg/ml)	Microgel Particles (mg/ml)	KCl (mg/ml)		
Dex-S	Dextran	85	0	0	Freeze dried directly	1.4～5.9
DN-S-1	Dextran-*b*-polyNIPAAm	85	0	0	Freeze dried directly	1.2～4.4
DN-S-2	Dextran-*b*-polyNIPAAm	85	0	0	Heated to 38 °C before freeze drying	2.7～7.1
Dex-P	Dextran	0	4.0	1.0	Freeze dried directly	30.4～143.6
DN-P-1	Dextran-*b*-polyNIPAAm	0	4.0	1.0	Freeze dried directly	8.7～65.0
DN-P-2	Dextran-*b*-polyNIPAAm	0	4.0	1.0	Heated to 38 °C before freeze drying	7.4～70.1

[a] The internal phase all samples is *p*-xylene and its volume fraction is 80 % v/v. [b] The polymer concentration in aqueous phase (distilled water) of all samples is 20 % w/v. [c] Concentration in distilled water. [d] Determined from the corresponding SEM micrographs. The experimental details are in **9.31**.

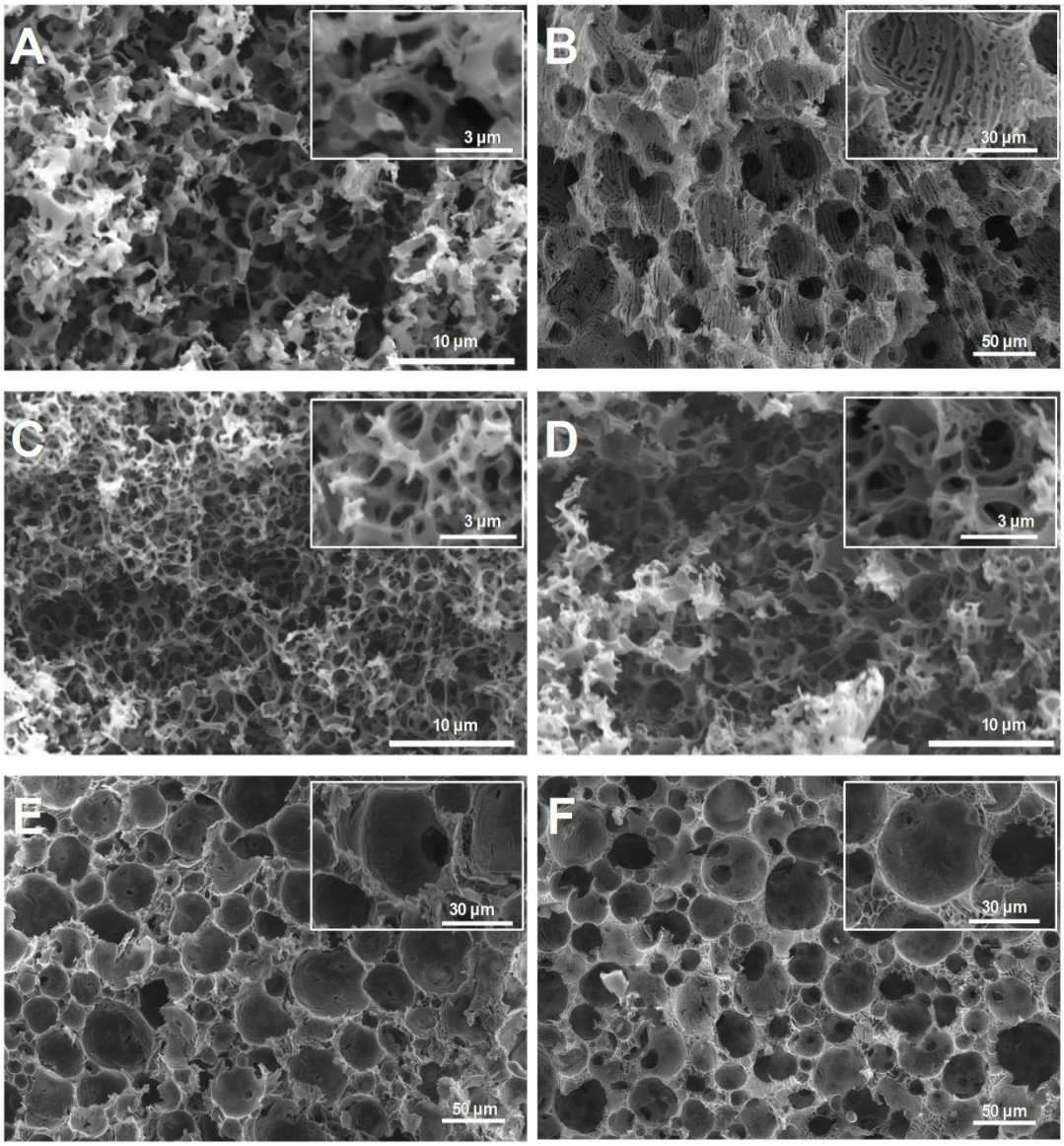

Figure 7-10: SEM images of dextran solid-HIPEs and dextran-*b*-polyNIPAAm thermo-responsive solid-HIPEs stabilised by surfactant Triton X405 or stimuli-responsive microgel particles; **A**: **Dex-S**; **B**: **Dex-P**; **C**: **DN-S-1**; **D**: **DN-S-2**; **E**: **DN-P-1**; **F**: **DN-P-2**.

A very thin layer of the *p*-xylene (oil phase) above the sedimented emulsion could be observed after the Triton X405 stabilised HIPEs being heated to 38 °C for 2 h, which indicated the precipitation of emulsions droplets. Microgel particle stabilised Pickering-HIPEs on the other hand were more stable at room temperature and no

phase separation was observed after being heated to 38 °C for 2 h. That is because the particles used as stabilisers in Pickering emulsions are irreversibly adsorbed at the interface of emulsions because of their high energy of attachment, which makes the resultant Pickering emulsions extremely stable.[193]

Turning to the differences in microstructure, SEM images of solid HIPEs (**Figure 7-10**) showed that solid-HIPEs obtained from Triton X405 stabilised emulsions (**Dex-S**, **DN-S-1** & **DN-S-2**) have an open porous network structure typical for polyHIPEs[15] with pore size ranges from 1 to 7 μm. However, Pickering solid-HIPEs (**Dex-P**, **DN-P-1** & **DN-P-2**) have 20% to 30% larger and partially (and not fully) opened combined with closed cell pores, which leads to a relatively low degree of pore interconnectivity. Pickering solid-HIPEs were much firmer to the touch than solid-HIPEs from surfactant stabilised emulsions (as mentioned in **Section 7.21**), probably because of the partially opened combined with closed cell pore structures. The pore sizes of all Pickering solid-HIPEs were generally in the range of 30 to 50 μm, although a few larger pores (above 70 μm) and smaller pores (below 20 μm) were observed. The substructure on the pore wall surface of Pickering solid-HIPEs, especially in **Dex-P**, could have been caused by the sublimation of water during freeze drying. The difference in pore structure, i.e. pore size and degree of interconnectivity, between solid-HIPEs made from Pickering or from traditional surfactant stabilised emulsions is similar to that seen between polyHIPEs produced from Pickering or surfactant stabilised emulsion templates[166], which are prepared by

radical polymerisation of styrene and maintain their porous structure by covalent crosslinks.

Table 7-4: Observations made during solubility tests of solid-HIPEs, thermo-responsive solid-HIPEs and double responsive solid-HIPEs in water above and below the LCST of dextran-*b*-polyNIPAAm

Sample Code	24 °C Water	38 °C Water
Dex-S & **Dex-P**	Dissolve instantly	Dissolves instantly
DN-S-1 & **DN-S-2**	Disintegrates into small pieces which sink to the bottom of the container and dissolve completely within 10 min	Floats in water, no apparent volume loss observed visually during 14 d
DN-P-1 & **DN-P-2**	Floating in water at first, then disintegrates into small pieces which slowly sink to the bottom of the container and dissolve completely within 10 min to 15 min	Floats in water, no apparent volume loss observed visually during 14 d

Several experiments were conducted in order to investigate and compare the dissolution behaviour of thermo-responsive solid-HIPEs in water below and above the LCST of dextran-*b*-polyNIPAAm (**Table 7-4**). Solid-HIPEs made of dextran (**Dex-S** & **Dex-P**), regardless whether they were prepared from Pickering or surfactant stabilised emulsions, were placed in distilled water and dissolved instantly at 24 °C and 38 °C as was expected for pure dextran. Dextran-*b*-polyNIPAAm thermo-responsive solid-HIPEs (**DN-S-1** & **DN-S-2**) were treated in the same way and also

dissolved at 24 °C, but the process took more than 10 min to complete. Double responsive solid-HIPEs **DN-P-1** and **DN-P-2** floated in water at 24 °C at the very beginning and it took some more time (about 10 to 15 min) to dissolve compared with **DN-S-1** and **DN-S-2** because of the relative low pore interconnectivities. In 38 °C water, because the polyNIPAAm block segments phase separated from water above the LCST of the block copolymer while simultaneously producing physical crosslinks through intermolecular interactions, all the solid-HIPEs made of dextran-*b*-polyNIPAAm were found floating in water without apparent volume loss for 14 d. It is worth to notice that this experimental results were same no matter whether the phase inversion of the polyNIPAAm copolymer was triggered (**DN-S-2** & **DN-P-2**, being heated to 38 °C before freeze drying) or not (**DN-S-1** & **DN-P-1)** during preparation, that might be because the solid-HIPEs were heated to temperatures above the LCST of dextran-*b*-polyNIPAAm as soon as it was contact with 38 °C warm water which triggered the physical aggregation of the polymers before they were totally hydrated and dissolved in water.

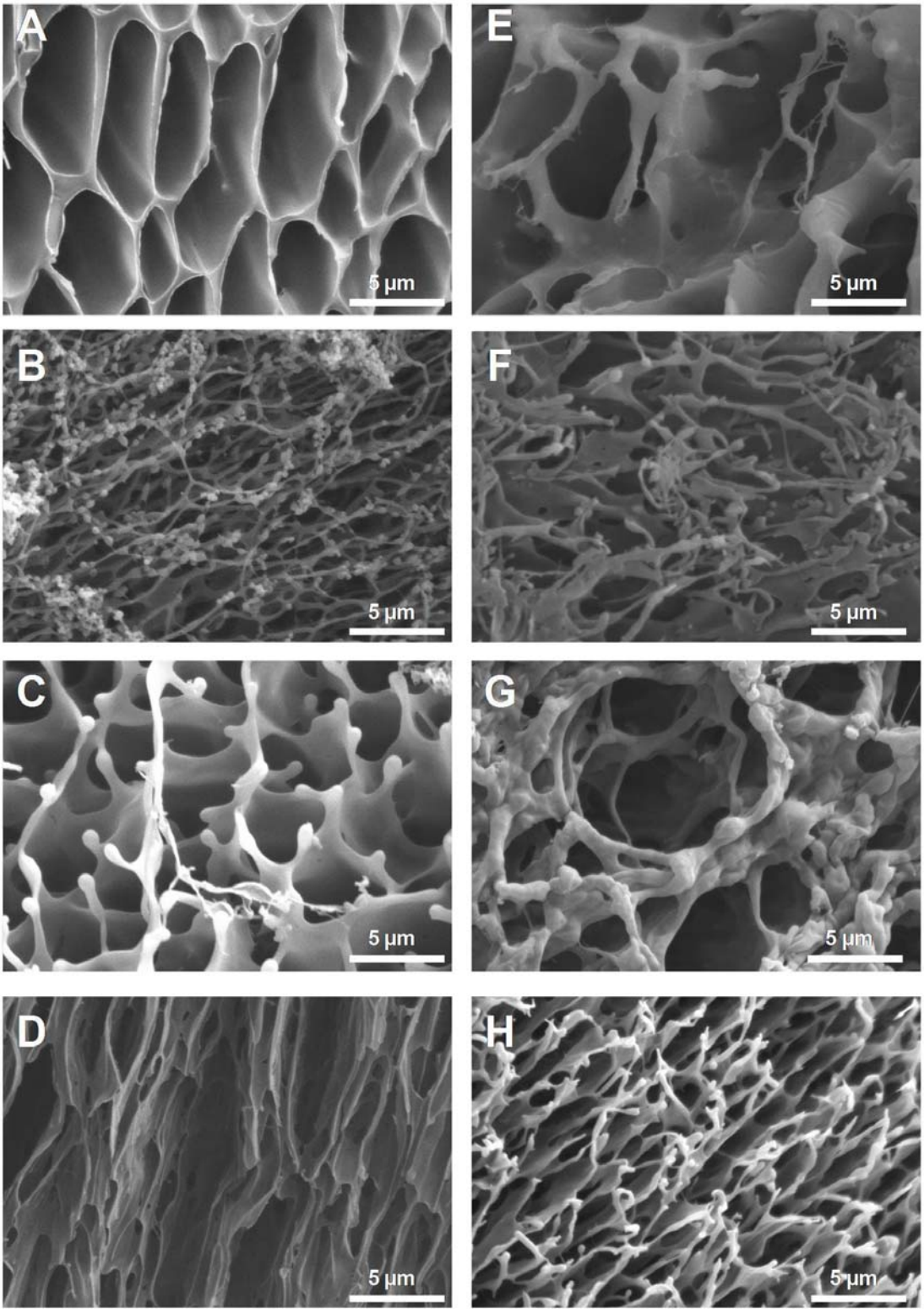

Figure 7-11: SEM images of double responsive solid-HIPEs after soaking in 38 °C water for 14 d: **A**~**D**. Sample **DN-P-1**; **E**~**H**. Sample **DN-P-2**.

The double responsive solid-HIPEs **(DN-P-1 & DN-P-2)** were freeze dried after being exposed to 38 °C warm water for 14 d and again characterised by SEM. The interaction between dextran-*b*-polyNIPAAm and water caused the pore morphology of the solid-HIPEs to change. Several different porous morphologies (**Figure 7-11**) were observed in their SEM images. Similar to other thermo-HIPEs, these pore morphologies with about 3~15 μm in diameter might be caused by the reorganisation/reshaping of the walls around the pore throats in the continuous phase. Also some fibrous morphologies can be rationalised by plasticisation of the polymer through water driven by the minimisation of interfacial energy.

7.3 CONCLUSIONS

Stable Pickering-HIPEs with an internal phase of 80 % v/v could be prepared using commercially available HAp nanoparticles directly without the need for surface modification. We also demonstrated that the pore size/pore throat size of the resulting dextran-GMA poly-Pickering-HIPE hydrogels could be adjusted within a certain range by changing ripening time, emulsifier concentration or dispersion conditions. By adding water soluble monomers in the aqueous phase, these Pickering-HIPEs stabilised by nontoxic biocompatible HAp nanoparticles, can be used as templates to manufacture highly porous materials.

HIPEs with thermo-responsive dextran-*b*-polyNIPAAm as solid constituent in the continuous phase and HAp nanoparticle or pH/thermo-responsive microgel particles

as sole emulsifier were successfully prepared. Similar to thermo-HIPEs prepared with Triton X405, after the oil phase was removed, solid-like foams, which were able to maintain their porous structure in an aqueous environment at 38 °C through aggregation of polyNIPAAm blocks, were obtained without the need for chemical crosslinks. Compared with solid-HIPEs prepared from surfactant stabilised HIPEs, these Pickering solid-HIPEs process better mechanical performance and larger pores, but lower interconnectivity.

Besides toluene and *p*-xylene, soybean oil and squalene could also be used as the oil phase of thermo-HIPEs stabilised either with Triton X405 or HAp nanoparticles. Soybean oil or squalene based thermo-HIPEs stabilised by HAp nanoparticle process higher viscosity and better stability than other thermo-HIPEs (e.g. thermo-HIPEs stabilised by Triton X405 or with toluene/*p*-xylene as oil phase). Moreover, these Pickering thermo-HIPEs prepared using nontoxic oils are more suitable for the purpose of *in vivo* application compared with toluene or *p*-xylene based thermo-HIPEs.

CHAPTER 8

CONCLUSIONS AND FUTURE WORK

In this final chapter, the concluding remarks of all the work in this thesis are presented and suggestions of further work are made. This thesis introduced several novel polysaccharide based stimuli-responsive polyHIPEs or solid-HIPEs prepared from o/w HIPEs either stabilised by traditional surfactant or colloidal particles. These stimuli responsive porous materials are intended to be used as injectable scaffolds for soft tissue engineering. Generally two thermo-responsive dextran based macroporous polymers, one ion-responsive alginate polyHIPE and two poly-Pickering-HIPEs/solid-HIPEs were prepared and studied. Attention has been focused on achieving injectability, suitable pore morphology for potential tissue engineering applications, biocompatibility and stimuli responsibility of these porous hydrogels.

8.1 CONCLUSIONS

o/w HIPE templating method is very effective in manufacturing porous hydrogels with well-defined porous structures. The main aim of this work was to develop suitable injectable porous scaffold systems based on o/w HIPE templated

macroporous polymers. By changing the crosslinking methods, emulsifiers, oil phases, type of stimuli-responsive monomers and macromonomers in the aqueous phase, we developed six types of novel scaffolds for soft tissue engineering (**Table 8-1**). All of these macroporous hydrogels possess an interconnected porous structure and hydrophilic solid constitute with turntable pore morphologies.

8.1.1 ION-RESPONSIVE VERSUS THERMO-RESPONSIVE MACROPOROUS HYDROGELS

Two types of stimuli-responsive materials, thermo-responsive polyNIPAAm and ion-responsive alginate, were used to prepare macroporous hydrogels. The stimuli-responsive behaviours of these polyHIPE/thermo-HIPE systems could be triggered under very mild conditions: ion-responsive methacrylate-modified alginate polyHIPEs (**Table 8-1 S2**) could be shrunk and swelled on demand in the presence of Ca^{2+} (Ca^{2+} could potentially even supplied by the surrounding tissue) or sodium citrate; thermo-responsive poly((dextran-GMA)-*co*-NIPAAm) polyHIPEs (**Table 8-1 S1**) had better mechanical properties after being heated to 38 °C in an aqueous environment. Dextran-*b*-polyNIPAAm based thermo-HIPEs (**Table 8-1 S4, S5 & S6**) could be used to produce interconnected macroporous solids using a thermal trigger close to human body temperature, as the polyNIPAAm part of thermo-responsive copolymer phase separated from water above the LCST (34 °C). We also demonstrated that covalently crosslinked polyHIPE hydrogels are indeed injectable

and their fragments produced during injection could be solidified by using Ca^{2+}-crosslinked alginate as adhesive. We believe this approach is generic and is a potentially versatile method that can be applied to produce other macroporous hydrogels. These two solidification mechanisms avoid the harsh condition required by other solidification methods (e.g. radical polymerisation) and do not need or produce toxic chemicals during solidification.

8.1.2 Covalent Crosslinking Versus Non-covalent Crosslinking of Macroporous Emulsion Templated Hydrogels

It was demonstrated that both covalently crosslinked polyHIPE hydrogels (**Table 8-1 S1 & S2**) and non-covalently crosslinked thermo-HIPEs (**Table 8-1 S3, S4, & S5**) possess good injectability. Covalently crosslinked polyHIPE hydrogels broke into small hydrogel fragments during extrusion through a hypodermic needle, but the well-defined pore structure characteristic for polyHIPE was maintained. The resulting hydrogel polyHIPE particles could be reformed into a monolithic scaffold with a solution-based alginate "adhesive" while maintaining the pore structure employing mild and biocompatible conditions. Because the aqueous phase of thermo-HIPEs is a mainly dextran-*b*-polyNIPAAm aqueous solution and there is no doubt that the HIPE is injectable at room temperature as is expected from an emulsion. The solidification of a thermo-HIPE can simply be triggered by heating it above its LCST. The porous

structure of the thermo-responsive solid-HIPE was maintained by aggregation of polyNIPAAm blocks within the copolymer. We believe that both of these two crosslinking methods could be applied in the manufacturing of injectable scaffolds for soft tissue engineering.

8.1.3 TRADITIONAL SURFACTANTS VERSUS COLLOIDAL PARTICLES AS EMULSIFIER FOR HIPE TEMPLATES

Compared with traditional surfactants, such as Triton X405 used to stabilise o/w HIPEs, colloidal particles, such as HAp nanoparticles and stimuli-responsive microgel particles, possess many advantages for manufacturing HIPE templated macroporous hydrogels for biomedical applications. These two types of nontoxic biocompatible particles are more suitable for *in vivo* use compared to the toxic or non-biocompatible surfactants and potentially provide extra functions, such as promote hard tissue cell proliferation (HAp nanoparticles) or as they could be used as nano-carrier for gene, growth factor or drug delivery (stimuli-responsive microgel particles). Compared with Triton X405 stabilised polyHIPEs/thermo-HIPEs (**Table 8-1 S1 S2, & S4**), poly-Pickering-HIPEs/thermo-HIPEs (**Table 8-1 S3 S5 & S6**) have much bigger pores with diameter exceeding 30 μm, which is more suitable for tissue engineering applications.

8.1.4 ORGANIC SOLVENTS VERSUS NONTOXIC OILS AS INTERNAL/DISPERSED PHASE FOR HIPE TEMPLATES

Obviously most organic solvents, such as toluene and *p*-xylene used as oil phase for o/w HIPEs, are not suitable for *in vivo* use. It is intended to inject thermo-HIPEs directly into the target area. In this case common water immiscible organic solvents cannot be used. Soybean oil and squalene as the oil phase of thermo-HIPEs (**Table 8-1 S5**) provide safer options for *in vivo* use.

Table 8-1: 6 types of injectable polyHIPE/thermo-HIPE hydrogels investigated in this thesis

Code	Name	Emulsifier	Oil phase	Solidification method
		Covalently crosslinked polyHIPE hydrogels		
S1	Poly((dextran-GMA)-*co*-NIPAAm) polyHIPEs	Triton X405	Toluene	Thermo-responsive & ion-responsive solidification
S2	Methacrylate-modified alginate polyHIPEs	Triton X405	Toluene	Ion-responsive solidification
S3	Dextran-GMA poly-Pickering-HIPEs	HAp nanoparticles	Toluene or soybean oil	Radical polymerisation
		Thermo-HIPEs (non-covalently crosslinked hydrogels)		
S4	Dextran-*b*-polyNIPAAm thermo-HIPEs	Triton X405	*p*-Xylene , soybean oil or squalene	Thermo-responsive solidification
S5	Dextran-*b*-polyNIPAAm Pickering thermo-HIPEs	HAp nanoparticles	*p*-Xylene , soybean oil or squalene	Thermo-responsive solidification
S6	Dextran-*b*-polyNIPAAm Pickering thermo-HIPEs	Microgel particles	*p*-Xylene	Thermo-responsive solidification

8.1.5 FINAL CONCLUDING REMARKS

It was demonstrated that the strategy used to prepare injectable scaffolds for soft tissue engineering (**Figure 1-1**) in this thesis is feasible and reliable. By using o/w HIPEs as template, we prepared injectable scaffolds with interconnected porous structures, turntable pore size/pore throat size and biocompatible hydrophilic natural polysaccharides (dextran or alginate) as the solid constitute of the scaffolds. By incorporating environmental stimuli-responsive materials (polyNIPAAm and alginate) into the injectable system, the scaffolds could be *in vivo* solidified triggered by body temperature or Ca^{2+} ions from the body. The use of nontoxic oils (soybean oil or squalene) as the oil phase and HAp nanoparticle as the emulsifier eliminated all cytotoxic compounds from thermo-HIPEs, which allows them to be potentially used directly *in vivo*. Moreover, using colloidal particles as emulsifiers allowed to tailor the pore size of polyHIPEs and thermo-HIPEs to the levels that suitable for cell proliferation.

It is hoped that the promising results obtained for these 6 injectable polysaccharide porous scaffolds presented in this thesis will encourage researchers to further explore the stimuli-responsive porous materials prepared from o/w HIPEs and their applications in tissue engineering and regenerative medicine.

8.2 RECOMMENDATIONS FOR FUTURE WORK

Many challenges remain to be overcome to optimise the performance of the scaffolds described in this thesis, the following requires further works:

- The mechanical performance of stimuli-responsive hydrogels prepared from o/w HIPEs, including the strength, stiffness and toughness, can be further diversified to meet the requirements of different biologic tissues.

- Some more studies should be conducted on cell seeding and cultivation on these stimuli-responsive scaffolds.

- Animal studies would provide real *in vivo* data for macroporous scaffolds.

- Proper cell encapsulation methods should be developed in order to protect the cells during premixing with thermo-HIPEs and provide nutrition or other necessary molecular (e.g. growth factors) during *in vivo* cell proliferation.

- Some other biological “adhesives” should be explored to bond polyHIPE hydrogel fragments in this thesis to meet different mechanical properties needs or *in vivo* degradation requirements

- Effect of HAp nanoparticles used to prepare macroporous scaffold on soft tissue cells should be explored.

CHAPTER 9

MATERIALS AND METHODS

9.1 MATERIALS

The following materials were purchased from Sigma-Aldrich Company Ltd. (Poole, UK): dextran from leuconostoc ssp. ($M_w \approx 40{,}000$ Da), alginate from brown algae (viscosity of 2 % solution at 25 °C ≈ 250 mPa.s), glycidyl methacrylate (GMA) (97+ %), methacrylic anhydride (94%), dimethyl sulfoxide (DMSO), free of water (99.9%), *N*-isopropylacrylamide (97%), *p*-xylene (99+%), ammonium persulfate (APS) (98+%), *N,N,N',N'*-tetramethylethylenediamine (TEMED) (99+%), triethylamine (GPC grade), sodium dodecylbenzenesulfonate (NaDBS) (technical grade), glacial acetic acid (GPC grade), *N,N'*-methylenebisacrylamide (BIS) (99.5+%), Triton X405 solution (polyethylene glycol tert-octylphenyl ether, 70% in H_2O), hydroxyapatite (HAp) nanoparticles (particle size < 200 nm), methyl myristate (99+ %), 2,2'-azobis(isobutyronitrile) (AIBN) (98+%), Amberlyst 15 ion exchange resin, dialysis tubing (diameter: 27 mm, molecular weight cut off (MWCO): 12,000 Da), acrylic acid (AA) (99+%), soybean oil (soya oil from glycine max), squalene (98+%), glutaraldehyde (25%), sodium phosphate monobasic (99+%),

sodium phosphate dibasic (99+%). sodium citrate (99+%) and ammonium cerium (IV) nitrate (99+ %) was obtained from Acros (Thermo Fisher Scientific Ltd., Loughborough, UK). Toluene (99+%), nitric acid (69+%), *N*,*N*-dimethylformamide (DMF) (GPC grade), sodium chloride (99+%), hydrochloride acid (HCl) (36+%), calcium chloride (94+%), sodium hydroxide (99+%), ethanol (99.7+%), acetone (99.8%), methanol (99.8%), potassium hydroxide (KOH) (99+%), potassium chloride (KCl) (99+ %) and 12-well BD Falcon™ cell culture insert companion plates (BDH-brand, Cat. No. 353503) were purchased from VWR (Leics., UK). 4-(Dimethylamino)pyridine (DMAP) (99%) was purchased from Alfa Aesar Ltd. (Lancashire, UK). Cellulose extraction soxhlet thimbles (inner diameter = 19 mm, outer length = 90 mm) were bought from Whatman (Whatman International Ltd. Maidstone, England). Deuterium oxide (D_2O) (99.8 atom% D) was supplied by Merck Ltd. (Darmstadt, Germany). Dialysis tubing (diameter: 29 mm, MWCO: 1,000 Da) was purchased from Spectrum Laboratories, Inc. (Breda, NL). A549 human type II tumour cells (A549) were obtained from American Type Culture Collection (# CCL 183; American Type Culture Collection, Virginia, USA); Dulbecco's Modified Eagle Medium (DMEM) was purchased from Invirtogen Ltd (Paisley, UK); Foetal Bovine Serum (FBS) was obtained from PAA Laboratories, (Somerset, UK). Osmiumtetroxide aqueous solution (4%) was purchased from TAAB (TAAB Laboratories, Berkshire, UK) and 1,1,1,3,3,3-hexamethyldisilazane (HMDS) (98+%) was from AVOCADO (AVOCADO Research Chemical Ltd., Lancashire UK).

Dialysis tubing with 12,000-14,000 MWCO was purchased from Medicell (Medicell International Ltd., UK). Pork muscle was purchased from my local Sainsbury's Supermarket Ltd. (London, UK). Piped nitrogen was supplied by BOC and passed through a calcium carbonate, sodium hydroxide and self-indicating-silica drying column. All materials were used as received.

9.2 SYNTHESIS OF DEXTRAN-GMA

Dextran-GMA was synthesis following the procedure described by Dijk-Wolthuis et al.[208] Dextran (25.0 g, 0.625 mmol) was dissolved in 225 ml DMSO. An atmosphere of nitrogen atmosphere was maintained throughout the reaction. DMAP (5.0 g, 0.041 mol) was added. After DMAP was dissolved in DMSO, GMA (6.2 g, 0.041 mol) was added in one portion. The solution was stirred at room temperature for 48 h. The reaction was stopped by adding 7.0 ml of a 36% aqueous HCl. The reaction mixture was transferred to a dialysis tube (MWCO = 12,000 Da) and dialysed against distilled water for 3 d (distilled water was changed twice a day until no impurities can be found in the ^{1}H-NMR spectra). Finally, dextran-GMA was freeze dried and a white fluffy product was obtained, which was stored at -20 °C in a freezer prior use.

The degree of substitution of dextran by GMA was quantified using ^{1}H-NMR spectra of dextran and dextran-GMA.[281] ^{1}H-NMR spectra were recorded on a Bruker DRX 400 (400 MHz) in D_2O at room temperature. ^{1}H-NMR spectra were processed using the software MestReNova (version 6.1.0). The NMR analysis was carried out

according to reference[208]. Specifically, the anomeric proton of the glucose ring of dextran (H_a) was clearly observed at δ = 4.9 ppm and the proton at the anomeric carbon of the α-1, 3 linkages ($H_{a'}$) was at δ = 5.1 ppm. The signals from the methacryloyl protons of glyceryl methacrylate (H_c) were observed (CH_3 at δ=1.8 ppm and $=CH_2$ at δ 5.7 ppm and δ 6.1 ppm. The results (**Figure 9-1**) are in agreement with the ^{1}H-NMR spectra in van Dijk-Wolthuis et al.s work.[281]

The degree of substitution of dextran-GMA was calculated by measuring the ratio between the average value of the integrals of the double-bond protons (δ = 5.6 to 6.3 ppm) and the integrals of the anomeric protons signals (δ = 4.8 to 5.6 ppm) in the ^{1}H-NMR spectrum of dextran-GMA in deuteroxide (**Figure 9-1**). The formula to calculate the degree of vinylic substitution to glucose unit is:

$$DS = \frac{\frac{1}{2}(\delta_{6.13} + \delta_{5.628})}{\delta_{5.1} + \delta_{4.9}} \qquad 9.1$$

The degree of substitution of dextran-GMA prepared is 34%.

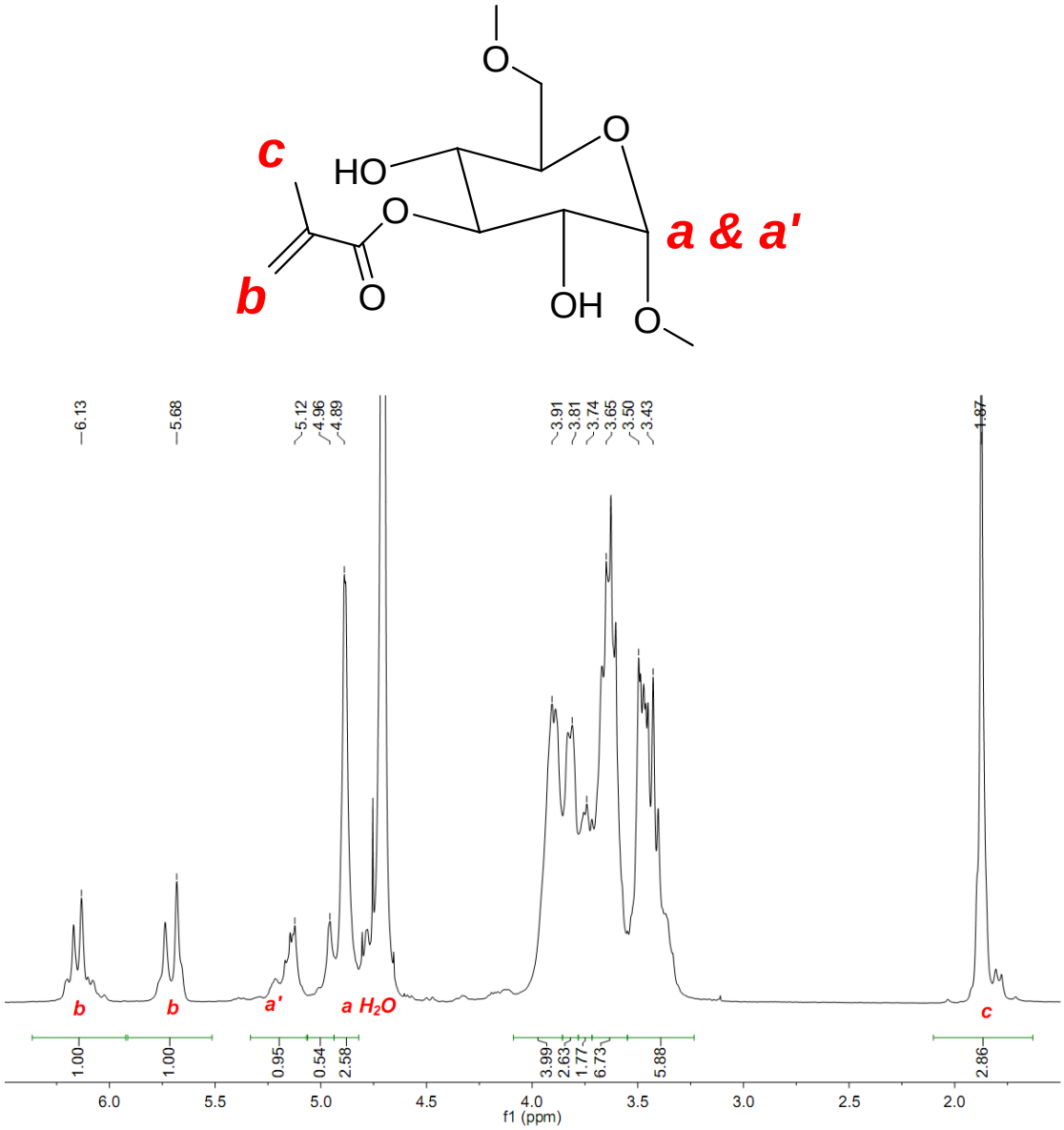

Figure 9-1: The ^{1}H-NMR spectra of dextran-GMA dissolved in D_2O.

9.3 DEXTRAN-GMA AND POLY((DEXTRAN-GMA)-*CO*-NIPAAM) POLYHIPE HYDROGEL PREPARATION (DG1, DN1 & DN2)

HIPEs were prepared in a 100 ml glass reaction vessel and stirred by a D-shaped PTFE paddle (the length of the paddle is 3.5 cm) connected to an overhead stirrer in

air atmosphere. During the preparation of the emulsions the stirring rate was kept constant at 450 rpm. The continuous aqueous phase of the HIPE contained up to two monomers (dextran-GMA and NIPAAm) and Triton X405 as surfactant. The dispersed phase, a 1.0 % w/v AIBN toluene solution, was slowly added to the homogeneous continuous phase (the compositions of continuous phase are listed in (**Table 9-1**). The duration of the dropwise addition of the dispensed phase was about 30 min and at the end of the addition, stirring was prolonged for a further 15 min to allow better homogenisation of the HIPE. The resulting emulsion was transferred into a soda glass sample tube with 2.5 cm outside diameter. The height of the emulsion level in the sample tube was controlled to be 0.5 cm in order to obtain cylindrical polyHIPE hydrogel with around 2.3 cm diameter and 0.5 cm height for oscillatory mechanical measurements. Then the sample was polymerised in a preheated oven at 60 °C for 24 h in air. A glass cutter was used to gently break the soda glass tube without damaging the cylindrical hydrogel. The foams were then soaked in DMSO in order to replace toluene. DMSO was exchanged three times a day with fresh DMSO for one week. Finally, the foams were soxhlet extracted with water for 2 d and then freeze dried for another 2 d. The compositions of the HIPEs are summarised in **Table 9-1**:

Table 9-1: Emulsion compositions of poly(dextran-GMA) and poly((dextran-GMA)-*co*-NIPAAm) polyHIPE hydrogels.

Sample Code	Aqueous phase [a] (volume fraction)	Aqueous phase composition [b]: Dextran-GMA/ NIPAAm/ Triton X405/ AIBN (% w/v : % w/v : % w/v: % w/v)
DG1	10	20 : 0 : 8.5 : 9
DGN1	10	10 : 10 : 8.5: 9
DGN2	10	4 : 16 : 8.5: 9

[a] Volume of the organic phase relative to the total volume of the emulsion.
[b] Concentration of Dextran-GMA, NIPAAm, Triton X405 and initiator AIBN in distilled water.

9.4 ELEMENTAL ANALYSIS OF POLY((DEXTRAN-GMA)-*CO*-NIPAAM) POLYHIPE HYDROGELS

Elemental analysis of poly((dextran-GMA)-*co*-NIPAAm) polyHIPEs was carried out by Mr. Stephen Boyer at the London Metropolitan University. It is used to determine the NIPAAm content in the polyHIPE hydrogel. And the results of elemental analysis are listed in **Table 9-2**:

.

Table 9-2: Elemental analysis results of poly((dextran-GMA)-*co*-NIPAAm) polyHIPEs

Sample	C (%)	H (%)	N (%)
DN1	47.16	6.68	3.25
DN2	49.91	7.44	5.32

The analysis of the ratio of dextran/NIPAAm is based on the molecular formula of poly((dextran-GMA)-*co*-NIPAAm) and calculated as follow:

$$X:Y:Z=\frac{N\%}{14}:\frac{(\frac{C\%}{12}-\frac{6}{14}N\%)}{7\times GMA_{sub}\%+6}:\frac{(\frac{C\%}{12}-\frac{6}{14}N\%)\times GMA_{sub}\%}{7\times GMA_{sub}\%+6} \quad 9.2$$

Where X is the molecular ratio of NIPAAm units of dextran-*b*-polyNIPAAm; Y is the molar percentage of glucose units of dextran; and Z is the molar percentage of GMA. C% is the weight percentage of carbon; N% is the weight percentage of nitrogen, as determined by elemental analysis; GMA_{sub} is the degree of substitution of dextran-GMA. The results of the calculation are as follows:

DN1: NIPAAm units: glucose units: GMA units = 0.8:1:0.36;

DN2: NIPAAm units: glucose units: GMA units =1.73:1:0.36.

9.5 OSCILLATORY MECHANICAL MEASUREMENTS OF POLY(DEXTRAN-GMA) AND POLY((DEXTRAN-GMA-*CO*-NIPAAM) POLYHIPE HYDROGELS.

Cylindrical dextran-GMA and poly((dextran-GMA)-*co*-NIPAAm) polyHIPE hydrogels with a diameter of 2.3 cm, and a height of 0.5 cm were used for this experiment. A TA Instruments AR1000 rheometer equipped with 2.0 cm standard steel parallel plates and a steel hotplate was used to record the storage modulus G' and loss modulus G" change of polyHIPE hydrogels. The shear modulus G' and the loss modulus G" were measured by heating samples from 25 °C to 50 °C at 0.5 °C/min at 1.0 Hz with 3.0% strain. This method is adapted from by the literature[282-283]. The result are shown in **Figure 3-3**.

9.6 SYNTHESIS OF METHACRYLATE-MODIFIED ALGINATE

The synthesis and characterisation of methacrylate-modified alginate followed the procedure reported by Smeds et al.[225] Briefly, after alginate (4.0 g) was dissolved in distilled water (200 ml) to make a 2.0 % w/v solution, methacrylic anhydride (15 ml) was added at once at room temperature. The pH of the solution was adjusted to 8 by dropwise addition of concentrated NaOH (5.0 M) (the pH of this solution was monitored by using a pH meter (CyberScan pH11, Eutech Instrument, Singapore)). The solution was incubated at 5 °C for 24 h. The polysaccharide was purified by

precipitation into ethanol (400 ml) and subsequently washed with ethanol (about 1 L). The sample was dried under vacuum at room temperature for 3 d. 3.0 g product was obtained and the yield was 75%.

The degree of methacrylation of methacrylate-modified alginate was determined from the ^{1}H-NMR spectrum in D_2O (**Figure 9-1**). ^{1}H-NMR spectra were recorded on a Bruker DRX 400 (400 MHz) in D_2O at room temperature. ^{1}H-NMR spectra were processed using the software MestReNova (version 6.1.0). The relative integrations of the anomeric protons of the glucose ring of alginate at δ = 4.9 ppm to methacrylate proton peaks (methylene protons at δ = 6.1 and 5.7 ppm and the methyl group peak, δ = 1.9 ppm) were used to determine the degree of substitution of alginate with methacrylate units. The molar ratio of glucose to methacrylate groups to glucose units was determined to be 1.00:0.44.

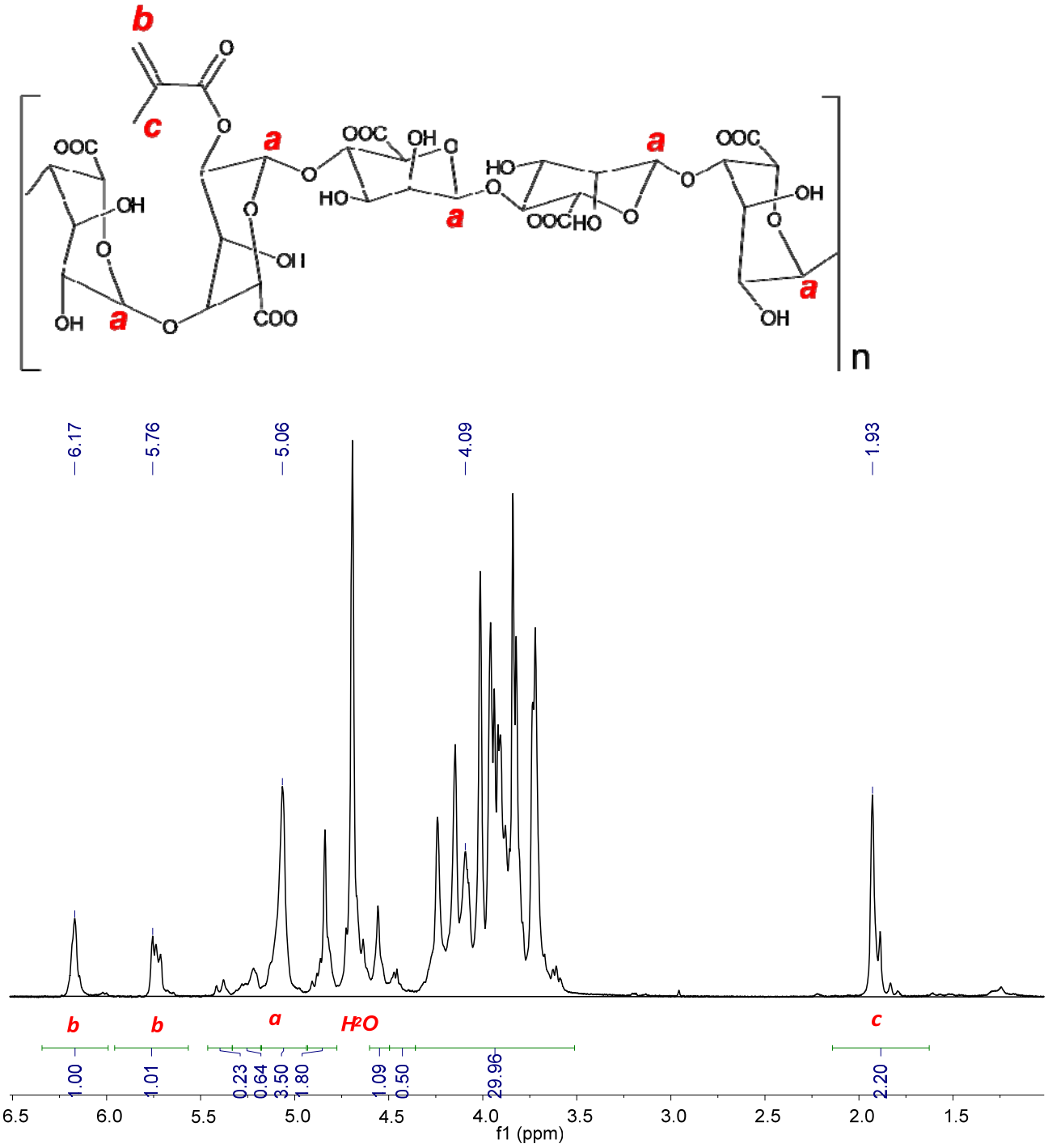

Figure 9-2: The ^{1}H-NMR spectra of methacrylate-modified alginate dissolved in D_2O.

9.7 PREPARATION OF HYDROGEL POLYHIPES PHMA FROM METHACRYLATE-MODIFIED ALGINATE

Methacrylate-modified alginate (0.35 g) obtained in **Section 9.6** was dissolved in distilled water (5.0 ml) together with Triton X405 (0.44 g) at room temperature. A solution of AIBN in toluene (1.0 wt%, 20 ml) was added under stirring (500 rpm) at room temperature for 4 h. The shear force necessary for the dispersion of the organic phase into the aqueous phase was provided by an IKA RW 20 Digital overhead stirrer (IKA Labortechnik, Germany) with a D-shaped PTFE paddle (the width of the paddle was 3.5 cm). A HIPE was obtained after complete addition of the organic phase. The resulting emulsion was transferred to soda glass sample tube with 2.5 cm outside diameter. The filling level of the emulsion (liquid) in the sample tube was 0.5 cm in order to obtain cylindrical polyHIPE hydrogel with about 2.1 to 2.3 cm diameter and 0.5 cm height for oscillatory mechanical measurements. The sample was cured in an oven at 60 °C for 24 h in air. The polyHIPE was soxhlet-extracted with methanol for 24h, then with acetone for a further 24 h. Finally, the methacrylate-modified alginate polyHIPE was dried in an oven at 60 °C for 24 h. Then the sample was immersed in distilled water (100 ml) for more than 6 h to reach its equilibrium swelling and freeze dried for 2 d.

9.8 IONIC CROSSLINKING AND DE-CROSSLINKING OF A HYDROGEL POLYHIPE MADE FROM METHACRYLATE-MODIFIED ALGINATE

9.8.1 IONIC CROSSLINKING OF A METHACRYLATE-MODIFIED ALGINATE POLYHIPE HYDROGEL PHMA

A piece of freeze-dried methacrylate-modified alginate polyHIPE hydrogel **PHMA** was equilibrated in 100 ml distilled water for 6 h. The hydrogel was taken out of the water and thoroughly shaken to remove excess water until no water could be visually observed on the surface of the hydrogel. **PHMA** was then soaked in 200 ml either 1.8 mM, 4 mM or 100 mM aqueous $CaCl_2$ solution for 24 h. The ionically crosslinked sample was soaked in about 100 ml distilled water for 2 h before being freeze dried for more than 3 d.

9.8.2 IONIC DE-CROSSLINKING OF IONICALLY CROSSLINKED METHACRYLATE-MODIFIED ALGINATE BASED POLYHIPE HYDROGEL PHMA

A piece of freeze-dried ionically and covalently crosslinked methacrylate-modified alginate polyHIPE **PHMA** were equilibrated in distilled water (100 ml) for 6 h. The hydrogel was taken out of the water and thoroughly shaken to remove excess water until no water could be visually observed in the surface of the sample. It was then

soaked in 200 ml 100 mM sodium citrate aqueous solution for 24 h. The ionically de-crosslinked sample was soaked in distilled water (about 100 ml) for 2 h before freeze drying.

9.9 OSCILLATORY MECHANICAL MEASUREMENTS OF METHACRYLATE-MODIFIED ALGINATE POLYHIPE HYDROGEL PHMA

Cylindrical methacrylate-modified alginate polyHIPE hydrogel **PHMA** with a diameter of 2.2 cm and a height of 0.5 cm were used for oscillatory rheology. A TA Instruments AR1000 rheometer equipped with a 2.0 cm standard steel parallel plate was used to record the storage modulus (G') and loss modulus (G") of methacrylate-modified alginate polyHIPE hydrogel. The frequencies scanned ranged from 20 to 120 rad/s. This method is similar to that used by Fernandez et al.[282] and Bajomo et al.[283]. The ionically crosslinked methacrylate-modified alginate polyHIPE hydrogel was prepared by soaking in 100 ml 100 mM aqueous $CaCl_2$ solution for 24 h. After ionic crosslinking, the hydrogel shrunk to 1.8 cm in diameter and 0.3 cm height. The crosslinked hydrogel was soaked in distilled water (50 ml) to remove any residual $CaCl_2$. Similarly to disrupt the ionic crosslinking, the ionically crosslinked samples were soaked in aqueous sodium citrate solution (100 ml, 100 mM) for 24 h. The hydrogel recovered its initial physical dimensions of 2.2 cm in diameter and 0.5 cm in height. The resulting sample was then washed with distilled water (50 ml) to remove

any remaining sodium citrate. Samples were stored in 100 ml distilled water at room temperature.

9.10 EQUILIBRIUM WATER UPTAKE RATIO OF METHACRYLATE-MODIFIED ALGINATE POLYHIPE HYDROGEL PHMA

The water uptake of methacrylate-modified alginate polyHIPE hydrogel **PHMA** was determined gravimetrically. The weight of the dry sample was measured directly. The weight of swollen samples was measured by weighing methacrylate-modified alginate hydrogels, which were equilibrated in 200 ml distilled water for 24 h after wiping off any excess water with tissue from the monolith surface. The water uptake ratio (R_w) was calculated as follows:

$$R_w = \frac{W_w - W_d}{W_d} \times 100\% \qquad 9.3$$

where W_w is the weight of the hydrogel swollen to equilibrium in distilled water and W_d is the weight of the freeze-dried hydrogel. The water uptake of polyHIPE PHMA was 8000±250 % w/w at fully swollen state and 3000±100 % w/w at fully shrunken state.

9.11 RATE OF SHRINKING AND SWELLING OF METHACRYLATE-MODIFIED ALGINATE POLYHIPE HYDROGEL PHMA

Cylindrical methacrylate-modified alginate polyHIPE hydrogel PHMA (obtained in S**ection 9.7**) with a diameter of 2.1 cm was used for these experiments. A Sony W55 digital camera (in video mode) was used to record a sample's shrinking behaviour in 100 ml 100 mM $CaCl_2$ and swelling behaviour in 100 ml 100 mM sodium citrate at room temperature. The diameter of the sample was measured from the video every minute during shrinking and every 30 s during swelling. The dimensions of methacrylate-modified alginate polyHIPE hydrogels were calibrated by a ruler placed next to the monolith in the video. After 3 h, the dimensions of the sample did not show any further changes in both swelling and shrinking experiments.

9.12 INJECTABILITY OF POLY((DEXTRAN-GMA)-*CO*-NIPAAM) POLYHIPE HYDROGEL DN2 AND METHACRYLATE-MODIFIED ALGINATE POLYHIPE HYDROGEL PHMA

Several pieces (about 3 ml in volume) of polyHIPE hydrogel (poly((dextran-GMA)-*co*-NIPAAm) polyHIPE hydrogel **DN2** or methacrylate-modified alginate polyHIPE hydrogel **PHMA**) were immersed in distilled water for 24 h. They were loaded into a 5 ml syringe (Becton, Dickinson U.K. Limited, Oxford UK) and gently pressed

through a hypodermic needle with an inner diameter of 1.1 mm in to a round bottom flask containing about 10 ml distilled water. The resulting injected hydrogel fragments were then lyophilised for 3 d for SEM characterisation. Hydrogel **DN2** or **PHMA** was also injected into a 1.5 cm×1.5 cm×1.5 cm pork muscle at room temperature which was then freeze dried with hydrogel present in the muscle tissue. In order to observe the injected hydrogel within the muscle in SEM, one part of the muscle was sliced away. The injected hydrogels were then lyophilised for 3 d together with the muscle for SEM characterisation.

9.13 REFORMING OF INJECTED HYDROGEL DN2 OR PHMA SCAFFOLDS

Several pieces (about 3 ml in volume) of polyHIPE hydrogel (poly((dextran-GMA)-*co*-NIPAAm) polyHIPE hydrogel **DN2** or methacrylate-modified alginate polyHIPE hydrogel (**PHMA)**) were immersed in distilled water to reach equilibrium and were then soaked in 50 ml aqueous alginate solution with two difference alginate concentrations separately (0.2 % w/v and 1.0 % w/v) for 24 h. The hydrogel was loaded into a 5 ml syringe and gently passed through a hypodermic needle (inner diameter = 1.1 mm) into a cellulose extraction thimble (inner diameter = 19 mm, outer length = 90 mm, Whatman International Ltd. Maidstone, England). The injected polyHIPE hydrogel fragments were confined within the closed end of a soxhlet thimble using a plastic syringe plunger (diameter = 1.3 cm), which was tightly fixed inside the thimble (acting as a shape template) with the help of two plastic cable ties.

The whole set-up was soaked in a 100 ml 50 mM aqueous $CaCl_2$ solution for 24 h to trigger the solidification of the alginate solution in these polyHIPE hydrogel fragments. After the soxhlet thimble was removed, the injected polyHIPE hydrogel fragments had formed a single cylinder shaped hydrogel monolith (diameter ≈ 1.3 cm, height ≈ 1 cm). The reforming procedure is illustrated in **Figure 9-3**.

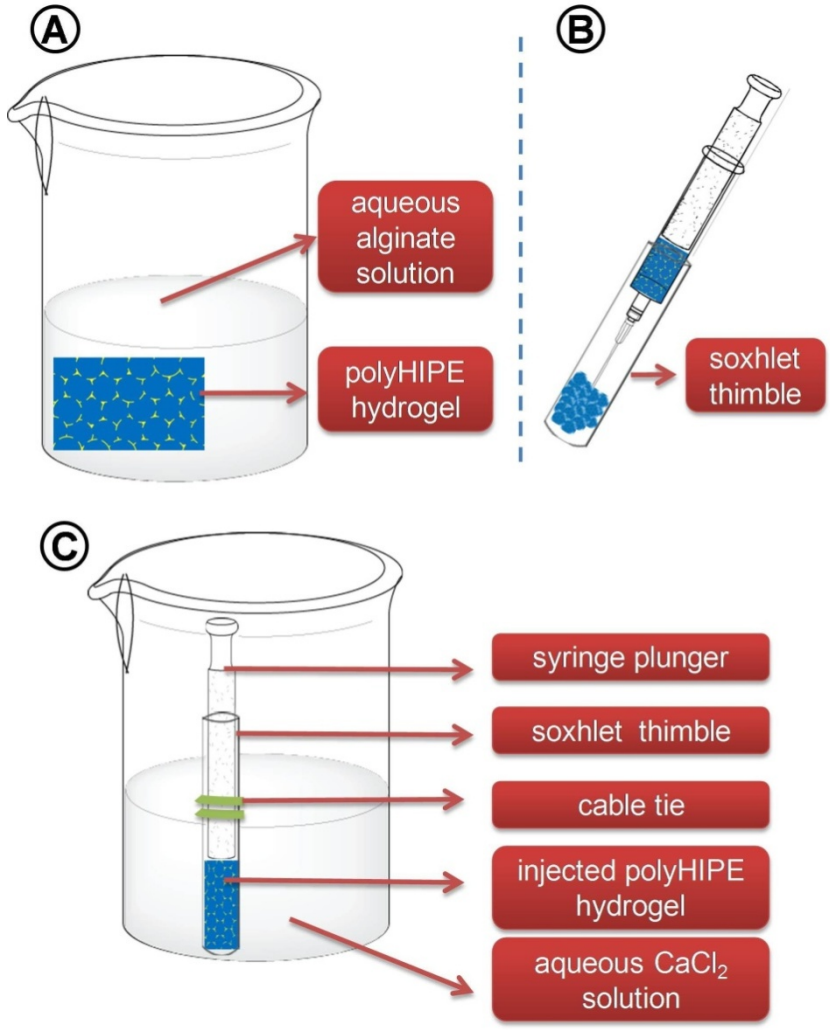

Figure 9-3: Reforming of injected hydrogel scaffolds: **A**: hydrogel pieces were soaked in aqueous alginate solution for 24 h; **B**: the hydrogels were loaded in a 5 ml syringe and gently passed through a hypodermic needle into a cellulose extraction thimble; **C**: the injected hydrogel fragments were confined in the soxhlet extraction thimble using the plunger of the plastic syringe, which was tightly fixed in the thimble by two plastic cable ties. The whole set-up was soaked in aqueous $CaCl_2$ solution for 24 h.

9.14 SYNTHESIS OF DEXTRAN-*b*-POLYNIPAAM COPOLYMER

Dextran (5.00 g; 0.125 mmol) was dissolved in distilled water (50 ml) in a three necked flask. The solution was placed in an oil bath at 27 °C and purged with nitrogen. The nitrogen atmosphere was maintained throughout the copolymerisation reaction. Cerium (IV) ammonium nitrate (5.50 g, 0.01 mol), nitric acid (6.10 g, 69%) and NIPAAm (5.00 g, 0.043 mol) were added to the reaction system. After 4 h, the reaction was stopped through addition of sodium hydroxide solution (1 N). The reaction mixture was transferred to a dialysis tube (MWCO = 12,000 Da) and dialysed against distilled water for 3 d (distilled water was changed twice a day). A white fluffy product was obtained after freeze drying and the yield is 44%. The ratio of dextran glucose units to NIPAAm repeat units was determined by comparing the ^{1}H-NMR spectra of dextran, NIPAAm and dextran-*b*-NIPAAm copolymer in D_2O. ^{1}H-NMR spectra were recorded on a Bruker DRX 400 (400 MHz) in D_2O at room temperature. ^{1}H-NMR spectra were processed using the software MestRe-C (version 4.8.1.1). The NMR analysis was carried out according to reference[248]. Specifically, signals corresponding to the anomeric proton of the glucose ring of dextran at δ = 4.9 ppm and the proton at the anomeric carbon of the α-1,3 linkages at δ = 5.1 ppm were clearly observed both in the ^{1}H-NMR spectra of dextran and the dextran-*b*-polyNIPAAm copolymer. The proton signals of NIPAAm, such as the two isopropyl group methyl signals (δ = 1.1 ppm), the isopropyl methine group (δ =3.8 ppm) and the

backbone CH & CH_2 groups (δ = 1.8 ppm & δ = 1.5 ppm), were identified in the ^{1}H-NMR spectra of NIPAAm and dextran-*b*-polyNIPAAm block copolymer. The ratio of glucose units of dextran to NIPAAm units was 1.00:0.67. The ^{1}H-NMR spectra of dextran-*b*-polyNIPAAm dissolved in D_2O is shown in **Figure 9-4**.

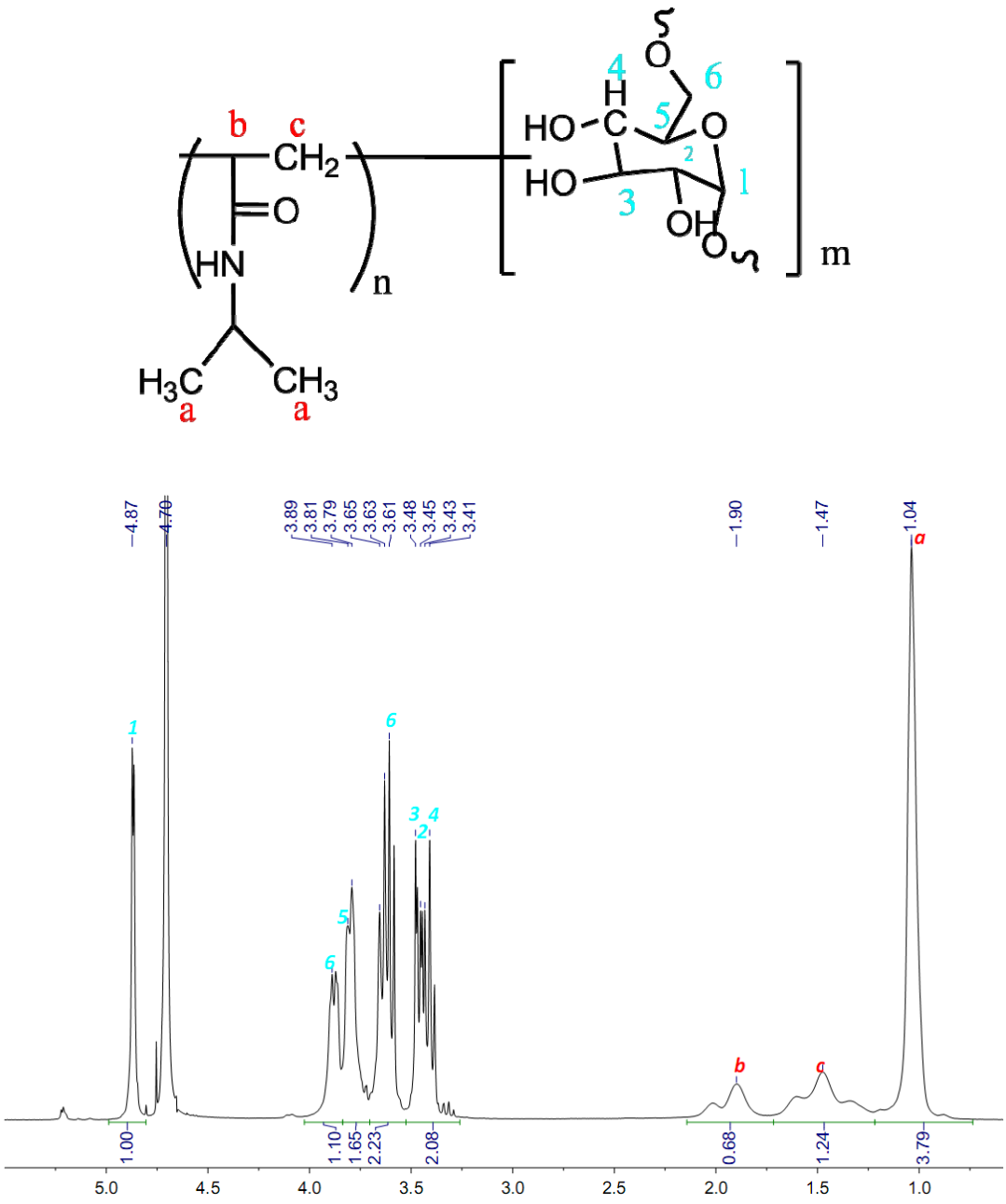

Figure 9-4: The ^{1}H-NMR spectra of dextran-*b*-polyNIPAAm dissolved in D_2O.

9.15 GPC ANALYSIS OF DEXTRAN AND DEXTRAN-*b*-POLYNIPAAM

The molecular weight of dextran-*b*-polyNIPAAm was measured by aqueous GPC by Smithers RAPRA Technology Ltd. (UK) using their standard procedures. The GPC system was calibrated with pullulan polysaccharide. The GPC results were listed in **Table 9-3**.

Table 9-3: GPC results of dextran and dextran-*b*-polyNIPAAm.

Sample	Description	Mw	Mn	Polydispersity
Dextran	Purchased from Sigma-Aldrich	40,000	18,500	2.2
Dextran-*b*-polyNIPAAm	Obtained in **Section 9.14**	28,000	13.600	2.1

9.16 DETERMINATION OF THE LOWER CRITICAL SOLUTION TEMPERATURE OF DEXTRAN-*b*-POLYNIPAAM

A 0.2 % w/v dextran-*b*-polyNIPAAm block copolymer solution in water (10 ml) was placed into a glass test tube. The tube was placed in a thermostated water bath and heated from 24 °C to 38 °C at a rate of 4 °C/h and then allowed to cool to room temperature. The transparent solution became cloudy suddenly when the temperature

reached 34 °C. It became transparent again when the temperature dropped below 34 °C, indicating the LCST of dextran-*b*-polyNIPAAm block copolymer to be 34 °C.

9.17 SYNTHESIS OF POLYNIPAAM HOMOPOLYMER N1

The aqueous redox polymerisation of NIPAAm was adapted from a procedure reported by Schild et al.[1] The polymerisation was carried out at 0 °C. Briefly, NIPAAm (2.22 g, 20.0 mmol) and APS (0.83 g, 3.6 mmol) were dissolved in 60 ml phosphate buffer (buffer composition: distilled water (500 ml), Na_2HPO_4 (0.576 g), NaH_2PO_4 (0.758 g), NaCl (4.2417 g); titrated to pH 7.4 using 0.1 M NaOH) and then TEMED (4.32 ml, 28.3 mmol) was added in one portion. The reaction mixture was stirred using a magnetic stirrer for 15 h under nitrogen at 0 °C in an ice bath. The resulting mixture was dialysed (MWCO = 1,000 Da) against distilled water for 48 h (and exchanged for freshly distilled water 4 times per day) at room temperature. A white fluffy product 1.82 g (82%) was obtained after freeze drying.

9.18 GPC ANALYSIS OF POLYNIPAAM HOMOPOLYMER N1

A PL-GPC 50 fitted with a PL-BV 400RT Viscometer was used, fitted with a PLgel 5 μm MIXED-D 300 × 7.5 mm GPC column (Polymer Laboratories, Shropshire, UK). The mobile phase was DMF with 1 % v/v triethylamine and 1 % v/v glacial acetic

acid. The standards used to calibrate GPC system were poly(methyl methacylate) (Polymer Laboratories).The GPC result of polyNIPAAm **N1** is as follow: M_n = 37,600 and M_w = 96,200.

9.19 DENSITY AND POROSITY OF SOLID HIPE DN0 AND THERMO-HIPE DN1, DN2 AND DN3

The matrix or skeleton density of solid-HIPEs and thermo-responsive solid-HIPEs (ρ_m) was measured by helium pycnometry (Accupyc 1330, Micromeritics, Dunstable UK). The envelop density ρ_H and the porosity were obtained using an envelope density analyzer (Geopyc 1360, Micromeritics, Dunstable, UK). The porosity was calculated using the following equation:

$$porosity = (1 - \frac{\rho_H}{\rho_m}) \times 100\%$$

The results are lisetd in following table:

Table 9-4: Density, porosity, pore volume of solid-HIPE and thermo-responsive solid-HIPEs.

Sample Code	Absolute Density (g/cm^3) [a]	Envelope Density (g/cm^3) [b]	Porosity (%)[b]	Pore Volume (cm^3/g) [b]
DN0	1.490	0.245	83.6	3.416
DN1	1.438	0.131	90.0	6.928
DN2	1.500	0.145	90.4	6.243
DN3	1.466	0.123	91.6	7.448

[a] Determined using GeoPyc 1360. [b] Determined using AccuPyc 1330.

9.20 PREPARATION OF DEXTRAN, DEXTRAN-*b*-POLYNIPAAM AND POLYNIPAAM SOLID-HIPES

Preparation of thermo-responsive solid-HIPE **DN1** serves as an example: Dextran-*b*-polyNIPAAm copolymer (0.050 g) was dissolved in 2.5 ml distilled water together with Triton X405 (0.21 g) at room temperature. The solution was placed into a reaction vessel equipped with an overhead stirrer with a D-shaped paddle. *p*-Xylene (22.5 ml; dispersed phase) was added using an addition funnel under stirring (450 rpm) at room temperature. The duration of the dropwise addition of the dispensed phase was about 30 min. A HIPE was obtained after the addition of *p*-xylene was complete. Approximately 2.5 ml of the *p*-xylene-containing HIPE was taken up in a 5 ml syringe and gently passed through a hypodermic needle (inner diameter = 1.1 mm)

into a round bottom flask. The emulsion was heated to 38 °C for 30 min in an oil bath, and the resulting material was lyophilised for 2 d. The final product was a white soft solid. The yield was approximately 73% (attributed to the loss caused of the HIPE by incomplete transfer of the very viscous HIPE from the reaction vessel into the container for the freeze dryer). The compositions of dextran and dextran-*b*-polyNIPAAm HIPEs are listed as follow:

Table 9-5: Composition of dextran and dextran-*b*-polyNIPAAm copolymer HIPE formulations.

Sample Code	Aqueous phase /oil phase (v:v)	Polymer in aqueous phase	Aqueous phase composition[a]: Polymer/Triton X405 (% w/v : % w/v)	Organic Phase
DN0	1 : 9	dextran	20 : 8.5	*p*-xylene
DN1	1 : 9	dextran-*b*-polyNIPAAm	20 : 8.5	*p*-xylene
DN2	1 : 4	dextran-*b*-polyNIPAAm	20 : 8.5	*p*-xylene
DN3	1 : 9	dextran-*b*-polyNIPAAm	25 : 8.5	*p*-xylene

[a] Concentration of dextran or dextran-*b*-polyNIPAAm copolymers and Triton X405 in distilled water

9.21 PREPARATION OF A POLYNIPAAM SOLID ABOVE ITS LCST

PolyNIPAAm **N1** (0.30 g) was dissolved in 1.5 ml distilled water and water was removed from the solution using a rotary evaporator with the water bath set to 40 °C to yield a transparent solids which was freeze-dried prior to use.

9.22 SOLUBILITY TESTS OF THERMO-RESPONSIVE SOLID-HIPES AND POLYNIPAAM

Approx 0.09 g of the thermo-responsive solid-HIPE **DN1** (and similarly for polyNIPAAm **N1)** was placed into a glass beaker containing distilled water (200 ml) at either 24 °C or 38 °C. The time of dissolution was defined as the time when the solid came in contact with water until the visual disappearance of all solid. Dissolution times of thermo-responsive solid-HIPE **DN1** are listed in **Table 6-3.** The dissolution time of polyNIPAAm **N1** at 24 °C is around 12 min.

9.23 PREPARATION OF HAP NANOPARTILCE STABILISED HIPES

HAp nanoparticles purchased Sigma-Aldrich Company Ltd. (Poole, UK) with particle size less than 200 nm (10 mg or 5 mg), 1.0 ml distilled water and 4.0 ml methyl myristate were added into a soda glass tube with a diameter of 2.5 cm. The mixture was then homogenised at 5,000 rpm for 15 s or 15,000 rpm for 25 s using a Polytron

PT10–35 GT batch homogenizer (Kinematica, Switzerland with a 9 mm rotor). Optical pictures of HIPEs were taken using a Canon 20D digital camera with Canon 60mm EF-S macro lens and Canon Speedlite 580EX flash light. These optical pictures can be found in **Figure 7-2**.

9.24 PREPARATION OF HAP NANOPARTICLE STABILISED DEXTRAN-GMA POLY-PICKERING-HIPES PPH1 TO PPH8 AND DEXTRAN-GMA POLYMIPE DGS

0.20 g dextran-GMA was dissolved in 1.0 ml distilled water together with different amount of HAp nanoparticles (**Table 9-6**) and 50 mg APS in a 25 mm diameter soda glass tube. 4.0 ml of oil phase (either methyl myristate or soybean oil) was added at on portion into the glass tube and homogenised at 2,000 rpm for 1.0 min. The emulsion was cured in an oven at 60 °C for 24 h followed by soxhlet extraction with methanol for 24 h and acetone for a further 24 h. Finally, the product was dried in an oven at 60 °C for 24 h. Then the sample was immersed in distilled water (100 ml) for 24 h and finally freeze dried for 2 d. The compositions and dispersion conditions are listed in **Table 9-6**.

Table 9-6: Compositions of hydrogel polyHIPEs **PPH1-PPH8** obtained from dextran-GMA HAp nanoparticle stabilised poly-Pickering-HIPEs and a dextran-GMA stabilised emulsion template **DGS**

Sample	Aqueous phase composition[a]: Dextran-GMA/APS/HAp Particle (% w/v:% w/v:% w/v)	Homogenising speed and duration	Oil phase type	Ripening time before polymerisation
PPH1[b]	20:5:1	15,000 rpm, 25 s	methyl myristate	0 d
PPH2[b]	20:5:1	5,000 rpm, 15 s	methyl myristate	0 d
PPH3[b]	20:5:1	5,000 rpm, 15 s	methyl myristate	7 d
PPH4[b]	20:5:1	5,000 rpm, 15 s	methyl myristate	14 d
PPH5[b]	20:5:0.5	5,000 rpm, 15 s	methyl myristate	0 d
PPH6[b]	20:5:0.3	5,000 rpm, 15 s	methyl myristate	0 d
PPH7[b]	20:5:1	5,000 rpm, 15 s	soybean oil	0 d
PPH8[b]	20:5:1	5,000 rpm, 15 s	soybean oil	7 d
DGS[c]	20:5:0	20,000 rpm, 60 s	methyl myristate	0 d

[a] The aqueous phase of all samples is a 20 % w/v dextran-GMA aqueous solution with 50 mg/ml ammonium persulfate (APS) as radical initiator and HAp nanoparticles as emulsifier. [b] Dextran-GMA poly-Pickering-HIPEs with 80% nominal pore volume. [c] Dextran-GMA stabilised emulsion templated hydrogel with about 70% nominal pore volume.

9.25 THERMO GRAVIMETRIC ANALYSIS (TGA) OF HAP STABILISED DEXTRAN-GMA POLYHIPE HYDROGELS

The amount of HAp nanoparticles incorporated into the dextran-GMA poly-Pickering-HIPE hydrogels was determined using a thermo gravimetric analyser (TGA Q500, TA Instruments, UK). Approximately 4 mg of the dried hydrogel obtained in **Section 9.24** were placed on a platinum holder and heated to 800 °C at a heating rate of 10 °C min^{-1} under a flow of air (60 ml min^{-1}). The HAp nanoparticle content was taken as the residual weight above 600°C (above the degradation temperature of crosslinked dextran-GMA). At least 3 individual samples were investigated to obtain an average value for each polyHIPE. The results are listed in **Table 9-7**.

Table 9-7: The amount of HAp nanoparticles incorporated into the dextran-GMA poly-Pickering-HIPE hydrogels as determined by TGA

Sample	**PPH1**	**PPH2**	**PPH3**	**PPH4**	**PPH5**	**PPH6**	**PPH7**	**PPH8**
Incorporated HAp nanoparticle proportion (% w/v)	3.9	4.4	1.8	2.3	1.6	1.4	3.9	1.9

9.26 DETERMINATION OF THE PORE SIZE/PORE THROAT SIZE DISTRIBUTION OF HAP STABILISED DEXTRAN-GMA POLY-PICKERING-HIPE HYDROGELS

The average pore size and pore throat size of all HAp stabilised dextran-GMA polyHIPEs were measured from SEM images using of Image-Pro Plus 6.0. In practice, several SEM micrographs were prepared of each specimen and more than 150 pores (or pore throats) were measured to determine the number distribution of pore and pore throat sizes.

9.27 DROPLET SIZE OF HAP NANOPARTICLE STABLISED PICKERING-HIPES DETERMINED BY OPTICAL MICROSCOPY

Optical microscopy images of HAp stabilised Pickering-HIPEs stabilised by 1.0 % w/v HAp nanoparticles produced through homogenisation at 15,000 rpm for 25 s were taken with an optical microscope (Olympus BX51M) by placing an emulsion sample onto a glass slide. The droplet size of the emulsion templates was determined by using image tool software (Image-Pro Plus 6.0). The image of this HIPE can be found in **Figure 7-3**.

9.28 PREPARATION OF HAP NANOPARTICLE OR TRITON X405 STABILISED DEXTRAN-*b*-POLYNIPAAM BASED THERMO-HIPES WITH SOYBEAN OIL OR SQUALENE AS OIL PHASE

The composition of dextran-*b*-polyNIPAAm copolymer HIPEs stabilised by Triton X405 and independently HAp nanoparticles are listed in **Table 9-8**.

Preparation of HIPE **DN-HAp-Soybean** serves as an example:

Dextran-*b*-polyNIPAAm copolymer (0.050 g) was dissolved in 2.5 ml distilled water together with HAp nanoparticles (0.025 g) at room temperature. The solution was placed into a reaction vessel equipped with an overhead stirrer equipped with a D-shaped paddle. 10 ml of the dispersed phase (soybean oil) was added (the duration of the dropwise addition of the dispensed phase was about 30 min) with an addition funnel under stirring (450 rpm) at room temperature. A HIPE was obtained after the addition of soybean oil was complete.

The composition of dextran-*b*-polyNIPAAm copolymer HIPEs with soybean oil or squalene as oil phase, Triton X405 or HAp nanoparticles as emulsifier are listed as follow:

Table 9-8: Compositions of dextran-*b*-polyNIPAAm copolymer HIPEs with soybean oil or squalene as oil phase, Triton X405 or HAp nanoparticles as emulsifier

Sample Code [a]	Oil phase	Emulsifier [b]		Polymer dissolved in aqueous phase [c]	Aqueous phase volume/oil phase volume (v:v)
		Triton X405 (mg/ml)	HAp nanoparticles (mg/ml)		
DN-S-*p*-Xylene	*p*-Xylene	85	0	Dextran-*b*-polyNIPAAm	1:4
DN-S-Soybean	Soybean oil	85	0		
DN-S-Squalene	Squalene	85	0		
DN-HAp-*p*-Xylene	*p*-Xylene	0	10		
DN-HAp-Soybean	Soybean oil	0	10		
DN-HAp-Squalene	Squalene	0	10		

[a] The internal phase volume of all samples 80 % v/v. [b] Concentration of emulsifiers in aqueous phase (distilled water). [c] Dextran-*b*-polyNIPAAm concentration in aqueous phase (distilled water) of all samples is 20 % w/v.

9.29 SYNTHESIS OF POLYNIPAAM-*CO*-AA MICROGEL PARTICLES

PolyNIPAAm-*co*-AA gel particles were kindly prepared by Wei Yuan. The polyNIPAAm-*co*-AA gel particles were synthesised in a surfactant-containing aqueous medium[279-280]. NIPAAm (6.38 g; 54.8 mmol), BIS (0.093 g, 0.6 mmol) and AA (0.216 g; 3.0 mmol) were mixed with 150 ml of a 0.01 M solution of odium dodecylbenzenesulfonate (NaDBS) in a 250 ml round-bottom flask equipped with

condenser. The monomer-containing solution was purged with nitrogen for 2 h. Polymerisation was initiated by adding 0.5 ml of a 7.5 % w/w aqueous ammonium persulfate (APS) solution and was terminated by blowing air into the flask after the polymerisation was allowed to proceed for 2 h at 60 °C at a stirring speed of 200 rpm. The reaction mixture was purified by dialysis (MWCO = 12,000-14,000) followed by ion exchange (Amberlyst 15 resin) and then freeze-dried. Dialysis against distilled water was carried out at 60 °C until the conductivity of the aqueous media became constant (the conductivity of the distilled water was monitored by using HANNA HI 8733 conductivity meter, HANNA Instruments Hellas, Greece). The exchange resin was regenerated with 5 % w/v HCl solution and washed to neutral in a column prior to use.

9.30 PREPARATION OF HAP NANOPARTICLE STABILISED DEXTRAN- *b*-POLYNIPAAM SOLID THERMO-HIPE DN-HAP-*P*-XYLENE

Dextran-*b*-polyNIPAAm copolymer (0.050 g) was dissolved in 2.5 ml distilled water containing an aqueous suspension of HAp nanoparticles at a concentration of 10 mg/ml at room temperature. The mixture was placed in a reaction vessel equipped with an overhead stirrer with a D-shaped paddle. 10 ml of a dispersed phase (either *p*-xylene or soybean oil or squalene) was added (the duration of the dropwise addition of the dispensed phase was 30 min) with an addition funnel under stirring (450 rpm)

at room temperature. A HIPE was obtained after the addition of the dispersed phase was complete.

In order to obtain solid HIPEs for SEM characterisation, approximately 2.5 ml of a *p*-xylene-containing HAp nanoparticle stabilised HIPE was taken up in a 5 ml syringe and gently passed through a hypodermic needle (inner diameter = 1.1 mm) into a round bottom flask. The emulsion was heated to 38 °C for 30 min in an oil bath and the resulting material lyophilised for 2 d.

9.31 PREPARATION OF MICROGEL STABILISED DEXTRAN AND DEXTRAN- *b*-POLYNIPAAM PICKERING SOLID-HIPES

A 0.4 % w/v polyNIPAAm-*co*-AA gel particle suspension was prepared employing a 1 mM KCl solution using 50 ml free standing centrifuge tubes for HIPE preparation. The pH of this suspension was adjusted to 6.8 through dropwise addition of a 0.1 M aqueous solution of KOH solution into this suspension (the pH of thes suspension was monitored by a pH meter CyberScan pH11, Eutech Instrument, Singapore). Dextran (or dextran-*b*-polyNIPAAm copolymer) (0.050 g) was dissolved in 2.5 ml of the suspension at room temperature. The mixture was placed into a reaction vessel equipped with an overhead stirrer with a D-shaped paddle. 10 ml of the dispersed phase (*p*-xylene) was slowly added (the drop wise duration was about 30 min) with an addition funnel under stirring (400 rpm) at room temperature. A HIPE was obtained

after the addition of *p*-xylene was complete. The resulting HIPE was divided into two parts: the first part, about 2.5 ml HIPE was lyophilised for 2 d after emulsification was stopped; the second part, approximately 2.5 ml of the HIPE was firstly loaded into a 5 ml syringe and gently passed through a hypodermic needle (inner diameter = 1.1 mm) into a round bottom flask, before the emulsion was heated to 38 °C for 30 min in an oil bath. The resulting material was lyophilised for 2 d. The yield was approximately 81% (attributed to the loss caused by incomplete transfer of the very viscous HIPE from the reaction vessel to freeze dryer). The composition of dextran and dextran-*b*-polyNIPAAm HIPEs stabilised by polyNIPAAm-*co*-AA gel particles are listed in as follow:

Table 9-9: Composition of dextran and dextran-*b*-polyNIPAAm copolymer HIPEs stabilised by polyNIPAAm-*co*-AA microgel particles

Sample Code [a]	Polymer in aqueous phase [b]	Aqueous phase[c]			Post treatment after HIPE was prepared
		Triton X405 (mg/ml)	Microgel Particles (mg/ml)	KCl (mg/ml)	
Dex-S	Dextran	85	0	0	Freeze dried directly
DN-S-1	Dextran-*b*-polyNIPAAm	85	0	0	Freeze dried directly
DN-S-2	Dextran-*b*-polyNIPAAm	85	0	0	Heated to 38 °C before freeze drying
Dex-P	Dextran	0	4.0	1.0	Freeze dried directly
DN-P-1	Dextran-*b*-polyNIPAAm	0	4.0	1.0	Freeze dried directly
DN-P-2	Dextran-*b*-polyNIPAAm	0	4.0	1.0	Heated to 38 °C before freeze drying

[a] The internal phase all samples is *p*-xylene and its volume fraction is 80 % v/v. [b] The polymer concentration in aqueous phase (distilled water) of all samples is 20 % w/v. [c] Concentration in distilled water. [d] Determined from the corresponding SEM micrographs.

9.32 CELL CULTURE AND CYTOXICITY ASSESSMENT OF O/W HIPE TEMPLATED SCAFFOLDS.

The cytoxicity assessment work was kindly performed by Andrew Chong, and the procedure is as follow: Poly((dextran-GMA)-*co*-NIPAAm) polyHIPE (**DNG2),** methacrylate-modified alginate based polyHIPE **PHMA** and thermo-HIPEs (**DN2** and **DN3**) were cut to about 4×4×4 mm^3 sized cubes using a scalpel and subsequently sterilized under UV light for 90 min at 0.120 J and 80 W (BLX-254, Vilber Lourmat, France). The scaffold was immersed in DMEM supplemented with 10% FBS (2 ml per well) in a 12-well plate and left in an incubator (37 °C, 5% CO_2) overnight. The following day, a suspension of A549 cell (2 µl, 1x10^5 cells/µl, labeled with a Vybrant cell tracer kit) was seeded on the scaffolds and incubated at 37 °C, 5% CO_2. The culture medium (DMEM supplemented with 10% FBS) was changed every 2 d by removing the inserts and replacing them.

On day 4, the culture medium was removed, scaffolds washed twice with phosphate buffer (1:5.25 of 0.2 M NaH_2PO_4 to 0.2 M Na_2HPO_4, pH 7.5) and fixed with 2.5% glutaraldehyde in phosphate buffer (as above) for 40 min at 37 °C. For the purpose of cell fixation, the phosphate buffer was then removed and replaced with phosphate buffer (as above) containing 1% osmium tetroxide and left at 37 °C for a further 1 h. Subsequently, the scaffolds were dehydrated by 3 sequential washes of ethanol (100%)

for 5 min each and then incubated twice in HMDS for 5 min each to remove water completely.

9.33 SEM CHARACTERISATION OF SCAFFOLDS WITH ENTRAPPED CELLS

The internal structure of all polyHIPEs, thermo-HIPEs or solid HIPEs samples and entrapped cells in these samples after cell culture were studied by scanning electron microscopy (Hitachi S-3400N, Berkshire, UK). All samples were sputtered with gold (Edwards Pirani 501 scancoat) for 2 min in an argon atmosphere to guarantee sufficient electrical conductivity.

REFERENCES AND NOTES

1 Langer, R. & Vacanti, J. P. Tissue Engineering. *Science* **260**, 920-926, (1993).

2 Slaughter, B. V., Khurshid, S. S., Fisher, O. Z., Khademhosseini, A. & Peppas, N. A. Hydrogels in Regenerative Medicine. *Adv. Mater.* **21**, 3307-3329, (2009).

3 MacArthur, B. D. & Oreffo, R. O. C. Bridging the gap. *Nature* **433**, 19-19, (2005).

4 Scott, J. H. Scaffold Design and Manufacturing: From Concept to Clinic. *Adv. Mater.* **21**, 3330-3342, (2009).

5 Shastri, V. P. In vivo Engineering of Tissues: Biological Considerations, Challenges, Strategies, and Future Directions. *Adv. Mater.* **21**, 3246-3254, (2009).

6 Langer, R. Perspectives and Challenges in Tissue Engineering and Regenerative Medicine. *Adv. Mater.* **21**, 3235-3236, (2009).

7 Vacanti, J. P. & Langer, R. Tissue engineering: the design and fabrication of living replacement devices for surgical reconstruction and transplantation. *The Lancet* **354**, S32-S34, (1999).

8 Griffith, L. G. & Naughton, G. Tissue Engineering--Current Challenges and Expanding Opportunities. *Science* **295**, 1009-1014, (2002).

9 Langer, R. & Vacanti, J. Tissue engineering. *Science* **260**, 920, (1993).

10 Shoichet, M. S. Polymer Scaffolds for Biomaterials Applications. *Macromolecules* **43**, 581-591, (2009).

11 Hou, Q., Bank, P. A. D. & Shakesheff, K. M. Injectable scaffolds for tissue regeneration. *J. Mater. Chem.* **14**, 1915-1923, (2004).

12 Drury, J. L. & D.J. Mooney. Hydrogels for tissue engineering: scaffold design variables and applications. *Biomaterials* **24**, 4337-4351, (2003).

13 Griffith, L. G. Emerging Design Principles in Biomaterials and Scaffolds for Tissue Engineering. *Ann. NY Acad. Sci* **961**, 83, (2002).

14 Kretlow, J. D., Klouda, L. & Mikos, A. G. Injectable matrices and scaffolds for drug delivery in tissue engineering. *Adv. Drug Delivery Rev.***59**, 263-273, (2007).

15 Cameron, N. R. High internal phase emulsion templating as a route to well-defined porous polymers. *Polymer* **46**, 1439-1449, (2005).

16 Zhang, H. & Cooper, A. I. Synthesis and applications of emulsion-templated porous materials. *Soft Matter* **1**, 107, (2005).

17 Ravikrishna, R., Green, R. & Valsaraj, K. T. Polyaphrons as Templates for the Sol–Gel Synthesis of Macroporous Silica. *J. Sol-Gel Sci. Technol.* **34**, 111-122, (2005).

18 Barbetta, A., Massimi, M., Devirgiliis, L. C. & Dentini, M. Enzymatic cross-linking versus radical polymerization in the preparation of gelatin polyHIPEs and their performance as scaffolds in the culture of hepatocytes. *Biomacromolecules* **7**, 3059-3068, (2006).

19 Q Hou, P. B., KM Shakesheff Injectable scaffolds for tissue regeneration. *J. Mater. Chem.* **14**, 1915-1923, (2004).

20 Fuchs, J. R., Nasseri, B. A. & Vacanti, J. P. Tissue engineering: a 21st century solution to surgical reconstruction. *Ann. Thorac. Surg.* **72**, 577-591, (2001).

21 Bisceglie, V. Über die antineoplastische Immunität: heterologe Einpflanzung von Tumoren in Hühnerembryonen. *Ztschr f Krebsforsch* **40**, 122-140, (1933).

22 Bianco, P. & Robey, P. G. Stem cells in tissue engineering. *Nature* **414**, 118-121, (2001).

23 Zhang, S., Gelain, F. & Zhao, X. Designer self-assembling peptide nanofiber scaffolds for 3D tissue cell cultures. *Semin. Cancer Biol.* **15**, 413-420, (2005).

24 Ruoslahti, E. & Pierschbacher, M. D. New Perspectives in Cell Adhesion: RGD and Integrins. *Science* **238**, 491-497, (1987).

25 Ruoslahti, E. Fibronectin and its Receptors. *Annu. Rev. Biochem* **57**, 375-413, (1988).

26 Yamada, K. M. Adhesive recognition sequences. *J. Biol. Chem.* **266**, 12809-12812, (1991).

27 Lisa, E. F., George, C. E., Jr., Jeffrey, T. B., Franklin, T. M. & Farshid, G. Advanced Material Strategies for Tissue Engineering Scaffolds. *Adv. Mater.* **21**, 3410-3418, (2009).

28 Sachlos, E. & Czernuszka, J. T. Making Tissue Engineering Scaffolds Work. Review: The application of solid freeform fabrication technology to the production of tissue engineering scaffolds *Eur. Cell. Mater.* **5**, 29-40, (2003).

29 Wu, J. Z., Cutlip, R. G., Andrew, M. E. & Dong, R. G. Simultaneous determination of the nonlinear-elastic properties of skin and subcutaneous tissue in unconfined compression tests. *Skin Res. Technol.* **13**, 34-42, (2007).

30 Goulet, R. W., Goldstein, S. A., Ciarelli, M. J., Kuhn, J. L., Brown, M. B. & Feldkamp, L. A. The relationship between the structural and orthogonal

compressive properties of trabecular bone. *J. Biomech.* **27**, 375-377, 379-389, (1994).

31 Yang, S., Leong, K.-F., Du, Z. & Chua, C.-K. The Design of Scaffolds for Use in Tissue Engineering. Part I. Traditional Factors. *Tissue Eng.* **7**, 679, (2001).

32 Mow, V. C. & Huiskes, R. *Basic Orthopaedic Biomaechanics and Mechano-Biology*. 3rd edn, (Lippincott Williams and Wilkins, 2005).

33 Quapp, K. M. & Weiss, J. A. Material Characterization of Human Medial Collateral Ligament. *J. Biomech. Eng.* **120**, 757-763, (1998).

34 M. Klisch, S. & Lotz, J. C. Application of a fiber-reinforced continuum theory to multiple deformations of the annulus fibrosus. *J. Biomech.* **32**, 1027-1036, (1999).

35 Miller-Young, J. E., Duncan, N. A. & Baroud, G. Material properties of the human calcaneal fat pad in compression: experiment and theory. *J. Biomech.* **35**, 1523-1531, (2002).

36 Weinberg, E. J. & Kaazempur-Mofrad, M. R. A large-strain finite element formulation for biological tissues with application to mitral valve leaflet tissue mechanics. *J. Biomech.* **39**, 1557-1561, (2006).

37 Langelaan, M. L. P., Boonen, K. J. M., Polak, R. B., Baaijens, F. P. T., Post, M. J. & van der Schaft, D. W. J. Meet the new meat: tissue engineered skeletal muscle. *Trends Food Sci. Tech.* **21**, 59-66, (2010).

38 Bokhari, M., Carnachan, R. J., Cameron, N. R. & Przyborski, S. A. Novel cell culture device enabling three-dimensional cell growth and improved cell function. *Biochem. Biophys. Res. Commun.* **354**, 1095-1100, (2007).

39 Mikos, A., Thorsen, A., Czerwonka, L., Bao, Y., Langer, R., Winslow, D. & Vacanti, J. Preparation and Characterization of Poly (L-Lactic Acid) Foams. *Polymer* **35**, 1068, (1994).

40 Christenson, E. M., Soofi, W., Holm, J. L., Cameron, N. R. & Mikos, A. G. Biodegradable Fumarate-Based PolyHIPEs as Tissue Engineering Scaffolds. *Biomacromolecules* **8**, 3806-3814, (2007).

41 Harris, L., Kim, B. & Mooney, D. Open pore biodegradable matrices formed with gas foaming. *J. Biomed. Mater. Res. A* **42**, 396-402, (1998).

42 O'Brien, F., Harley, B., Yannas, I. & Gibson, L. Influence of freezing rate on pore structure in freeze-dried collagen-GAG scaffolds. *Biomaterials* **25**, 1077-1086, (2004).

43 Huang, Q., Goh, J., Hutmacher, D. & Lee, E. In Vivo Mesenchymal Cell Recruitment by a Scaffold Loaded with Transforming Growth Factor β1 and the Potential for in Situ Chondrogenesis. *Tissue Eng.* **8**, 469-482, (2002).

44 Hutmacher, D., Sittinger, M. & Risbud, M. Scaffold-based tissue engineering: rationale for computer-aided design and solid free-form fabrication systems. *Trends Biotechnol.* **22**, 354-362, (2004).

45 Nam, Y. & Park, T. Porous biodegradable polymeric scaffolds prepared by thermally induced phase separation. *J. Biomed. Mater. Res.* **47**, 8-17, (1999).

46 Ma, P. X. Scaffolds for tissue fabrication. *Mater. Today* **7**, 30-40, (2004).

47 Croll, T., Gentz, S., Mueller, K., Davidson, M., O'Connor, A., Stevens, G. & Cooper-White, J. Modelling oxygen diffusion and cell growth in a porous, vascularising scaffold for soft tissue engineering applications. *Chem. Eng. Sci.* **60**, 4924-4934, (2005).

48 Kweon, H., Yoo, M., Park, I., Kim, T., Lee, H., Lee, H., Oh, J., Akaike, T. & CS Cho. A novel degradable polycaprolactone networks for tissue engineering. *Biomaterials* **24**, 801-808, (2003).

49 Dado, D. & Levenberg, S. Cell-scaffold mechanical interplay within engineered tissue. *Semin. Cell Dev. Biol.* **20**, 656-664, (2009).

50 Spoerke, E. D., Murray, N. G., Li, H., Brinson, L. C., Dunand, D. C. & Stupp, S. I. A bioactive titanium foam scaffold for bone repair. *Acta Biomater.* **1**, 523-533, (2005).

51 Tschon, M., Fini, M., Giavaresi, G., Torricelli, P., Rimondini, L., Ambrosio, L. & R Giardino. In vitro and in vivo behaviour of biodegradable and injectable PLA/PGA copolymers related to different matrices. *Int. J. Artif. Organs* **30**, 352-362, (2007).

52 Han, D. & Hubbell, J. Synthesis of polymer network scaffolds from L-lactide and poly (ethylene glycol) and their interaction with cells. *Macromolecules* **30**, 6077, (1997).

53 Herrero-Vanrell, R. & Molina-Martinez, I. PLA and PLGA microparticles for intravitreal drug delivery: an overview. *J. Drug Deliv. Sci. Technol.* **17**, 11-17, (2007).

54 Habraken, W., Wolke, J., Mikos, A. & Jansen, J. Injectable PLGA microsphere/calcium phosphate cements: physical properties and degradation characteristics. *J. Biomater. Sci., Polym. Ed.* **17**, 1057-1074, (2006).

55 Kim, M., Choi, Y., Yang, S., Hong, H., Cho, S., Cha, S., Pak, J., Kim, C., Kwon, S. & Park, C. Muscle regeneration by adipose tissue-derived adult stem cells attached to injectable PLGA spheres. *Biochem. Biophys. Res. Commun.* **350**, 499-499, (2006).

56 Eliaz, R. & J Kost. Characterization of a polymeric PLGA-injectable implant delivery system for the controlled release of proteins. *J. Biomed. Mater. Res.* **50**, 388-396, (2000).

57 Mahoney, M. & Anseth, K. Contrasting effects of collagen and bFGF-2 on neural cell function in degradable synthetic PEG hydrogels. *J. Biomed. Mater. Res. A* **81A**, 269-278, (2007).

58 Nuttelman, C., Tripodi, M. & Anseth, K. In vitro osteogenic differentiation of human mesenchymal stem cells photoencapsulated in PEG hydrogels. *J. Biomed. Mater. Res. A* **68A**, 773-782, (2004).

59 Lee, K. Y. & Mooney, D. J. Hydrogels for Tissue Engineering. *Chem. Rev.* **101**, 1869-1880, (2001).

60 Ossipov, D. & Hilborn, J. First injectable poly(vinyl clcohol) hydrogel formed by mixing of functional PVA components. *Abstr. Paper Am. Chem. Soc.* **231**, (2006).

61 Payne, R. G., Yaszemski, M. J., Yasko, A. W. & Mikos, A. G. Development of an injectable, in situ crosslinkable, degradable polymeric carrier for osteogenic cell populations. Part 1. Encapsulation of marrow stromal osteoblasts in surface crosslinked gelatin microparticles. *Biomaterials* **23**, 4359-4371, (2002).

62 Payne, R. G., McGonigle, J. S., Yaszemski, M. J., Yasko, A. W. & Mikos, A. G. Development of an injectable, in situ crosslinkable, degradable polymeric carrier for osteogenic cell populations. Part 2. Viability of encapsulated marrow stromal osteoblasts cultured on crosslinking poly(propylene fumarate). *Biomaterials* **23**, 4373-4380, (2002).

63 Payne, R. G., McGonigle, J. S., Yaszemski, M. J., Yasko, A. W. & Mikos, A. G. Development of an injectable, in situ crosslinkable, degradable polymeric carrier for osteogenic cell populations. Part 3. Proliferation and differentiation of encapsulated marrow stromal osteoblasts cultured on crosslinking poly(propylene fumarate). *Biomaterials* **23**, 4381-4387, (2002).

64 Shi, X., Hudson, J., Spicer, P., Tour, J., Krishnamoorti, R. & Mikos, A. Rheological behaviour and mechanical characterization of injectable poly(propylene fumarate)/single-walled carbon nanotube composites for bone tissue engineering. *Nanotechnology* **16**, S531-S538, (2005).

65 Kempen, D. H. R., Lu, L., Kim, C., Zhu, X., Dhert, W. J. A., Currier, B. L. & Yaszemski, M. J. Controlled drug release from a novel injectable biodegradable microsphere/scaffold composite based on poly(propylene fumarate). *J. Biomed. Mater. Res. A* **77**, 103-111, (2006).

66 Yaremchuk, M. J. Facial skeletal reconstruction using porous polyethylene implants. *Plast. Reconstr. Surg.* **111**, 1818-1827, (2003).

67 Moreira-Gonzalez, A., Jackson, I. T., Miyawaki, T., Barakat, K. & DiNick, V. Clinical outcome in cranioplasty: Critical review in long-term follow-up. *J. Craniofac. Surg.* **14**, 144-153, (2003).

68 Hong, Y., Song, H., Gong, Y., Mao, Z., Gao, C. & Shen, J. Covalently crosslinked chitosan hydrogel: Properties of in vitro degradation and chondrocyte encapsulation. *Acta Biomater.* **3**, 23-31, (2007).

69 Cheng, W., Jin, D., Pei, G., Zeng, X., Tang, G., Li, H. & DY Xiang. Biocompatibility of goat osteoblasts with a novel injectable scaffold material composed with chitosan-beta-tricalcium phosphate in vitro. *Tissue Eng.* **12**, 1083-1083, (2006).

70 Jin, R., Hiemstra, C., Zhong, Z. & Feijen, J. Enzyme-mediated fast in situ formation of hydrogels from dextran-tyramine conjugates. *Biomaterials* **28**, 2791-2800, (2007).

71 Tomme, S. V., Nostrum, C. v., Smedt, S. d. & WE Hennink. Degradation behavior of dextran hydrogels composed of positively and negatively charged microspheres. *Biomaterials* **27**, 4141-4148, (2006).

72 Tomme, S. V., Geest, B. D., Braeckmans, K., Smedt, S. D., Siepmann, F., Siepmann, J., Nostrum, C. & WE Hennink. Mobility of model proteins in hydrogels composed of oppositely charged dextran microspheres studied by protein release and fluorescence recovery after photobleaching. *J. Control. Rel.* **110**, 67-78, (2005).

73 Maia, J., Ferreira, L., Carvalho, R., Ramos, M. & Gil, M. Synthesis and characterization of new injectable and degradable dextran-based hydrogels. *Polymer* **46**, 9604-9614, (2005).

74 Tomme, S. R. V., Steenbergen, M. J. v., Smedt, S. C. D., Nostrum, C. F. v. & Hennink, W. E. Self-gelling hydrogels based on oppositely charged dextran microspheres. *Biomaterials* **26**, 2129-2135, (2005).

75 Buschmann, M., Gluzband, Y., Grodzinsky, A., Kimura, J. & Hunziker, E. Chondrocytes in agarose culture synthesize a mechanically functional extracellular matrix. *J. Orthop. Res.* **10**, 745-758, (1992).

76 Michael D. Buschmann, Y. A. G. A. J. G. J. H. K. E. B. H. Vol. 10 745-758 (1992).

77 Landa, N., Feinberg, M., Holbova, R., Miller, L., Cohen, S. & Leor, J. Novel injectable alginate scaffold attenuates progressive infarct expansion and preserves left ventricular systolic and diastolic function late after myocardial infarction. *Eur. Heart J.* **27**, 149-149, (2006).

78 Leor, J., Miller, L., Feinberg, M., Shachar, M., Landa, N., Holbova, R. & Cohen, S. A novel injectable alginate scaffold promotes angiogenesis and preserves left ventricular geometry and function after extensive myocardial infarction in rat. *Circulation* **110**, 279-279, (2004).

79 Park, Y., Tirelli, N. & Hubbell, J. Photopolymerized hyaluronic acid-based hydrogels and interpenetrating networks. *Biomaterials* **24**, 893-900, (2003).

80 Beier, J., Stern-Straeter, J., Foerster, V., Kneser, U., Stark, G. & Bach., A. Tissue engineering of injectable muscle: Three-dimensional myoblast-fibrin injection in the syngeneic rat animal model. *Plast. Reconstr. Surg.* **118**, 1113-1121, (2006).

81 Peretti, G., Xu, J., Bonassar, L., Kirchhoff, C., Yaremchuk, M. & MA Randolph. Review of injectable cartilage engineering using fibrin gel in mice and swine models. *Tissue Eng.* **12**, 1151-1168, (2006).

82 Payne, R., Yaszemski, M., Yasko, A. & Mikos, A. Development of an injectable, in situ crosslinkable, degradable polymeric carrier for osteogenic cell populations. Part 1. Encapsulation of marrow stromal osteoblasts in surface crosslinked gelatin microparticles. *Biomaterials* **23**, 4359-4371, (2002).

83 Ibusuki, S., Fujii, Y., Iwamoto, Y. & Matsuda, T. Tissue-engineered cartilage using an injectable and in situ gelable thermoresponsive gelatin: Fabrication and in vitro performance. *Tissue Eng.* **9**, 371-384, (2003).

84 Chen, J. & Cheng, T. Thermo-responsive chitosan-graft-poly(N-isopropylacrylamide) injectable hydrogel for cultivation of chondrocytes and meniscus cells. *Macromol. Biosci.* **6**, 1026-1039, (2006).

85 Rowley, J. A., Madlambayan, G. & Mooney, D. J. Alginate hydrogels as synthetic extracellular matrix materials. *Biomaterials* **20**, 45-53, (1999).

86 Kempen, D. H. R., Lu, L. C., Kim, C., Zhu, X., Dhert, W. J. A., Currier, B. L. & Yaszemski, M. J. Controlled drug release from a novel injectable biodegradable micro sphere/scaffold composite based on poly(propylene fumarate). *Journal of Biomedical Materials Research Part A* **77A**, 103-111, (2006).

87 Shin, H., Ruhé, P. Q., Mikos, A. & Jansen, J. In vivo bone and soft tissue response to injectable, biodegradable oligo(poly(ethylene glycol) fumarate) hydrogels. *Biomaterials* **24**, 3201-3211, (2003).

88 Behravesh, E., Zygourakis, K. & Mikos, A. Adhesion and migration of marrow-derived osteoblasts on injectable in situ crosslinkable poly(propylene fumarate-co-ethylene glycol)-based hydrogels with a covalently linked RGDS peptide *J. Biomed. Mater. Res. A* **65A**, 260-270, (2003).

89 Davis, K., Burdick, J. & Anseth, K. Photoinitiated crosslinked degradable copolymer networks for tissue engineering applications. *Biomaterials* **24**, 2485-2495, (2003).

90 Kwon, I. & Matsuda, T. Photo-iniferter-based thermoresponsive block copolymers composed of poly(ethylene glycol) and poly(N-isopropylacrylamide) and chondrocyte immobilization. *Biomaterials* **27**, 986-995, (2006).

91 Anseth, K., Metters, A., Bryant, S., Martens, P., Elisseeff, J. & Bowman, C. N. In situ forming degradable networks and their application in tissue engineering and drug delivery. *J. Control. Rel.* **78**, 199-209, (2002).

92 Li, Q., Wang, J., Shahani, S., Sun, D., Sharma, B., Elisseeff, J. & KW Leong. Biodegradable and photocrosslinkable polyphosphoester hydrogel. *Biomaterials* **27**, 1027-1034, (2006).

93 Timmer, M., Ambrose, C. & Mikos, A. Evaluation of thermal- and photo-crosslinked biodegradable poly(propylene fumarate)-based networks. *J. Biomed. Mater. Res. A* **66A**, 811-818, (2003).

94 Na, K., Park, J., Kim, S., Sun, B., Woo, D., Chung, H. & Park, K. Delivery of dexamethasone, ascorbate, and growth factor (TGF beta-3) in thermo-reversible hydrogel constructs embedded with rabbit chondrocytes. *Biomaterials* **27**, 5951-5957, (2006).

95 Kim, S. & Healy, K. Synthesis and characterization of injectable poly(N-isopropylacrylamide-co-acrylic acid) hydrogels with proteolytically degradable cross-links. *Biomacromolecules* **4**, 1214-1223, (2003).

96 Ho, E., Lowman, A. & Marcolongo, M. Synthesis and characterization of an injectable hydrogel with tunable mechanical properties for soft tissue repair. *Biomacromolecules* **7**, 3223-3228, (2006).

97 Kuo, C. & Ma, P. Ionically crosslinked alginate hydrogels as scaffolds for tissue engineering: Part 1. Structure, gelation rate and mechanical properties. *Biomaterials* **22**, 511-521, (2001).

98 Mano, J. Stimuli-Responsive Polymeric Systems for Biomedical Applications. *Adv. Eng. Mater.* **10**, 515-527, (2008).

99 Alarcon, C. d. l. H., Pennadam, S. & Alexander, C. Stimuli responsive polymers for biomedical applications. *Chem. Soc. Rev.* **34**, 276-285, (2005).

100 Tokarev, I. & Minko, S. Stimuli-Responsive Porous Hydrogels at Interfaces for Molecular Filtration, Separation, Controlled Release, and Gating in Capsules and Membranes. *Adv. Mater.* **9999**, NA, (2010).

101 Barker, S. L. R., Ross, D., Tarlov, M. J., Gaitan, M. & Locascio, L. E. Control of Flow Direction in Microfluidic Devices with Polyelectrolyte Multilayers. *Anal. Chem.* **72**, 5925-5929, (2000).

102 Urry, D. W. Five axioms for the functional design of peptide-based polymers as molecular machines and materials: Principle for macromolecular assemblies. *Pept. Sci.* **47**, 167-178, (1998).

103 Ju, H., Kim, S. & Lee, Y. pH/temperature-responsive behaviors of semi-IPN and comb-type graft hydrogels composed of alginate and poly (N-isopropylacrylamide). *Polymer* **42**, 6851, (2001).

104 Huang, J., Wang, X., Qi, W. & Yu, X. Temperature sensitivity and electrokinetic behavior of a N-isopropylacrylamide grafted microporous polyethylene membrane. *Desalination* **146**, 345, (2002).

105 Schild, H. G. Poly(N-isopropylacrylamide): experiment, theory and application. *Prog. Polym. Sci.* **17**, 163, (1992).

106 Bergbreiter, D. E., Case, B. L., Liu, Y.-S. & Caraway, J. W. Poly(N-isopropylacrylamide) Soluble Polymer Supports in Catalysis and Synthesis. *Macromolecules* **31**, 6053-6062, (1998).

107 Cho, J. H., Kim, S.-H., Park, K. D., Jung, M. C., Yang, W. I., Han, S. W., Noh, J. Y. & Lee, J. W. J. W. Chondrogenic differentiation of human mesenchymal stem cells using a thermosensitive poly(N-isopropylacrylamide) and water-soluble chitosan copolymer. *Biomaterials* **25**, 5743-5751, (2004).

108 Westhaus, E. & Messersmith, P. B. Triggered release of calcium from lipid vesicles: a bioinspired strategy for rapid gelation of polysaccharide and protein hydrogels. *Biomaterials* **22**, 453-462, (2001).

109 Partap, S., Rehman, I., Jones, J. R. & Darr, J. R. Supercritical Carbon Dioxide in Water Emulsion-Templated Synthesis of Porous Calcium Alginate Hydrogels. *Adv. Mater.* **18**, 501-504, (2006).

110 Sone, H., Fugetsu, B. & Tanaka, S. Selective elimination of lead(II) ions by alginate/polyurethane composite foams. *J. Hazard. Mater.* **162**, 423-429, (2009).

111 Seki, H. & Suzuki, A. Adsorption of Lead Ions on Composite Biopolymer Adsorbent. *Ind. Eng. Chem. Res.* **35**, 1378-1382, (1996).

112 Jaya, B., Ruma, S. & Bajpai, A. K. Binary biopolymeric beads of alginate and gelatin as potential adsorbent for removal of toxic Ni^{2+} ions: A dynamic and equilibrium study. *J. Appl. Polym. Sci.* **103**, 2581-2590, (2007).

113 Li, Z., Ramay, H. R., Hauch, K. D., Xiao, D. & Zhang, M. Chitosan-alginate hybrid scaffolds for bone tissue engineering. *Biomaterials* **26**, 3919-3928, (2005).

114 Zmora, S., Glicklis, R. & Cohen, S. Tailoring the pore architecture in 3-D alginate scaffolds by controlling the freezing regime during fabrication. *Biomaterials* **23**, 4087-4094, (2002).

115 Dvir-Ginzberg, M., Gamlieli-Bonshtein, I., Agbaria, R. & Cohen, S. Liver Tissue Engineering within Alginate Scaffolds: Effects of Cell-Seeding Density on Hepatocyte Viability, Morphology, and Function. *Tissue Eng.* **9**, 757-766, (2003).

116 Matthew, I. R., Browne, R. M., Frame, J. W. & Millar, B. G. Subperiosteal behaviour of alginate and cellulose wound dressing materials. *Biomaterials* **16**, 275-278, (1995).

117 Balakrishnan, B., Mohanty, M., Umashankar, P. R. & Jayakrishnan, A. Evaluation of an in situ forming hydrogel wound dressing based on oxidized alginate and gelatin. *Biomaterials* **26**, 6335-6342, (2005).

118 Alexander, D. A., Hyun Joon, K. & David, J. M. Alginate Hydrogels as Biomaterials. *Macromol. Biosci.* **6**, 623-633, (2006).

119 Tønnesen, H. H. & Karlsen, J. Alginate in Drug Delivery Systems. *Drug Dev. Ind. Pharm.* **28**, 621-630, (2002).

120 Grant, G. T., Morris, E. R., Rees, D. A., Smith, P. J. C. & Thom, D. Biological interactions between polysaccharides and divalent cations: The egg-box model. *FEBS Letters* **32**, 195-198, (1973).

121 Stevens, M. M., Qanadilo, H. F., Langer, R. & Prasad Shastri, V. A rapid-curing alginate gel system: utility in periosteum-derived cartilage tissue engineering. *Biomaterials* **25**, 887-894, (2004).

122 Quist, A. P., Rhee, S. K., Lin, H. & Lal, R. Physiological Role of Gap-Junctional Hemichannels: Extracellular Calcium-Dependent Isosmotic Volume Regulation. *J. Cell Biol.* **148**, 1063-1074, (2000).

123 Yamaguchi, T., Chattopadhyay, N., Kifor, O., Sanders, J. L. & Brown, E. M. Activation of p42/44 and p38 Mitogen-Activated Protein Kinases by Extracellular Calcium-Sensing Receptor Agonists Induces Mitogenic Responses in the Mouse Osteoblastic MC3T3-E1 Cell Line. *Biochem. Biophys. Res. Commun.* **279**, 363-368, (2000).

124 Wan, L., Jiang, J., Arnold, D., Guo, X., Lu, H. & Mow, V. Calcium Concentration Effects on the Mechanical and Biochemical Properties of Chondrocyte-Alginate Constructs. *Cell. Mol. Bioeng.* **1**, 93-102, (2008).

125 Chung, H. J., Kim, I. K., Kim, T. G. & Park, T. G. Highly Open Porous Biodegradable Microcarriers: In Vitro Cultivation of Chondrocytes for Injectable Delivery. *Tissue Eng. Part A* **14**, 607-615, (2008).

126 Galeska, I., Kim, T. K., Patil, S. D., Bhardwaj, U., Chatttopadhyay, D., Papadimitrakopoulos, F. & Burgess, D. J. Controlled release of dexamethasone from PLGA microspheres embedded within polyacid-containing PVA hydrogels. *APPS J.* **7**, E231-E240, (2005).

127 Jaklenec, A., Wan, E., Murray, M. E. & Mathiowitz, E. Novel scaffolds fabricated from protein-loaded microspheres for tissue engineering. *Biomaterials* **29**, 185-192, (2008).

128 Lao, L., Tan, H., Wang, Y. & Gao, C. Chitosan modified poly(L-lactide) microspheres as cell microcarriers for cartilage tissue engineering. *Colloids Surf., B* **66**, 218-225, (2008).

129 Hong, Y., Gao, C., Shi, Y. & Shen, J. Preparation of porous polylactide microspheres by emulsion-solvent evaporation based on solution induced phase separation. *Polym. Adv. Technol.* **16**, 622-627, (2005).

130 Zhao, H., Ma, L., Gao, C. & Shen, J. A composite scaffold of PLGA microspheres/fibrin gel for cartilage tissue engineering: Fabrication, physical properties, and cell responsiveness. *J. Biomed. Mater. Res. B Appl. Biomater.* **88B**, 240-249, (2009).

131 Sarkar, S., Lee, G. Y., Wong, J. Y. & Desai, T. A. Development and characterization of a porous micro-patterned scaffold for vascular tissue engineering applications. *Biomaterials* **27**, 4775-4782, (2006).

132 Kang, S.-W., Yang, H. S., Seo, S.-W., Han, D. K. & Kim, B.-S. Apatite-coated poly(lactic-*co*-glycolic acid) microspheres as an injectable scaffold for bone tissue engineering. *J. Biomed. Mater. Res. A* **85A**, 747-756, (2008).

133 Kang, S.-W., Jeon, O. & Kim, B.-S. Poly(lactic-*co*-glycolic acid) Microspheres as an Injectable Scaffold for Cartilage Tissue Engineering. *Tissue Eng.* **11**, 438-447, (2005).

134 Hong, Y., Gong, Y., Gao, C. & Shen, J. Collagen-coated polylactide microcarriers/chitosan hydrogel composite: Injectable scaffold for cartilage regeneration. *J. Biomed. Mater. Res. A* **85A**, 628-637, (2008).

135 Kang, S.-W., Seo, S.-W., Choi, C. Y. & Kim, B.-S. Porous Poly(Lactic-*co*-Glycolic Acid) Microsphere as Cell Culture Substrate and Cell Transplantation Vehicle for Adipose Tissue Engineering. *Tissue Eng. Part C Methods* **14**, 25-34, (2008).

136 Rouquerol, J., Avnir, D., Fairbridge, C., Everett, D., Haynes, J., Pernicone, N., Ramsay, J., Sing, K. & Unger, K. Recommendations for the characterization of porous solids. *Pure Appl. Chem.* **66**, 1739, (1994).

137 Barbetta, A., Dentini, M., Zannoni, E. & Stefano, M. D. Tailoring the porosity and morphology of gelatin-methacrylate polyHIPE scaffolds for tissue engineering applications. *Langmuir* **21**, 12333-12341, (2005).

138 MM Stevens, H. Q., R Langer, V Prasad. A rapid-curing alginate gel system: utility in periosteum-derived cartilage tissue engineering. *Biomaterials* **25**, 887-894, (2004).

139 KT Nguyen, J. W. Photopolymerizable hydrogels for tissue engineering applications. *Biomaterials* **23**, 4307-4314, (2002).

140 Temenoff, J., Shin, H., Conway, D., Engel, P. & Mikos, A. In Vitro Cytotoxicity of Redox Radical Initiators for Cross-Linking of Oligo(poly(ethylene glycol) fumarate) Macromers. *Biomacromolecules* **4**, 1605-1613, (2003).

141 Ma, P. X. & Choi, J.-W. Biodegradable Polymer Scaffolds with Well-Defined Interconnected Spherical Pore Network. *Tissue Eng.* **7**, 23-33, (2001).

142 Jeong, B., Bae, Y. & Kim, S. Drug release from biodegradable injectable thermosensitive hydrogel of PEG-PLGA-PEG triblock copolymers. *J. Control. Rel.* **63**, 155-163, (2000).

143 Shung, A. K., Behravesh, E., Jo, S. & Mikos, A. G. Crosslinking characteristics of and cell adhesion to an injectable poly(propylene fumarate-co-ethylene glycol) hydrogel using a water-soluble crosslinking system. *Tissue Eng.* **9**, 243-254, (2003).

144 Mathur, A., Moorjani, S. & Scranton, A. Methods for synthesis of hydrogel networks: A review. *J. Macromol. Sci., Rev. Macromol. Chem. Phys.* **C36**, 405-430, (1996).

145 Place, E. S., George, J. H., Williams, C. K. & Stevens, M. M. Synthetic polymer scaffolds for tissue engineering. *Chem. Soc. Rev.* **38**, 1139-1151, (2009).

146 Hafeman, A., Li, B., Yoshii, T., Zienkiewicz, K., Davidson, J. & Guelcher, S. Injectable Biodegradable Polyurethane Scaffolds with Release of Platelet-derived Growth Factor for Tissue Repair and Regeneration. *Pharm. Res.* **25**, 2387-2399, (2008).

147 Harris, L. D., Kim, B.-S. & Mooney, D. J. Open pore biodegradable matrices formed with gas foaming. *J. Biomed. Mater. Res.* **42**, 396-402, (1998).

148 Yeong, W.-Y., Chua, C.-K., Leong, K.-F. & Chandrasekaran, M. Rapid prototyping in tissue engineering: challenges and potential. *Trends Biotechnol.* **22**, 643-652, (2004).

149 Tuzlakoglu, K. & Reis, R. L. Biodegradable Polymeric Fiber Structures in Tissue Engineering. *Tissue Eng. Part B Rev.* **15**, 17-27, (2009).

150 Moutos, F. T., Freed, L. E. & Guilak, F. A biomimetic three-dimensional woven composite scaffold for functional tissue engineering of cartilage. *Nat. Mater.* **6**, 162-167, (2007).

151 Woodfield, T. B. F., Malda, J., de Wijn, J., Péters, F., Riesle, J. & van Blitterswijk, C. A. Design of porous scaffolds for cartilage tissue engineering using a three-dimensional fiber-deposition technique. *Biomaterials* **25**, 4149-4161, (2004).

152 Cooper, J. A., Lu, H. H., Ko, F. K., Freeman, J. W. & Laurencin, C. T. Fiber-based tissue-engineered scaffold for ligament replacement: design considerations and in vitro evaluation. *Biomaterials* **26**, 1523-1532, (2005).

153 O'Brien, F. J., Harley, B. A., Yannas, I. V. & Gibson, L. J. The effect of pore size on cell adhesion in collagen-GAG scaffolds. *Biomaterials* **26**, 433-441, (2005).

154 Barnes, C. P., Sell, S. A., Boland, E. D., Simpson, D. G. & Bowlin, G. L. Nanofiber technology: Designing the next generation of tissue engineering scaffolds. *Adv. Drug Delivery Rev.* **59**, 1413-1433, (2007).

155 Barbetta, A., Dentini, M., Vecchis, M. S. D., Filippini, P., Formisano, G. & Caiazza, S. Scaffolds based on biopolymeric foams. *Adv. Funct. Mater.* **15**, 118-124, (2005).

156 Kovačič, S., Štefanec, D. & Krajnc, P. Highly Porous Open-Cellular Monoliths from 2-Hydroxyethyl Methacrylate Based High Internal Phase Emulsions (HIPEs): Preparation and Void Size Tuning. *Macromolecules* **40**, 8056-8060, (2007).

157 Lissant, K. J. Geometry of Emulsions. *J. Soc. Cosmet. Chem.* **21**, 141-154, (1970).

158 Lissant, K. J. The geometry of high-internal-phase-ratio emulsions. *J. Colloid Interface Sci.* **22**, 462-468, (1966).

159 Menner, A. & Bismarck, A. New Evidence for the Mechanism of the Pore Formation in Polymerising High Internal Phase Emulsions or Why polyHIPEs Have an Interconnected Pore Network Structure. *Macromol. Symp.* **242**, 19-24, (2006).

160 Williams, J. & Wrobleski, D. Spatial distribution of the phases in water-in-oil emulsions. Open and closed microcellular foams from cross-linked polystyrene. *Langmuir* **4**, 656, (1988).

161 Cameron, N. R. & Barbetta, A. The influence of porogen type on the porosity, surface area and morphology of poly (divinylbenzene) PolyHIPE foams. *J. Mater. Chem.* **10**, 2466, (2000).

162 Palocci, C., Barbetta, A., Grotta, A. L. & Dentini, M. Porous biomaterials obtained using supercritical CO_2-water emulsions. *Langmuir* **23**, 8243-8251, (2007).

163 Butler, R., Davies, C. M. & Cooper, A. I. Emulsion Templating Using High Internal Phase Supercritical Fluid Emulsions. *Adv. Mater.* **13**, 1459-1463, (2001).

164 Butler, R., Hopkinson, I. & Cooper, A. I. Synthesis of Porous Emulsion-Templated Polymers Using High Internal Phase CO2-in-Water Emulsions. *J. Am. Chem. Soc.* **125**, 14473-14481, (2003).

165 Williams, J. & Wrobleski, D. High internal phase water-in-oil emulsions: influence of surfactants and cosurfactants on emulsion stability and foam quality. *Langmuir* **7**, 1370-1377, (1991).

166 Menner, A., Ikem, V., Salgueiro, M., Shaffer, M. & Bismarck, A. High internal phase emulsion templates solely stabilised by functionalised titania nanoparticles. *Chem. Commun.*, 4274-4276, (2007).

167 Hayman, M. W., Smith, K. H., Cameron, N. R. & Przyborski, S. A. Growth of human stem cell-derived neurons on solid three-dimensional polymers. *J. Biochem. Bioph. Methods* **62**, 231-240, (2005).

168 David, D. & Silverstein, M. S. Porous polyurethanes synthesized within high internal phase emulsions. *J. Polym. Sci., Part A: Polym. Chem.* **47**, 5806-5814, (2009).

169 Akay, G., Birch, M. A. & Bokhari, M. A. Microcellular polyHIPE polymer supports osteoblast growth and bone formation in vitro. *Biomaterials* **25**, 3991-4000, (2004).

170 Busby, W., Cameron, N. R. & Jahoda, C. A. B. Tissue engineering matrixes by emulsion templating. *Polym. Int.* **51**, 871-881, (2002).

171 Freed, L. E., Marquis, J. C., Nohria, A., Emmanual, J., Mikos, A. G. & Langer, R. Neocartilage formation in vitro and in vivo using cells cultured on synthetic biodegradable polymers. *J. Biomed. Mater. Res.* **27**, 11-23, (1993).

172 Naotaka, K. Hydrophilic polymeric material. *U.S. Patent* **Patent No.: US 6,048,908**, (1997).

173 Naotaka, K. Hydrophilic polymeric material and method of preparation. *U.S. Patent* **Patent No.: 6,218,440**, (2001).

174 Krajnc, P., Stefanec, D. & Pulko, I. Acrylic Acid ‘‘Reversed’’PolyHIPEs. *Macromol. Rapid Commun.* **26**, 1289, (2005).

175 Kulygin, O. & Silverstein, M. Porous poly(2-hydroxyethyl methacrylate) hydrogels synthesized within high internal phase emulsions. *Soft Matter* **3**, 1525-1529, (2007).

176 Langer, R. Selected advances in drug delivery and tissue engineering. *J. Control. Rel.* **62**, 7, (1999).

177 Barbetta, A., Massimi, M., Di Rosario, B., Nardecchia, S., De Colli, M., Devirgiliis, L. C. & Dentini, M. Emulsion Templated Scaffolds that Include Gelatin and Glycosaminoglycans. *Biomacromolecules* **9**, 2844-2856, (2008).

178 Francisco, F.-T., Jan, C. M. v. H., Jens, C. T., Thierry, M., Ralf, W. & Neil, R. C. Reversible Immobilization onto PEG-based Emulsion-templated Porous Polymers by Co-assembly of Stimuli Responsive Polymers. *Adv. Mater.* **21**, 55-59, (2009).

179 Zhang, H. & Cooper, A. I. Thermoresponsive ldquoParticle Pumpsrdquo: Activated Release of Organic Nanoparticles from Open-Cell Macroporous Polymers. *Adv. Mater.* **19**, 2439-2444, (2007).

180 Lim, H., Kassim, A., Huang, N., Khiewc, P. & Chiu, W. Three-dimensional flower-like brushite crystals prepared from high internal phase emulsion for drug delivery application. *Colloid. Surface Physicochem. Eng. Aspect.* **345**, 211-218, (2009).

181 Dayeh, V. R., Chow, S. L., Schirmer, K., Lynn, D. H. & Bols, N. C. Evaluating the toxicity of Triton X-100 to protozoan, fish, and mammalian cells using fluorescent dyes as indicators of cell viability. *Ecotoxicol. Environ. Saf.* **57**, 375-382, (2004).

182 Dias, N., Mortara, R. A. & Lima, N. Morphological and physiological changes in Tetrahymena pyriformis for the in vitro cytotoxicity assessment of Triton X-100. *Toxicol. in Vitro* **17**, 357-366, (2003).

183 Rosety M, O. F., Rosety-Rodríguez M, Rosety JM, Rosety I, Carrasco C, Ribelles A. Acute toxicity of anionic surfactants sodium dodecyl sulphate (SDS) and linear alkylbenzene sulphonate (LAS) on the fertilizing capability of gilthead (Sparus aurata L.) sperm. *Histol. Histopathol.* **16**, 839-843, (2001).

184 Borenfreund, E. & Shopsis, C. Toxicity monitored with a correlated set of cell-culture assays. *Xenobiotica* **15**, 705-711, (1985).

185 Grant, R. L., Yao, C., Gabaldon, D. & Acosta, D. Evaluation of surfactant cytotoxicity potential by primary cultures of ocular tissues: I. Characterization of rabbit corneal epithelial cells and initial injury and delayed toxicity studies. *Toxicology* **76**, 153-176, (1992).

186 Ward, R. K., Hubbard, A. W., Sulley, H., Garle, M. J. & Clothier, R. H. Human keratinocyte cultures in an in vitro approach for the assessment of surfactant-induced irritation. *Toxicol. in Vitro* **12**, 163-165, (1998).

187 Ikem, V. *O.*, Menner, A. & Bismarck, A. High Internal Phase Emulsions Stabilized Solely by Functionalized Silica Particles. *Angew. Chem., Int. Ed.* **47**, 8277-8279, (2008).

188 Akartuna, I., Studart, A. R., Tervoort, E. & Gauckler, L. J. Macroporous Ceramics from Particle-stabilized Emulsions. *Adv. Mater.* **20**, 4714-4718, (2008).

189 Arditty, S., Whitby, C. P., Binks, B. P., Schmitt, V. & Leal-Calderon, F. Some general features of limited coalescence in solid-stabilized emulsions. *Eur. Phys. J. E* **11**, 273-281, (2003).

190 Menner, A., Verdejo, R., Shaffer, M. & Bismarck, A. Particle-Stabilized Surfactant-Free Medium Internal Phase Emulsions as Templates for Porous Nanocomposite Materials:poly-Pickering-Foams. *Langmuir* **23**, 2398-2403, (2007).

191 Hermant, M. C., Klumperman, B. & Koning, C. E. Conductive Pickering-poly (high internal phase emulsion) composite foams prepared with low loadings of single-walled carbon nanotubes. *Chem. Commun.* **2009**, 2738, (2009).

192 Zifu, L., Tian, M., Jianfang, W. & To, N. High Internal Phase Emulsions Stabilized Solely by Microgel Particles. *Angew. Chem.* **121**, 8642-8645, (2009).

193 Binks, B. P. Particles as surfactants--similarities and differences. *Curr. Opin. Colloid Interface Sci.* **7**, 21-41, (2002).

194 Bernard, P. B. & Jhonny, A. R. Inversion of Emulsions Stabilized Solely by Ionizable Nanoparticles13. *Angew. Chem.* **117**, 445-448, (2005).

195 Blaker, J. J., Lee, K.-Y., Li, X., Menner, A. & Bismarck, A. Renewable nanocomposite polymer foams synthesized from Pickering emulsion templates. *Green Chem.* **11**, 1321-1326, (2009).

196 Wenxin, W., He, L., Racha Cheikh Al, G., Lloyd, H., Michael, F., Kevin, M. S., Brian, S. & Cameron, A. Biodegradable Thermoresponsive Microparticle Dispersions for Injectable Cell Delivery Prepared Using a Single-Step Process. *Adv. Mater.* **21**, 1809-1813, (2009).

197 Lévesque, S. G., Lim, R. M. & Shoichet, M. S. Macroporous interconnected dextran scaffolds of controlled porosity for tissue-engineering applications. *Biomaterials* **26**, 7436-7446, (2005).

198 Barbetta, A., Barigelli, E. & Dentini, M. Porous Alginate Hydrogels: Synthetic Methods for Tailoring the Porous Texture. *Biomacromolecules* **10**, 2328-2337, (2009).

199 Hayman, M. W., Smith, K. H., Cameron, N. R. & Przyborski, S. A. Enhanced neurite outgrowth by human neurons grown on solid three-dimensional scaffolds. *Biochem. Biophys. Res. Commun.* **314**, 483-488, (2004).

200 Karageorgiou, V. & Kaplan, D. Porosity of 3D biomaterial scaffolds and osteogenesis. *Biomaterials* **26**, 5474-5491, (2005).

201 Bokhari, M. A., Akay, G., Zhang, S. & Birch, M. A. The enhancement of osteoblast growth and differentiation in vitro on a peptide hydrogel--polyHIPE polymer hybrid material. *Biomaterials* **26**, 5198-5208, (2005).

202 Busby, W., Cameron, N. R. & Jahoda, C. A. B. Emulsion-Derived Foams (PolyHIPEs) Containing Poly(ε-caprolactone) as Matrixes for Tissue Engineering. *Biomacromolecules* **2**, 154-164, (2001).

203 Yulia, L., Inbal, L.-M., Shulamit, L. & Michael, S. S. A degradable, porous, emulsion-templated polyacrylate. *J. Polym. Sci., Part A: Polym. Chem.* **47**, 7043-7053, (2009).

204 Zhang, X., Li, J., Li, W. & Zhang, A. Synthesis and Characterization of Thermo- and pH-Responsive Double-Hydrophilic Diblock Copolypeptides. *Biomacromolecules* **8**, 3557-3567, (2007).

205 Yakushiji, T., Sakai, K., Kikuchi, A., Aoyagi, T., Sakurai, Y. & Okano, T. Graft Architectural Effects on Thermoresponsive Wettability Changes of Poly(N-isopropylacrylamide)-Modified Surfaces. *Langmuir* **14**, 4657-4662, (1998).

206 Yamato, M., Akiyama, Y., Kobayashi, J., Yang, J., Kikuchi, A. & Okano, T. Temperature-responsive cell culture surfaces for regenerative medicine with cell sheet engineering. *Prog. Polym. Sci.* **32**, 1123-1133.

207 Kumar, A., Srivastava, A., Galaev, I. Y. & Mattiasson, B. Smart polymers: Physical forms and bioengineering applications. *Prog. Polym. Sci.* **32**, 1205-1237, (2007).

208 van Dijk-Wolthuis, W. N. E., Franssen, O., Talsma, H., van Steenbergen, M. J., Kettenes-van den Bosch, J. J. & Hennink, W. E. Synthesis, Characterization, and Polymerization of Glycidyl Methacrylate Derivatized Dextran. *Macromolecules* **28**, 6317-6322, (1995).

209 Lee, K. Y., Rowley, J. A., Eiselt, P., Moy, E. M., Bouhadir, K. H. & Mooney, D. J. Controlling Mechanical and Swelling Properties of Alginate Hydrogels Independently by Cross-Linker Type and Cross-Linking Density. *Macromolecules* **33**, 4291-4294, (2000).

210 Wu, C. & Wang, X. Globule-to-Coil Transition of a Single Homopolymer Chain in Solution. *Physical Review Letters* **80**, 4092, (1998).

211 Kwon, I. K. & Matsuda, T. Photo-iniferter-based thermoresponsive block copolymers composed of poly(ethylene glycol) and poly(N-isopropylacrylamide) and chondrocyte immobilization. *Biomaterials* **27**, 986-995, (2006).

212 Qin, S., Geng, Y., Discher, D. E. & Yang, S. Temperature-Controlled Assembly and Release from Polymer Vesicles of Poly(ethylene oxide)-*block*-poly(*N*-isopropylacrylamide). *Adv. Mater.* **18**, 2905-2909, (2006).

213 Sigurdson, L., Carney, D. E., Hou, Y., Hall, L., Hard, R., Hicks, W., Bright, F. V. & Gardella, J. A. A comparative study of primary and immortalized cell adhesion characteristics to modified polymer surfaces: Toward the goal of effective re-epithelialization. *J. Biomed. Mater. Res.* **59**, 357-365, (2002).

214 Verrier, S., Blaker, J. J., Maquet, V., Hench, L. L. & Boccaccini, A. R. PDLLA/Bioglass® composites for soft-tissue and hard-tissue engineering: an in vitro cell biology assessment. *Biomaterials* **25**, 3013-3021, (2004).

215 A. D. Sezer, J. A. Release characteristics of chitosan treated alginate beads: II. Sustained release of a low molecular drug from chitosan treated alginate beads. *Journal of Microencapsulation* **16**, 687-696, (1999).

216 Roy, I. & Gupta, M. N. Smart Polymeric Materials: Emerging Biochemical Applications. *Chemistry & Biology* **10**, 1161-1171, (2003).

217 Fourest, E. & Volesky, B. Alginate Properties and Heavy Metal Biosorption by Marine Algae. *Appl. Biochem. Biotechnol.* **67**, 215-226, (1997).

218 Zhao, B. & Moore, J. S. Fast pH- and Ionic Strength-Responsive Hydrogels in Microchannels. *Langmuir* **17**, 4758-4763, (2001).

219 Zhang, K., Luo, Y. & Li, Z. Synthesis and Characterization of a pH- and Ionic Strength-Responsive Hydrogel. *Soft Materials* **5**, 183 - 195, (2007).

220 Luo, Y., Zhang, K., Wei, Q., Liu, Z. & Chen, Y. Poly(MAA-co-AN) hydrogels with improved mechanical properties for theophylline controlled delivery. *Acta Biomater.* **5**, 316-327, (2009).

221 Liu, H., Zhen, M. & Wu, R. Ionic-Strength- and pH-Responsive Poly[acrylamide-*co*-(maleic acid)] Hydrogel Nanofibers. *Macromol. Chem. Phys.* **208**, 874-880, (2007).

222 Horkay, F., Tasaki, I. & Basser, P. J. Osmotic Swelling of Polyacrylate Hydrogels in Physiological Salt Solutions. *Biomacromolecules* **1**, 84-90, (2000).

223 Jeon, C. H., Makhaeva, E. E. & Khokhlov, A. R. Swelling behavior of polyelectrolyte gels in the presence of salts. *Macromol. Chem. Phys.* **199**, 2665-2670, (1998).

224 Jeon, O., Bouhadir, K. H., Mansour, J. M. & Alsberg, E. Photocrosslinked alginate hydrogels with tunable biodegradation rates and mechanical properties. *Biomaterials* **30**, 2724-2734, (2009).

225 Smeds, K. A. & Grinstaff, M. W. Photocrosslinkable polysaccharides for *in situ* hydrogel formation. *J. Biomed. Mater. Res.* **54**, 115-121, (2001).

226 Choi, Y. S., Hong, S. R., Lee, Y. M., Song, K. W., Park, M. H. & Nam, Y. S. Study on gelatin-containing artificial skin: I. Preparation and characteristics of novel gelatin-alginate sponge. *Biomaterials* **20**, 409-417, (1999).

227 Kulkarni, A. R., Soppimath, K. S., Aminabhavi, T. M., Dave, A. M. & Mehta, M. H. Glutaraldehyde crosslinked sodium alginate beads containing liquid pesticide for soil application. *J. Control. Rel.* **63**, 97-105, (2000).

228 Bajpai, S. K. & Tankhiwale, R. Investigation of water uptake behavior and stability of calcium alginate/chitosan bi-polymeric beads: Part-1. *React. Funct. Polym.* **66**, 645-658, (2006).

229 Sakai, S. & Kawakami, K. Synthesis and characterization of both ionically and enzymatically cross-linkable alginate. *Acta Biomater.* **3**, 495-501, (2007).

230 Doner, L. W. & Bécard, G. Solubilization of gellan gels by chelation of cations. *Biotechnol. Tech.* **5**, 25-28, (1991).

231 Loutit, J. F., Mollison, P. L., Young, I. M. & Lucas, E. J. Citric acid-sodium citrate-glucose mixtures for blood storage. *Exp. Physiol.* **32**, 183, (1943).

232 Drageta, K. I., Steinsvågb, K., Onsøyenb, E. & Smidsrøda, O. Na- and K-alginate; effect on Ca2+-gelation. *Carbohydr. Polymer* **35**, 1-6.

233 Draget, K. I., Simensen, M. K., Onsøyen, E. & Smidsrød, O. Gel strength of Ca-limited alginate gels made in situ. *Hydrobiologia* **260-261**, 563-565, (1993).

234 Carnachan, R. J., Bokhari, M. A., Przyborski, S. A. & Cameron, N. R. Tailoring the morphology of emulsion-templated porous polymers. *Soft Matter* **2**, 608-616, (2006).

235 Elisseeff, J., McIntosh, W., Anseth, K., Riley, S., Ragan, P. & Langer, R. Photoencapsulation of chondrocytes in poly(ethylene oxide)-based semi-interpenetrating networks. *J. Biomed. Mater. Res.* **51**, 164-171, (2000).

236 Behravesh, E., Jo, S., Zygourakis, K. & Mikos, A. G. Synthesis of in Situ Cross-Linkable Macroporous Biodegradable Poly(propylene fumarate-co-ethylene glycol) Hydrogels. *Biomacromolecules* **3**, 374-381, (2002).

237 Nguyen, K. T. & West, J. L. Photopolymerizable hydrogels for tissue engineering applications. *Biomaterials* **23**, 4307-4314, (2002).

238 Komath, M. & Varma, H. Development of a fully injectable calcium phosphate cement for orthopedic and dental applications. *Bull. Mater. Sci.* **26**, 415-422, (2003).

239 Salem, A. K., Rose, F. R. A. J., Oreffo, R. O. C., Yang, X., Davies, M. C., Mitchell, J. R., Roberts, C. J., Stolnik-Trenkic, S., Tendler, S. J. B., Williams, P. M. & Shakesheff, K. M. Porous Polymer and Cell Composites That Self-Assemble In Situ. *Adv. Mater.* **15**, 210-213, (2003).

240 Gutowska, A., Jeong, B. & Jasionowski, M. Injectable gels for tissue engineering. *Anat. Rec.* **263**, 342-349, (2001).

241 Alsberg, E., Anderson, K. W., Albeiruti, A., Franceschi, R. T. & Mooney, D. J. Cell-interactive Alginate Hydrogels for Bone Tissue Engineering. *J. Dent. Res.* **80**, 2025-2029, (2001).

242 Kamal, H. B., Kuen Yong, L., Eben, A., Kelly, L. D., Kenneth, W. A. & David, J. M. Degradation of Partially Oxidized Alginate and Its Potential Application for Tissue Engineering. *Biotechnol. Progr.* **17**, 945-950, (2001).

243 Shapiro, L. & Cohen, S. Novel alginate sponges for cell culture and transplantation. *Biomaterials* **18**, 583-590, (1997).

244 Chen, J.-P. & Cheng, T.-H. Preparation and evaluation of thermo-reversible copolymer hydrogels containing chitosan and hyaluronic acid as injectable cell carriers. *Polymer* **50**, 107-116, (2009).

245 Cai, Q., Wan, Y., Bei, J. & Wang, S. Synthesis and characterization of biodegradable polylactide-grafted dextran and its application as compatilizer. *Biomaterials* **24**, 3555-3562, (2003).

246 Cai, Q., Yang, J., Bei, J. & Wang, S. A novel porous cells scaffold made of polylactide-dextran blend by combining phase-separation and particle-leaching techniques. *Biomaterials* **23**, 4483-4492, (2002).

247 Ciardelli, G., Chiono, V., Vozzi, G., Pracella, M., Ahluwalia, A., Barbani, N., Cristallini, C. & Giusti, P. Blends of Poly-(ε-caprolactone)and Polysaccharides in Tissue Engineering Applications. *Biomacromolecules* **6**, 1961-1976, (2005).

248 Wang, L., Tu, K., Li, Y., Zhang, J., Jiang, L. & Zhang, Z. Synthesis and characterization of temperature responsive graft copolymers of dextran with poly (N-isopropylacrylamide). *React. Funct. Polym.* **53**, 19, (2002).

249 Chauvierre, C., Labarre, D., Couvreur, P. & Vauthier, C. Radical emulsion polymerization of alkylcyanoacrylates initiated by the redox system dextran-cerium (IV) under acidic aqueous conditions. *Macromolecules* **36**, 6018, (2003).

250 Bertholon, I., Lesieur, S., Labarre, D., Besnard, M. & Vauthier, C. Characterization of Dextran&Poly(isobutylcyanoacrylate) Copolymers Obtained by Redox Radical and Anionic Emulsion Polymerization. *Macromolecules* **39**, 3559-3567, (2006).

251 Umbreit, J. N. & Strominger, J. L. Relation of Detergent HLB Number to Solubilization and Stabilization of D-Alanine Carboxypeptidase from Bacillus subtilis Membranes. *Proc. Nat. Acad. Sci. USA* **70**, 2997-3001, (1973).

252 Petrov, P., Petrova, E. & Tsvetanov, C. B. UV-assisted synthesis of super-macroporous polymer hydrogels. *Polymer* **50**, 1118-1123, (2009).

253 Dinu, M. V., Ozmen, M. M., Dragan, E. S. & Okay, O. Freezing as a path to build macroporous structures: Superfast responsive polyacrylamide hydrogels. *Polymer* **48**, 195-204, (2007).

254 Chung, H., Kim, T. W., Kwon, M., Kwon, I. C. & Jeong, S. Y. Oil components modulate physical characteristics and function of the natural oil emulsions as drug or gene delivery system. *J. Control. Rel.* **71**, 339, (2001).

255 Shingel, K. I., Faure, M.-P., Azoulay, L., Roberge, C. & Deckelbaum, R. J. Solid emulsion gel as a vehicle for delivery of polyunsaturated fatty acids: implications for tissue repair, dermal angiogenesis and wound healing. *J. Tissue Eng. Regen. Med.* **2**, 383-393, (2008).

256 Woodard, J. R., Hilldore, A. J., Lan, S. K., Park, C. J., Morgan, A. W., Eurell, J. A. C., Clark, S. G., Wheeler, M. B., Jamison, R. D. & Wagoner Johnson, A. J. The mechanical properties and osteoconductivity of hydroxyapatite bone scaffolds with multi-scale porosity. *Biomaterials* **28**, 45-54, (2007).

257 Cai, Y., Liu, Y., Yan, W., Hu, Q., Tao, J., Zhang, M., Shi, Z. & Tang, R. Role of hydroxyapatite nanoparticle size in bone cell proliferation. *J. Mater. Chem.* **17**, 3780-3787, (2007).

258 Ginebra, M. P., Traykova, T. & Planell, J. A. Calcium phosphate cements as bone drug delivery systems: A review. *J. Control. Rel.* **113**, 102-110, (2006).

259 Yuasa, T., Miyamoto, Y., Ishikawa, K., Takechi, M., Momota, Y., Tatehara, S. & Nagayama, M. Effects of apatite cements on proliferation and differentiation of human osteoblasts in vitro. *Biomaterials* **25**, 1159-1166.

260 Pissiotis, E. & Spngberg, L. S. W. Biological evaluation of collagen gels containing calcium hydroxide and hydroxyapatite. *J. Endod.* **16**, 468-473, (1990).

261 Kano, S., Yamazaki, A., Otsuka, R., Ohgaki, M., Akao, M. & Aoki, H. Application of hydroxyapatite-sol as drug carrier. *Bio-Med. Mater. Eng.* **4**, 283-290, (1994).

262 Paul, W. & Sharma, C. P. Porous hydroxyapatite nanoparticles for intestinal delivery of insulin. *Trends Biomate. Artif. Organs* **14**, 37, (2001).

263 Babensee, J. E., McIntire, L. V. & Mikos, A. G. Growth Factor Delivery for Tissue Engineering. *Pharm. Res.* **17**, 497-504, (2000).

264 Zhu, S. H., Huang, B. Y., Zhou, K. C., Huang, S. P., Liu, F., Li, Y. M., Xue, Z. G. & Long, Z. G. Hydroxyapatite Nanoparticles as a Novel Gene Carrier. *J. Nanopart. Res.* **6**, 307-311, (2004).

265 Olton, D., Li, J., Wilson, M. E., Rogers, T., Close, J., Huang, L., Kumta, P. N. & Sfeir, C. Nanostructured calcium phosphates (NanoCaPs) for non-viral gene delivery: Influence of the synthesis parameters on transfection efficiency. *Biomaterials* **28**, 1267-1279, (2007).

266 Colver, P. J. & Bon, S. A. F. Cellular Polymer Monoliths Made via Pickering High Internal Phase Emulsions. *Chem. Mater.* **19**, 1537-1539, (2007).

267 Li, Y. & Weng, W. Surface modification of hydroxyapatite by stearic acid: characterization and in vitro behaviors. *J. Mater. Sci. - Mater. Med.* **19**, 19-25, (2008).

268 Binks, B. P. & Lumsdon, S. O. Influence of Particle Wettability on the Type and Stability of Surfactant-Free Emulsions. *Langmuir* **16**, 8622-8631, (2000).

269 Fujii, S., Okada, M. & Furuzono, T. Hydroxyapatite nanoparticles as stimulus-responsive particulate emulsifiers and building block for porous materials. *J. Colloid Interface Sci.* **315**, 287-296, (2007).

270 Brugger, B., Rosen, B. A. & Richtering, W. Microgels as Stimuli-Responsive Stabilizers for Emulsions. *Langmuir* **24**, 12202-12208, (2008).

271 Ngai, T., Auweter, H. & Behrens, S. H. Environmental Responsiveness of Microgel Particles and Particle-Stabilized Emulsions. *Macromolecules* **39**, 8171-8177, (2006).

272 Sun, T., Jackson, S., Haycock, J. W. & MacNeil, S. Culture of skin cells in 3D rather than 2D improves their ability to survive exposure to cytotoxic agents. *J. Biotechnol.* **122**, 372-381, (2006).

273 Aveyard, R., Binks, B. P. & Clint, J. H. Emulsions stabilised solely by colloidal particles. *Adv. Colloid Interf.Sci.* **100-102**, 503-546, (2003).

274 Tsujino, I., Ako, J., Honda, Y. & Fitzgerald, P. J. Drug delivery via nano-, micro and macroporous coronary stent surfaces. *Expert Opin. Drug Deliv.* **4**, 287-295, (2007).

275 Risbud, M. V., Hardikar, A. A., Bhat, S. V. & Bhonde, R. R. pH-sensitive freeze-dried chitosan-polyvinyl pyrrolidone hydrogels as controlled release system for antibiotic delivery. *J. Control. Rel.* **68**, 23-30, (2000).

276 Hutmacher, D. Scaffolds in tissue engineering bone and cartilage. *Biomaterials* **21**, 2529-2543, (2000).

277 Taylor, P. Ostwald ripening in emulsions. *Colloid. Surface Physicochem. Eng. Aspect.* **99**, 175-185, (1995).

278 Kabalnov, A. S., Pertzov, A. V. & Shchukin, E. D. Ostwald ripening in emulsions: I. Direct observations of Ostwald ripening in emulsions. *J. Colloid Interface Sci.* **118**, 590-597, (1987).

279 Ogawa, K., Suzuki, H., Wang, B., Yoshida, R. & Kokufuta, E. Preparation of Thermosensitive Submicrometer Gel Particles with Anionic and Cationic Charges. *Langmuir* **15**, 4289-4294, (1999).

280 Ogawa, K., Nakayama, A. & Kokufuta, E. Preparation and Characterization of Thermosensitive Polyampholyte Nanogels. *Langmuir* **19**, 3178-3184, (2003).

281 W. N. E. van Dijk-Wolthuis, O. F., H. Talsma, M. J. van Steenbergen, J. J. Kettenes-van den Bosch, and W. E. Hennink. Synthesis, Characterization, and Polymerization of Glycidyl Methacrylate Derivatized Dextran. *Macromolecules* **28**, 6317, (1995).

282 Fernandez, E., Lopez, D., Lopez-Cabarcos, E. & Mijangos, C. Viscoelastic and swelling properties of glucose oxidase loaded polyacrylamide hydrogels and the evaluation of their properties as glucose sensors. *Polymer* **46**, 2211-2217, (2005).

283 Bajomo, M., Steinke, J. H. G. & Bismarck, A. Inducing pH Responsiveness via Ultralow Thiol Content in Polyacrylamide (Micro)Gels with Labile Crosslinks. *J. Phys. Chem. B* **111**, 8655-8662, (2007).